Environmental
Studies
Revolving
Funds

041 Field Measurements of Sediment Transport on the Scotian Shelf

Volume I

The Radio-isotope Experiment

Canada

June 1986

The Environmental Studies Revolving Funds are financed from special levies on the oil and gas industry and administered by the Canada Oil and Gas Lands Administration for the Minister of Energy, Mines and Resources, and by the Northern Affairs Program for the Minister of Indian Affairs and Northern Development.

ENVIRONMENTAL STUDIES REVOLVING FUNDS

REPORT No. 041

June 1986

FIELD MEASUREMENTS OF SEDIMENT TRANSPORT ON THE SCOTIAN SHELF

Volume I

The Radio-Isotope Experiment

Donald O. Hodgins
Georges Drapeau
Lewis H. King

Seaconsult Marine Research Ltd.
820-1200 West 73rd Avenue
Vancouver, British Columbia

Scientific Advisor: Carl L. Amos

The correct citation for this report is:

Hodgins, D.O., G. Drapeau and L.H. King. 1986. Field measurements of sediment transport on the Scotian Shelf. Volume I The radio-isotope experiment. Environmental Studies Revolving Funds Report 041. Ottawa. 160 p.

Published under the auspices
of the Environmental Studies
Revolving Funds
ISBN 0-920783-40-6

SUMMARY

Seabed mobility on Sable Island Bank is an important factor for the planning and design of oil and gas pipelines. This study undertook detailed sand transport and boundary layer current measurements, for the first time, at two sites on the Bank close to Sable Island. An innovative technique using radio-isotope tracers to tag mobile sand layers was used to measure bedload transport. Detailed bathymetry, and 500 kHz side scan sonar surveys were made on each site, supplemented by sediment grab samples and bottom still photographs. Burst sampled current meter data were collected 50 cm above the seabed, and coincident wave and meteorological data were compiled for the interpretation of results. The study results are presented in two volumes. Volume I describes the radio-isotope experiment and the geological setting for each site, together with background wave, current, and wind conditions. Certain sediment transport rates and the connections with storms are established. The boundary layer measurements, and the application of simple transport models to predict the tracer results, are discussed in Volume II.

Experiment Objectives:

- to provide estimates of the sand transport rate at two sites, Olympia to the north of the island and Venture on the SE shoreface, during the winter storm season and relate these rates to storm events,
- to determine mobile layer depths,
- to establish procedures for future shelf tracer studies.

Tracer Methods

The 1-km^2 Venture site (43°56.4'N, 59°39.6'W) was located on the eastern flank of a shoreface-connected ridge characterized by a uniform distribution of well-sorted fine sand ($0.17<D_{50}<0.20$ mm) with a silt tail of about 1%, over a coarse sand lag layer ($D_{50}\sim 1$ mm). The fine sand on the ridge was tagged with 1.2 kg of irradiated ground glass containing Iridium 192 (74.4-day half-life) having a D_{50} of 0.37 mm. The total activity upon deployment was 1.52 Ci with approximately 7×10^6 grains of tracer.

The Olympia site (44°00.4'N, 59°52.0'W) was situated on a gentle northward gradient with little local relief. Two sediment types: a moderate to well-sorted sand ($0.30<D_{50}<0.45$ mm) with a 1 to 3% fine silt fraction, over a medium to coarse sand ($0.40<D_{50}<0.75$ mm) with negligible fines were present. The coarse sand lag layer was tagged with 1.5 kg of glass having a D_{50} of 0.57 mm, irradiated to have an activity of 1.59 Ci over 2.8×10^6 grains at the time of deployment.

Four detection surveys were made by towing a NaI crystal scintillometer over the tracer clouds on lines approximately 10 m apart. The scintillometer was mounted in a weighted sled that positioned the sensor 50 mm above the sea bed. The sled was navigated relative to the ship using an ORE TrackPoint acoustic ranging system. The ship was navigated with a Syledis network established on Sable Island. Tracer maps with a relative accuracy of $\pm$10 m were obtained.

Results

Baseline surveys of the radiation cloud patterns were completed immediately after deployment on Sept. 25 and 26, 1984 to give the initial shape and location. Three surveys (Oct. 25 and 26, 1984, Jan. 15 and 18, 1985 and Feb. 18 and 19, 1985) were made subsequently. A good mix of tracer and sediment was obtained by the October survey following passage of a hurricane in mid-October, and significant movement of the cloud at Venture was detected between later surveys in response to winter storms.

It was found that the coarse sand lag layer at Olympia was comparatively stable under storm conditions. Little net movement of the cloud was detected and dispersion was small. Mean velocities of the cloud centroid were of the order of 0.3 to 0.5 m/d.

By contrast the fine sand layer at Venture was found to be mobile. Net movements of 50 to 70 m were detected giving mean velocities of 1 to 2 m/day. Calculated and cored mobile layer depths of 10 to 30 cm were found, which yield mean sand transport rates of 17 to 20 kg/m/hr averaged over 30 to 83 day periods. A consistent direction of movement

was not found; rather the cloud appears to have been transported in directions consistent with wave and current conditions between detections. Thus significant movement is expected to be sporadic, linked to storms, and characterized by transport rates during storms much higher than the above mean values.

Conclusions

This study has shown that radio-isotope tracer experiments can be carried out on continental shelves using available navigation techniques. This is true even in the stormy winter season. The tracer data provided valuable information on the net transport directions, and indicated the amount of dispersion and advection produced by combined wave-current conditions. They also provided quantitative estimates of the mobile layer thickness and transport rates averaged over the intervals between surveys at the Venture location.

RÉSUMÉ

La Mobilité des fonds marins est un facteur important dans la conception et la planification de pipe-lines transportant pétrole et gaz sur le banc de l'Île de Sable. Cette étude a permis, pour la première fois, des mesures détaillées du transport de sable et du courant de la couche limite et ce, à deux endroits sur le banc près de l'Île de Sable. Le transport des sédiments fut mesuré grâce à une technique innovatrice utilisant des traceurs radio-isotopes pour suivre le mouvement des couches de sable. À chaque station ont été obtenus une bathymétrie détaillée, un profil par sonar à balayage latéral (500 kHz), des échantillons de sédiment prélevés à la benne ainsi que des photographies du fond. Des données de courantomètre furent collectées, de façon intermittente, à 50 cm du fond et, pour aider à l'interprétation des résultats, les conditions météorologiques et de la houle ont été compilées. Les résultats de cette étude sont présentés en deux volumes. Le Volume I décrit l'expérience des traceurs radio-isotopes, l'environnement géologique de chaque site ainsi que les conditions prévalentes de houle, courant et vent. Certains taux de transport sédimentaire sont établis ainsi que les liens avec des tempêtes. Dans le volume II sont discutées les mesures de la couche limite et l'application de simples modèles de transport pour prédire le mouvement des traceurs.

Objectifs de l'expérience

- fournir des estimations du taux de transport de sable à 2 stations (Olympia au nord de l'Île et Venture au sud-est) au cours de la saison de tempête hivernale et relier ces taux aux tempêtes,
- déterminer l'épaisseur de la couche mobile,
- établir des procédures pur de futures études de transport côtier utilisant des traceurs.

Méthode d'utilisation des traceurs

Le site de Venture (43°56.4'N, 59°39.6'W) couvrant 1 km^2 et situé sur le flanc est d'une crête reliée au rivage était caractérisé par une distribution uniforme de sable fin de granulométrie étalée ($0.17<D_{50}<0.20$ mm) avec environ 1% de silt, couvrant une couche de sable

grossier ($D_{50}\sim1$ mm). 1.2 kg de verre moulu irradié (D_{50}=0.37 mm) contenant de l'Iridium 192 (demie-vie de 74.4 jours) fut mélangé au sable fin de la crête. L'activité totale lors du déploiement était de 1.52 Ci avec environ $7x10^6$ grains de traceur.

Le site d'Olympia (44°00.4'N, 59°52.0'W) était situe sur une pente douce, direction nord, comportant peu du relief. Deux types de sédiment: un sable de granulométrie allant de modérément a bien étalée ($0.30<D_{50}<0.45$ mm) avec une fraction de 1 à 3% de silt fin, couvrant du sable moyen à grossier ($0.40<D_{50}<0.75$ mm) avec une portion négligeable de sable fin. 1.5 kg de verre irradié (D_{50}=0.57mm) fut mélangé à la couche de sable grossier donnant une activité de 1.59 Ci au déploiement pour $2.8x10^6$.

Quatre campagnes de détection furent effectuées en remorquant un scintillateur à cristal de NaI au-dessus des nuages de traceur, sur des radiales séparées d'environ 10 m. Le scintillateur était monté sur un traîneau lesté, avec le senseur à 50 mm au-dessus de fond marin. La position du traîneau par rapport au navire était donnée par un système acoustique de positionement ORE TrackPoint et le navire lui-même positionné grâce à un réseau Syledis basé sur l'Île de Sable.

Résultats

Le 25 et 26 sept. 1984, immédiatement après le déploiement, des mesures furent effectuées donnant la forme et l'emplacement initials du nuage radioactif. Trois autres campagnes (25 et 26 oct. 1984, 15 et 18 jan. 1985 et 18 et 19 fév. 1985) furent ensuite complétées. En octobre, on a mesuré un bon melange du traceur et des sédiments suite au passage d'un ouragan à la mi-octobre et, entre chaque relevé subséquent, d'importants mouvements du nuage furent détectés, à Venture, en réponse aux tempêtes hivernales.

En comparaison, la couche de fond constitué de sable grossier s'est avérée plutôt stable sous l'effet des tempêtes. Peu de dispersion du nuage ainsi qu'un faible mouvement net furent observés. La vitesse moyenne du centre de masse du nuage variait de 0.3 à 0.5 m/j.

Par contre, la couche de sable fin, à Venture, s'est montrée très mobile. Des mouvements nets de 50 à 70 m furent détectés donnant des vitesses moyennes de 1 à 2 m/jour. Selon les calculs et les mesures, l'épaisseur de la couche mobile variait de 10 à 30 cm ce qui correspond à des taux de transport moyen de 17 à 20 kg/m/h pour des périodes de 30 à 80 jours. Aucune direction particulière du mouvement ne fut constatée; le nuage semble au contraire s'être déplacé selon les directions de la houle et du courant présents entre chaque détection. Donc les déplacements importants semblent sporadiques, liés aux tempêtes et caractérisés par des taux de transport beaucoup plus élevés lors des tempêtes que les valeurs moyennes reportées ci-haut.

Conclusions

Cette étude a démontré que des expériences utilisant des traceurs radio-isotopes peuvent être effectuées sur les plateaux continentaux avec les techniques de positionnement disponibles et ce, même durant la saison de tempête hivernale. Les données de traceur ont fourni précieuses informations sur les directions du transport net et ont indiqué le degré de dispersion et d'advection produit par l'effect combiné de la houle et du courant. Elles ont aussi fourni des estimés quantitatifs de l'épaisseur de la couche mobile et des taux de transport moyens pour chaque période entre les relevés, au site de Venture.

Table of Contents

Acknowledgements

The following organizations and personnel have contributed to this study.

Seaconsult Marine Research Ltd.

Donald O. Hodgins, Ph.D., P.Eng. (Project Manager)
Douglas G. Bliss, M.Sc. (Eng)., P.Eng.
Eric D. Kinsella, M.Sc.
Tony Bowen, Ph.D.
Lewis H. King, Ph.D.

INRS-Océanologie

Georges Drapeau, Ph.D. (Chief Scientist)
Bernard Long, Ph.D.

McElhanney Services Ltd.

Thomas W. Windeyer, B.Sc. (Chief Technician)
Oscar Blagdon, Capt. M.V. Arctic Prowler
Andy Power, C.L.S., P.Eng.
Peter Baer, C.L.S., P.Eng.

Earth and Ocean Research Ltd.

Dan Plasse, Ph.D.

Geological Survey of Canada

Carl L. Amos, Ph.D.

List of Figures

List of Tables

List of Drawings

Notations

$A(t)$ = remaining activity in the tracer cloud

a = absorption coefficient for a sand-water combination

C_e = equivalent concentration

C_m = mean concentration

$C(z)$ = concentration at depth z

D_{50} = median grain diameter

E = thickness of mobile sediment layer

f_o = calibration constant

$f(z)$ = calibration response as a function of depth

H_s = significant wave height

I_g = ionization constant of tracer in water

L = breath of seafloor for transport equation

l = width of seafloor area scanned by probe

M_t = mass of tracer

N = radiation count rate

Q = bedload transport rate

R_L = lower limit on count rates above background

T_p = wave period associated with H_s

t = time gap of integration (2 x integration constant)

V = velocity of detection

V_m = mean velocity of the mobile sediment traction layer

V_c = mass velocity of the tracer

z = vertical coordinate (depth into seabed)

σ_r = chosen standard deviation of tracer grains

ρ_s = density of sediment

μ_o = linear absorption coefficient of the tracer

β = ratio of equivalent concentration to mean concentration

Acronyms

MEDS - Marine Environmental Data Service (Canada)

AES - Atmospheric Environment Service (Canada)

CEA - Commissariat l'Energie Atomique (France)

NOAA - National Oceanic & Atmospheric Administration (US)

BIO - Bedford Institute of Oceanography

BP - Before Present

1.0 INTRODUCTION

1.1 Sand Transport on Sable Island Bank

Sable Island Bank is generally perceived to be a region of very active sediment transport, particularly close to the island. This view is supported by such published accounts of the evolution of the island as that shown in Fig. 1.1.1. Amos and King (1984), in their survey of bedforms, note the presence of large scale features including sand ridges, sand waves, and 2-D megaripples around the island but conclude that the majority of these are moribund. Thus the frequency and degree to which sediments are transported and the relationship of the transport mechanics to tide and storm surge currents, and to storm-generated waves, are factors that are presently poorly understood.

The major objective of this study was to obtain, for the first time, quantitative measurements of sand transport, and to identify in a more qualitative fashion those factors causing significant transport. A radio-isotope tracing technique was selected for measuring sand movement at two separate sites, one on the north side of the island and one on the south-east flank (Fig. 1.1.2). A reasonably comprehensive environmental data set including sediment properties, wind, wave and boundary layer current measurements was also assembled for the period encompassing the tracer detection surveys.

1.2 Objectives of the Tracer Experiment

The tracer study had the following objectives:

- to provide a quantitative estimate of mass sand transport at each site during the winter storm season and relate this to bedform stability and storm events,
- to determine representative depths for the mobile layer, and
- to establish procedures and standards for future shelf tracer studies on the seafloor during storm seasons.

1.3 Overview of Procedures

To maximize the results of a experiment of this kind it is desirable to assemble a database that encompasses all the parameters involved in the

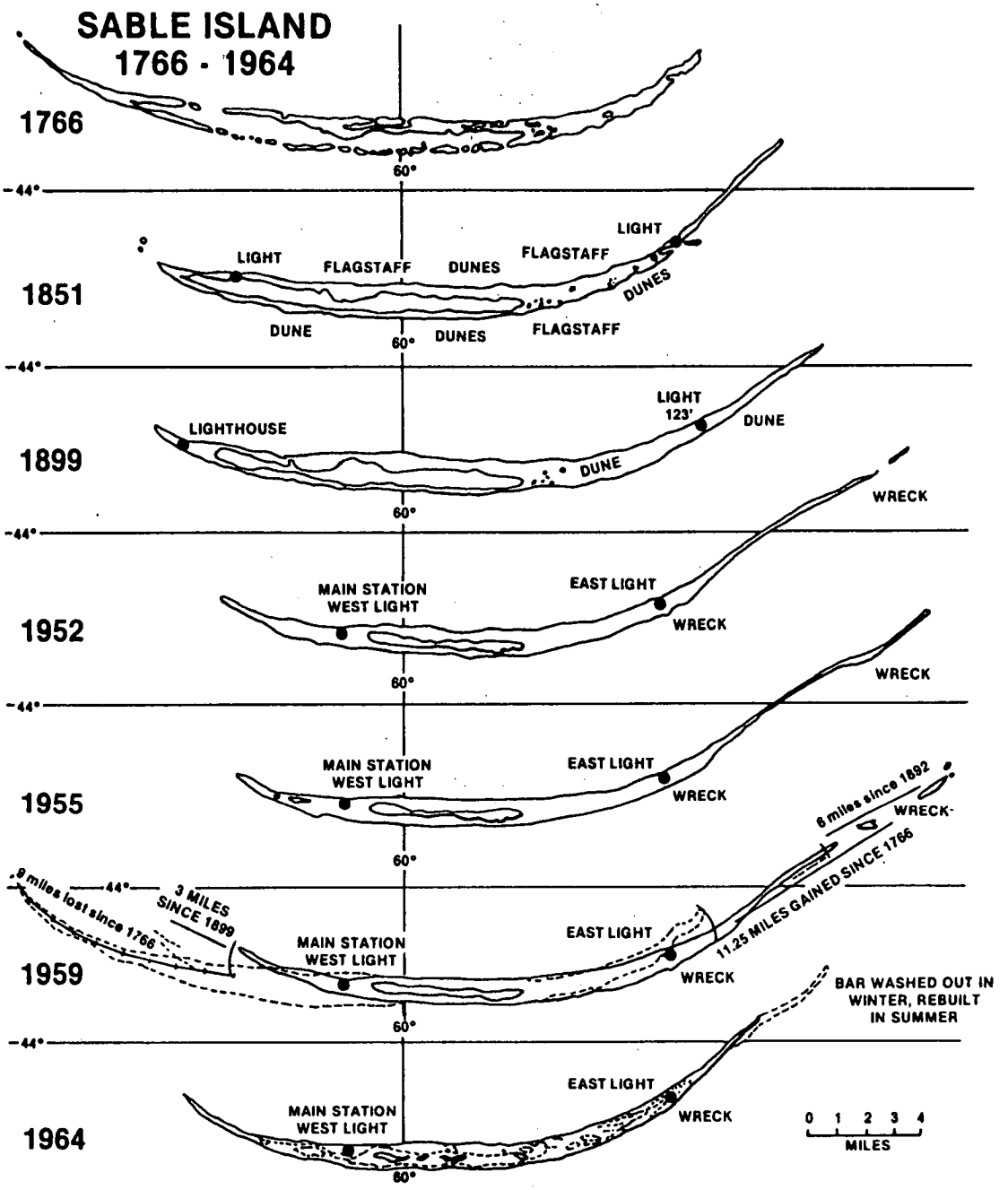

Fig. 1.1.1 Migration patterns of Sable Island (Cameron, 1965).

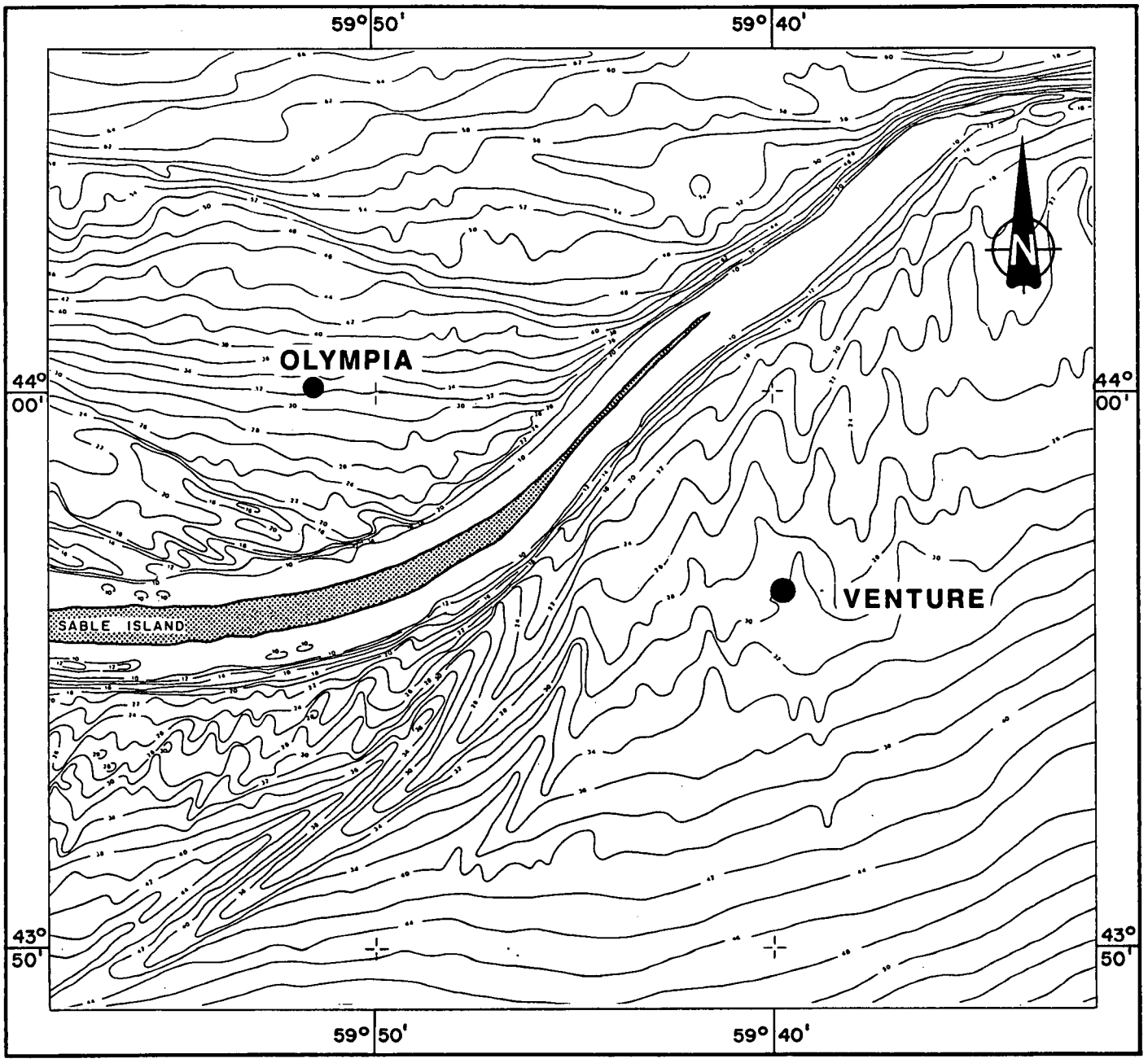

OLYMPIA : 44°00.38'N
59°51.95'W

VENTURE : 43°56.37'N
59°39.61'W

Fig. 1.1.2 Map showing the location of the Venture and Olympia survey sites.

sediment transport process. Thus reasonably comprehensive site investigations were made to describe the surficial sediments and bedforms, time-series of the bottom currents, surface waves and meteorological parameters were recorded, and the dispersion of the radioactive tracer was mapped to obtain quantitative measurements of the bottom sediment transport. The site investigations, consisted of a detailed bathymetric and side-scan survey of each one-kilometre square area, and sediment samples and bottom photographs were taken. Shallow seismic lines of each site were also obtained from the records archived at the BIO.

Burst current meter measurements were recorded in the boundary layer 0.5 m off the seafloor to monitor the key physical process driving sediment transport. At each site a Sea Data directional electromagnetic current meter with pressure gauge was deployed for the duration of the experiment and recorded currents at 1 Hz for 1024 s every 3 hours.

Wave records during the experiment were obtained from various Waverider buoys deployed in the East Sable Bank region and the meteorological parameters were obtained from the AES weather station on Sable Island.

The radio-isotope used for tagging the sand was deployed at each study site and its dispersion was measured with a scintillometer mounted on a sled towed behind the ship. After each tracer detection a contour map of the radioactive cloud was made. The sediment transport vectors and depth of mobile layer were calculated from these cloud maps. These quantitative results were then compared to environmental factors governing sand transport to more fully understand sediment movement around Sable Island.

The experiment took place over a five month period and featured four dedicated cruises for the site investigations, tracer detections and current meter servicing: the cruise programs are shown in Table 1.3.1.

Table 1.3.1

Outline of Dedicated Cruises for the Radio-Isotope Experiment

Date	Olympia Site 44°00.38'N 59°51.95'W	Venture Site 43°56.37'N 59°39.61'W
Cruise No. 1 22-28 Sept. 84	- Sea Data 635-9 deployed - four site markers deployed deployed - radio-isotope deployed - grab samples taken - bottom photographs taken - tracer detection survey	- Sea Data 635-12 deployed - four site markers deployed - radio-isotope deployed - grab samples taken - bottom photographs taken - tracer detection survey - side-scan survey
Cruise No. 2 24-29 Oct. 84	- tracer detection survey - side-scan survey - bathymetric survey - Sea Data 635-9 serviced	- tracer detection survey - side-scan survey - bathymetric survey - Sea Data 635-12 serviced
Cruise No. 3 11-18 Jan. 85	- service Sea Data 635-9 - tracer detection survey	- recover Sea Data 635-12 - deploy Sea Data 621 - tracer detection survey
Cruise No. 4 17-22 Feb. 85	- recover Sea Data 635-9 - recover corner markers - tracer detection survey - bottom grab samples taken	- deploy RALPH - tracer detection survey - recover RALPH - recover corner markers - service Sea Data 621 - bottom grab samples taken

2.0 SITE CHARACTERISTICS

The two sites selected for the study, Olympia and Venture, were chosen to examine contrasting conditions for sediment transport. Most importantly the seabed properties, especially the sand grain size distributions, are quite different. Olympia features a coarser sand than Venture. Details on the stratigraphy and seabed features are discussed in the following sections so that the interpretation of the radio-isotope tracer results can be placed in a proper geological perspective. Also, the wave and current conditions differ because of the influence of Sable Island. The Venture site is more exposed to severe wave conditions since it faces the open ocean than the Olympia location which is well sheltered by the island.

Finally both sites are very relevant to gas pipeline concerns. There are proposals for routes on both the North and South side of Sable Island, and the mobility of bottom sediments under winter storm conditions is of crucial importance to decisions on pipeline burial.

2.1 Geological Setting

(a) Stratigraphy

A diagrammatic section of the Scotian Shelf succession from an area south of Halifax across Emerald Basin and Emerald Bank is shown in Fig. 2.1.1 and illustrates the stratigraphic relationships between surficial formations and their relationship to underlying bedrock, topography, and both present and former sea level. The surficial succession of Quaternary age averages about 50 m in thickness and is comprised of five formations: Scotian Shelf Drift, Emerald Silt, Sambro Sand, Sable Island Sand and Gravel, and LaHave Clay (King, 1970). The table of formations recently modified by King and Fader (1985) is shown in Table 2.1.1. The sand facies of the Sable Island Sand and Gravel Formation comprises the seabed geological unit at the Olympia and Venture sites; thus, a more complete description of this unit is included below.

The Sable Island Sand and Gravel Formation is characterized on high resolution seismic records by weak, fairly continuous, coherent reflections. In most areas it occurs as a thin veneer deposit of less

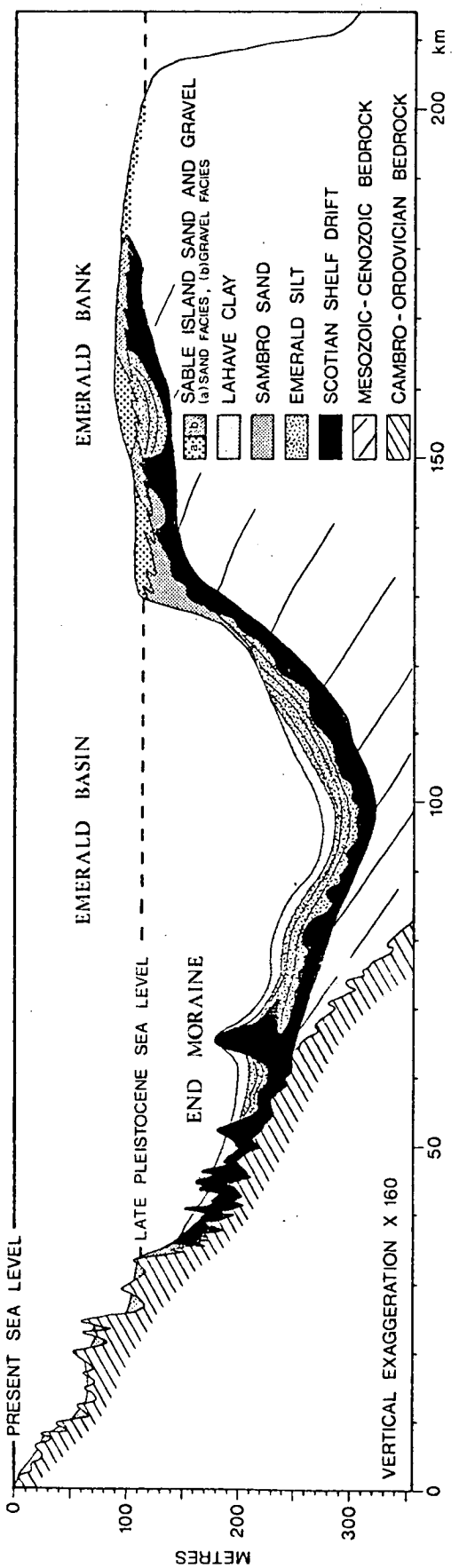

Fig. 2.1.1 Diagrammatic section of the Scotian Shelf surficial succession across Emerald Basin and Emerald Bank (King, 1980).

Table 2.1.1

Table of Quaternary Formations

Age	Formation	Lithostratigraphy	Thickness	Seismostratigraphy
HOLOCENE	LaHave Clay	Greyish brown, soft, silty clay grading to clayey silt, confined mainly to basins and depressions of shelf. Derived by winnowing of glacial sediments on banks and transported to basins. Time equivalent of Sable Island Sand and Gravel and Sambro Sand on banks	0-70 m	Generally transparent without reflections. Some weak continuous coherent reflections in base of section becoming stronger in nearshore sandy facies
	Sable Island Sand & Gravel	Fine to coarse, well-sorted sand grading to sub-rounded to rounded gravels. Unconformably overlies Emerald Silt and Scotian Shelf Drift, and derived from these deposits through reworking during Holocene transgression above 120 m present depth. Time equivalent of LaHave Clay in basins	0-50 m, generally veneer	Highly reflective seabed. Generally closely spaced continuous coherent reflections if deposit is of sufficient thickness to resolve
	Sambro Sand	Silty sand grading locally to gravelly sand and well-sorted sand. Deposited sublittorally with respect to the Pleistocene shoreline below 120 m present depth. Time equivalent to basal LaHave Clay and upper Emerald Silt, facies A.	0-20 m, generally veneer	Similar to Sable Island Sand and Gravel
PLEISTOCENE	Emerald Silt, facies C	Not well sampled	0-100 m	Discontinuous coherent reflections; transitional between facies A and glacial till
	Emerald Silt, facies B	Dark greyish brown, poorly sorted clayey and sandy silt with some gravel. Poorly developed rhythmic banding; proglacial in origin	0-40 m	Medium to low amplitude continuous coherent reflections, and to some degree a ponded sedimentational-style
	Emerald Silt, facies A	Dark greyish brown, poorly sorted clayey and sandy silt, some gravel. Well developed rhythmic banding; subglacial in origin. Time equivalent to Scotian Shelf Drift	0-100 m	High amplitude continuous coherent reflections, highly conformable to substrate irregularities
	Scotian Shelf Drift	Very dark greyish brown, cohesive glacial till comprised of poorly sorted sandy clay and silt with variable gravel	0-100 m	Incoherent reflections, sometimes with scattered point source reflections

than 0.3 m thickness unconformably overlying deposits of Emerald Silt and Scotian Shelf Drift. In these cases it is not resolved on the seismic profiles but, nevertheless, is a distinct formation as indicated by bottom sampling, and is continuous over large areas of the seabed. In many areas on the outer banks it increases in thickness to 50 m or more. By definition it is restricted to areas of seabed above the level of the lowest Late Pleistocene sea level stand (120 m) and continues upward to the present shoreline. The thickest deposits occur in relict offshore bars, sand ridges and sand wave fields. The formation is basal transgressive in origin and comprised of well-sorted and well-rounded particles of sand and gravel, mainly derived from the erosion of former glacial deposits on the banks and reworked in a high energy zone of the transgressing sea. It is divided into two facies on the basis of textural difference: (a) sand greater than 50% and (b) gravel greater than 50%. The upper part of the formation is currently being reworked.

(b) Geological History

The environmental history of the Scotian Shelf over the past 70,000 years (King and Fader, 1985) began with the advance of a thick continental ice sheet which probably extended to the shelf edge and most likely was responsible for extensive glacial erosion. A general recession of the ice began to occur at approximately 50,000 years BP which led to the development of an extensive floating ice shelf, pinned by contact with the seabed in the shallow bank areas. This stage dominated and gradually diminished over a period of approximately 34,000 years or to approximately 16,000 years BP. During this stage the glacial till (Scotian Shelf Drift) and glaciomarine sediments (Emerald Silt) were laid down as subglacial deposits.

The period between 16,000 and 10,000 years BP covers the time of lowest sea level, its subsequent transgression, and the disappearance of ice influence in the offshore. A prominent submarine terrace was cut sometime between 15,000 and 17,000 years BP at a depth of 120 m. It occurs at the boundary between the Sambro Sand and Sable Island Sand and Gravel. The terrace indicates the beginning of the Late Wisconsinan-Holocene transgression during which time Wisconsinan-Holocene

unconformity was cut, and the glacial sediments between the old and present shoreline were modified in respose to a high energy beach environment. As the transgression progressed across the outer banks it produced large areas of clean, well-sorted sands and gravels (Sable Island Sand and Gravel Formation) and the winnowed fines were deposited in the basins as LaHave Clay.

Subsequent developments during the Holocene and to the present include the reworking of the sand deposits on the outer shelf to form various bedforms including offshore bars, sand ridges, sand ribbons, sand waves and megaripples. They represent areas of present or past instability of the seabed.

2.2 Site Interpretation

Geological interpretation of the 1-km^2 sites at Olympia and Venture is based on detailed bathymetry, bottom sample, sidescan sonar (500 KHz) and high resolution seismic data. These data were collected on several different cruises during the field operation. The collection procedures and survey control are discussed under Sections 1.3 and 3.0 of this report. Bathymetric charts (Drawings 1 and 4) were prepared for each site and a detailed sidescan mosaic (Drawing 2) was compiled for the Olympia Site. Sediment properties, distribution of bedforms and other seabed features, and the seismostratigraphy were compiled on Drawings 3 and 5 and referred to as features charts. Sidescan data were collected at Venture but were not mosaiced since no distinct features were present in the charts.

2.2.1 Olympia Site

(a) Bathymetry

The bathymetry of the Olympia Site (Drawing 1) is shown at a scale of 1:2500 with a 0.5 m contour interval, and is based on 17 east-west oriented survey lines with a spacing of 50 to 100 m. The general water depths range from 33.0 to 36.5 m following a gentle gradient to the north. The contours are generally regular, conforming to the regional east-west trending contours of the shelf between the north shore of Sable Island and the Upper Gully, (Fig. 2.2.1) and they only deviate

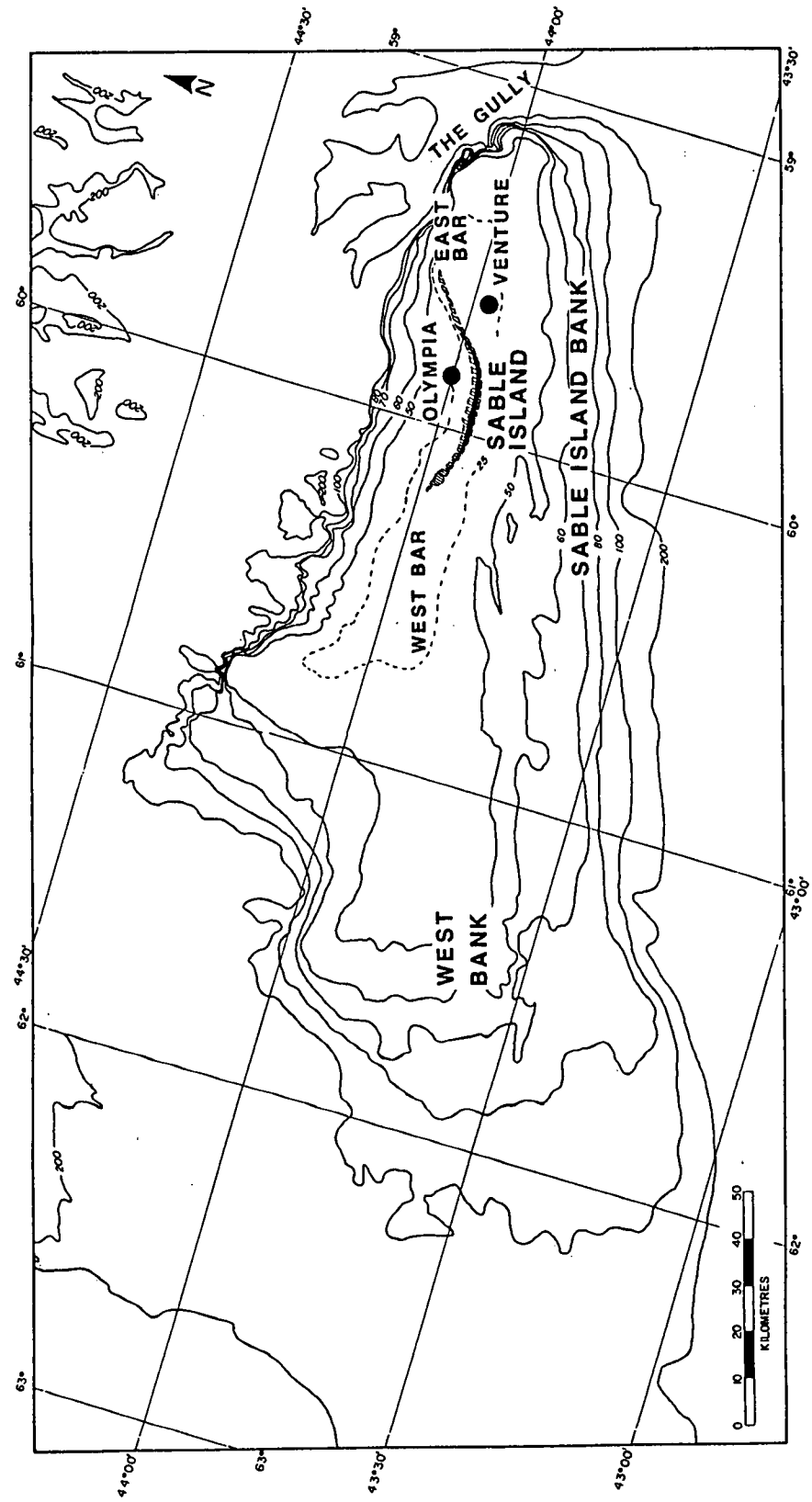

Fig. 2.2.1 Regional bathymetry around Sable Island Bank.

slightly around areas of local relief of approximately 0.5 m. The area showing greatest variation occurs in the southeast corner of the site where major bedforms appear to be best organized. A terrace of 175 to 250 m width cuts across the central portion of the site and is defined by the 34.0 and 34.5 m contours.

(b) Seabed Geology

The seabed sediment is comprised of the Sable Island Sand and Gravel Formation, sand facies, which at times contain a minor gravel component controlled by the distribution of bedforms. Sediment properties from a suite of 28 grab samples (Appendix 8.1) are shown on the features chart for the Olympia Site (Drawing 3) (references are indicated on the diagram) for comparison with the distribution of seabed features and bedforms interpreted from the sidescan mosaic (Drawing 2). On the basis of median diameter the samples fall into two categories, 0.30-0.45 mm and 0.40-0.75 mm; that is medium sand and medium to coarse sand. The latter generally have a small gravel component which is also indicated on the diagram. There is a direct correlation between these categories and the areas of light and dark tonal quality of the mosaic. The areas of light tonal quality are outlined on the features chart and designated as "B" and the dark patches as "A". Areas B are characterized by moderate to well-sorted, medium sand, generally with a fine silt fraction of 1 to 3% and a negligible gravel fraction. One exception, sample 26 shows a gravel fraction of 5.7% and may result from a positional error or the inclusion of a large gravel fragment. Areas A are characterized by moderate to well-sorted, medium to coarse sand with a fine fraction generally below 0.5%. The coarse fraction represents the dominant aspect of this category. This includes a well developed gravel fraction up to a maximum of 1.6% and a prominent coarse sand fraction.

The gravelly sand patches (A) of Drawing 2 (areas of dark tonal quality on the mosaic) vary widely in shape, size and distribution. For the most part, the patches are highly irregular and vary in size from 10 m diameter to large areas up to 500 m length. Some are elongate in shape with a general northeast-southwest trend and their trend axes are

indicated on the features diagram. These oriented patches are most common in the southeast quadrant of the Olympia Site. Some of the trends are comprised of discontinuous patches. These trends are thought to represent the troughs of major bedforms and will be discussed later. On the eastern half of the site approximately 15 to 20% of the seabed is covered by the gravel patches, whereas on the western half 70 to 80% is comprised of gravel patches. Trends are less evident on the western half.

The gravel patches are always associated with the occurrence of wave ripples which are illustrated in the mosaic (Drawing 2) and in Fig. 2.2.2 which shows their appearance in detail. The ripples have a uniform orientation across the entire site with their crests trending northwest-southeast. Their wavelengths are 1 to 1.5 m, characteristic of ripples in gravel and coarse sand. They sometines grade into the adjacent sand areas as illustrated in Fig. 2.2.2. Wave ripples of this magnitude are storm related. Both the wave ripples and the gravel and coarse sand occurrences contribute to high acoustic backscatter which provides the dark tonal quality of the sidescan sonograms.

The gravel patches are always depressed 0.5 to 1 m below the adjacent sand areas as illustrated in Fig. 2.2.2 and suggests they are related to bedform activity. As mentioned earlier some of the gravel patches have a distinct orientation, especially in the southeast quadrant of the site and this also suggests bedform related activity. The best defined trends have a wavelength of 100 to 150 m which according to the classification of Amos and King (1984) would place them in the category of sand waves. Although they do not have all the attributes of sand waves, especially because of their low amplitude of 0.5 to 1.0 m, they are best considered as low amplitude sand waves for the present time. Additional evidence for a sand wave interpretation comes from the occurrence of megaripple development on the sand waves. Their distribution is indicated on the features chart, and their crest line orientation is similar to that of the sand waves. They are illustrated in Fig. 2.2.3 and appear to be degraded in nature. Hummocky megaripples are also common over much of the seabed in the sand areas and they are illustrated in Fig. 2.2.2.

Fig. 2.2.2

Cruise - #1 M.V. Arctic Prowler 22-28 September 1984

Fix - 20 to 24, Line 0-2

Water Depth - 33 m

The area of dark tonal quality which defines the trough represents gravel and coarse sand with superimposed wave ripples (A). The areas of light tonal quality represent a seabed comprised of sand forming sand waves which have heights of 0.5 to 1 m and wavelengths of 100 to 150 m. Their axes trend northeast-southwest. Hummocky megaripples (B) give the seabed a mottled appearance. The wave ripples (A) have wavelengths of 1 to 1.5 m and their crests trend northwest-southeast. The wave ripples sometimes extend into the peripheral area of sand and decrease in wavelength. See Drawing 2 for location.

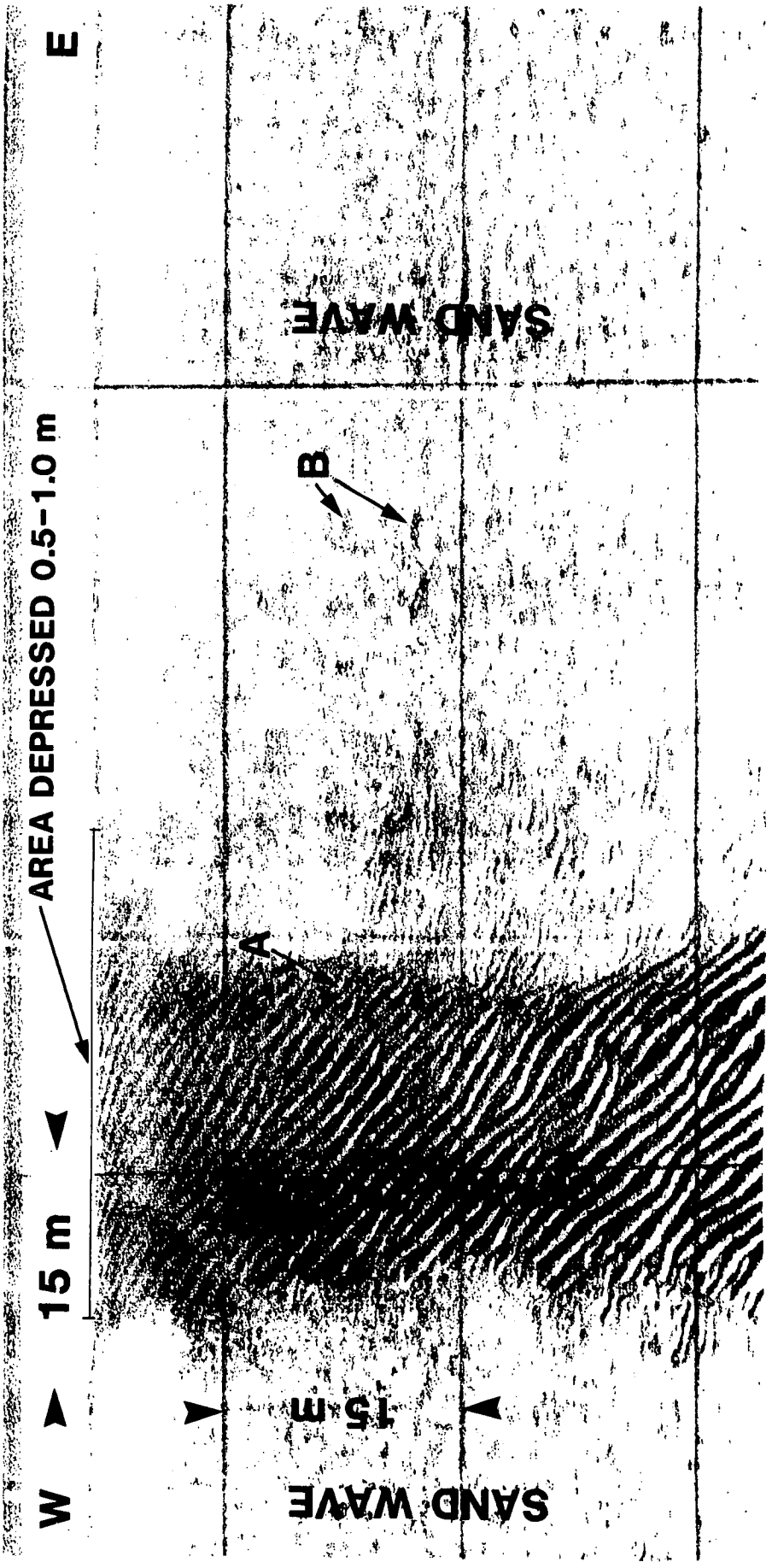

Fig. 2.2.2 Sidescan sonogram (500 KHz) near Olympia dump site showing the flanks of low amplitude sand waves separated by a shallow gravel trough.

Fig. 2.2.3

Cruise - #1 M.V Arctic Prowler 22-28 September 1984

Fix - 45 to 50, Line 0-6

Water Depth - 34 m

Sidescan sonogram of degraded megaripples (A) and wave ripples (B) near the Olympia dump site. The areas of light tonal quality are comprised of sand and the dark areas are gravel and coarse sand. The wave ripples (B) are developed in the gravel areas and have a wavelength of 1 to 1.5 m. The gravel occupies a shallow trough between low amplitude sand waves. The megaripples (A) are developed on the sand waves, have a wave length of 2 to 5 m, and their crests are oriented northeast-southwest. See Drawing 2 for location.

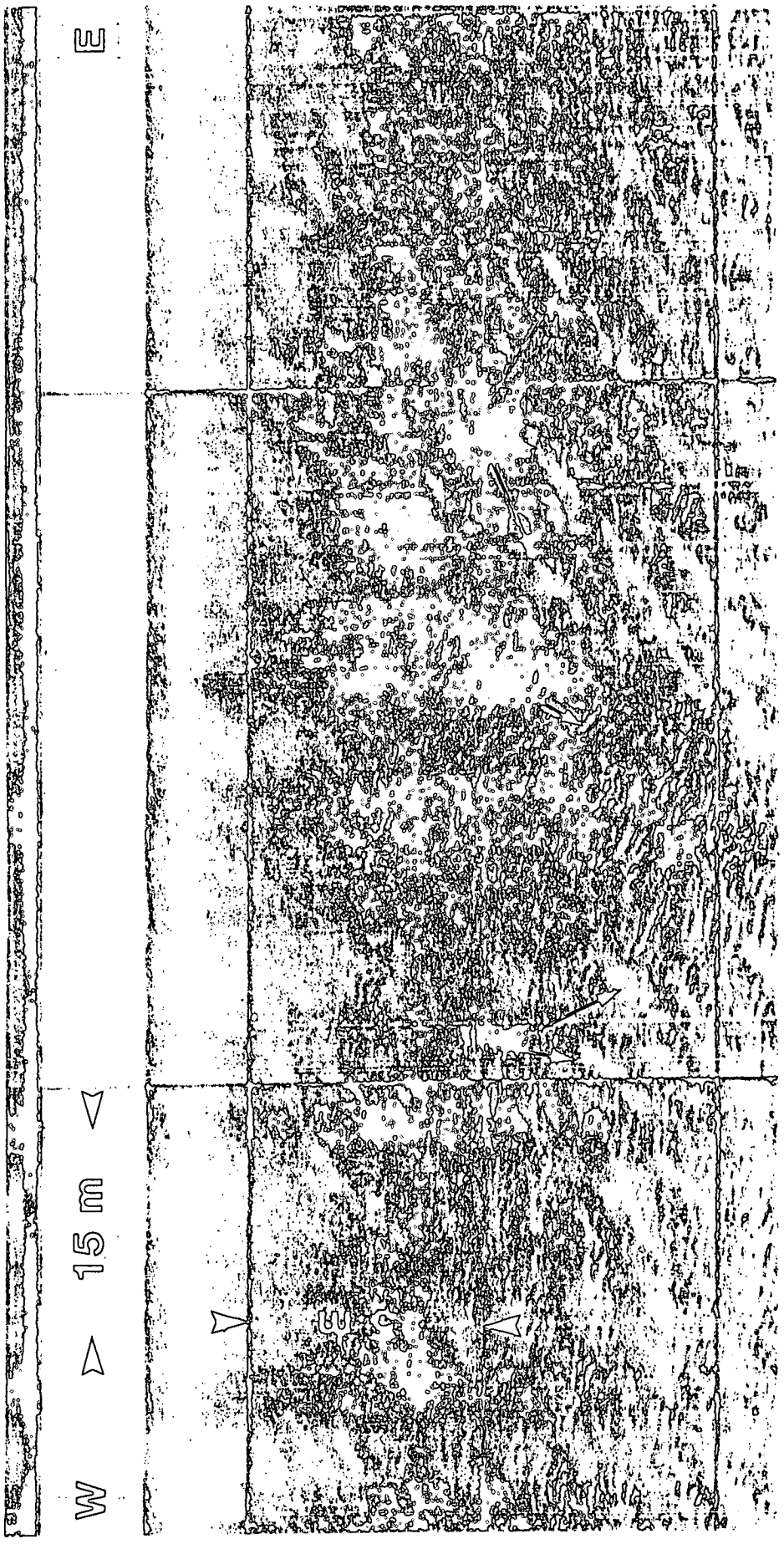

Fig. 2.2.3 Sidescan sonogram of degraded megaripples (A) and wave ripples (B) near the Olympia dump site.

Description of the seabed is further enhanced by two bottom photographs (Fig. 2.2.4). Photo (a) shows a sand seabed with a fine gravel component and was taken in a sand area (A) but close to a contact with a gravel patch. Several sand dollars, some partly buried, as well as a starfish are present in the photograph. Photo (b) is similar in appearance except that the sand is slightly finer in texture.

(c) Subsurface Geology

From regional considerations, the lowest reflection in the interpreted seismic profile (Drawing 3) represents the Winconsinan-Holocene unconformity formed by a transgressing sea following glaciation. Sable Island Sand and Gravel overlies the unconformity and has a thickness of 5 to 7 m. Several reflections occur within the section.

(d) Bedform Activity

The degraded nature of the bedforms recognized in the Olympia Site indicate an origin dominated by episodic events probably generated during major winter storms. Both the low amplitude sand waves and the superimposed degraded megaripples have similar orientations and may be activated by the west to east bottom currents.

2.2.2 Venture Site

(a) Bathymetry

The bathymetry of the Venture Site (Drawing 4) is presented at a scale of 1:2500 with a contour interval of 0.5 m, and is based on one north-south and 20 east-west survey lines spaced at approximately 50 to 75 m. The general water depths range from 28 to 32 m increasing in a southeast direction. The contours across the northern portion of the site define a gentle ridge striking to the east, and a shallow trough of similar orientation plunging gently to the east across the central portion of the site. The regional bathymetric configuration is comprised of a series of north-south parallel ridges and troughs plunging to the south off the shoreface of East Bar. The Venture Site is located on the eastern flank of one of these ridges referred to as a shoreface-connected sand ridge. The site bathymetry is an expression of local variations on the larger feature.

Photo - (a) 44°00.46'N 59°51.93W

Cruise - #1 M.V. Arctic Prowler 22-28 September 1984

Camera Station 8, Photo 3

Water Depth - 35 m

The bottom photograph shows a sand seabed with a fine gravel component taken close to a contact with a gravel patch. Several sand dollars, some partly buried, as well as a starfish are present in the photograph. See Drawing 2 for location.

Photo - (b) 44°00.39'N 59°51.79'W

Cruise - #1 M.V. Arctic Prowler 22-28 September 1984

Camera Station 8, Photo 2

Water Depth - 34.5 m

The bottom photograph shows a sand seabed with scattered shell fragments, several sand dollars and a starfish. See Drawing 2 for location.

(a)

(b)

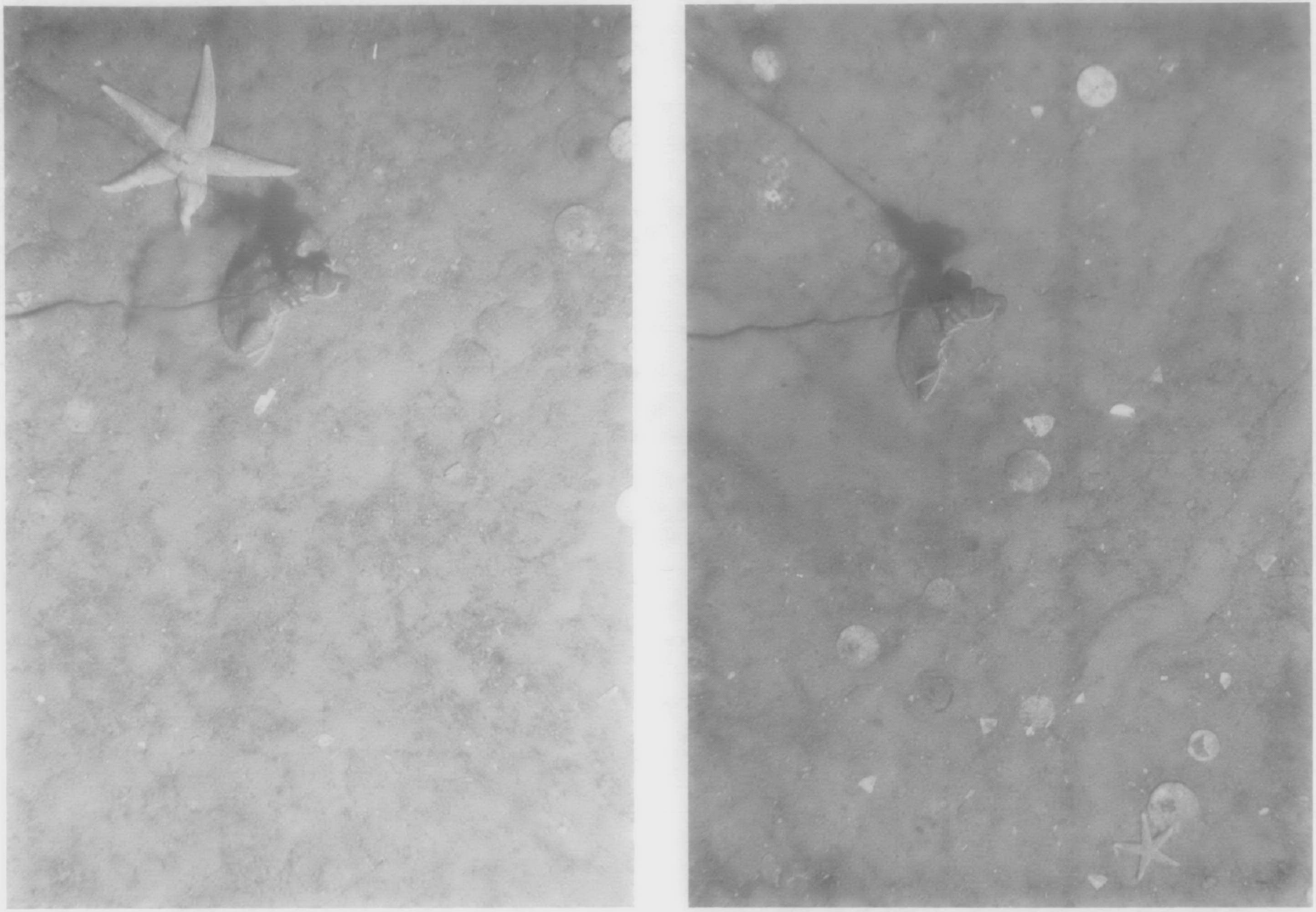

Fig. 2.2.4 Bottom photographs taken at Olympia site.

(b) Seabed Geology

The seabed geology is comprised of the Sable Island Sand and Gravel Formation, sand facies. Sediment properties from a suite of 32 samples are shown on the Venture features chart (Drawing 5) (references are indicated on diagram) for comparison with the distribution of bedforms interpreted from sidescan sonar records. All samples, with the exception of Sample 19 from the northeast corner of the site, show a uniform, well-sorted texture within the fine sand range with median diameters ranging from 0.17 to 0.20 mm and a silt tail of about 1%. Sample 19 is a coarse to very coarse sand (1.0 mm median diameter) with a gravel fraction of 7.9%. The sample is located 25 m to the west of the leading edge of the sand ridge; however, this may be in error because it appears to be more representative of the gravel area to the east of the leading edge. It is also possible that the sampler penetrated to the lag layer underlying the leading edge of sand.

The Venture Site is characterized by the occurrence of one major bedform: a shoreface-connected sand ridge (Amos and King, 1984) with its trough at the northeast corner of the site and its crest approximately 1 km to the west of the site. Thus, the greater part of the site is located on the eastern flank of this major bedform. From regional considerations, the sand ridge has a north-south axial trend, is approximately 7 m in height, and has a wavelength of 2500 m. The leading edge of the sand ridge is illustrated in Fig. 2.2.5. Wave ripples also occur within the site and are confined to the gravel area along the trough of the sand ridge (Fig. 2.2.5).

Small, shallow depressions of approximately 0.5 to 1.0 m diameter are common on the seabed of the Venture Site. They are illustrated in Fig. 2.2.6 and have a density of occurrence of approximately 0.05 to 0.07/m^2. Their origin is uncertain, but they may represent shallow burrows formed by skate resting on the seabed (C. Amos, GSC, pers. comm, 1985). The seabed description is further enhanced by two bottom photographs (Fig. 2.2.7). Both photos show a medium sand seabed with some long crested low amplitude ripples present. The occassional sand dollar is present in the

Figure - 2.2.5

Cruise - #1, M.V. Arctic Prowler 22-28 September 1984

Fix - 100 to 110, Line V-20

Water Depth - 29 to 30 m

Sidescan sonogram (500 KHz) near Venture dump site showing the leading edge (A) of a shoreface-connected sand ridge (light tonal quality) migrating to the east across an exposed lag layer of gravel and shells (dark tonal quality) in its associated trough. (See geological section in Drawing 5). (B) indicates unknown seabed features which are shallow elongate depressions oriented normal to the leading edge. (C) indicates wave ripples of 1.0 to 1.5 m wavelength that occur on the gravel seabed. See Drawing 5 for location.

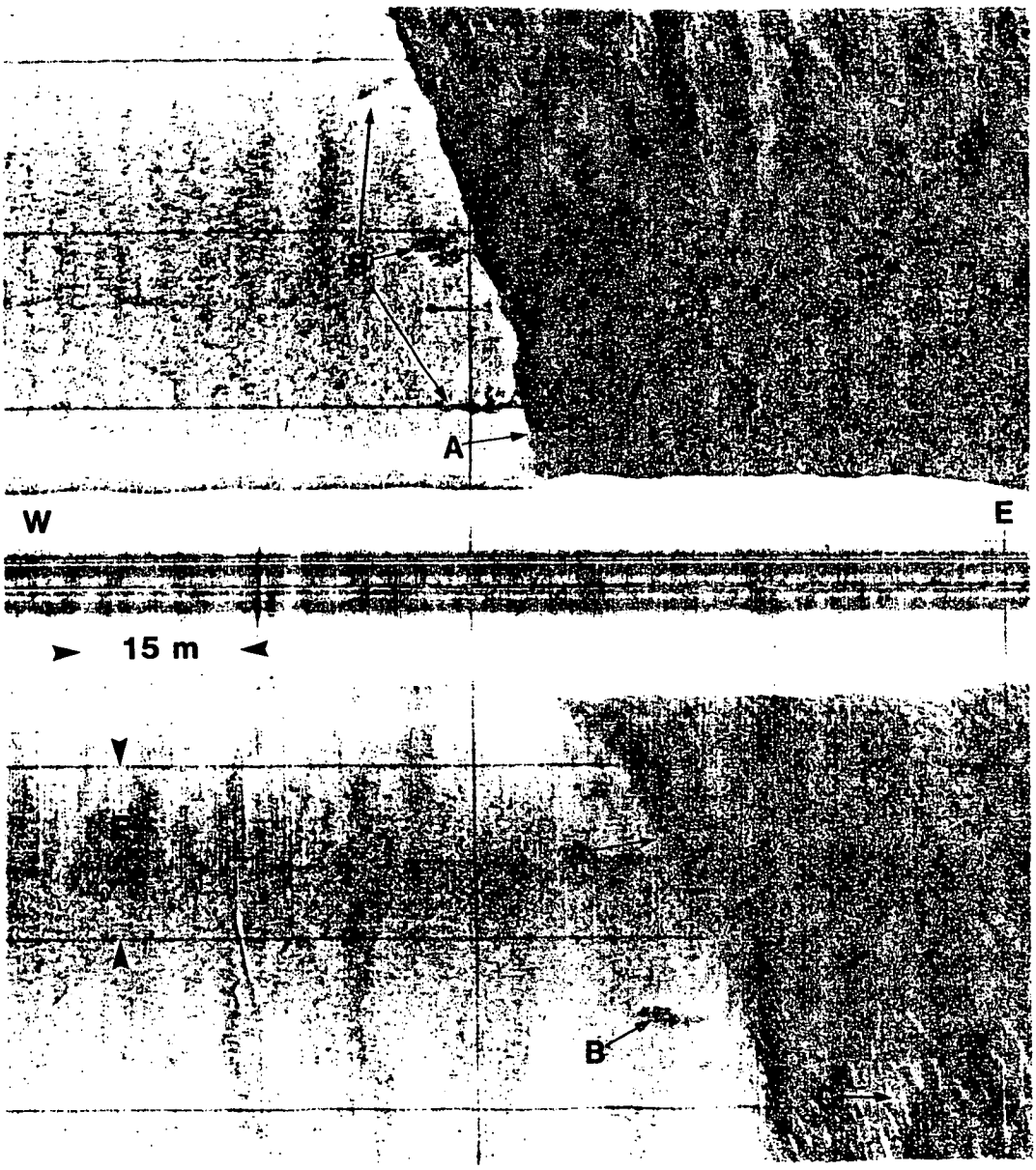

Fig. 2.2.5 Sidescan sonogram (500 KHz) near Venture dump site showing the leading edge (A) of a shoreface-connected sand ridge.

Figure - 2.2.6

Cruise - #1 M.V. Arctic Prowler 22-28 September 1984

Fix - 105 to 110, Line V-17

Water Depth - 28 m

Sidescan sonogram (500 KHz) of a sand seabed on the eastern flank of a sand ridge near the Venture dump site. Numerous small depressions (A) of 0.5 to 1 m diameter are randomly dispersed across the entire 1-km^2 site. They occur at a density of 0.05 to 0.07/m^2. It has been suggested that they represent shallow burrows formed by skate resting on the seabed (Amos, pers. comm.). See Drawing 5 for location.

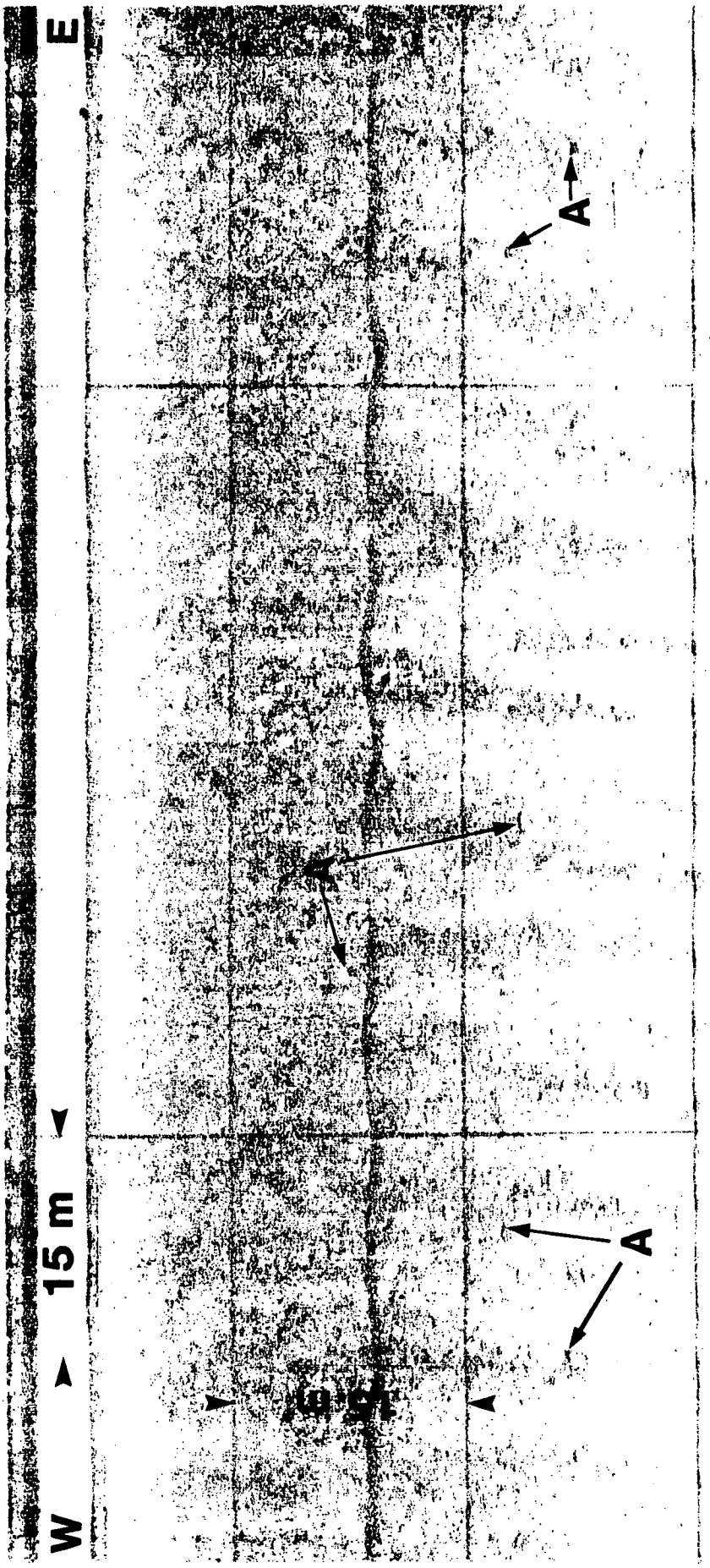

Fig. 2.2.6 Sidescan sonogram (500 KHz) of a sand seabed on the eastern flank of a sand ridge near the Venture dump site.

Photo (a) 45°56.30'N 59°39.51'W
Cruise: #1 M.V. Arctic Prowler
Camera Station 14, photo 14
Water Depth 30 m

Photo (b) 43°56.30'N 59°39.79'N
Cruise: #1 M.V. Arctic Prowler
Camera Station 11, photo 14
Water Depth 30 m

(b)

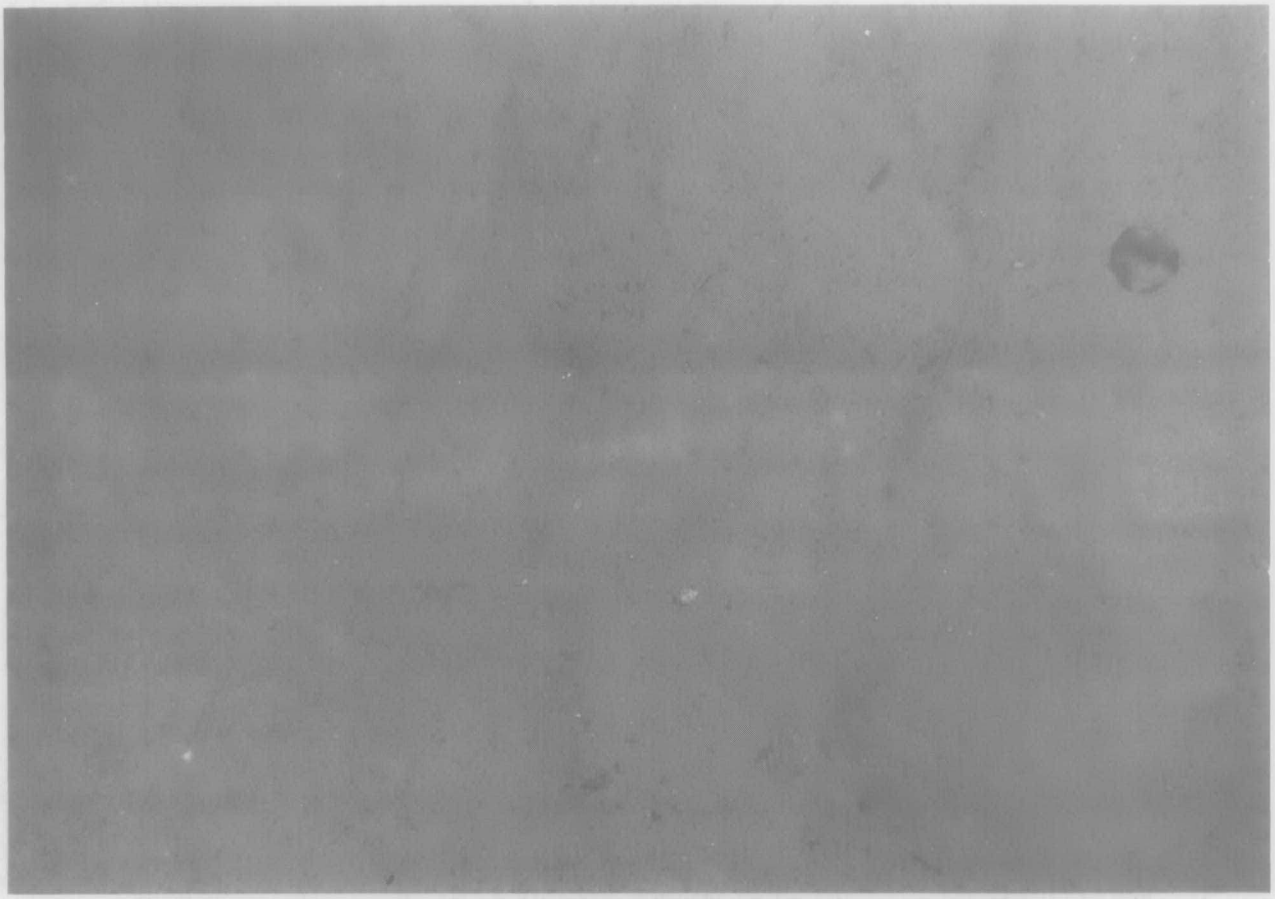

(a)

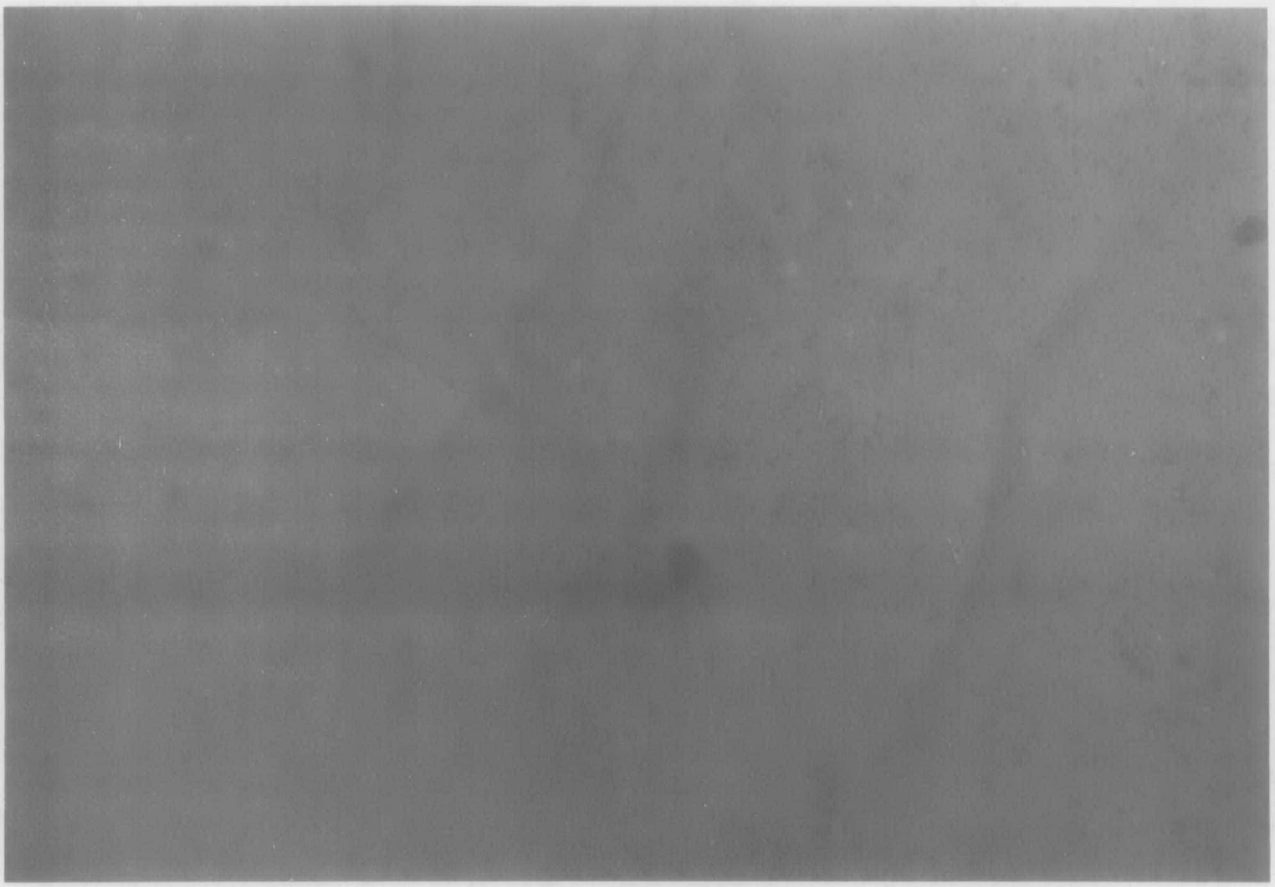

Fig. 2.2.7 Bottom photographs taken at Venture site.

photograph.

(c) Subsurface Geology

An interpreted seismic profile is shown in Drawing 5. From a regional knowledge of the area the Wisconsinan-Holocene unconformity forms the base of the Sable Island Sand and Gravel Formation. A lag layer which constitutes the base of the sand ridge occurs 7 m below the seabed along much of the section but crops out and defines the seabed near the eastern end of the section.

(d) Bedform Activity

According to Amos and King (1984) a sand ridge is a composite, flow parallel, linear accumulation of sand of measurable relief, formed by the superposition and migration of sand waves or megaripple fields. They are underlain by a lag layer which crops out for short distances in the trough areas between ridges (Geological section, Drawing 5). The lag layer is identified at the seabed by its dark tonal quality on sidescan sonograms (Fig. 2.2.5) and is comprised of gravel and shells with superimposed wave ripples. Their model (Amos and King, 1984) suggests that the leading edge of the sand ridge migrates easterly across the lag layer. Erosion cuts into the lag and lowers its surface while the winnowed sands are transported to the depositional areas of the ridge. As the ridge system migrates over the long term, each successive passage of a trough lowers the lag still further. The thickness of the sand above the lag approximately constitutes the thickness of the long term mobile layer.

Although the migration rate is not known, the excellent state of preservation of the leading edge suggests that the rate is at least measureable in terms of metres per year. Sediment transport is also difficult to assess across the surface of the sand ridge because there are no bedforms such as sand waves and megaripples to indicate the nature of the activity. It may be that the interaction of currents and waves inhibits the formation of such bedforms even though the degree of sediment transport could be quite large.

2.3 Physical Oceanography

Sediment transport in the study area will be dominated by combined wave-current conditions. This section presents an overview of known characteristics of the current and wave climates to the north and to the south of Sable Island.

2.3.1 Current Regimes

Olympia

Currents near the seabed in this region are comprised of tidal and non-tidal flows. The latter are associated with currents generated by weather systems moving over the Eastern seaboard, changes in seawater density, and to a small extent, by meanders of Gulf Stream water over the Scotian Shelf. Near Olympia these processes appear to be dominated by surge currents produced by meteorological forcing, although these show generally low coherence with local wind measured on Sable Island, and by tides. The tidal component is comparatively weak with speeds of 10 to 15 cm/s.

Non-tidal flows range up to 25 to 30 cm/s, two to three times larger than the tides, with a predominantly eastward orientation consistent with bedforms. Background currents are very weak, with speeds ranging from 4 to 8 cm/s. Maximum combined current speeds range up to 40 to 45 cm/s in a west to east direction.

Venture

As at Olympia, Venture currents are dominated by tides, and non-tidal flows linked to meteorological forcing. A sample of the total current at Venture, measured during this study, is shown in Fig. 2.3.1. For comparison the tidal portion of the flow is isolated in Fig. 2.3.2 together with the non-tidal component. All of these time-series exclude wave-induced currents and represent the low-frequency variations in the flow field.

These plots show that total currents range up to 30 to 32 cm/s, comprised of astronomical tides ranging from 20 to 25 cm/s, and residual flows of about 15 to 20 cm/s maximum. Spectra of the total and non-tidal currents (Fig. 2.3.3) show the strong contribution of both the duirnal

SITE NAME: VENTURE
LATITUDE: 43° 57' 22" N
LONGITUDE: 59° 40' 38" W
DEPTH: 30 m
METER ID: 621/1
DELTA T: 180 min

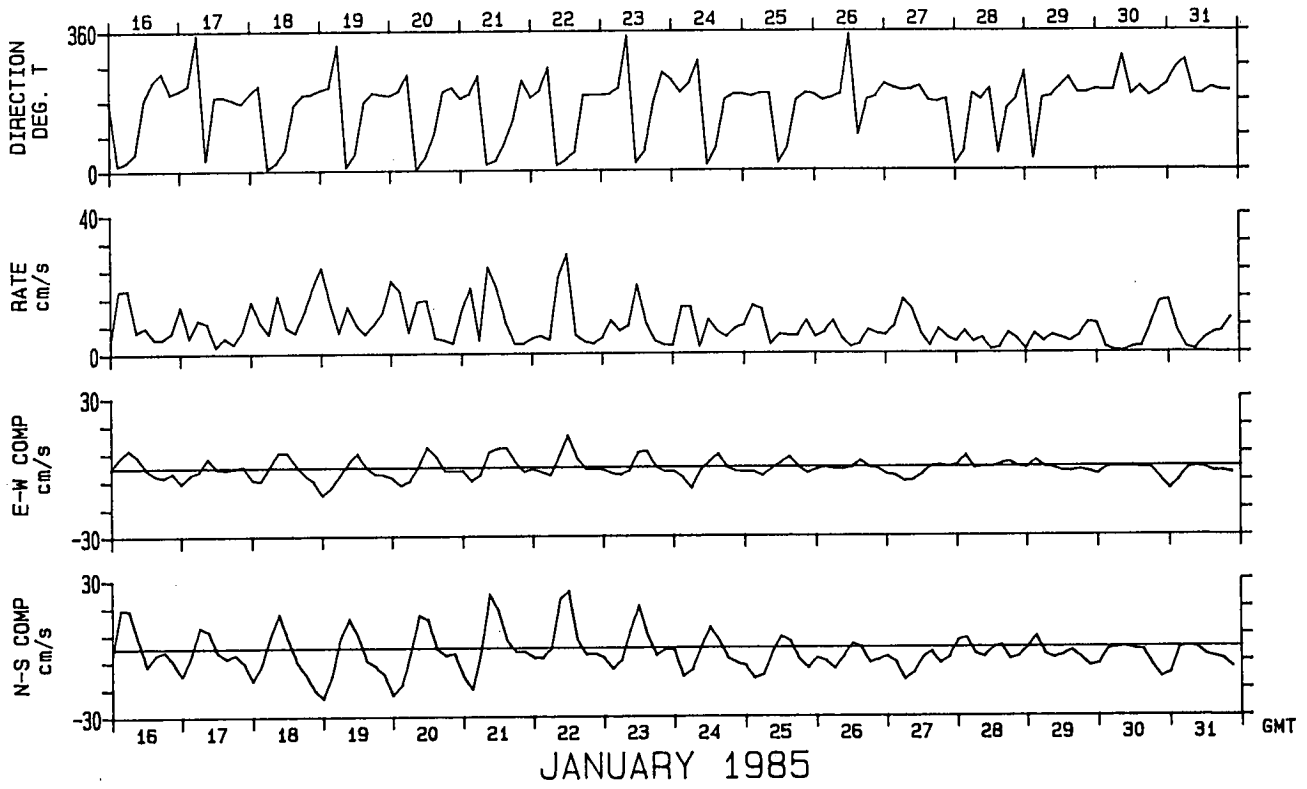

Fig. 2.3.1 Sample time-series of total measured current 50 cm off the bottom at the Venture site.

SITE NAME: VENTURE
LATITUDE: 43° 57' 22" N
LONGITUDE: 59° 40' 38" W
DEPTH: 30 m
METER ID: 621/1
DELTA T: 60 min

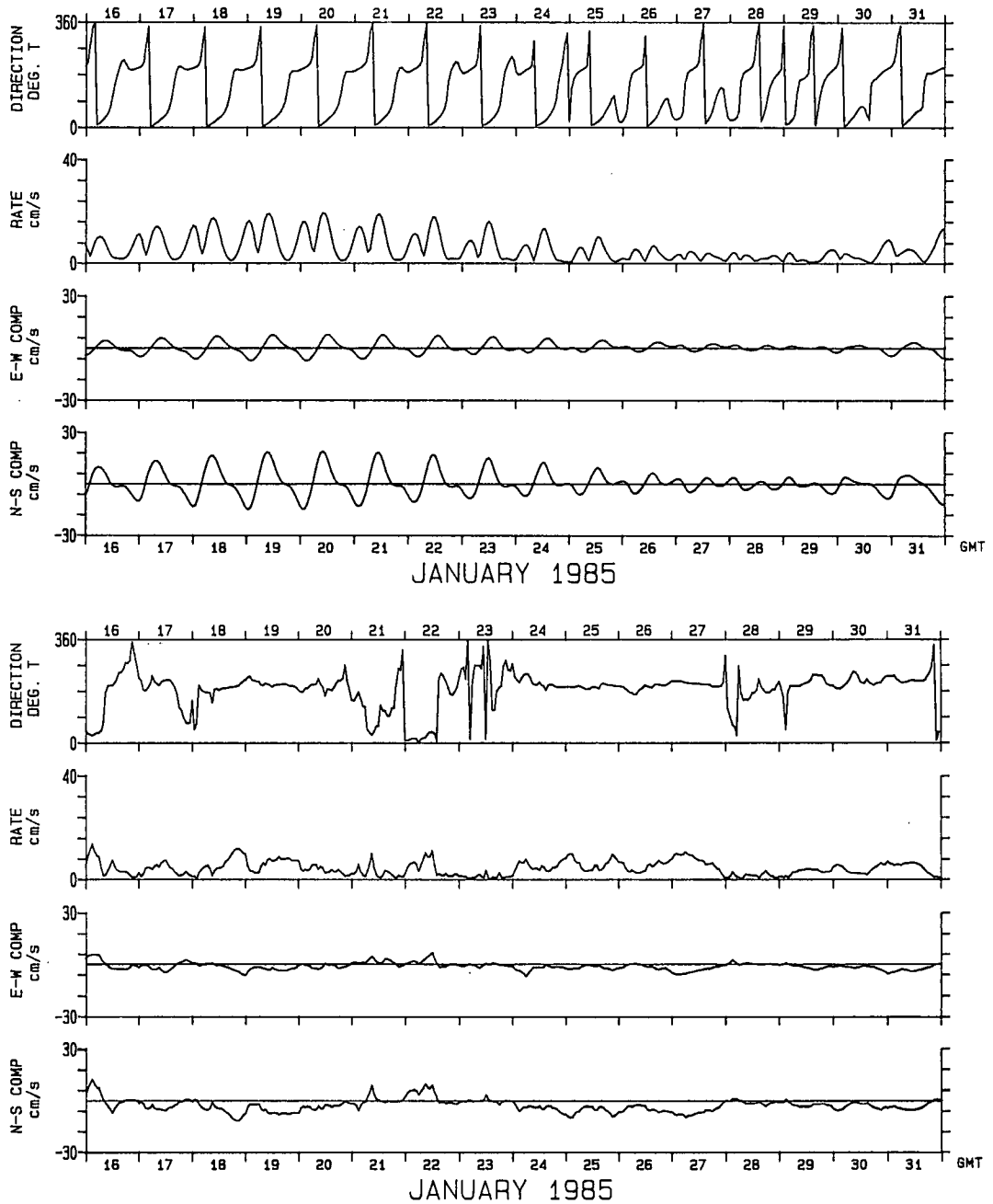

Fig. 2.3.2 Sample time-series of the tidal component of flow (upper panel) and the slowly-varying non-tidal component (lower panel) for Venture. The interval corresponds with that in Fig. 2.3.1 for total current.

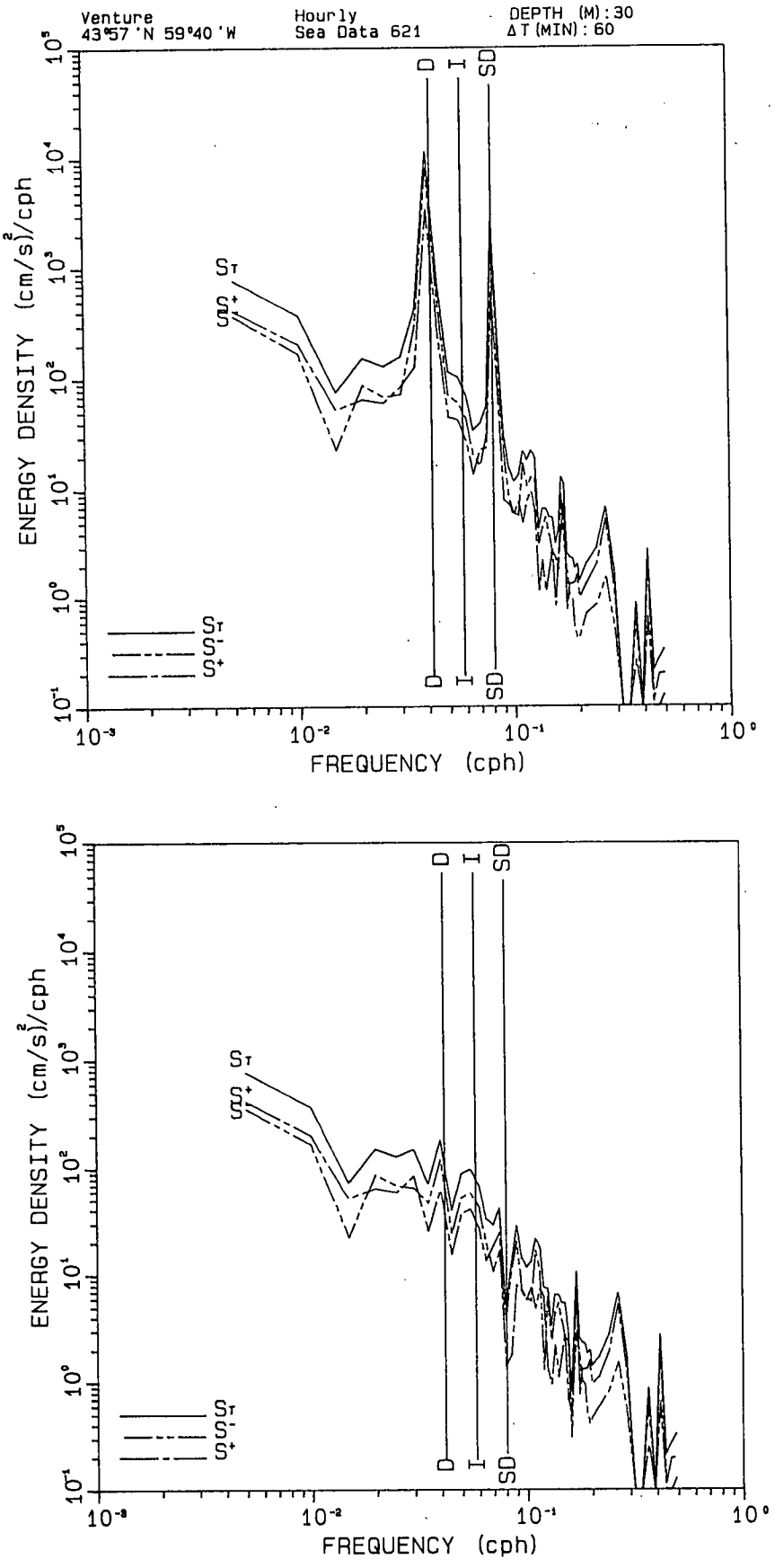

Fig. 2.3.3 Rotary spectra for total current (upper panel) and for non-tidal residual current (lower panel).

(D) and semi-duirnal (SD) tide relative to the slowly-varying non-tidal flows, and the absence of energy at the inertial frequecy (I). This latter feature indicates that the shallow shelf water response may be mainly barotropic during strong winter storm winds, but with a strong inertial response suppressed by the proximity to Sable Island.

Progressive vector diagrams for both total and non-tidal residual flows are shown in Fig. 2.3.4. These demonstrate clearly that the net circulation is SSW aligned with the sand ridges featured in this area. The inferred speed of this net motion is some 3 to 5 cm/s.

For much of the time these low frequency currents are below threshold to induce sediment motion. Therefore, it would appear that combined wave-current bottom stresses are responsible for the dispersion of sand. This is consistent with the tracer cloud observations at Venture, discussed below. To illustrate the combined flows, the burst sampled data from two storm records are plotted in Fig. 2.3.5 for the storm on January 21, 1985; these records are 6 hours apart. The mean flows corresponding to these burst records are as follows:

Record-length mean flow (cm/s)			Duration (°T)	Figure
u	v	R		
8.6	3.0	9.0	71	2.3.5 a
-2.2	-1.6	2.7	234	2.3.5 b

These values illustrate the dramatic difference between the averaged current and the magnitude of the maximum wave-induced flow speed--about a factor of 15 to 20. The two records reproduced here show waves with a strong N-S alignment corresponding with steady SSW winds during the storm.

2.3.2 Wave Climate

Wave conditions at both sites are typical of ocean areas dominated by extratropical storms having a strong seasonal dependence. The most reliable data for describing wave heights comes from composite Waverider

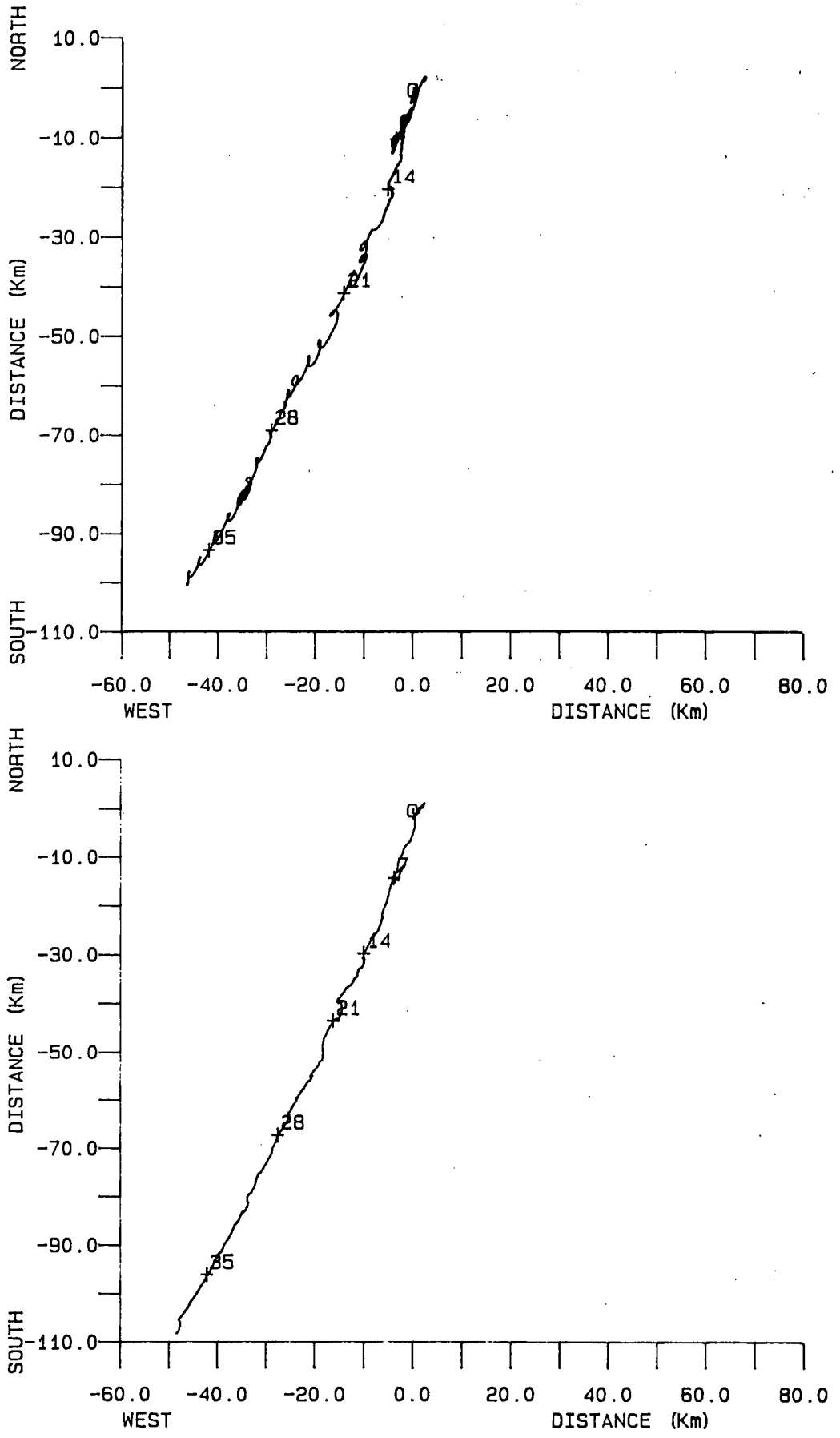

Fig. 2.3.4 Progressive vector diagrams at Venture for total current (top) and for residual current (bottom). Labels beside the PVD indicate elapsed time in days.

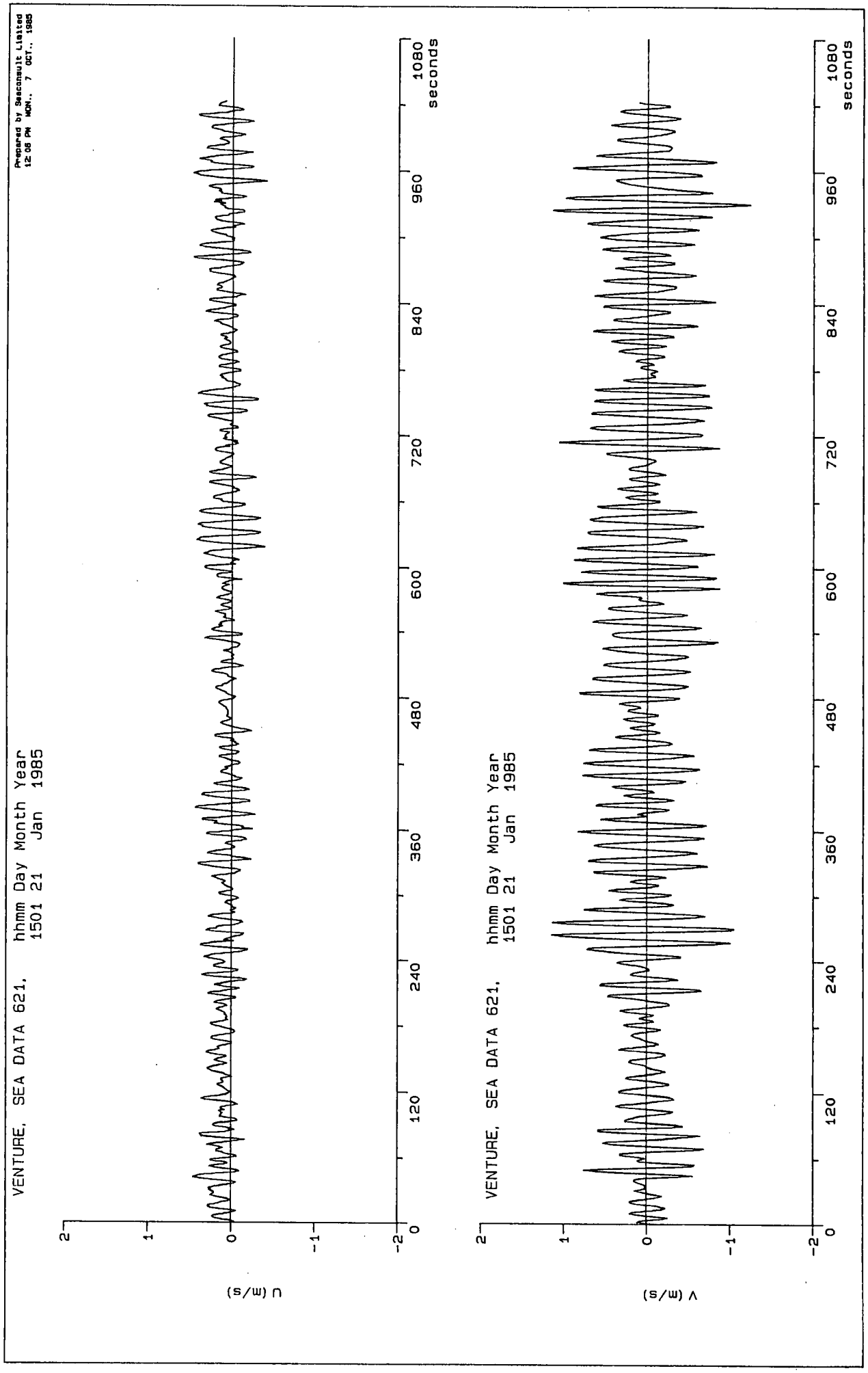

Fig. 2.3.5 (a) Sample of a burst current record at 15:01 Z, January 21, 1985 at Venture.

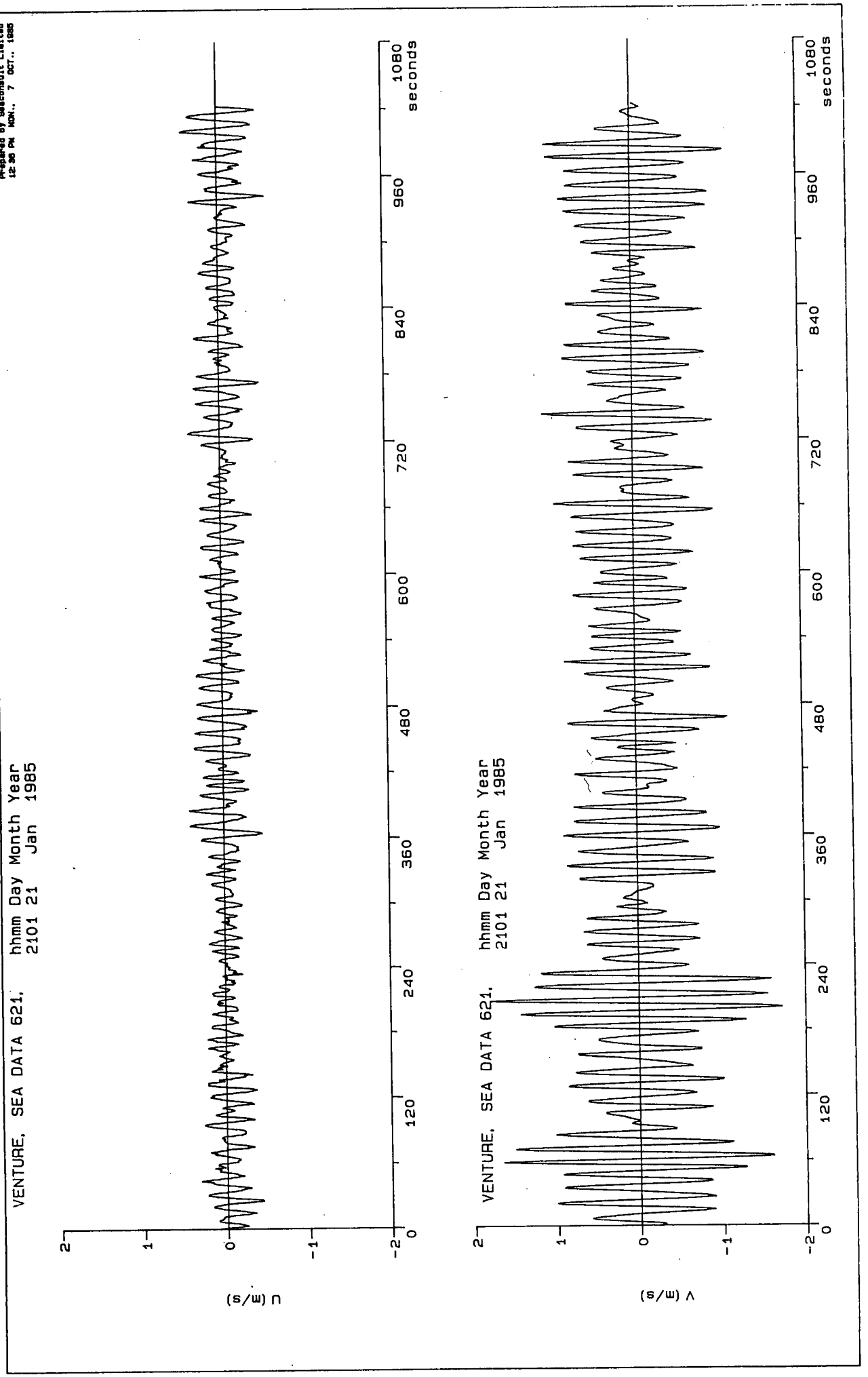

Fig. 2.3.5 (b) Same as (a) except that the time is 21:01 Z, January 21, 1985.

measurements collected around Sable Island since 1980. Two distributions for significant wave height are shown in Fig. 2.3.6; the first corresponding to the area south of Sable Island in 50 m of water shows that 80% of the waves are less than 3 m H_s and that 90% are less than 3.7 m. Thus the percentage of large waves (H_s>6 m) is very low (<1%) and linked directly to major storms. As a rough guideline the 1 and 5 year return wave heights predicted by this distribution are:

H_s (m)	Venture	Olympia
1-yr return	8.0	7.2
5-yr return	8.9	8.3

The distribution north of Sable Island is quite different: 80% of the heights are less than 2 m and 90% are less than 2.7 m. The occurrence of large waves, while still lower than south of the island, is appreciable reflecting the high incidence of N-NE storm winds from weather systems intensifying over Newfoundland and the Western Grand Banks in winter. Thus the 1 and 5-year return values for H_s are only slightly lower than over the Venture site.

Peak wave periods for heights ranging from 8 to 9 m vary from 10 to 14 s.

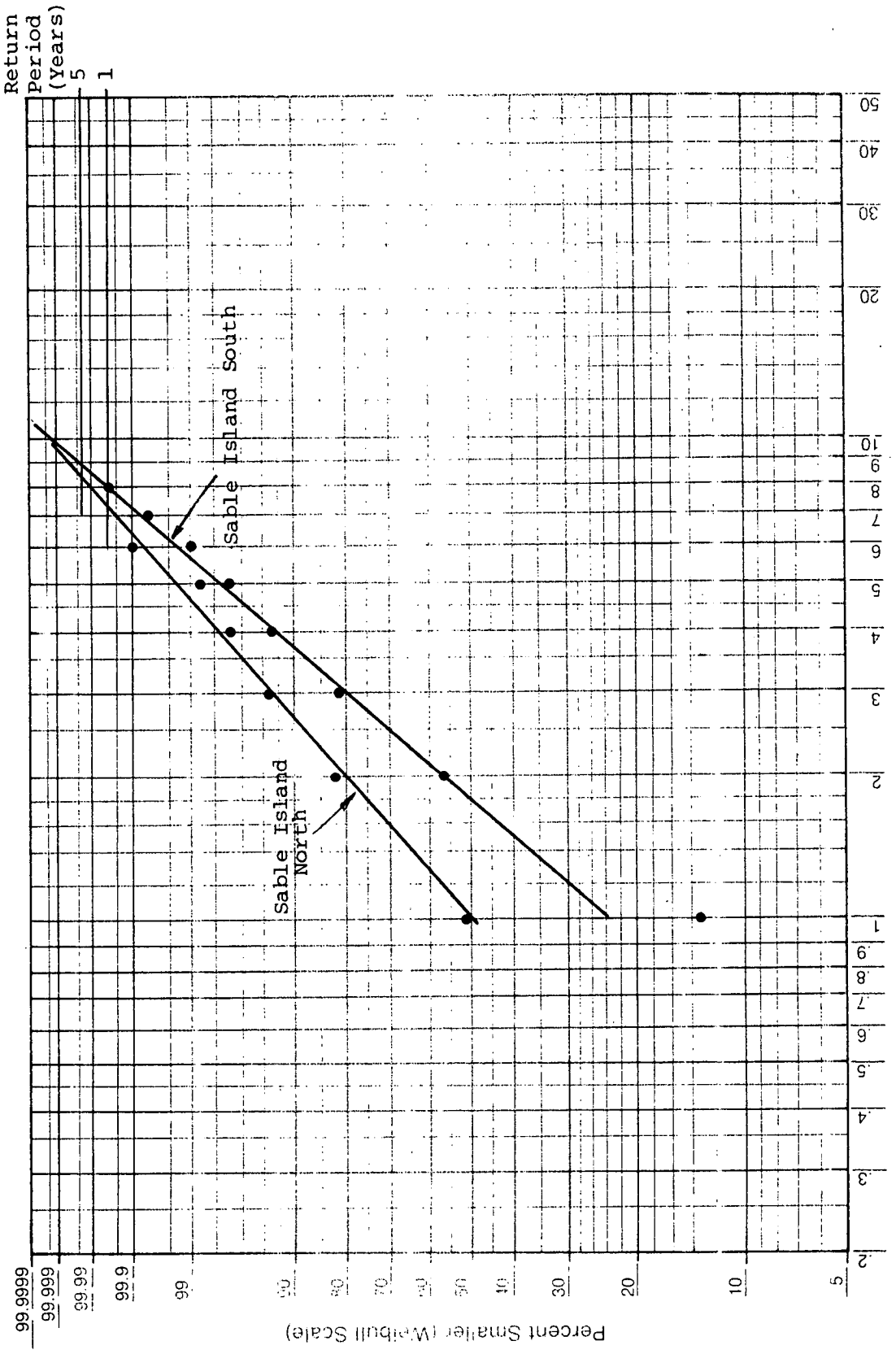

Fig. 2.3.6 Cumulative wave height distributions based on composite Waverider measurements to the south and to the north of Sable Island.

3.0 EXPERIMENTAL METHODS

3.1 Field Observations of Sand Movement Using Radioactive Tracers

(a) Introduction

Experimental methods to determine the transport of sand size sediments can be grouped under three categories:

1) The near bottom flow generated by the combined action of waves and currents is measured and coupled to sediment transport rate by means of sediment transport equations (e.g. Ackers-White (1973) formula).
2) Sensors are used to measure both the movement and concentration of sand grains (e.g. Optical Back Scatter Sensor combined with electromagnetic flow meters).
3) Sand grains are labeled, either coloured or radioactivated, so that the movement of these grains can be measured directly and used to determine the movement of the whole sediment mass.

One specific advantage of the third method is that it does not necessitate the maintenance of instruments on the study site. Measurements are limited only by the capacity to follow the tracer; it is particularly effective for long term experiments which was one of the objectives of this study on Sable Island Bank.

Inherent to the use of tracers is the problem of defining to what extent the observed movement of tracer grains is representative of the movement of the total mass of sediment within which the tracer grains have been injected. There are two premises: one is that the trajectory of the tracer grains is the same as that of the sediment in which they are injected, and the other is that the velocity of tracer is the same as the velocity of the sediment traction layer under investigation. The centroid of all tracer grains detected during a given survey is used to determine the mass velocity (V_c) of the tracer. The mass velocity of the tracer is determined by dividing the distance the tracer cloud centroid has moved between two detections by the time elapsed between these two detections. The first premise is less stringent than the second one and tracers with the same grain size and density as the parent sediment are assumed to follow similar paths. The representativeness of the movement

of the centroid of tracer grains to determine the sediment transport rate is more difficult to assess because sediment tracers are usually deposited at the water-sediment interface and their mixing within the sediment traction layer is not instantaneous. Alquier et al. (1970) have pointed out that the penetration of the tracer within the mobile sediment layer is time dependent and that the tracer concentration is not constant with depth within the sediment. The time dependence of the tracer integration within the sediment is interpreted differently depending on the type of tracer used.

Luminescent tracer experiments usually last only a few hours and are labour intensive. Duane and James (1980) point out that one man-year of effort was necessary to count 1000 separate size fractions that were collected during a two-hour experiment. These authors assumed steady state conditions and that the tracer attains an equilibrium concentration within 30 to 60 minutes after injection. Katoh et al. (1985) during experiments with luminescent tracers that lasted approximately five hours observed, however, that tracer concentrations had different distributions either increasing, decreasing or remaining constant as a function of time. Because of their short duration, luminescent tracer experiments are used to observe the movement of sediments over short distances and opinion differs on the interpretation to be given to the integration of the tracer within the mobile sediment layer.

The sediment tracer study on Sable Island Bank was planned to last several months rather than a few hours because of the generally low transport rates expected on the contenental shelf. Radioactive tracers are particularly suitable for long-term experiments like the present study where the movement of sediments results from the cumulative effect of many transport processes (Long, 1986).

The basic principle is to calculate the bedload transport rate Q using the mean velocity V_m of the mobile sediment layer of width L, usually taken as unit width, and the thickness of the mobile sediment layer E (Fig. 3.1.1). This volume rate is multiplied by the density of the

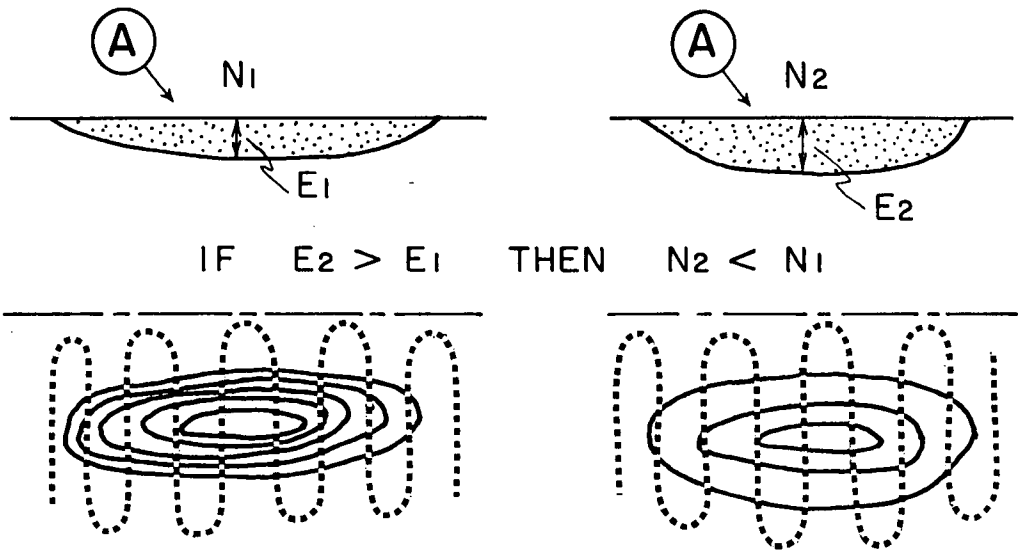

Figure 3.1.1 Tracer distribution within the mobile sediment layer. The deeper the tracer is buried the less radioactive activity, N, will be measured.

sediment (ρ_s=1.8 gr/cubic cm) to determine the transport in terms of mass per unit time per unit width, i.e.

$$Q = \rho_s \cdot V_m \cdot L \cdot E \qquad (3.1.1)$$

The unknowns are then V_m and E.

As discused above it is necessary to establish the relationship between V_c, the velocity of the centroid of tracer cloud, and the mean velocity V_m of the mobile sediment layer. The alternative, considered for this study, is to define the conditions for which V_c is equal to V_m; that condition is fulfilled when tracer grains are completely integrated into the sediment mobile layer. This is the condition "de bon melange" stipulated by Sausay (1967). The question that immediately comes to mind is how long does it take for the condition of thorough mixing of the tracer to be satisfied? Users of radioactive tracers from the Commissariat a l'Energie Atomique (A. Caillot, CEA, pers. comm., 1985) observed under stable environmental conditons that the velocity of centroid of the tracer grains diminishes during the first few days immediately following the tracer injection. Thereafter V_c tends to a constant velocity which is interpreted to be that of the mobile sediment layer with which the tracer is integrated. For the present study it implies that the thorough mixing and the identification of the tracer with the mobile sediment layer was partial at the time of the first detection, one day after injection, but was complete at the time of the second detection. Once the tracer is well mixed, it can also serve to determine the thickness of the mobile layer. Sauzay (1967) has developed a model to determine the thickness of penetration E of the tracer within the the sediment. This model is described in the next section.

(b) The Transport Equation

The first parameter to consider is the signal produced by the tracer cloud. The radioactivity level f(z) of the tagged sediment as a function of depth is measured with a scintillation probe. The probe is calibrated to conform to the penetrating power law for a point source:

$$f(z) = f_o \cdot \exp(-az) \qquad (3.1.2)$$

$$f(z) = f_o \cdot \exp(-az) \qquad (3.1.2)$$

where f_o and a are calibration constants; f_o is the probe response[1], a is the absorption coefficient for a water-sand combination, and z is the depth into the sediment. The sand tracer is not a point source and is distributed within the sediment over the seafloor. Equation (3.1.2) is then integrated from the water sediment interface (depth = 0) to a depth E corresponding to the lower limit of the sediment mobile layer.

$$N = \int_0^E f_o \cdot e^{-az} \, dz \qquad (3.1.3)$$

The count rate recorded by the probe is also a function of the tracer concentration as a function of depth, C(z), and is integrated in the equation.

$$N = \int_0^E f_o \cdot e^{-az} \cdot C(z) \, dz \qquad (3.1.4)$$

Considering first a hypothetical case where the concentration of the tracer is uniform for the whole depth E, then

$$C(z) = C_m \qquad (3.1.5)$$

The radiation count rate N is then easily determined by integrating (3.1.5) for the interval 0 to E

$$N = C_m \cdot f_o \cdot \frac{1}{a} [1-e^{-aE}] \qquad (3.1.6)$$

Knowing the initial amount of radioactivity injected A, as well as its half-life, the remaining activity A(t) at the time of a given survey can be determined. The hypothetical uniform tracer concentration C_m per unit area used in the preceeding equation can be expressed as

$$C_m = \frac{A(t)}{E} \qquad (3.1.7)$$

---

[1] (counts per second for 1 micro-Curie per square metre or c/s for 1 $\mu Ci/m^2$)

and substituting (3.1.7) in (3.1.6) gives

$$N = \frac{A(t)}{E} \cdot f_o \cdot \frac{1}{a} \cdot [1 - e^{-aE}] \qquad (3.1.8)$$

It remains to consider the initial hypothesis of constant tracer concentration with depth. The distribution of tracer within the sediment mobile layer can take different configurations. Sauzay (1967) has analysed different tracer distributions as a function of depth (Fig. 3.1.2) and he has integrated these data to obtain what is termed the equivalent concentration C_c

$$C_c = \int_0^E C(z) \cdot e^{-az} \cdot dz \; / \; \int_0^E e^{-az} \cdot dz \qquad (3.1.9)$$

The approach taken by Sauzay is to introduce the coefficient

$$\beta = \frac{C_c}{Cm} \qquad (3.1.10)$$

The maximum depth E is then obtained implicitely by solving the equation

$$N = \beta \cdot \frac{A(t)}{E} \cdot f_o \cdot \frac{1}{a} [1 - e^{-aE}] \qquad (3.1.11)$$

Experience has shown (Alquier et al., 1970) that a parabolic tracer distribution is the most realistic and the use of a constant value of 1.15 for β has produced consistent results (see Fig. 3.1.2).

3.2 Tracer Characteristics

(a) Choice of Radioactive Element

One important objective of radioactive sediment tracer experiments is not to interfere with the natural environment and to limit the presence of radioactive material to a time period long enough to bring the experiments to conclusion. This implies that naturally occuring radioactive elements have much too long a half-life to serve the purpose. The alternative is to use elements that can be radioactivated in a nuclear reactor and have a half-life suitable for a specific experiment. Commonly used elements are listed in Table 3.2.1.

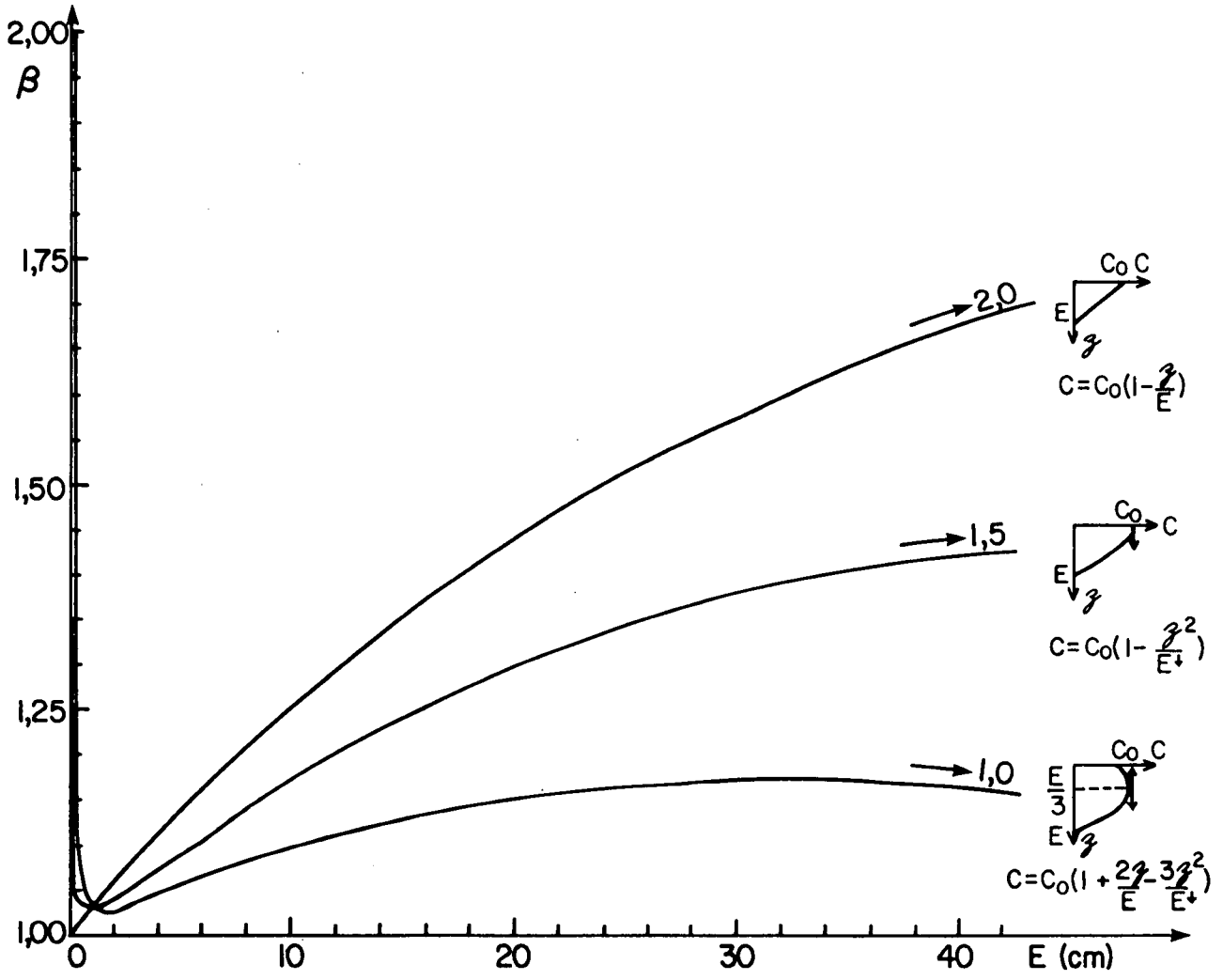

Fig. 3.1.2 Tracer distribution as a function of depth, after Sauzay (1967). The vertical axis is the ratio $\beta = C_c/C_m$ (uniform concentration/ equivalent concentration) and the horizontal axis is the sediment depth. The parameter β is a function of depth and distribution of tracer.

Table 3.2.1

Elements Commonly Used For Radioactive Sediment Tracing

Isotope	Au^{198}	Nd^{147}	Cr^{51}	Ir^{192}	Ta^{182}
Half-Life (days)	2.7	11.1	27	74.4	111
Gamma energy (keV)	410	90 400 700	320	205 612	Complex 1100

Table 3.2.2

Composition of Glass Used for Radioactive Tracers

Compound	Percentage
SiO_2	48
Al_2O_3	19
CaO	17
MgO	6
K_2O	5
TiO_2	5
Ir	0.3

(b) Sediment Tagging

There are two approaches for tagging sand size sediments with radioactive tracers: one is to coat endogenic sand with a compound containing the radioactive material, and the other is to use a glass of the same density and size as the endogenic sand in which the radioactive material is incorporated directly. This latter method (bulk labelling) has advantages; namely no loss of radioactive material by abrasion and a radioactivity proportional to the mass of the material. The Commissariat l'Energie Atomique in France (C.E.A) has used bulk labelling extensively and developed glasses to incorporate different radioactive elements. The composition for Iridium glass is listed in Table 3.2.2.

The glass chosen for a specific survey is ground to meet the unique requirements of the experiment and is irradiated in a nuclear reactor at a flux of 10^{12} and 10^{13} newtons per square centimetre per second ($N\ cm^{-2}\ s^{-1}$) from 24 hours to one week depending on the level of radioactivity to be reached. This radioactivated material needs then to "cool" for some time to eliminate the short-lived activated elements particularly Na^{24} (Caillot, 1970).

(c) Number of Radioactivated Sand Grains

The quantity of tracer needed for a specific experiment is determined on the basis of many parameters. When the quantity of tracer is expressed in terms of kilograms per Curie (kg/Ci), the parameters are as follows:

M_t = mass of tracer
D_{50} = median grain size
R_L = lower limit of count rates above background
l = width of seafloor scanned by probe
V = velocity of detection
t = time gap of integration (2 x integration constant)
f_o = calibration constant same as (3.1.2)
a = absorption coefficient same as (3.1.2)
μ_o = linear absorption coefficient of the tracer
I_g = ionization constant of tracer in water
σ_r = chosen standard deviation of tracer grains

L(h/2)= 50% distribution width of grain size

E = thickness of mobile layer

Courtois and Sauzay (1970) developed the following equation to describe the mass of the sediment

$$M_t = 1.25 \cdot \frac{(D_{50})^3}{V.l.t} \cdot \frac{R_L}{f_o} \cdot \frac{1-e^{-2aE}}{(1-e^{-aE})} \cdot \left(\frac{\mu_o . Ig}{\sigma_r}\right)^2 \left(1+1.05\left[\frac{L(h/2)}{D_{50}}\right]\right)^2 \quad (3.1.12)$$

(d) Specifications for the Tracer Used at Olympia and Venture Sites

The radioactive element chosen was Iridium 192 because its half-life of 74.4 days best suited the requirements for the Sable Island Sediment Transport Study. The energy spectrum of Ir 192 was spread between 205 and 612 keV with peaks at 295 keV (15.2%) 308 keV (15.8%), 316 keV (44.0%) and 468 keV (25.0%). The mean energy level of gamma radiation is 360 keV.

Because of the larger grain size, the weight of tracer required for the Olympia site was larger than for the Venture site. Independently of the level of activity used, it is recommended that the number of tracer grains should always exceed one million (10^6) (Sauzay, 1967).

The specifications for the radioactive tracer at Olympia and Venture sites are summarized on Table 3.2.3.

3.3 Equipment

(a) Tracer Injection System

Different tracer injection systems have been developed by the Commissariat l'Energie Atomique depending on the quantity of tracer to be released. For the Sable Island study, a multi-canister system was used because three canisters were needed to contain the quantity of tracer injected at each site. This system can contain up to six canisters of radioactive tracer. The canisters are mounted on a tripod (see Fig. 3.3.1). The release mechanism is operated by compressed air and is activated from the ship, so that the tracer can be released directly onto the seafloor, or some distance above it to produce a larger initial cloud. In the case of the present survey the radioactive

Table 3.2.3

Tracer Characteristics for Both Study Sites

Parameter	Venture Site	Olympia Site
Weight (Kg)	1.20	1.54
Activity (Ci) (as of 27 September, 1984)	1.517	1.590
Grain size limits (mm)	0.3-0.4	0.5-0.6
Grain size, D_{50} (mm)	0.37	0.57
Number of Grains	7.15×10^6	2.81×10^6
Activity per grain *(μCi)	0.212	0.565

* microcuries

Notes

The radioactive tracers prepared by CEA are shipped in specially designed ready-to-use cannisters as shown in the upper right corner of the figure. When triggered the bottom of the cannister opens and releases the tracer. A multi-cannister release system is used when more than one cannister is needed to contain the tracer load. The simultaneous release of all the cannisters is operated by compressed air and triggered from the ship so that the tracer can be released directly on the seafloor or some distance above it to obtain a wider initial spreading of the tracer.

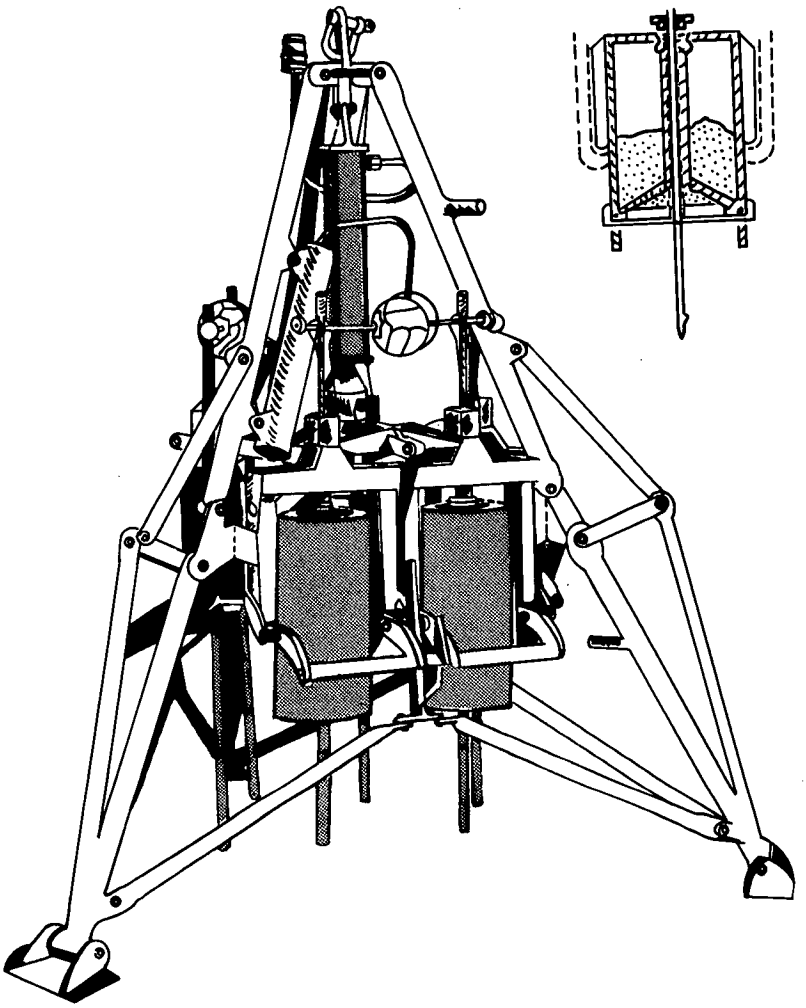

Fig. 3.3.1 Tracer injection system developed by CEA (France).

tracer was released 5 metres above the bottom.

(b) Detection Scintillometer and Sled

The scintillometer and all the detection equipment was developed by the Commissariat l'Energie Atomique. The basic components of the scintillometer were a 2.5 x 3.8 cm sodium iodide (NaI) crystal used as primary detector, linked to a photomultiplier tube. The scintillometer probe was contained within a waterproof stainless steel cylinder 5.3 cm in diameter by 36 cm long that weighs 2 kg. The stainless steel container had a thickness of 2 mm in front of the NaI crystal. This scintillation probe is a miniature compared with the RIST probe used by Duane, (1970). The calibration constant for the scintillometer mounted 5 cm above seafloor is f_o=60.54 to obtain counts per second for 1 micro-Curie covering 1 m^2 on the seafloor at a threshold of 50 kev (Sauzay, 1976, p. 48).

The scintillation probe was mounted on a sled that maintained the centre of the probe at a constant height of 5 cm above the seafloor. The sled is designed so that it can land on the bottom on either side (Fig. 3.3.2) without affecting the operation of the scintillometer. The sled is ballasted to weigh approximately 100 kg. Although the sled is light it works very well provided that the towing cable is long enough. For this study a cable length of 120 m was used and it was possible to work under quite rough conditions with heavy seas (4-5 m) and winds exceeding 30 knots. The limiting factor was the maneuverability of the ship in the heavy weather.

(c) Recording System

The signal received from the scintillometer is a frequency signal proportional to the count rate detected by the sensor. The recording system setup is shown in Fig. 3.3.3. This primary frequency signal was fed to two parallel-mounted signal analysers (IPP4). Different settings were used to condition the primary signal: (1) The integration time rate was set at 1.2 seconds which is most appropriate for survey speeds of the order of 1 m/s and, (2) the threshold was set at 50 keV which was the lowest level. This low level setting allowed the system to detect

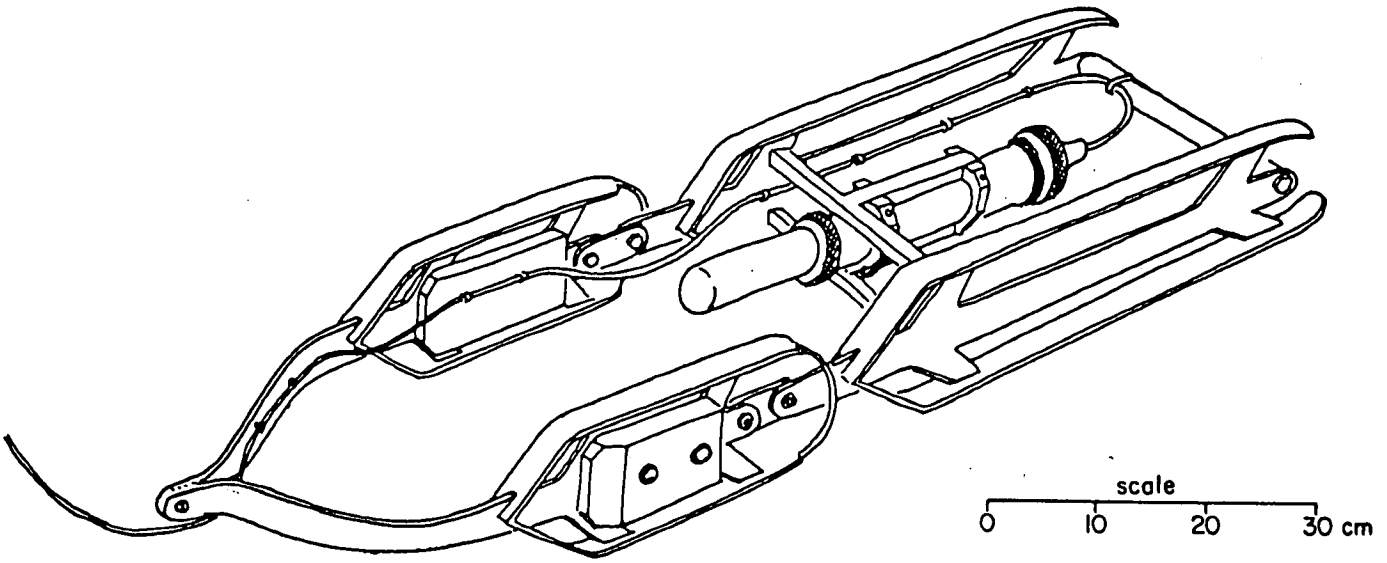

Fig. 3.3.2 Scintillation probe mounted on the towing sled. Probe is maintained at 5 cm above the seafloor.

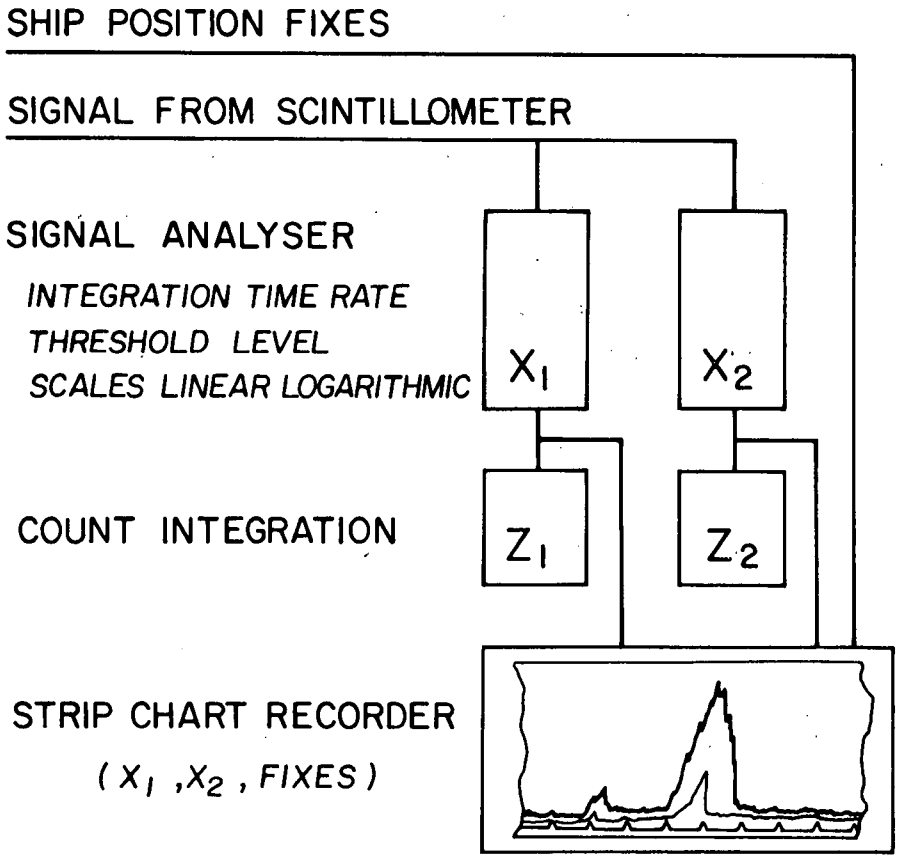

Fig. 3.3.3 Recording system used for tracer detection surveys.

low intensities of radioactivity although it made the detection system more prone to saturate at peak tracer concentrations; nevertheless, this is a lesser problem than obtaining a lower level of information. Also one signal analyser was set on a logarithmic scale to cope with all cases and the other signal analyser was set to different scales depending on the activity response foreseen for a given survey line. The aim was to obtain more details by operating the analyser near full scale. The processed signals from the signal analysers were fed to two count integrators that integrate count rates over a whole survey line. Finally both the linear scale and the logarithmic scale signals were sent to a strip chart analog recorder that simultaneously records ship position fixes. A typical record is shown in Fig. 3.3.4. The information recorded on the strip chart (signal levels and ship fixes) were used to plot the distribution of the radioactive tracer cloud, discussed in the next section.

(d) Navigation and Sled Positioning

Precise navigation is a concern for tracer studies. The navigation network used in this experiment consisted of a Syledis system with three beacons on Sable Island. This system, used to position the ship itself, was backed up by the ARGO system deployed on the Scotian Shelf. The position of the sled relative to the ship was monitored for surveys 2, 3 and 4 using an O.R.E. Trackpoint system. Navigation and positioning data were logged in an on-board computer and monitored for accuracy and consistency. The combined system had an overall positioning accuracy of the sled of $\pm$12 to $\pm$15 metres.

3.4 Data Processing

The analysis of sediment tracer data is approached differently whether the movement of sediments is one-dimensional (moving along only one axis) or two-dimensional (moving in different directions), and whether the sediments are transported by bedload processes only or by suspension as well.

Applications of sand size radioactive tracers for studying the transport of sediments are most often concerned with engineering

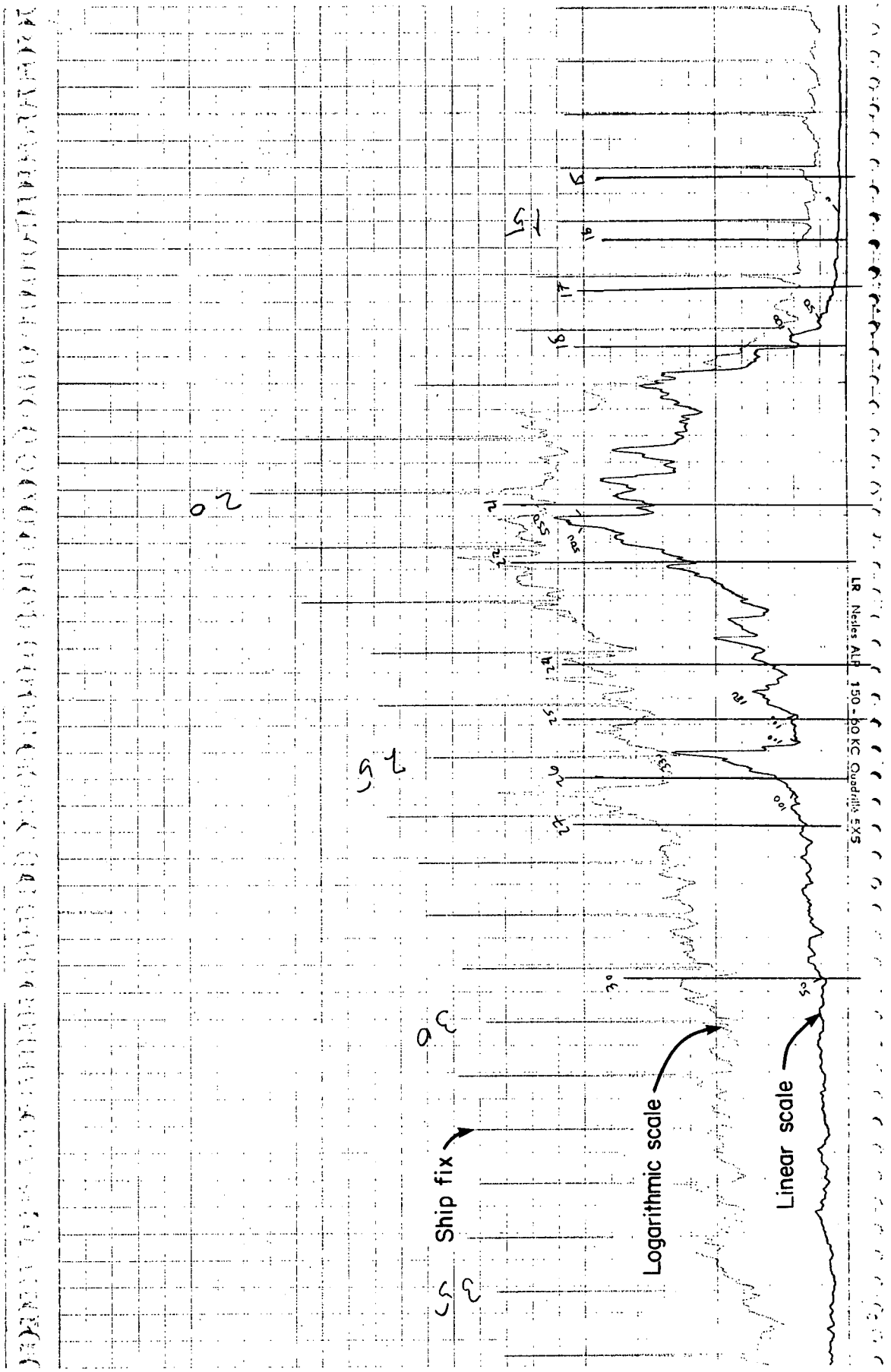

Fig. 3.3.4 Analog output of tracer detection system, showing linear and logarithmic recording scales and the ship's fix lines on the strip chart.

problems where the transport of sediments is one-dimensional driven primarily by wave generated longshore transport in the littoral zone,or the transport resulting from tidal currents in estuaries. The total count rate ("Bilan des taux de comptage"; Sauzay, 1967) applies to these one-dimensional sediment transport problems. The procedure elaborated by Sauzay is best explained by the example shown on Fig. 3.4.1. The overall axis of transport is predetermined, and the survey lines are run perpendicular to that axis. As mentioned in the preceeding section, it is important that the survey completely encompasses the tracer cloud. Each survey line produces two types of data: one is the analog graphic record of the radioactivity response of the tracer cloud, and the other is the cumulative count of the scintillations recorded during the survey of that line. The graphical record is used to map the isointensity contours (isopleths) of the tracer cloud, which is facilitated by the inscription of the ship track fixes directly on the analogue record. The map of the isocontours of the tracer cloud is very useful to visualize the tracer distribution. Quantitative measurements, are however, based on the determination of the centroid of the tracer cloud along the transport axis and on the evaluation of the thickness of the mobile sediment layer.

The equation for calculating the mobile thickness layer has been developed in Section 3.1. It has also been described in Section 3.3(c) that the total count of scintillations recorded along one survey line is recorded by a scintillation count integrator. It should be added, however, that this total count rate obtained at the end of each survey line needs to be normalized. The total count rate obtained during the survey of one line is directly related to the speed of the survey, because the total count is time dependent. The calibration of the detection system is based on the assumption that the dynamic detection is run at the speed of 1 m/s. The active area sensed by the scintillation probe is 1 m^2 and with the time integration constant of the system being set at 1 second, the count rates can be integrated as if it were a static survey, which facilitates the calibration of the detection probe. The recorded total count rate is then corrected to

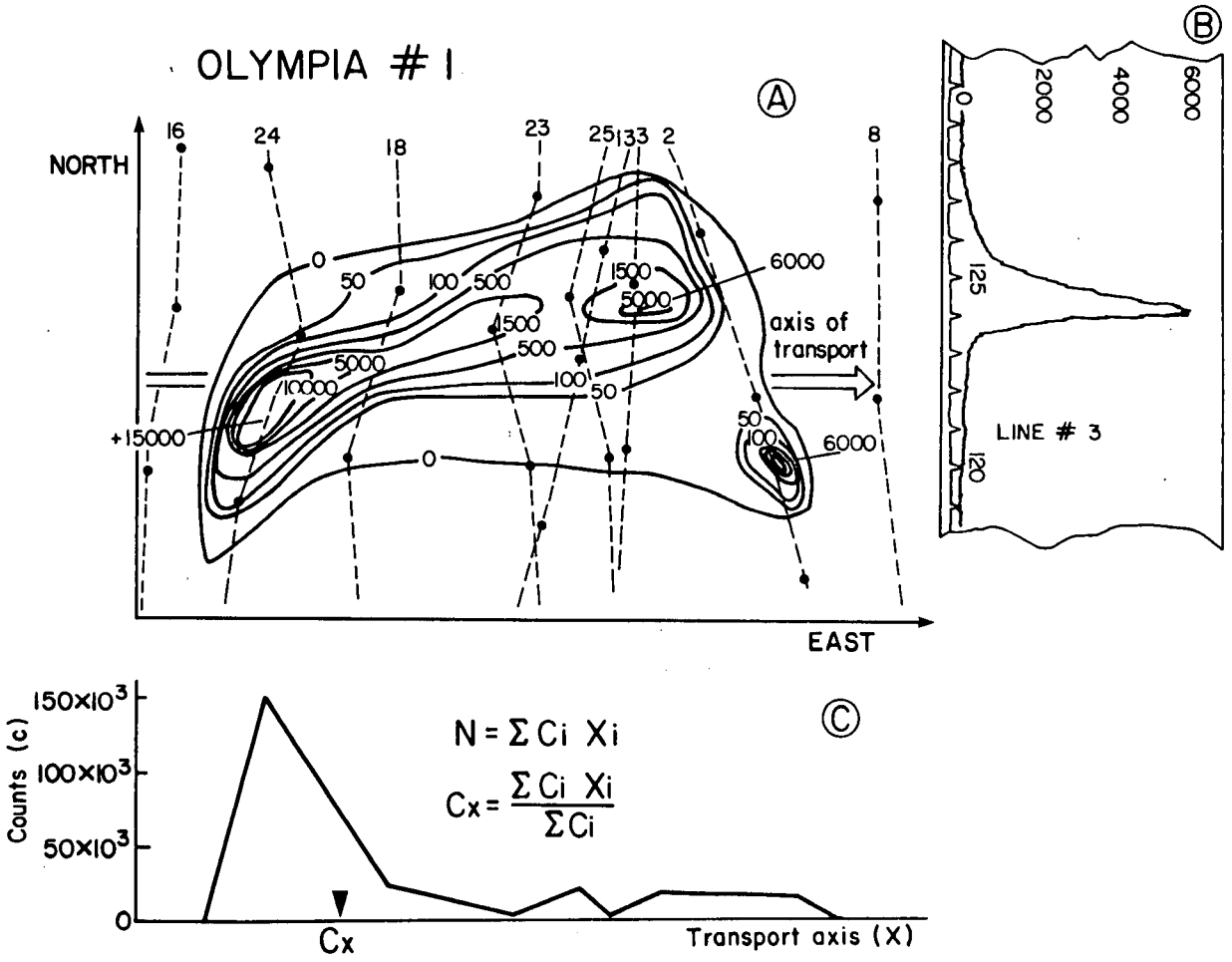

(a) Map of isopleths of measured radioactivity of the tracer cloud and ship's track superimposed on it.

(b) Graphic record of line no. 3 showing measured radioactivity and fixes.

(c) Total count of each survey line as a function of position along transport axis. Integration of this graph provides a total count 'N' for the whole detection and also the x-coordinate, Cx, of the centroid of the tracer cloud.

Fig. 3.4.1 Example of results from a tracer detection survey.

obtain a total count corresponding to a survey speed of 1 m/s. A second correction has to be made to subtract the background radiation level from the total count rate. A mean background radiation level (counts/second) is determined for the survey area by running the system for some time outside the tracer cloud and averaging the measured background radiation level.

An example of calculations to determine the centroid of the tracer cloud is shown in part C of Fig. 3.4.1. The basic assumption remains the same; that is, the movement of sediment is treated within a one-dimension system. The horizontal axis represents distances from a reference coordinate and the vertical axis the scintillation counts. The data collected for each survey line, that is the total count and the distance of that line from the reference coordinate, are plotted on the graph. The end result is that the distribution of the tracer cloud is defined by a one-dimensional section. Fig. 3.4.1 helps to visualize how the total count is obtained for the whole detection, and also the location of the centroid with respect to the reference coordinate. Part C of Fig. 3.4.1 is drawn to explain the procedure because in practice the location of the centroid and the total count are calculated quite simply. In fact, the total count is the quantity "N" identified in the transport equation (3.1.11).

The problem for the Sable Island Shelf study is that the transport of sediment is not unidirectional and the procedure just described must be modified. The map of the radioactive tracer cloud is used as the basis for the calculation of the centroid as well as the total radiation count. The isopleths of the tracer cloud are digitized and the surface area of each isopleth as well as the geographical coordinates of the centroid of the isopleth are calculated. The proper summation of these data provides the geographical coordinates of the centroid for the whole tracer cloud as well as the total scintillation count.

Comparison of the two methods was established using the first detection at the Olympia site and the difference between the two methods for locating the centroid was 3 metres. The total scintillation count rate

obtained by digitization was 1,834,601 compared with 2,096,165 for the method described in Fig. 3.4.1.

This difference between the two methods is easily explained by examining Fig. 3.4.1. The method based on the one-dimensional approximations uses in fact nine data points to determine both the centroid and the total count and, as shown by the diagram, necessarily assumes a linear distribution between the data points. By contrast, the method based on digitization of the isopleths of the tracer cloud makes use of all the information available and for this very reason is more accurate. In addition, it provides geographical coordinates of the centroid that account for tracer movement in all directions. This is essential for shelf surveys in areas like Sable Island Bank.

4.0 SUMMARY OF FIELD OPERATIONS

4.1 Olympia Site

At the Olympia site 1.54 kg of 0.5-0.6 mm glass activated to the level of 1.590 Ci was released using the tracer injection system described in section 3.3. The tracer injection system was lowered on the seafloor and then lifted 5 m above the bottom to obtain a larger initial cloud. The injection was completed on 23 Sept 84 at 22:36 GMT. The coordinates of the injection point are 44°00.35'N 59°52.00'W.

(a) Cruise No 1.

The first detection at the Olympia site was carried out on Sept. 25 and 26, 1984. The ship tracks of that detection are shown in Fig. 4.1.1 and the results of the survey are shown in Fig. 4.1.2. This survey took place two days after the injection and it is difficult to explain why the tracer shows two secondary concentration peaks separated from the main tracer concentration; the same situation is observed and discussed further for Venture. Calculations of the thickness of the mobile sediment layer are not meaningful because of the disparity between the quantity of tracer injected (A) and the total radiation count (N) obtained for that survey.

(b) Cruise No. 2

The second detection at the Olympia site took place on Oct. 25 and 26, 1984. The ship tracks for that detection are shown in Fig. 4.1.3. The results of the survey are shown on Fig. 4.1.4. This survey was undertaken under very good weather conditions and was very successful. The area covered by the tracer increased to 4258 sq. m from 1523 sq. m. at the time of first detection.

(c) Cruise No. 3

The third survey was undertaken on Jan. 15 and 18, 1985 in severe weather conditions with 30 knot winds and 5 m waves. To maintain headway and steerageway the ship was sailed at slow speed (3 knots) into the wind. Nonetheless the survey was very successful. As can be seen on Fig. 4.1.6 the survey outlined the high intensity peak of the tracer (49,000 cps) as well as the distribution of the tracer around that peak. The

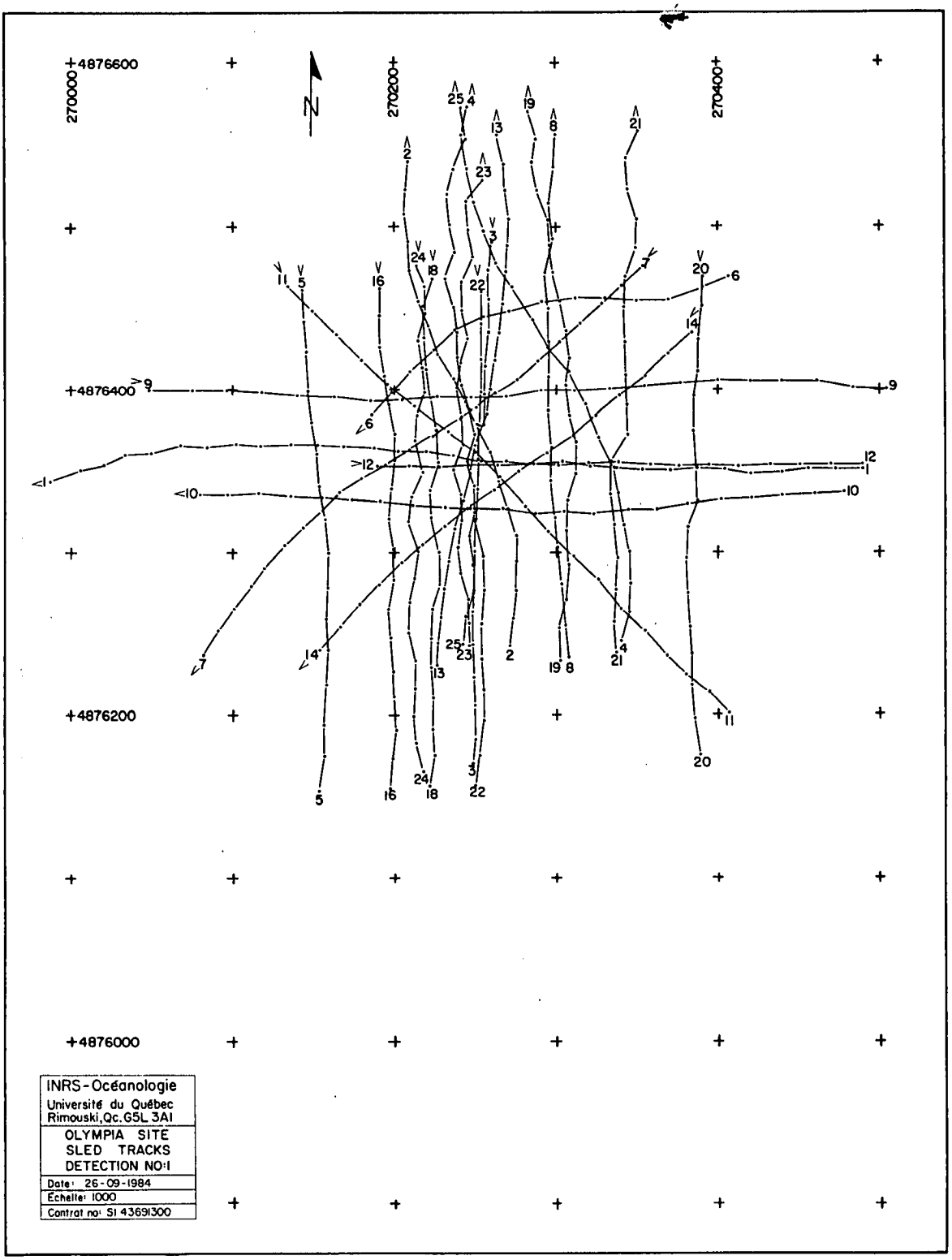

Fig. 4.1.1 Olympia site sled tracks for detection No. 1.

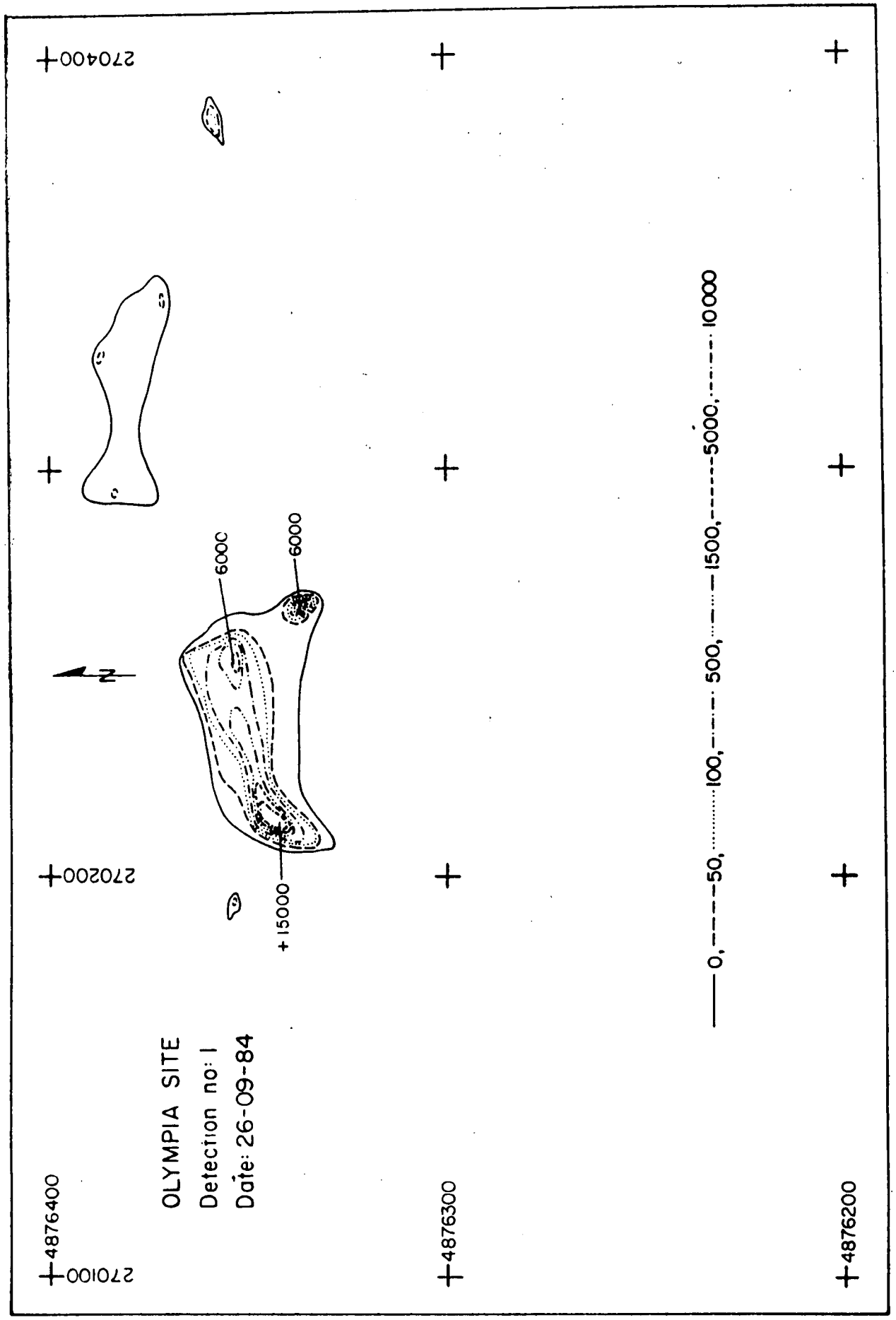

Fig. 4.1.2 Tracer cloud at Olympia after detection No. 1.

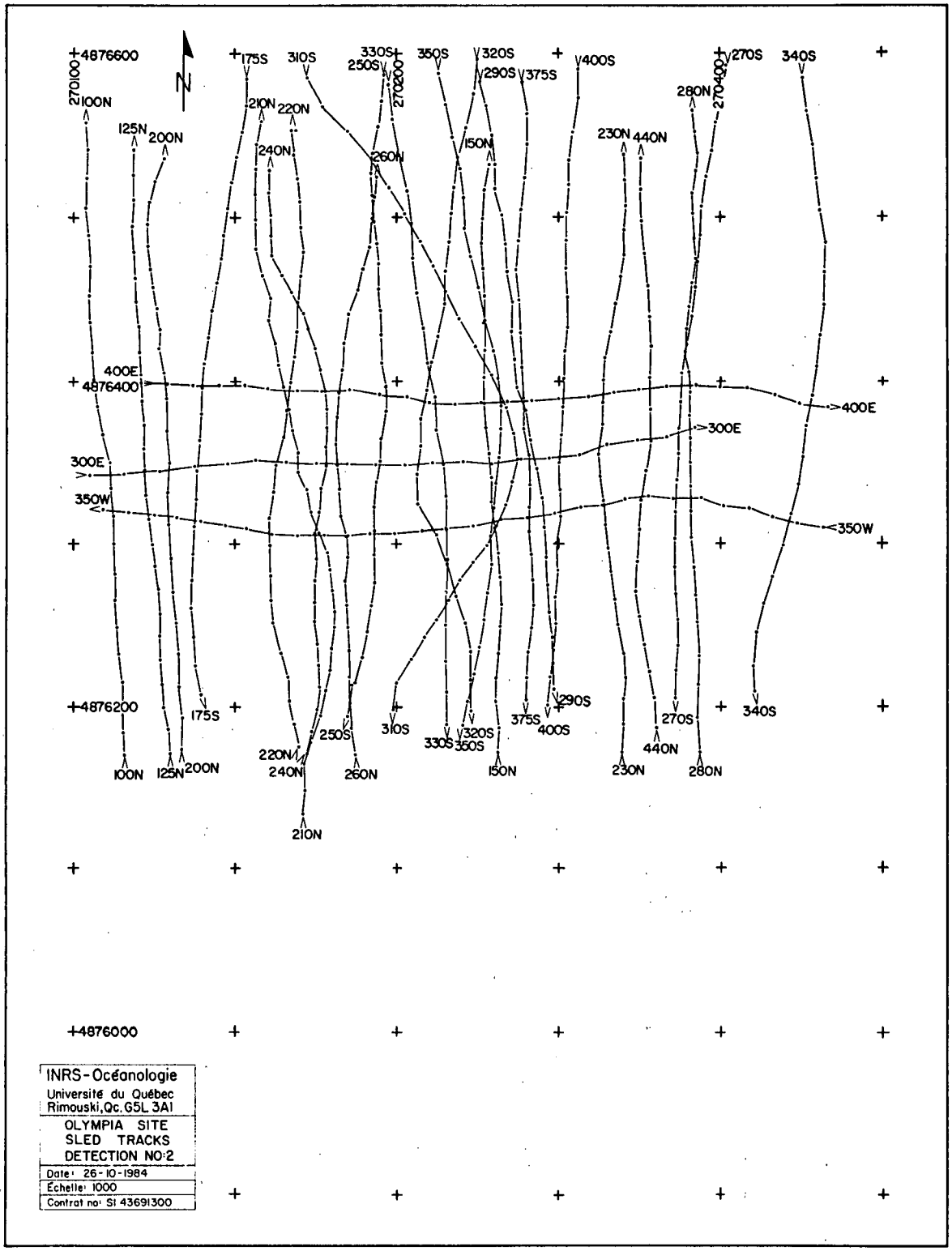

Fig. 4.1.3 Olympia site sled tracks for detection No. 2.

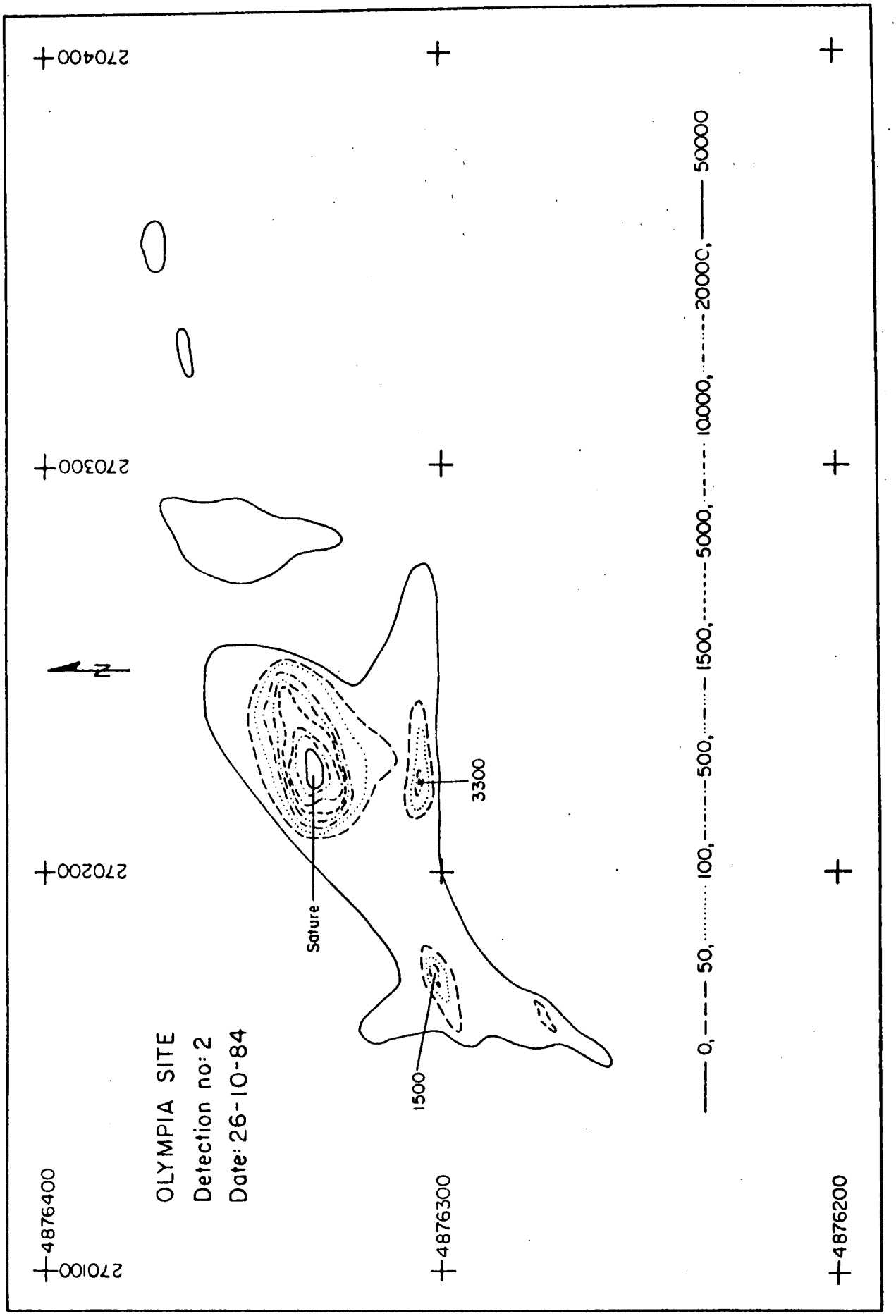

Fig. 4.1.4 Tracer cloud at Olympia after detection No. 2. "Saturé" means above 50,000 c.p.s.

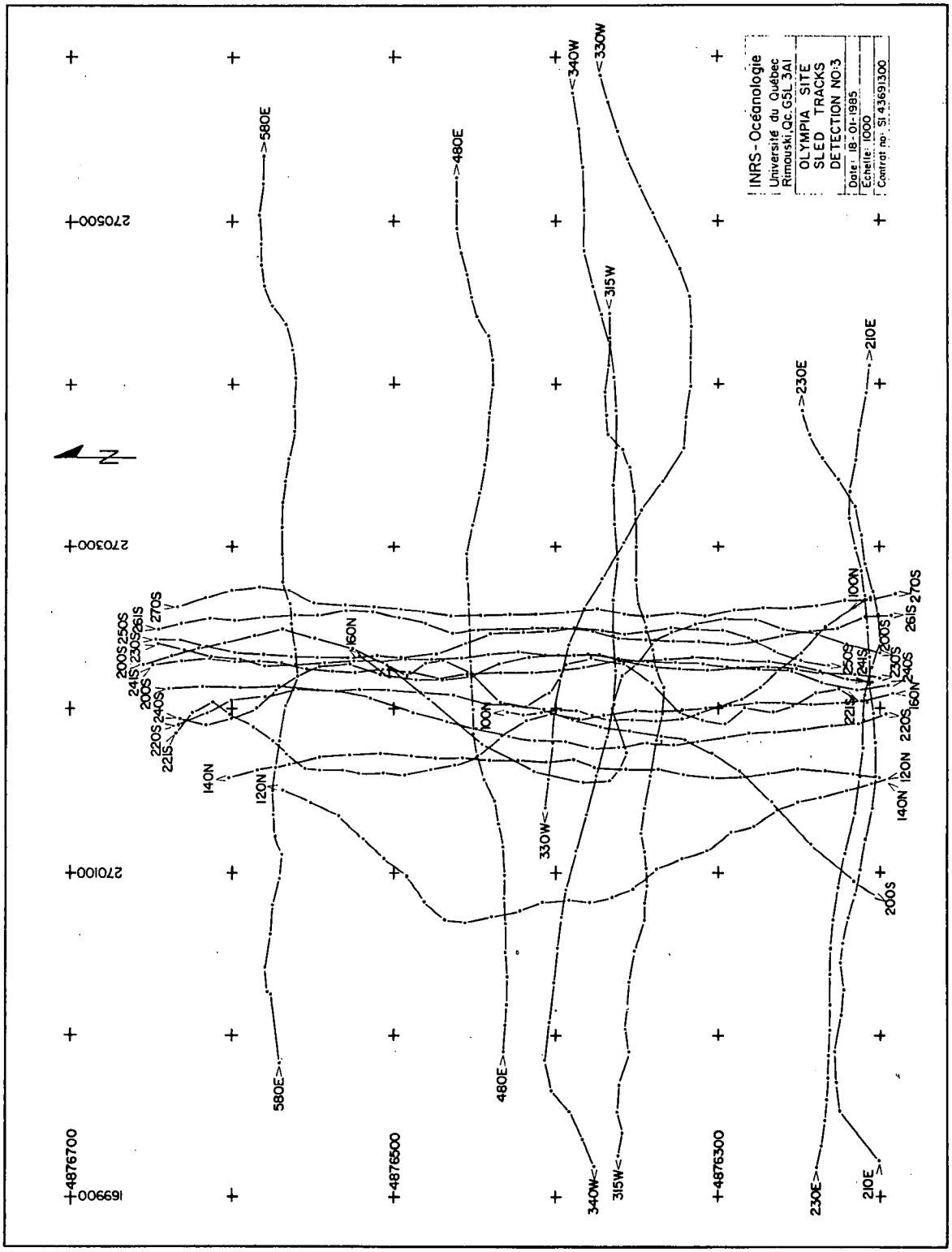

Fig. 4.1.5 Olympia site sled tracks for detection No. 3.

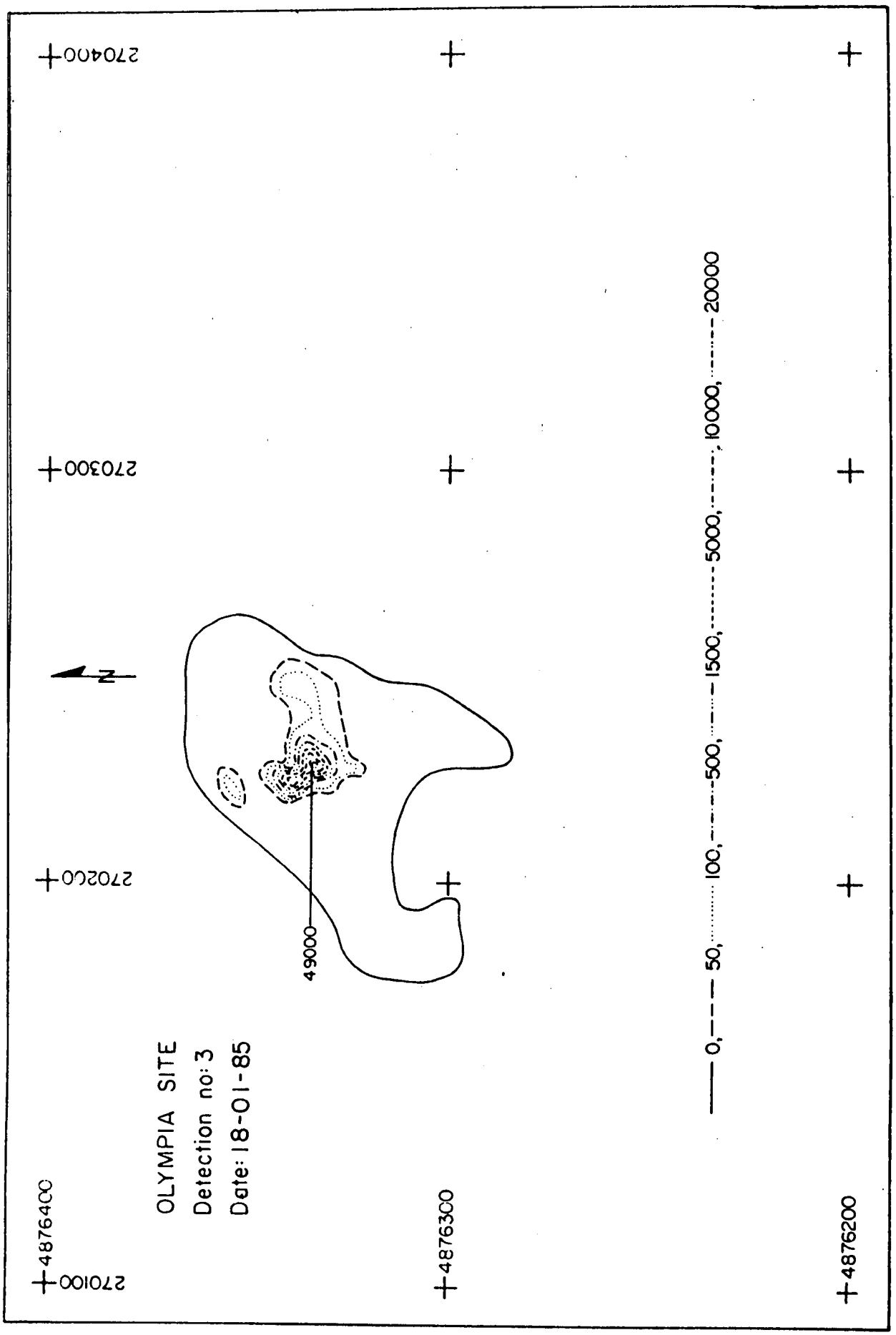

Fig. 4.1.6 Tracer cloud at Olympia after detection No. 3.

ship tracks for that survey are shown on Fig. 4.1.5.

(d) Cruise No.4

The fourth detection was performed on Feb. 18 and 19, 1985 under typical winter conditions. The ship tracks are plotted in Fig. 4.1.7. The results of the survey are outlined on Fig. 4.1.8. This survey took place five weeks after the third one and at a time the tracer activity had dropped from 35 to 26 percent of the initial injection level. However, the radioactivity measured during this fourth survey is comparatively much lower than for the third survey. In fact, the discrepancy is such that either the coarser grain tracer has been covered by more mobile finer sand or, although the survey indicated that the tracer cloud had been completely encompassed, some of the tracer has not been detected. The location of the centroid of tracer cloud for this survey is then somewhat questionable because it is based on the assumption that the radioactivity isopleths are accurately outlining the location of all the tracer grains.

4.2 Venture Site

At the Venture site 1.20 kg of 0.3-0.4 mm glass activated to the level of 1.514 Ci was released following the same procedure as for the Olympia site. The injection was completed on 24 Sept. 1984 at 10:30 GMT. The coordinates of the injection point are 43°56.40'N, 59°39.60'W.

(a) Cruise No.1

The first survey at the Venture site began one day after the initial injection on Sept. 25 and 26, 1984. It was not expected that the tracer would have spread so much nor that the three high concentration peaks would be found. Although it was not planned, a multi-point injection favors a better dispersion of the tracer. For example, Lavelle et al. (1978) chose a triangular injection pattern (injection points 100 m apart) for their radioactive tracer sediment study on Long Island Shelf. The main objective of the first survey was to locate the tracer; mixing of the tracer with the mobile bedload layer would not generally have been adequate for a calculation of the thickness of the mobile layer. The ship tracks are shown in Fig. 4.2.1 and the results of the survey in

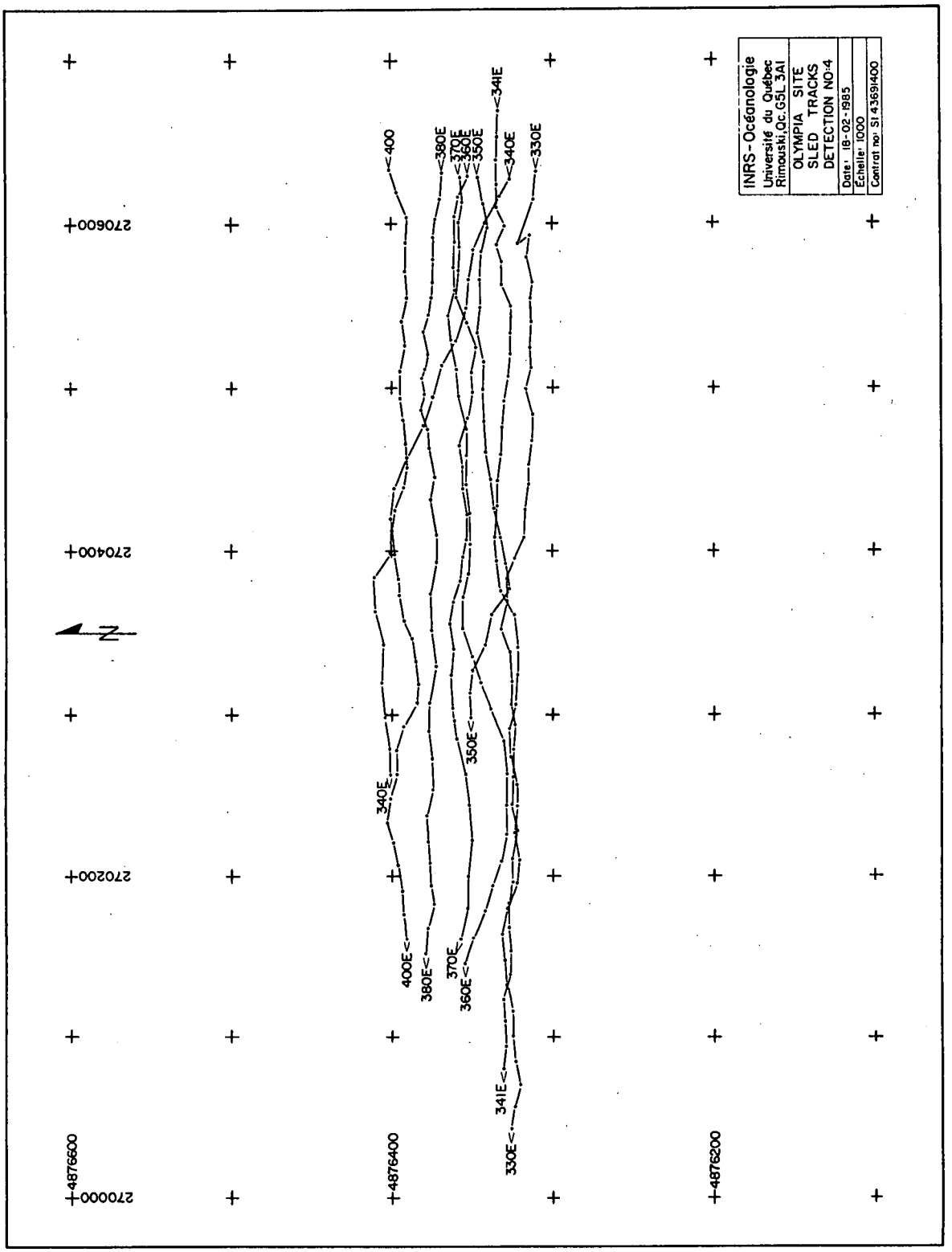

Fig. 4.1.7 Olympia site sled tracks for detection No. 4.

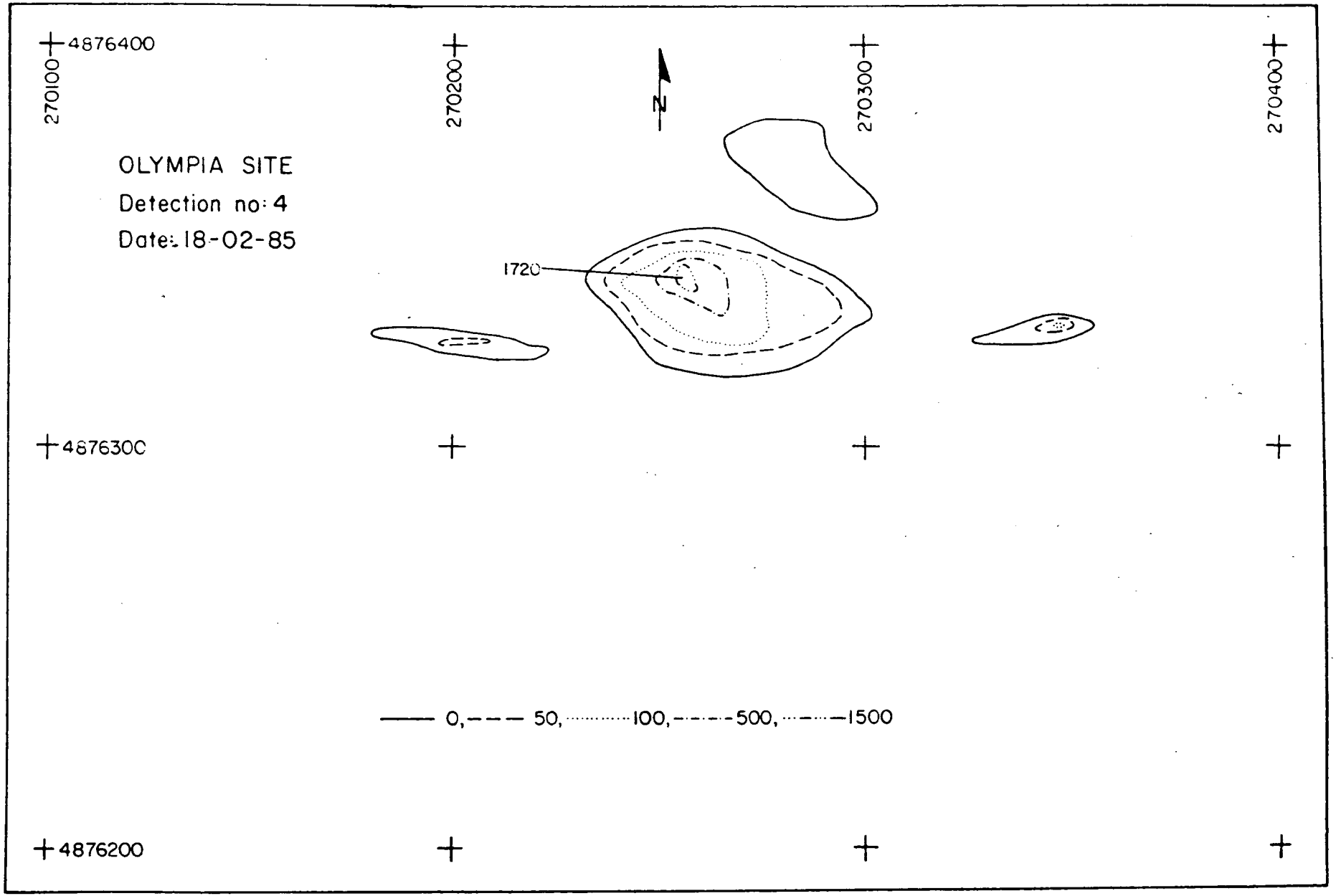

Fig. 4.1.8 Tracer cloud at Olympia after detection No. 4.

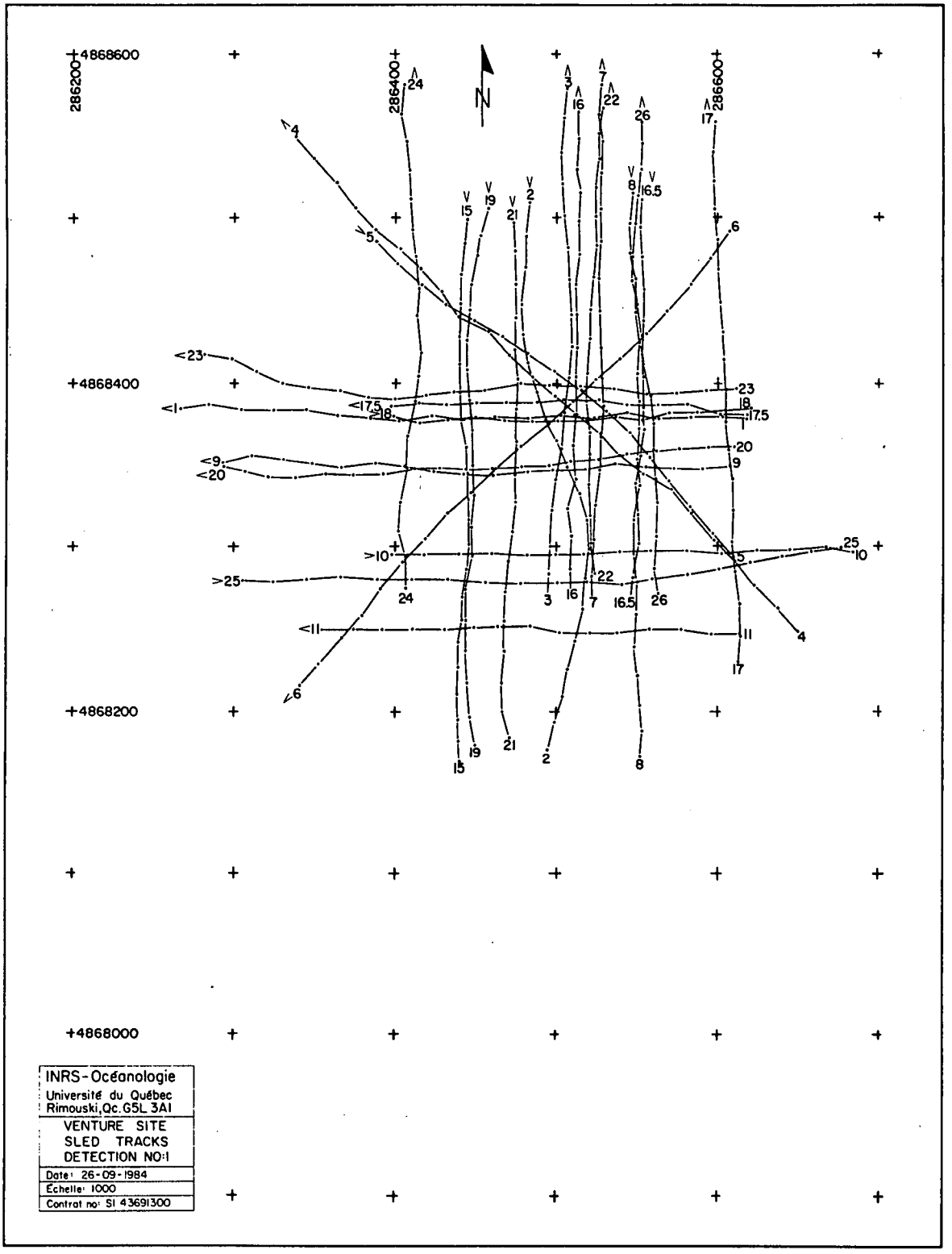

Fig. 4.2.1 Venture site sled tracks for detection No. 1.

Fig. 4.2.2.

(b) Cruise No. 2

The second survey of Venture site (26-27 October, 1984) benefited from very good weather conditions and was very extensive. The ship tracks are plotted in Fig. 4.2.3. The results of that survey are shown in Fig. 4.2.4. and reveal that the Venture tracer cloud had dispersed considerably, covering an area of some 61,500 m^2.

(c) Cruise No. 3

The third survey took place on Jan. 17, 1985 under the same severe weather conditions as those encounterd at the Olympia site. The ship's tracks are reproduced in Fig. 4.2.5 and the results of the survey appear on Fig. 4.2.6. The area covered by the tracer is similar with that of the second survey except that it has moved northeastward.

(d) Cruise No. 4

The fourth survey was carried out on Feb. 19 and 20, 1985. The weather conditions being typical for winter. The ship tracks are shown in Fig. 4.2.7 and the results of the survey in Fig. 4.2.8. The isopleths show that the peak response of the tracer has diminished considerably by comparison with the third survey. By contrast with the fourth survey on Olympia site however, this lower peak activity is explained by the spreading of the tracer over a larger area, that is 83,700 m^2 as compared with 67,800 m^2 for the third survey. In fact, the tracer recovery for this fourth survey is 32 percent as compared with 26 percent for the third survey. In addition to spreading considerably the shape of the tracer cloud has changed elongating North-South.

4.3 Basic Environmental Data

(a) Wind Time-Series

Wind, temperature and pressure records from the AES weather observation station on Sable Island (Fig. 4.3.1) are plotted in Appendix 8.2 for the duration of the radio-isotope experiment; i.e., the middle of September, 1984 to the end of February 1985. The winter months of December, January and February show higher windspeeds for longer periods of time, usually prevailing from the West. Windspeeds, especially in January, are

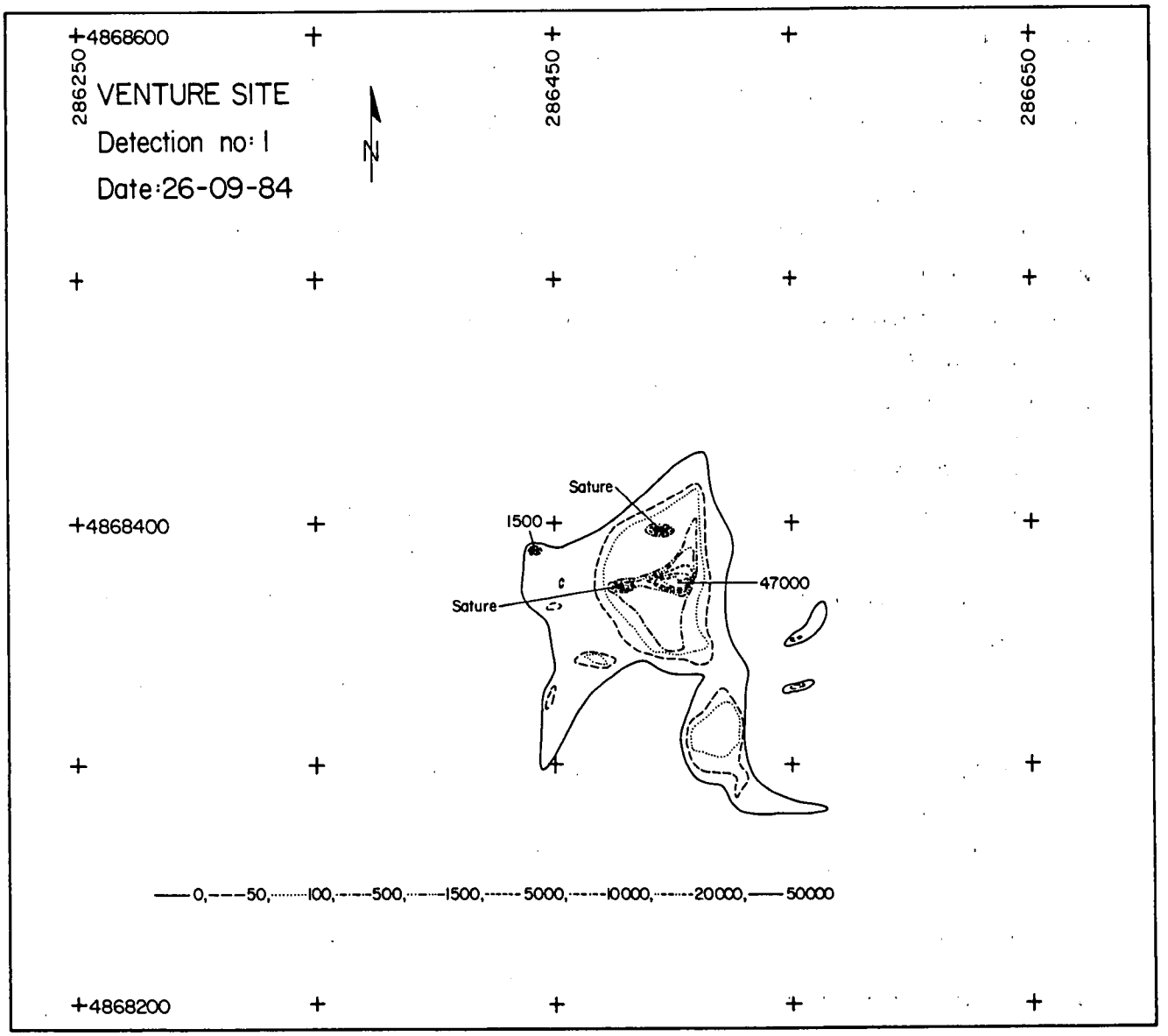

Fig. 4.2.2 Tracer cloud at Venture after detection No. 1.

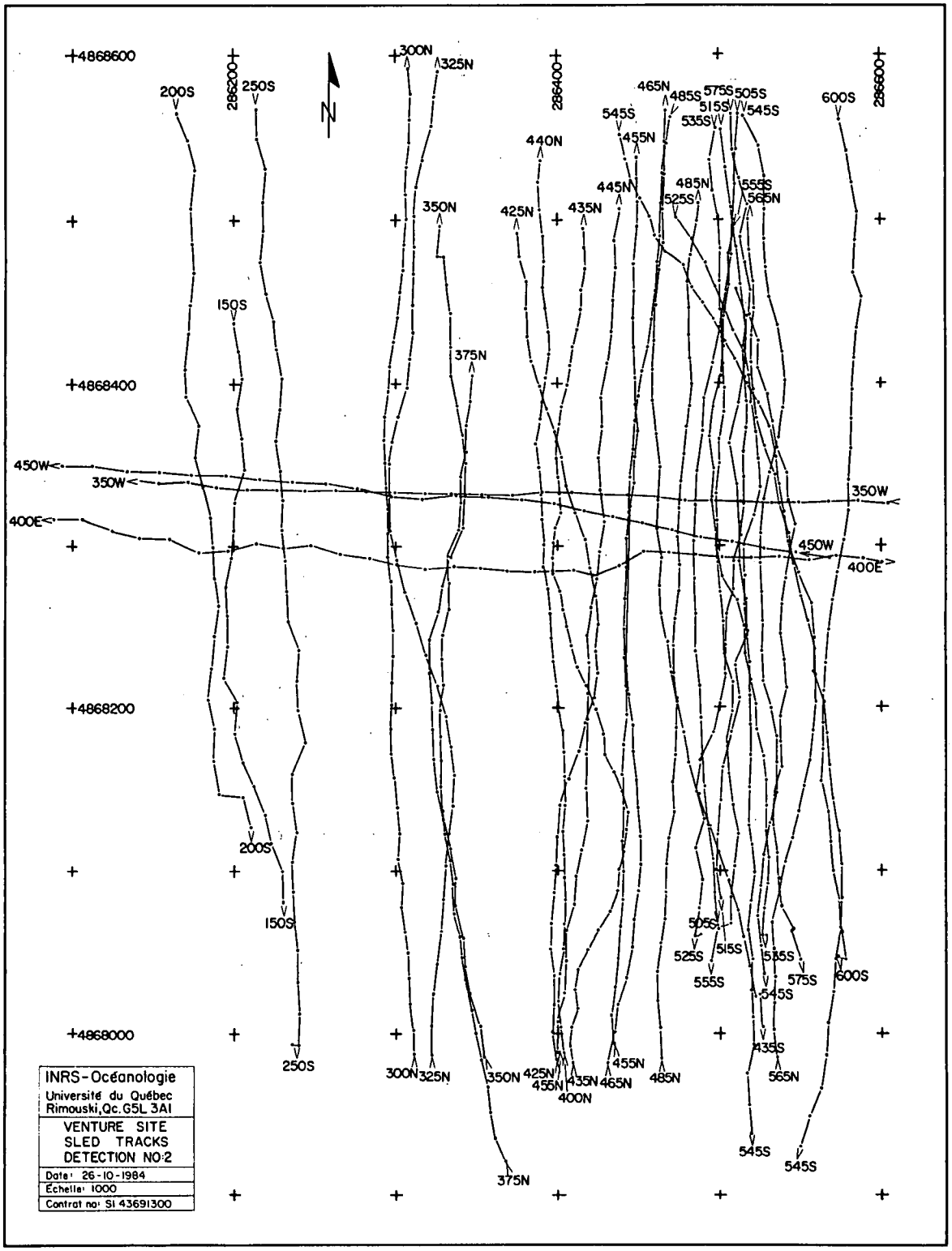

Fig. 4.2.3 Venture site sled tracks for detection No. 2.

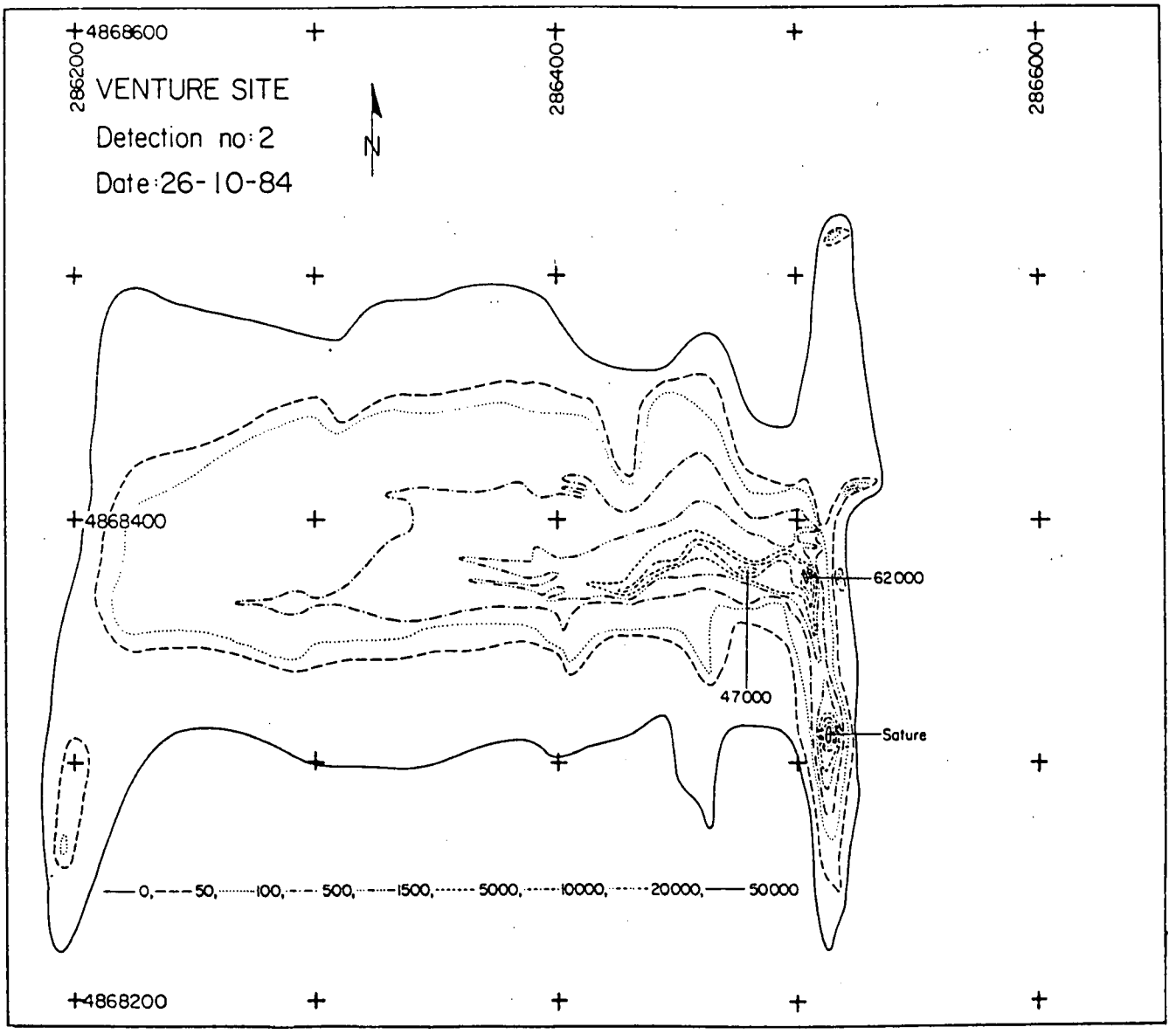

Fig. 4.2.4 Tracer cloud at Venture after detection No. 2.

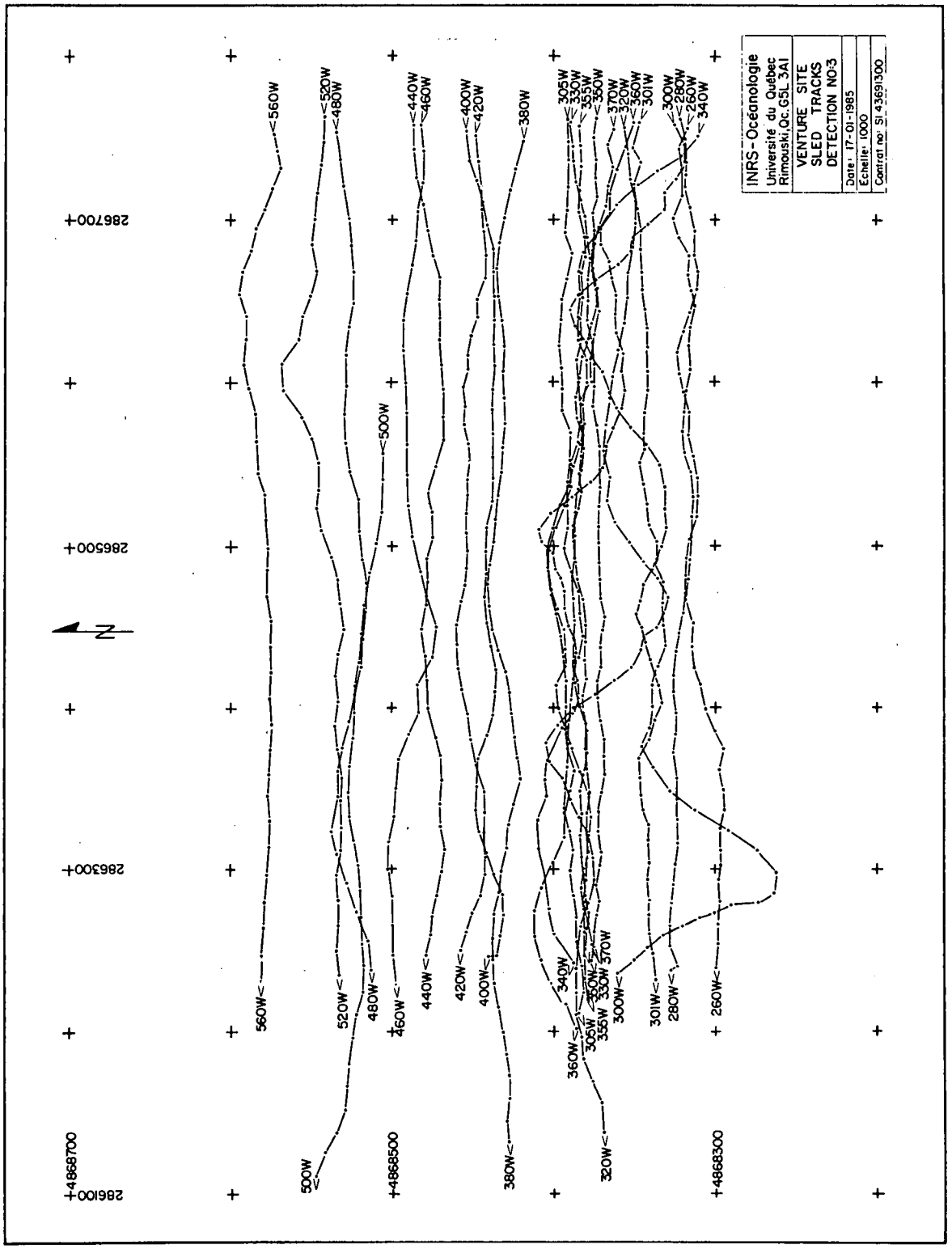

Fig. 4.2.5 Venture site sled tracks for detection No. 3.

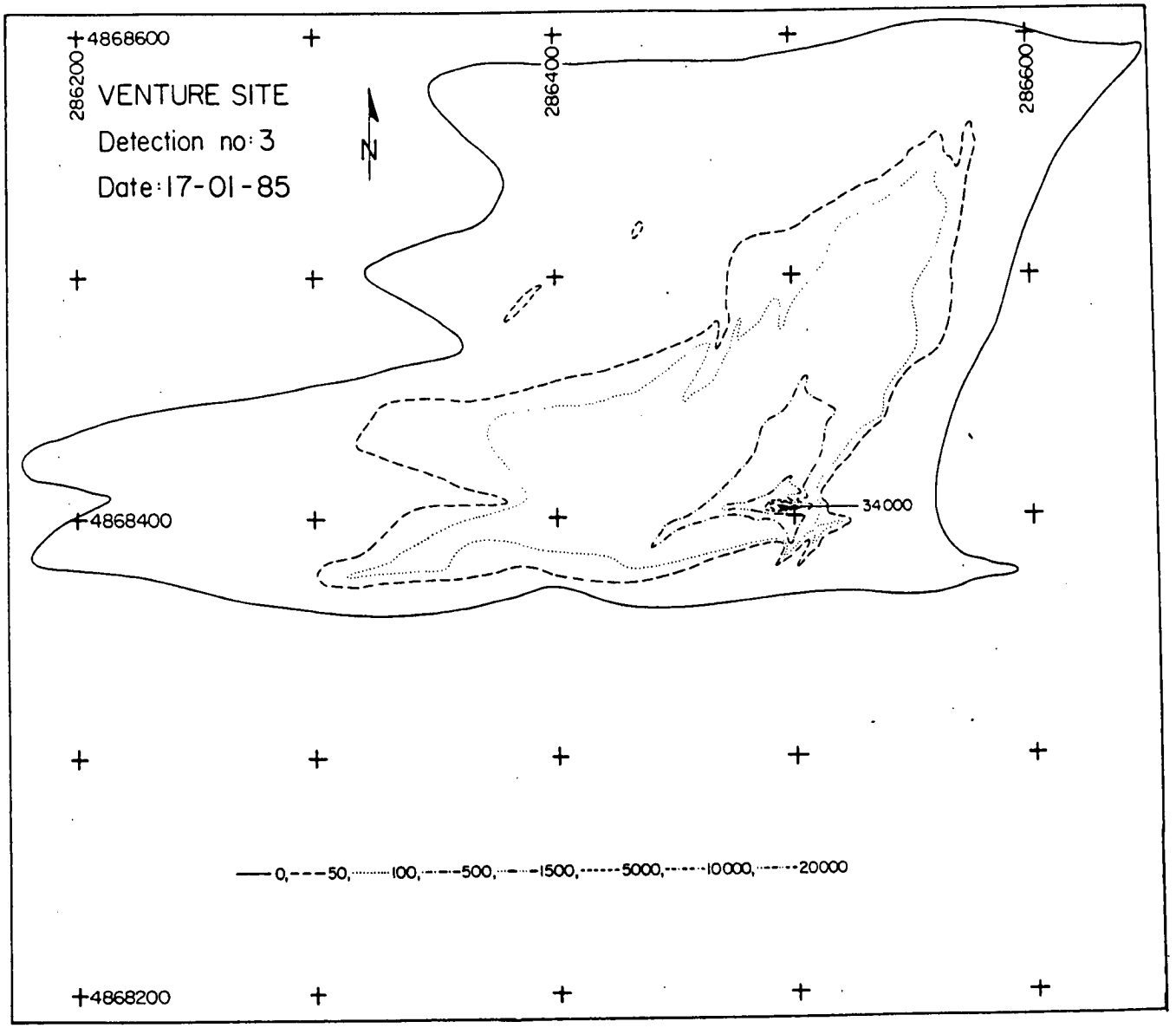

Fig. 4.2.6 Tracer cloud at Venture after detection No. 3.

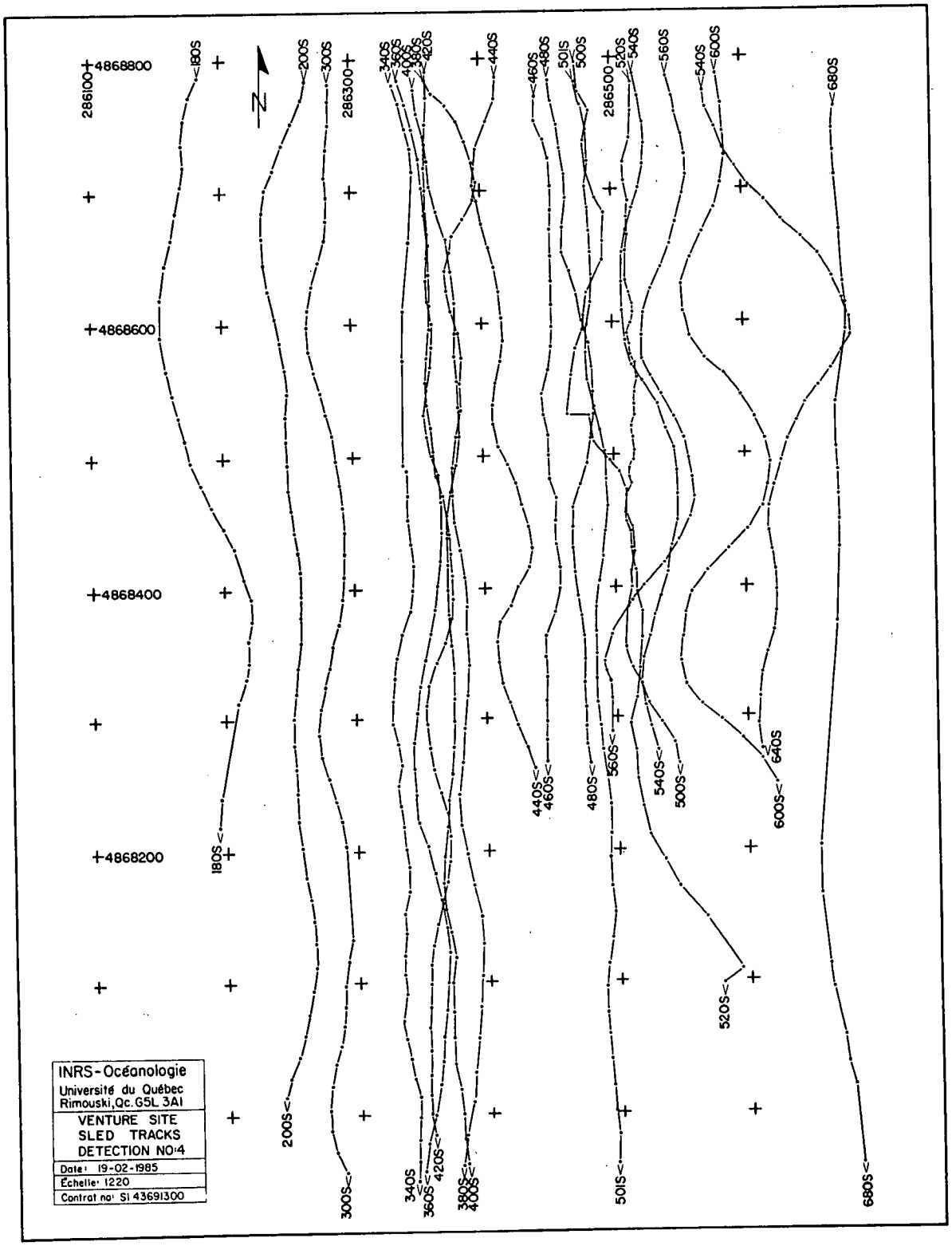

Fig. 4.2.7 Venture site sled tracks for detection No. 4.

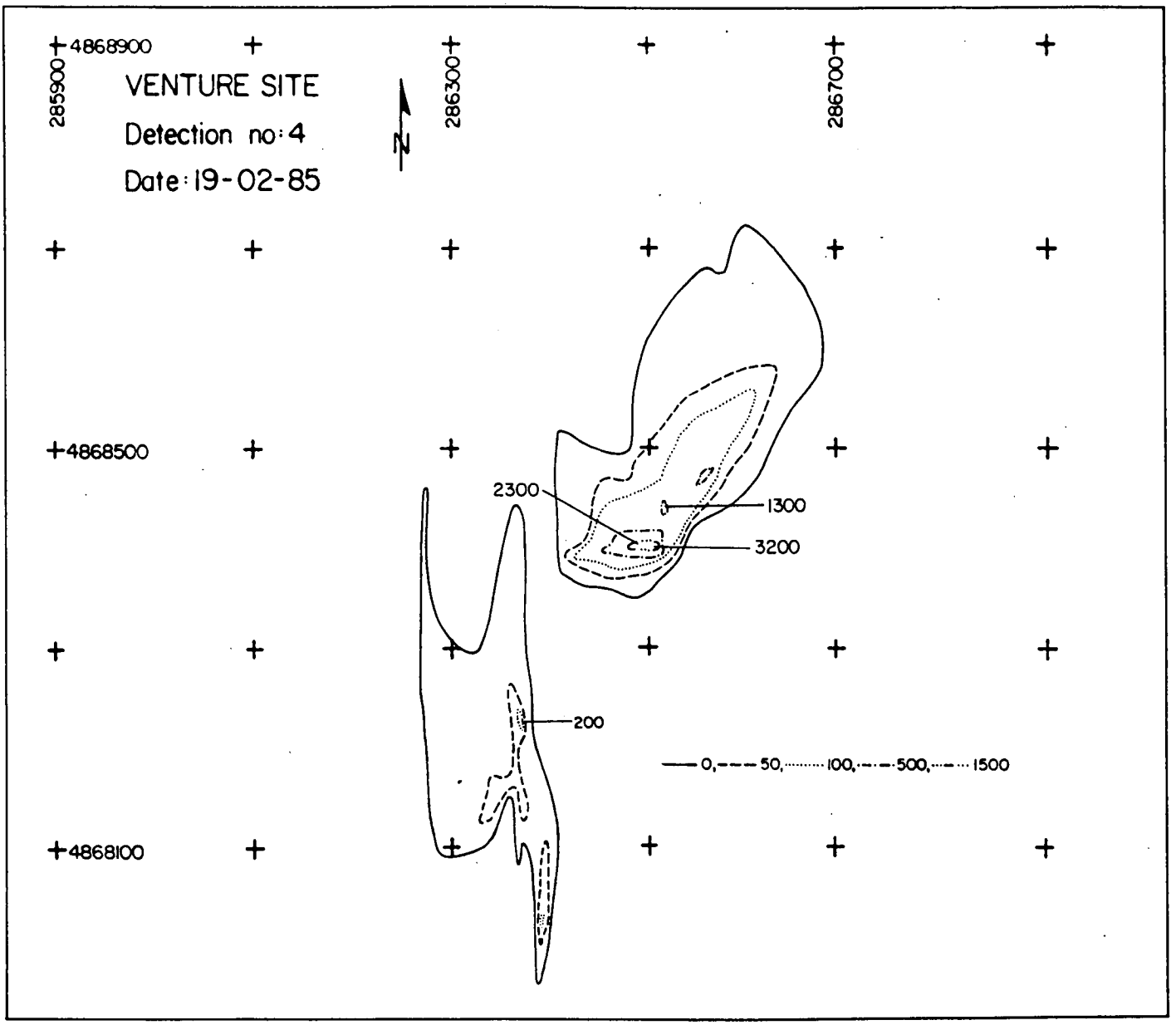

Fig. 4.2.8 Tracer cloud at Venture after detection No. 4.

frequently over 20 knots.

(b) Wave Time-Series

Time-series of significant wave height, reproduced in Appendix 8.3 for the study period, were compiled from wave buoys located at various drilling rigs around Sable Island. On the south side of the island two Waverider sites were operating, Glenelg E-58 and West Venture C-62, which gave a near-continuous wave record close to the Venture site. Two stations, West Venture N-91 and West Venture B-92, provided some data north of Sable Island to give a wave history for the Olympia study site. (see Fig. 4.3.1 for the location of the Waverider sites).

(c) Major Storms

The first major storm to occur after the initial tracer deployment was Hurricane Josephine, which lasted from midnight October 15, 1984 to noon October 19, 1984. This storm had persistant winds of 25 to 35 knots and was properly classified as a moderate gale. The important thing to notice about this storm is that the winds were generally from the East whereas other storms, identified below, have been from the West. The maximum significant wave height at the Venture site was about 6 m with an associated period of 10 to 11 s. This storm was most likely responsible for the southwest dispersal of the tracer during the first deployment period, Sept 28-Oct. 28, 1984 (compare Fig. 4.2.2 with Fig. 4.2.4). The surface analysis chart for Josephine, at about the time of maximum influence on East Bar, is reproduced in Fig. 4.3.2.

No data are available for the wave conditions at the Olympia site but it would have been much more protected from waves by the East Bar.

Smaller storms from the West on Nov. 15 and 18, 1984 created deep water significant wave heights of 5.1 m and 5.3 m respectively.

The winter storm season occurred from the beginning of December 1984 to the end of the experiment in February 1985. There was a large storm in early December and after Dec. 22, 1984 a succession of winter storms until February 15, 1985. Generally, the winter storms were from the southwest - northwest sector. Major characterisitcs of the storms are

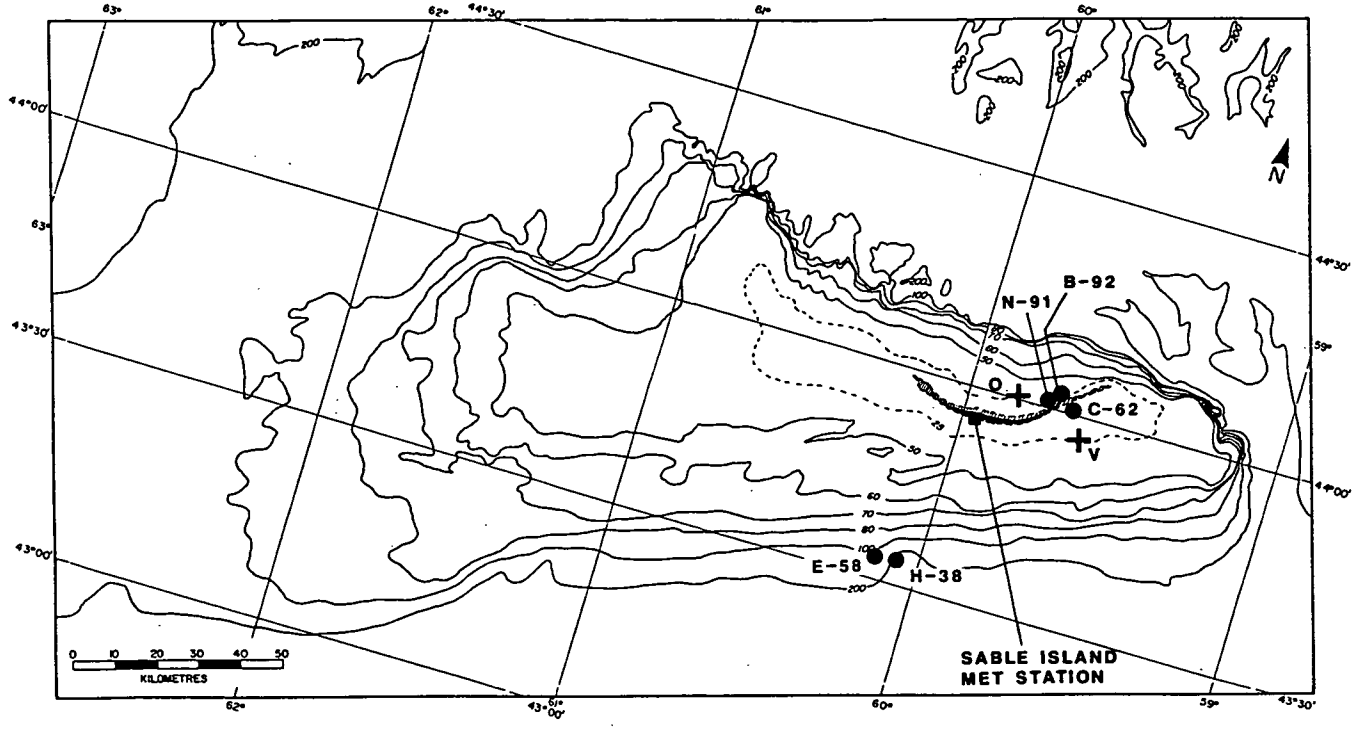

LEGEND

O	OLYMPIA	44°00.58'N 59°51.95'W
V	VENTURE	43°56.37'N 59°38.61'W
E-58	GLENELG	43°37.43'N 60°09.95'W
H-38	GLENELG	43°37.80'N 60°05.30'W
C-62	W. VENTURE	44°01.07'N 59°40.00'W
N-91	W. VENTURE	44°00.77'N 59°44.47'W
B-92	W. VENTURE	44°02.03'N 59°43.55'W

Fig. 4.3.1 Location of Waverider buoys providing data for the radio-isotope experiment.

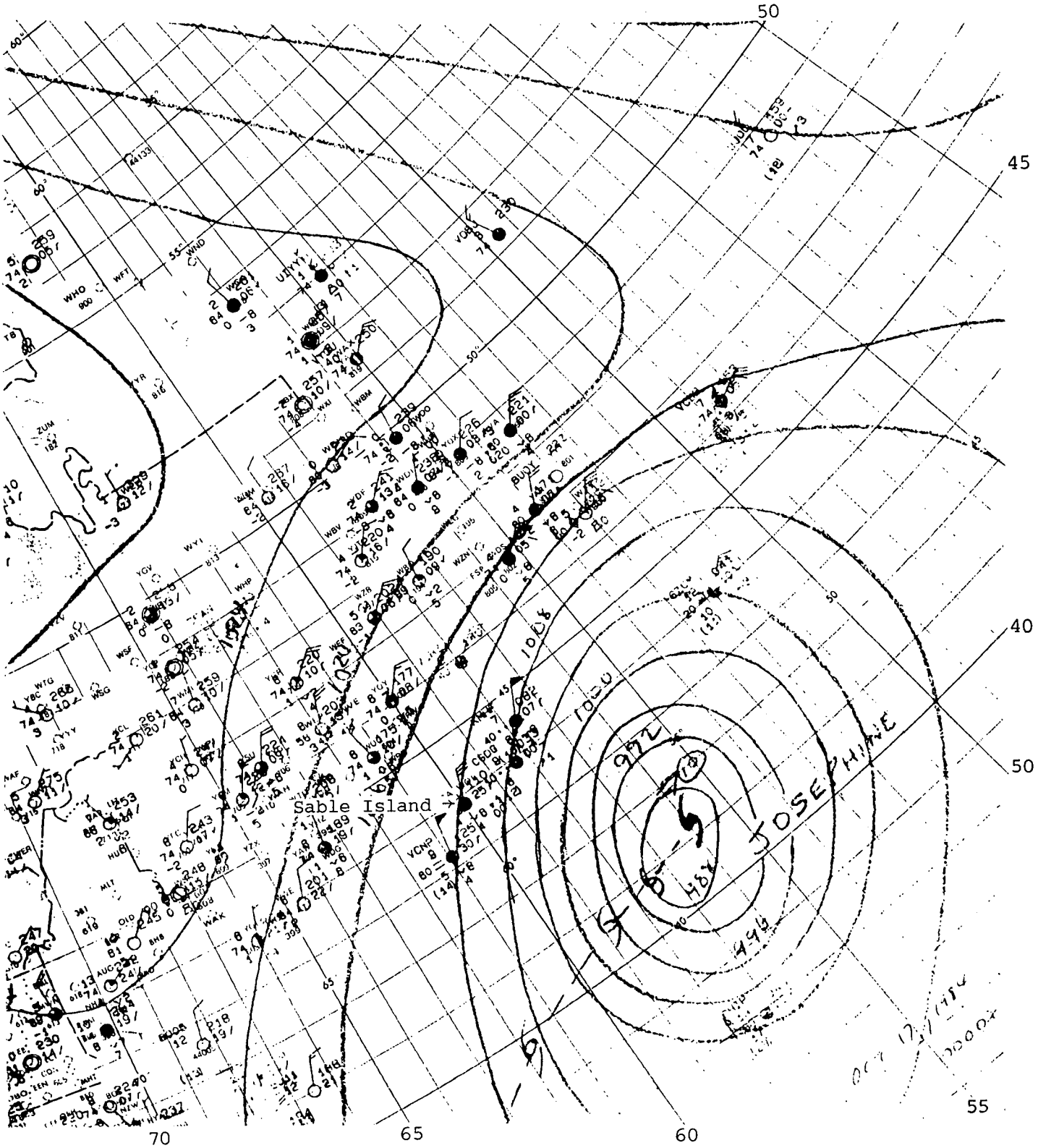

Fig. 4.3.2 Surface weather chart showing the structure of Hurricane Josephine (00:00Z October 17, 1984) with winds of 30 to 50 knots NE on Sable Island.

Venture (43°56.4'N, 59°39.6'W)
Olympia (44°00.4'N, 59°52.0'W)

outlined in Table 4.3.1.

The sediment transport processes at both the study sites appear to be storm dominated. The background current due to tides is insufficent to move the sediment, and it would appear to take storm waves which usually have a significant wave height of over 5 m and the wind-driven current to generate tranport at either site. The Olympia site is more protected and will have smaller wave heights for storms from the northeast through south to the west, than the Venture Site.

Table 4.3.1

Storms at Sable Island During the Radio-Isotope Experiment

Date	Beaufort Storms Classification	Wind Dir. (°T)	Max. Deep Water Sig. Wave Height $(H_S)_{max}$ (m)	Period Assoc. with (H_S) max (S)
16-19 Oct 84	Moderate gale	NE	6.54	10.50
15 Nov 84	Moderate gale	NW	5.14	9.10
18 Nov 84	Moderate gale	NW	5.25	11.38
6 - 8 Dec 84	Fresh gale	E → W	7.69	13.65
22 Dec 84	Fresh gale	SE	4.01	9.75
25-28 Dec 84	Fresh gale	W	6.92	10.50
5 - 8 Jan 85	Strong gale	W	7.81	10.50
9-10 Jan 85	Moderate gale	W	5.74	13.65
12-14 Jan 85	Moderate gale	WNW	4.69	9.10
15-17 Jan 85	Moderate gale	W	6.47	10.50
20-24 Jan 85	Fresh gale	WSW	8.35	11.38
27-29 Jan 85	Moderate gale	W	-	-
13-15 Feb 85	Moderate gale	E → W	5.43	13.65

5.0 DISCUSSION OF RESULTS

5.1 Winter Survey on Sable Island Bank

One result of this study has been to confirm that sediment tracer surveys can be accomplished on the Scotian Shelf during the winter season. This issue was a concern at the planning phase of present study. The success of these winter surveys results from the combination of many factors. The survey ship **M.V. Arctic Prowler** and its crew proved to be capable of working effectively under adverse conditions. One problem particular to radioactive sediment tracer surveys is that they have to be carried on at slow speeds, ideally at 1 m/s (2 knots) although a speed of 3 knots is satisfactory. This was achieved by sailing the survey lines upwind exclusively. Another anticipated problem was the difficulty of maintaining the detection sled on the bottom, since the pitching action of the ship would tend to pull it irregularly along the seabed. The detection sled was ballasted to weigh approximately 100 kg and it was towed with a 120 m long cable. That combination resulted in a well "tuned" damped mechanical system in which the sled acted as the mass of the system, the cable as the spring, and the fluid resistance as the damper. Had the detection sled been lifting off the seafloor, it would had showed up immediately on the analog strip chart records.

5.2 Thickness of the Mobile Sediment Layer

The transport equation developed in Section 3.1 determines the thickness of the mobile sediment layer. This contrasts, for example, the approach taken by Lavelle et al. (1978), where the thickness of the mobile layer was not evaluated specifically. In (3.1.11) the thickness of the mobile layer (E) is a function dependent on three constants and two parameters: the total tracer radiation count measured during the detection (N), and the total radioactivity of the tracer after allowing for decay A(t). A(t) is a well defined parameter and the estimation of the thickness E essentially relies on the ability to measure N correctly.

It is important to consider the sensitivity of this method for determining the thickness E. Equation (3.1.11) shows that E is a non-linear function of the ratio A(t)/N where A(t) is the total

radioactivity of the tracer and N is the activity measured during a specific survey. This relationship is illustrated by the diagram shown in Fig. 5.2.1. For higher values of the ratio N/A(t), the estimate of E is precise but for lower values of N/A(t) the estimation of E becomes unreliable.

Table 5.2.1 summarizes the results of analyzing the tracer cloud data from Sable Island Bank. N/A ratios are shown in the fourth column of the table. The thickness results for Olympia are quite erratic but those for Venture site are consistent.

A fifth cruise aboard **C.S.S. Dawson** was organised by the Atlantic Geoscience Centre of the Geological Survey of Canada (C.L. Amos) in October 1985 to locate whatever radioactive tracer was left at Venture, 13 months after injection of the initial 1.5 kg of radioactive glass. By that time the radioactivity was reduced to 2.47 per cent of its original level. The radioactive tracer was located and cored using a vibrocorer. The core was logged using an integration interval of 100 s at a threshold of 50 kev. The results showed a maximum concentration of tracer between 10 and 20 cm below the seafloor (Drapeau, 1986). This direct verification of depth of mixing of the tracer within the mobile sediment layer is assumed to be representative of the traction layer of sediments considering the length of time that the tracer was present at the site and had been subjected to a complete cycle of seasonal conditions.

5.3 Mean Velocity of the Mobile Sediment Layer

Comparisons of the tracer surveys described in chapter 4 show a very complex evolution and movement of the tracer clouds at each site. The movement of the clouds is schematized in Fig. 5.3.1. Both study sites, Olympia and Venture, are shown on the same figure to illustrate the difference between the two sites; the centroid of the tracer cloud moved little at Olympia while it moved considerable distances at Venture. The figure also shows the locations of highest concentrations of tracer as they were surveyed.

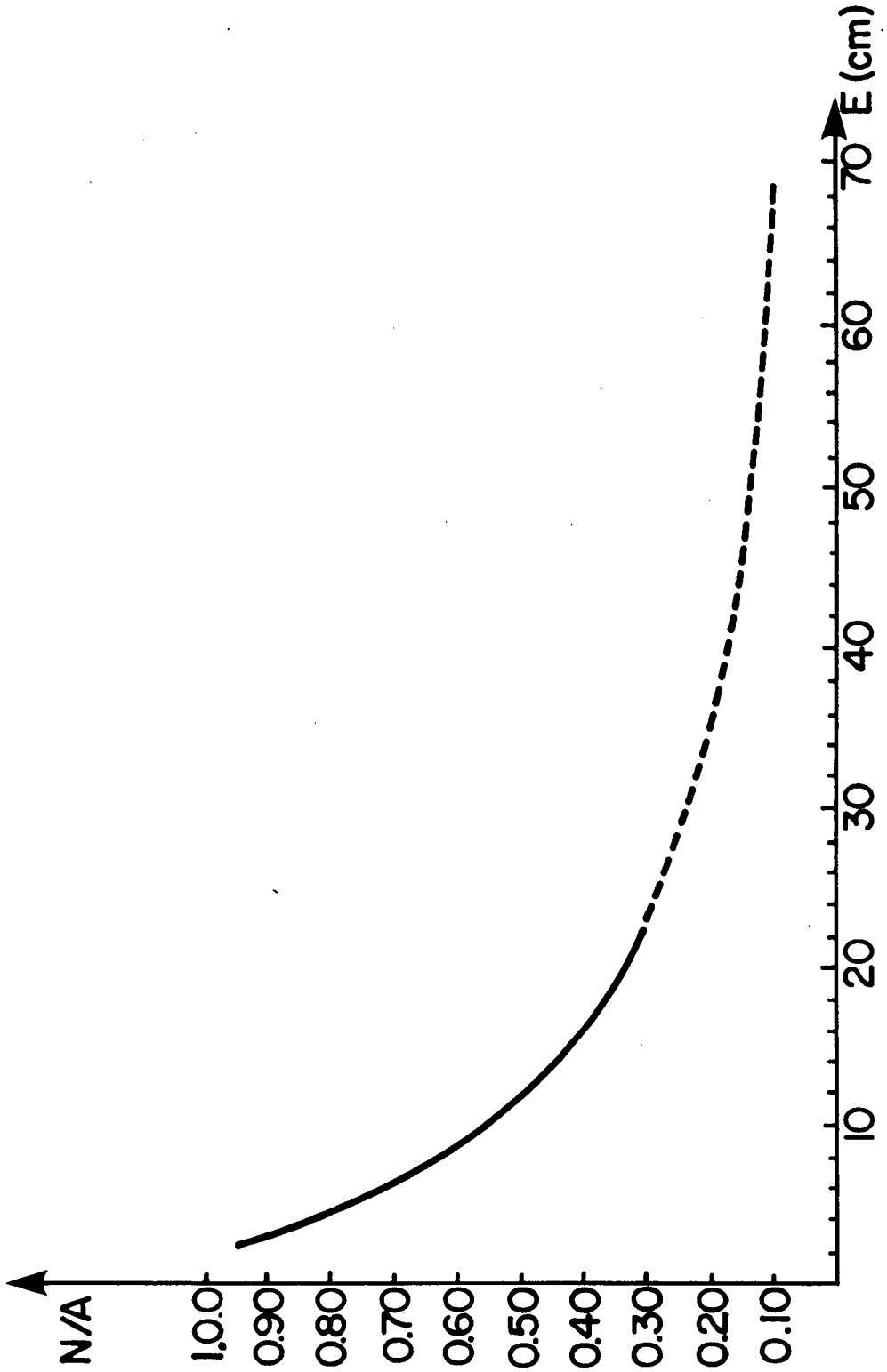

Fig. 5.2.1 Graph of ratio N/A (N: detected activity; A: total activity) versus the depth E, of tracer within the sediment. It outlines the sensitivity of the method used to determine the thickness of the sediment mobile layer.

Table 5.2.1

Mobile Sediment Layer Thickness

Site Detection	Total Activity A (counts)	Measured Activity N (counts)	N/A (%)	Mobile Layer Thickness (cm)
Olympia				
1	96,258,600	1,834,701	1.90	-
2	74,155,466	7,669,618	10.34	66.98*
3	34,223,262	965,197	2.82	245.63*
4	24,931,583	411,757	1.65	419.46*
Venture				
1	91,839,180	5,402,102	5.88	-
2	70,753,098	33,897,820	47.91	12.70
3	32,652,249	8,346,988	25.56	27.85
4	23,787,377	7,519,920	31.60	21.91

* unreliable data, see Fig. 5.2.1

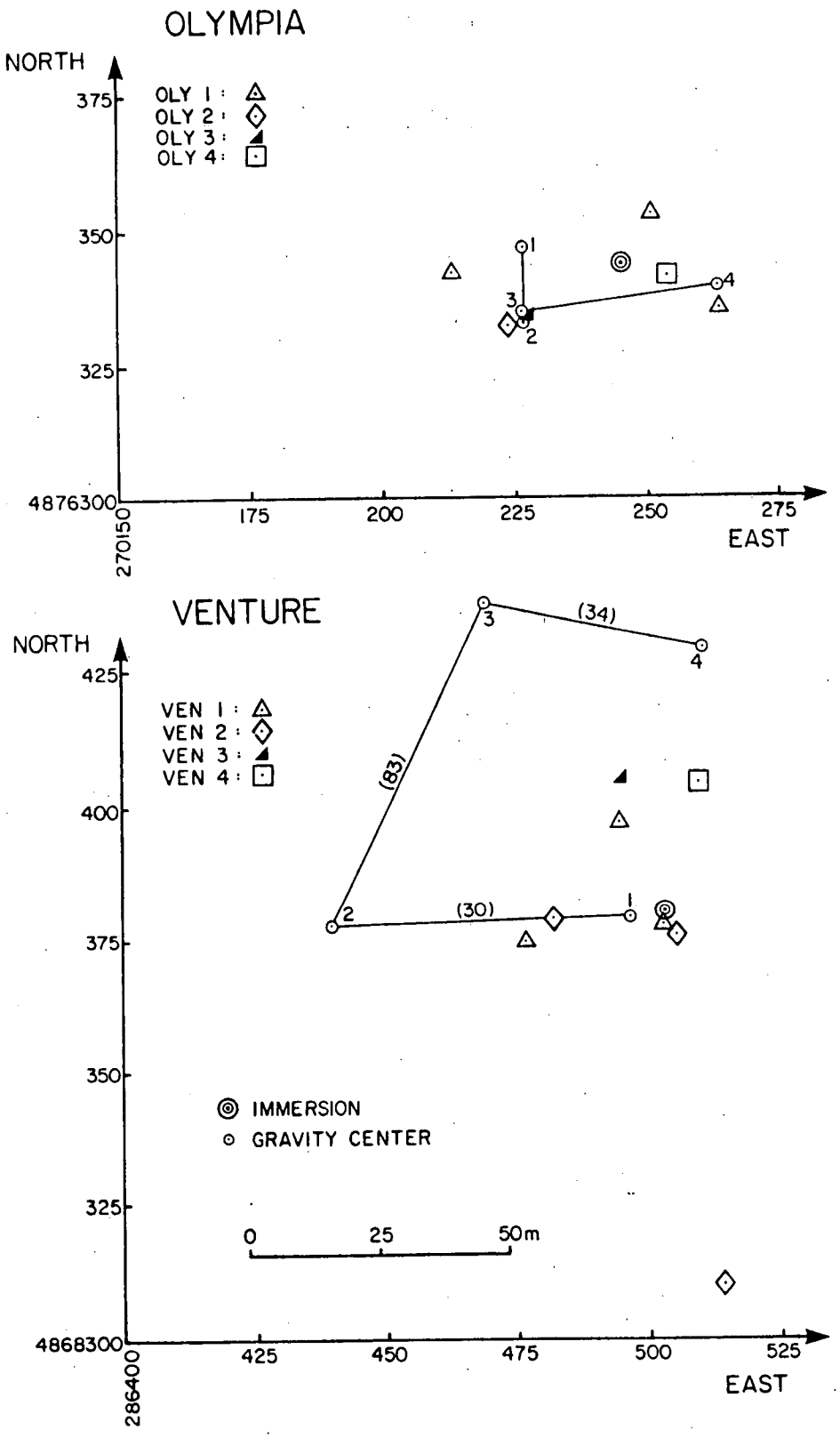

Fig. 5.3.1 Locations of the tracer immersion positions, the peak concentration points, and the centroids of each cloud. The numbers in brackets indicate the number of days between surveys. Both sites are to the same scale and use UTM coordinates.

Olympia Site: The first survey at Olympia showed three tracer concentration points distributed about the positioned immersion point as shown in Fig. 5.3.1. The peak concentration points for detections 2 and 3 were closest to the highest concentration point of detection 1. The figure also shows that the centroid of the tracer cloud hardly moved during the time between the first three surveys. As explained before, the tracer cloud location for the fourth survey is questionable because of the low tracer level obtained for that detection.

Venture Site: The three high tracer concentration points of detection 1, the two high points of detection 2, and the high tracer concentration for detections 3 and 4 are shown in the lower panel of Fig. 5.3.1. The two high concentration points of detection 2 are very close to two concentration points of detection 1 and some of these points are juxtaposed on the immersion point of the tracer. These small positional differences are well within the limits of navigation accuracy. The tracer source is thus interpreted to have been stationary at Venture as well as at Olympia. Tracer source stationarity has also been observed by other workers; for instance those of the Commissariat a l'Energie Atomique (A. Caillot, CEA pers. comm., 1985) and Lavelle et al. (1978).

As already explained in section 3.1.1 the movement of the centroid of the tracer cloud is one key parameter to determine the sediment transport rate. At Venture, the centroid of the tracer cloud has moved similar distances from one survey to the next, although the time interval between the surveys is not the same.

5.4 Sediment Transport Rates

Olympia: The most striking result here is that the centroid of the tracer cloud moved little during the whole experiment. This most likely results from the choice of a coarser tracer to match the lag sand present at that location and the sheltering afforded by Sable Island. Not surprisingly, the tracer behaved like that coarser lag sand and did not move much. It is also possible that the tracer had been partly covered by the finer sand winnowing over the Olympia area. Partial

Table 5.3.1

Sediment Transport Rates

Site Detection	Mass Velocity (m/day)	Area (m^2)	Transport (kg/m/hr)	Transport (m^3/m/hr)
Olympia				
1-2	0.429	1523-4884	-	-
2-3	0.0241	4884-3791	-	-
3-4	0.235	3791-2746	-	-
Venture				
1-2	2.29	7772-61,543	18.23	10.13×10^{-3}
2-3	0.666	61,543-67,846	16.78	9.32×10^{-3}
3-4	1.95	67,846-91,018	20.27	11.26×10^{-3}

burial may, for example, have made detection of the peak concentration point in survey 4 very difficult. Hence the centroid position would be very uncertain also.

The sensitivity test for the calculation of the mobile layer thickness E indicates that the results for Olympia shown in Table 5.2.1 are unreliable. Combined with the fact that the tracer hardly moved at Olympia, it is not possible to determine reliable transport rates for that site.

Venture: The movement of the tracer is important at Venture site; the tracer was dispersed over a wide area and the centroid of the tracer cloud moved considerable distances from its source as shown in Fig. 5.3.1.

Calculations of sediment transport rates for Venture are summarized in Table 5.3.1. The transport rates are uniform throughout the experiment. A transport rate of 20.27 kg/m/hr, taking the density of the mobile traction sediment layer as 1.8 g/cm^3 is equivalent to 98.64 m^3/m/yr. These transport rates are long term averages. In fact, the transport of sediments is expected to be quite episodic with rates proportional to the third to the sixth power of the nearbed flow velocity. This implies that sediment transport is very intense during storms, with rates perhaps one to two orders of magnitude larger than the mean value measured with tracers (see also Drapeau and Long, 1984).

5.5 Direction of Sediment Transport

The direction of sediment transport as measured by radioactive tracers follows the path of the centroid of the tracer cloud during the experiment (Fig. 5.3.1). Thus when interpreting the direction of transport it should be borne in mind that if transport has been in more than one direction in the interval between two detections, only the net result is measured by the change of location of the centroid of the tracer. Moreover, if the tracer has been moved in many directions it is likely that it will be dispersed over a wide area.

In the Sable Island area storm generated currents and waves are obvious

agents causing sediment transport. The combined action of wave agitation and wind-generated currents would generally be oriented with the forcing wind field. It is reasonable to link changes in sediment transport direction to storm events in the wind and wave records.

For example, it has been found that the direction of sediment transport is westward at Venture between the first survey (25 Sept. 1984) and the second one (26 Oct. 1984). According to wave height records available, the major event during that period occured when characteristic wave heights in shallow water reached 5.5 m on October 16 and then gradually fell to 4 m by October 19. (See e.g. Station 142, West Venture C-62, located between Venture and Sable Island). These waves were generated by the tropical hurricane Josephine and would have progressed westward over the survey site on October 16th. As the tracer had been injected shortly before the storm, it was prone to move and to become dispersed over a very large area (61,543 m^2 at the Venture site).

Subsequently the movement at Venture changed direction and the centroid moved northeastward between the second (26 Oct. 1984) and the third survey (17 Jan. 1985). The direction of transport cannot be linked to one major event during that interval but rather to many winter storms that almost continuously succeed each other during that season (see Table 4.3.1). Partial wave records at station 142 show events of 6 metre characteristic wave heights and wind records from Sable Island indicate that 20 to 30 knot winds blow mostly from the west during the winter. The southwesterly exposure of Venture to storm winds and waves is consistent with the observed transport direction. The sediment transport direction shifted east between the third (17 Jan. 1985) and the fourth survey (19 Feb. 1985) at Venture. The probable transport direction at Olympia site between the third and the fourth survey is eastward, similar to that at the Venture site.

5.6 Bedload And Suspended Load Transport Processes

The experiments on Sable Island Bank were planned to study primarily the bedload transport at the two sites. Furthermore the experiments at each location were designed with somewhat different perspectives in mind. The

grain size of the glass used as tracer was chosen at Olympia to match the 0.4-0.6 mm lag sand which had a median grain size of 0.5 mm. At Venture the median grain size of the glass used is 0.37 mm. This difference in tracer grain size has produced substantially different results for the two experimental sites, the most obvious being that the tracer moved greater distances at Venture than at Olympia.

Tracers integrate all sediment transporting processes that are active between surveys. The tracer cloud patterns thus represent the physical manifestation of the natural processes at work which may include movement along the bed and in suspension.

One parameter examined to illustrate the relative importance of bedload versus suspended load transport is the area covered by the tracer as a function of its radioactivity shown in Fig. 5.6.1. The diagrams for Olympia and Venture are drawn at the same scale to indicate the difference between the two tracer clouds. The larger grain size and less severe forcing conditions at the Olympia site contribute to the very much smaller movement and dispersal there. The relative compactness of the tracer cloud pattern at Olympia site is one criterion with which to recognize bedload transport. Conversely we expect that the dispersal of the tracer, being one order of magnitude larger at Venture, is due to suspension of the tagged grains. This would account for transport over longer distances. The dispersal of tracer at the Venture site agrees well with NOAA experiments on the Long Island inner shelf (Lavelle et al., 1978). These authors report that for their spring-summer experiment the time sequence shows diffusive growth of the radioactive cloud pattern but little advection. In that case, the cloud covered an area of some 29,000 m^2, 69 days after the beginning of the experiment. During the fall-winter experiment on the inner Long Island shelf the radioactive cloud covered 251,000 m^2, 36 days after the beginning of the experiment. In this latter case, Lavelle and his colleagues also identified elliposidal patterns of some contours as advective features.

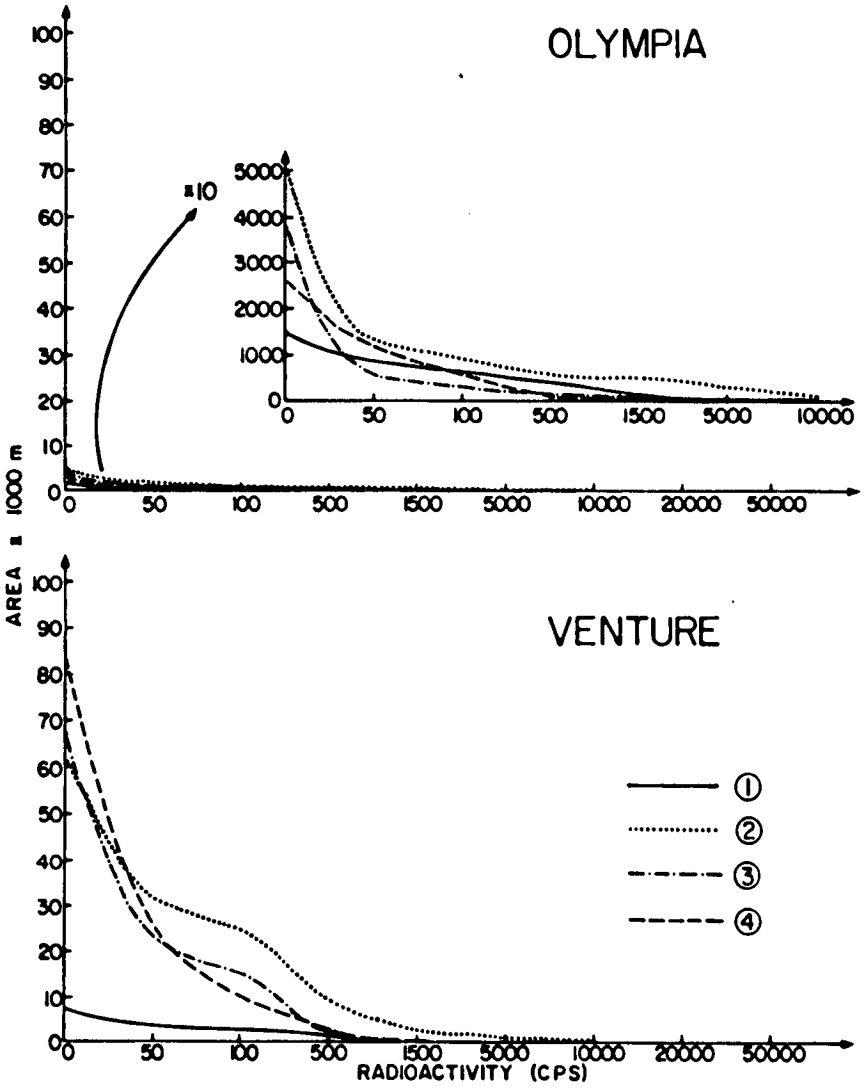

Fig. 5.6.1 Area distribution as a function of radioactivity above natural level. The figure shows for a given detection the area covered by each level of radioactivity. The same scale is used for both sites and the insert on the Olympia graph is enlarged ten times.

6.0 CONCLUSIONS AND RECOMMENDATIONS

The radio-isotope tracing experiment reported here represents the first attempt to directly measure bedload transport rates on Sable Island Bank. It was also the first time tracing techniques have been used in such an energetic and difficult working environment. With respect to the original objectives the following conclusions have been reached.

On Sand Transport

1) The coarse sand lag layer at Olympia is comparatively stable under winter storm conditions. Transport rates were negligible and cloud dispersion produced by material suspension appeared to be very small. Mean transporting velocities were of the order of 0.2 to 0.4 m/day. The medium sand layer (0.3 to 0.45 mm median diameter--not tagged) may be more mobile as evidenced by some suspected burial of the tagged lag layer.

2) The fine sand ($D_{50} \sim 0.17$ to 0.20 mm) layer at Venture was tagged with 0.37 mm sand tracer. Considerable net movement of the cloud and dispersion of tracer grains was measured. Mean transporting velocities ($\sim$ one month averages) were of the order of 1 to 2 m/day. Calculated and cored mobile layer thicknesses of 10 to 30 cm gave sand transport rates of 17 to 20 kg/m/hr. Maximum transport rates in storms are expected to be up to one order of magnitude greater.

3) Transport directions at Venture appear correlated to wind and wave directions.

On the tracer method

1) It is possible to conduct radio-isotope experiments on Sable Island Bank in winter provided surveys are carried out between storms. Navigation with systems such as Syledis set up on Sable Island give satisfactory ship positioning accuracy; however, a range-bearing system to position the sled relative to the ship, within ± 5 m, is manditory. The ORE Trackpoint instrument proved to be satisifactory in the present experiment.

2) The sensitivity of the transport model to the precision with which

the tracer cloud is mapped on all surveys demands complete, accurate surveying procedures. The objective is to account for all the tracer in each survey. Inaccurate surveys lead to exceedingly unrealistic mobile layer depths. This proved to be the case at Olympia. There the lag layer was tagged, and it is possible that finer sands intermittently covered the tracer. The results appear much more reasonable at Venture and it is concluded that the tracer there remained in the fine-sand ridge over the lag layer without being covered by deposited sand.

3) The selection of tracer grain size is crucial. The glass injected at Venture was more closely matched to a coarser lag (0.4 mm) than to the finer sand ridge material (0.15 - 0.20 mm), and this may give unrepresentatively low transport rates for the finer material. Detailed size distributions were not available prior to this study so that the size mismatch was unexpected.

Recommendations

The study reported here has provided initial estimates of sand mobility at sites with different exposures and different seabed geologies on Sable Island Bank. The tracer techniques were carried out with equipment and procedures applied in the past mainly in the littoral zone under much less difficult working conditions. The accuracy of results is limited here by a number of factors, including positioning, vertical tracer distributions in the surficial sediments, and grain size distributions for the tracer material. Several recommendations can be made to improve future tracer studies.

1) A reasonably comprehensive knowledge of the surficial geology at each site is required in order to design the tracer. Specifically the material properties comprising the mobile layer--grain size distributions and specific gravities--must be known, distinctly from those same properties for underlying lag deposits. The objectives are to tag mobile layers in preference to stable lag layers, and in this way avoid interpretation difficulty due to possible burial, and to give a precise match of tracer to mobile material.

2) Scintillometer positioning relative to the ship with accuracies of

±5 m is desirable. Ship positioning with a similar accuracy is necessary to ensure adequate positional accuracy for the individual track lines. Acoustic devices such as the ORE Trackpoint between the scintillometer sled and the ship are recommended for all surveys. Also adequate time must be allowed to complete a survey at sea under less than ideal conditions since the accuracy of the results is directly related to how well N (total radiation count) can be measured within each survey. In areas like Sable Island this can amount to 18 to 24 operational hours.

3) Quantitative transport estimates depend on a measure of how far the tracer grains are mixed into the seabed materials (the dimension E). It can be calculated as described above or measured by coring in the cloud. It is recommended that the capacity for coring and measuring E be available on each detection survey in future studies using radioactive tracers.

7.0 REFERENCES

Ackers, P. and W.R. White, 1973. Sediment Transport: New Approach and Analysis. Jour. Hydr. Division, ASCE, 99, (HY11), November, 2041-2060.

Alquier, M., G. Courtois, G. Gruat et G. Sauzay, 1970. La notion de bon mélange dans l'emploi de traceurs (Vitesse débitantet vetesse du cêntre de gravit d'un nuage de traceurs dans l'étude d'un coulement). Houille Blanche, 25(7), 643-650.

Amos, C.L. and E.L. King, 1984. Bedforms of the Canadian Eastern Seaboard: A Comparison with Global Occurrences. Marine Geology, 57, 167-208.

Amos, C., D. Hodgins, G. Drapeau and B. Long, 1985. Sand Transport Measurements Around Sable Island - a Shelf Edge, Tidal Environment. Symposium on modern and ancient clastic deposits. State University of Utrecht, 26-28 Aug. 1985.

Anguenot, M., A. Caillot et G. Courtois, 1968. Utilisation de traceurs radioactifs à l'étude sédimentologique de Lac de Maracaibo. CEA Internal Report DR/SAR.S/68-7/GC/JJ.

Caillot, A., 1970. Les méthodes de marquage des sédiments par des indicateurs radioactifs. Houille Blanche, 25(7), 661-674.

Cameron, H.L., 1965. The Shifting Sands of Sable Island. Geogr. Rev., 55(4), 463-476.

Courtois, G. et G. Souzay, 1970. Les masses de sédiments à injecter dans une expérience de traceurs radioactifs en sédimentologie dynamique. Houille Blanche, 25(7), 629-642.

Davison, A., 1984. A Pre-Dredging Sand Mobility Study using a Radioisotope Tracer. Proc. 19th Coastal Eng. Conf., ASCE, 2063-2076.

Drapeau, G., 1986. Radio-Isotope Tracer and Near-Bed Current Study in the Sable Island Area. Unpublished Manuscript, INRS-Océanologie, 34pp.

Drapeau, G. and B. Long, 1984. Measurements of Bedload Transport in the Nearshore Zone Using Radioisotopic Sand Tracers. Proc. 19th Coastal Eng. Conf., ASCE, 1252-1264.

Duane, D.B., 1970. Tracing Sand Movement in the Littoral Zone; Progress in the Radioisotopic Sand Tracer (RIST) Study, July 1968-February 1969. US Army Corps of Engineers, Coastal Engineering Center, MP4-70.

Duane, D.B. and W.R. James, 1980. Littoral Transport in the Surf Zone Elucidated by an Eulerian Sediment Tracer Experiment. Jour. Sed. Petrology, 50, 929-942.

Katoh, K., N. Tanaka, T. Kondoh, M. Akaishi and K. Terasaki, 1985. Field Observation of Local Movements in the Surf Zone Using Fluorescent Sand Tracer (second report). Rept. Port and Harbour Research Institute of Japan, 24, 63 pp.

King, L.H., 1970. Surficial Geology of the Halifax-Sable Island map area. Marine Science Paper 1, Ottawa, 16 pp.

King, L.H., 1980. Aspects of Regional Surficial Geology Related to Site Investigation Requirements -- Eatern Canadian Shelf. in Offshore Site Investigation, (Ardus, D.A., Ed.), Graham & Trotman Ltd. London, 291 pp.

King, L.H. and G.B. Fader, 1985. Wisconsinan Glaciation of the Continental Shelf -- Southeast Atlantic Canada. GSC Open File Report, 126.

Lavelle, J.W., D.J.P. Swift, D.E. Gadd, W.L. Stubblefield, F.N. Case, H.R. Brashear and K.W. Haff, 1978. Fair Weather and Storm Sand Transport on the Long Island, New York, Inner Shelf. Sedimentology, 25, 823-842.

Long, B.N.F., 1986. Techniques de Tracage, Chapter 4 In Bottom Sediment Transport - Present Knowledge and Industry Needs, ESRF Report No. 027, Ottawa, Canada.

Sauzay, G., 1967. Méthode de bilan des taux de comptage d'indicateurs radioactifs pour la determination de debit de charriage de lits dablelux. Thèse Doctoral, Toulouse, 162 pp.

Tola, F., 1982. The Use of Radioactive Tracers in Dynamic Sedimentolgy. Note CEA-N-2261, 162 pp.

Vincent, C.E., R.A. Young and D.J.P Swift, 1982. On the Relationship Between Bedload and Suspended Sand Transport on the Inner Shelf, Long Island, New York. J. Geophys. Res., 87(66), 4164-4170.

8.0 APPENDICES

Appendix 8.1 Bottom Sample Data

WENTWORTH SOIL CLASSIFICATION

UNIFIED SOIL CLASSIFICATION

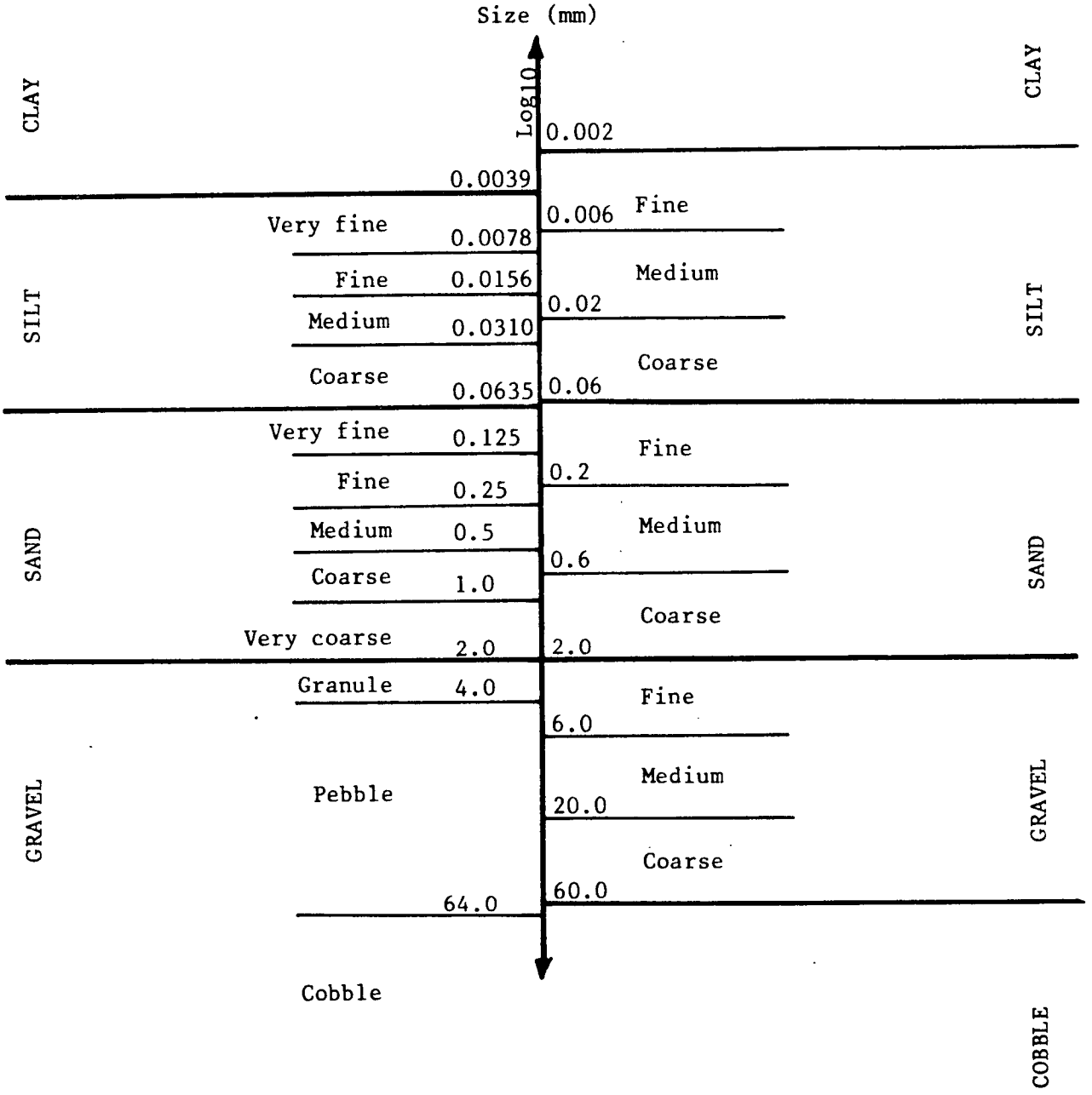

Seaconsult

Marine Research Ltd.

Seaconsult Marine Research Ltd.

GRAIN SIZE CURVE

CLIENT:	
PROJECT NUMBER:	
LAB. NUMBER:	
LOCATION:	Grab #1 Olympia
HOLE:	SAMPLE:
DEPTH:	
TECHNICIAN:	DATE:

COBBLES	GRAVEL SIZES		SAND SIZES			SILT	CLAY
	COARSE	FINE	COARSE	MEDIUM	FINE		

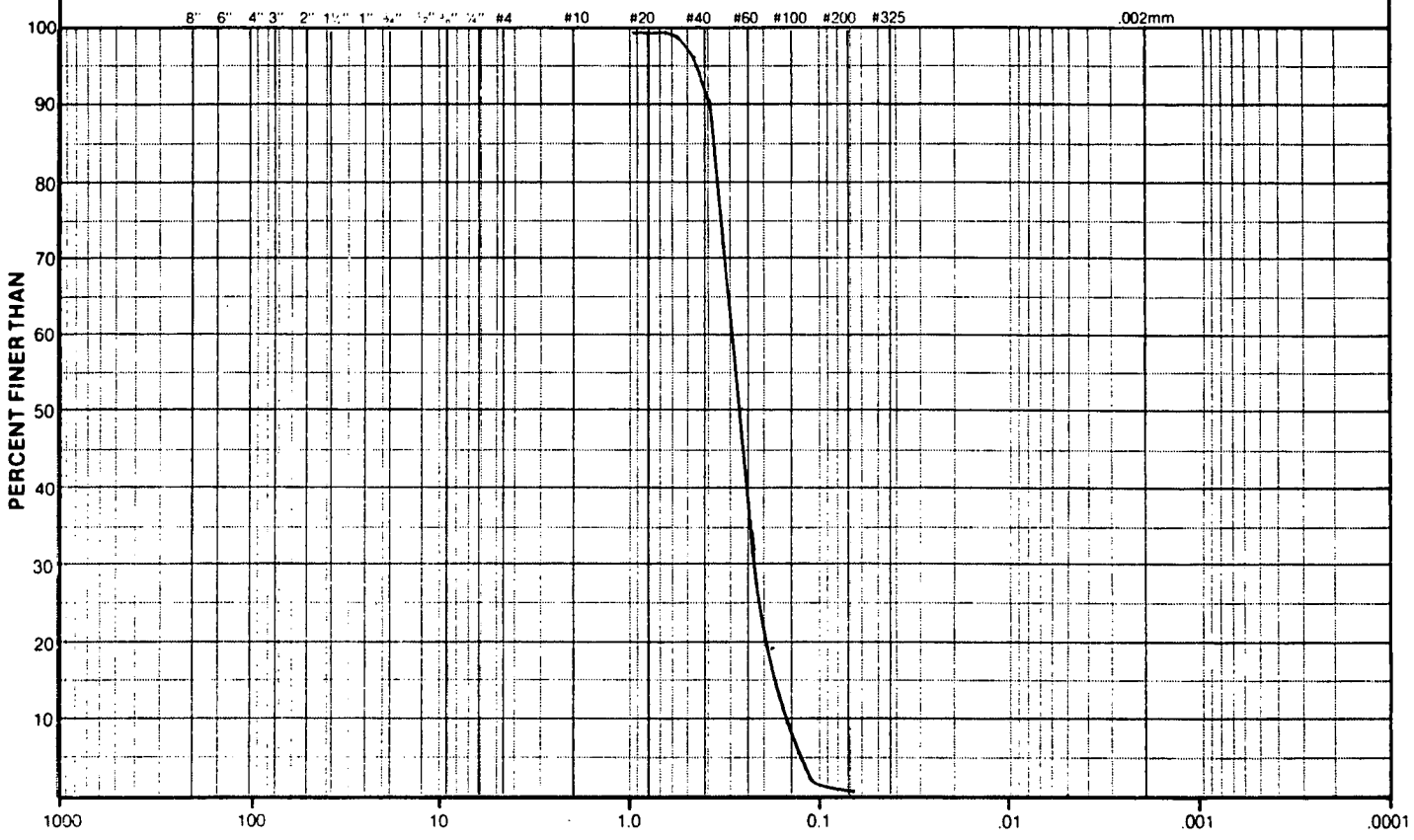

REMARKS: D_{50} = 0.28 mm , D_{90} = 0.30 mm

NOTE: UNIFIED SOIL CLASSIFICATION SYSTEM

SUMMARY

D_{10} =	mm	GRAVEL	0.10 %
D_{30} =	mm	SAND	98.80 %
D_{60} =	mm	SILT	0.55 %
C_U =	mm	CLAY	0.55 %
C_C =	mm		

Seaconsult Marine Research Ltd.

GRAIN SIZE CURVE

CLIENT:	
PROJECT NUMBER:	
LAB. NUMBER:	
LOCATION:	Grab #7 Olympia
HOLE:	SAMPLE:
DEPTH:	
TECHNICIAN:	DATE:

COBBLES	GRAVEL SIZES		SAND SIZES			SILT	CLAY
	COARSE	FINE	COARSE	MEDIUM	FINE		

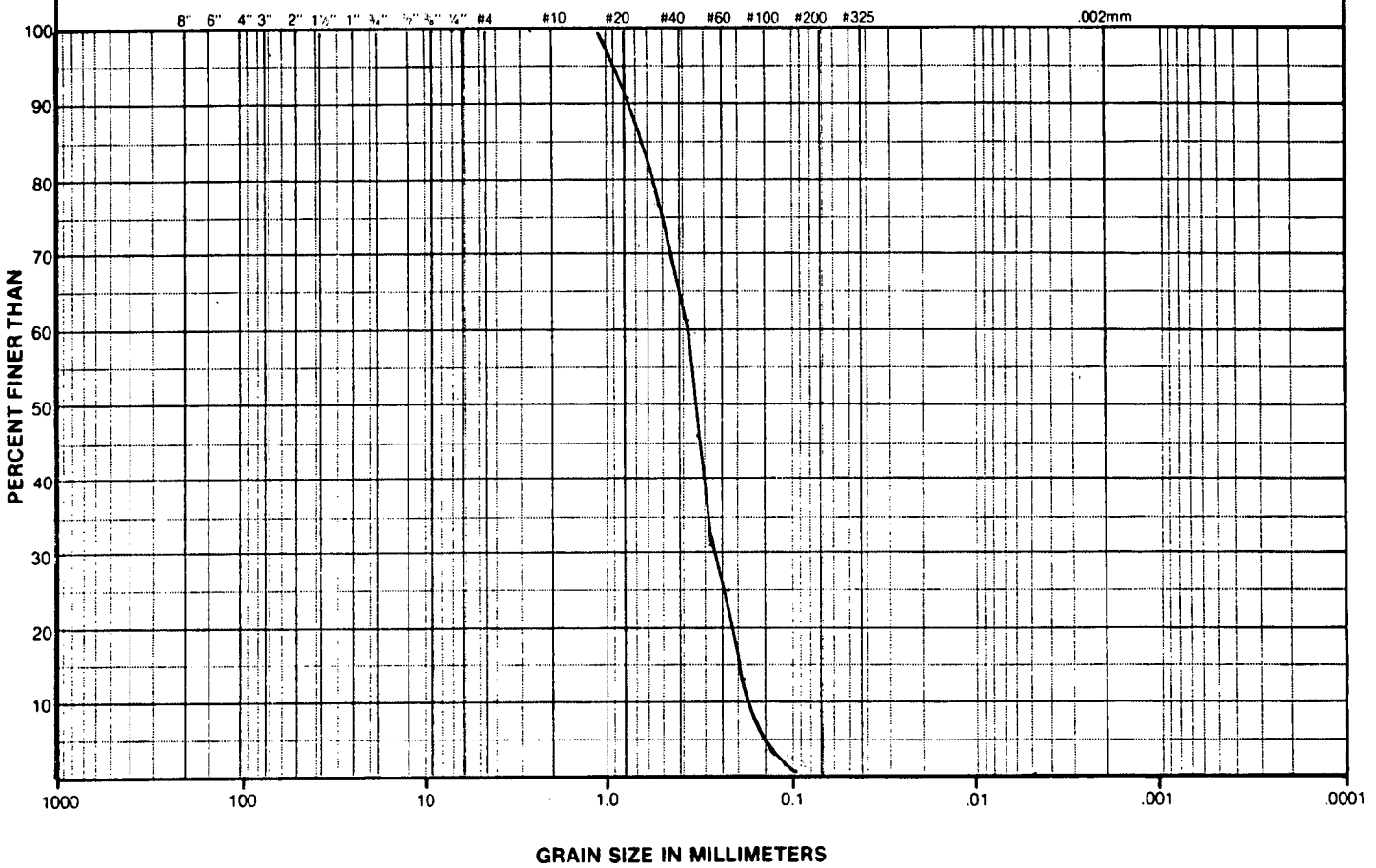

REMARKS: D_{50}= 0.38 mm , D_{90}= 0.78 mm

NOTE: UNIFIED SOIL CLASSIFICATION SYSTEM

SUMMARY

D_{10} =	mm	GRAVEL	0.20 %
D_{30} =	mm	SAND	98.90 %
D_{60} =	mm	SILT	0.45 %
C_U =	mm	CLAY	0.45 %
C_C =	mm		

Seaconsult Marine Research Ltd.

GRAIN SIZE CURVE

CLIENT:	
PROJECT NUMBER:	
LAB. NUMBER:	
LOCATION:	Grab #8 Olympia
HOLE:	SAMPLE:
DEPTH:	
TECHNICIAN:	DATE:

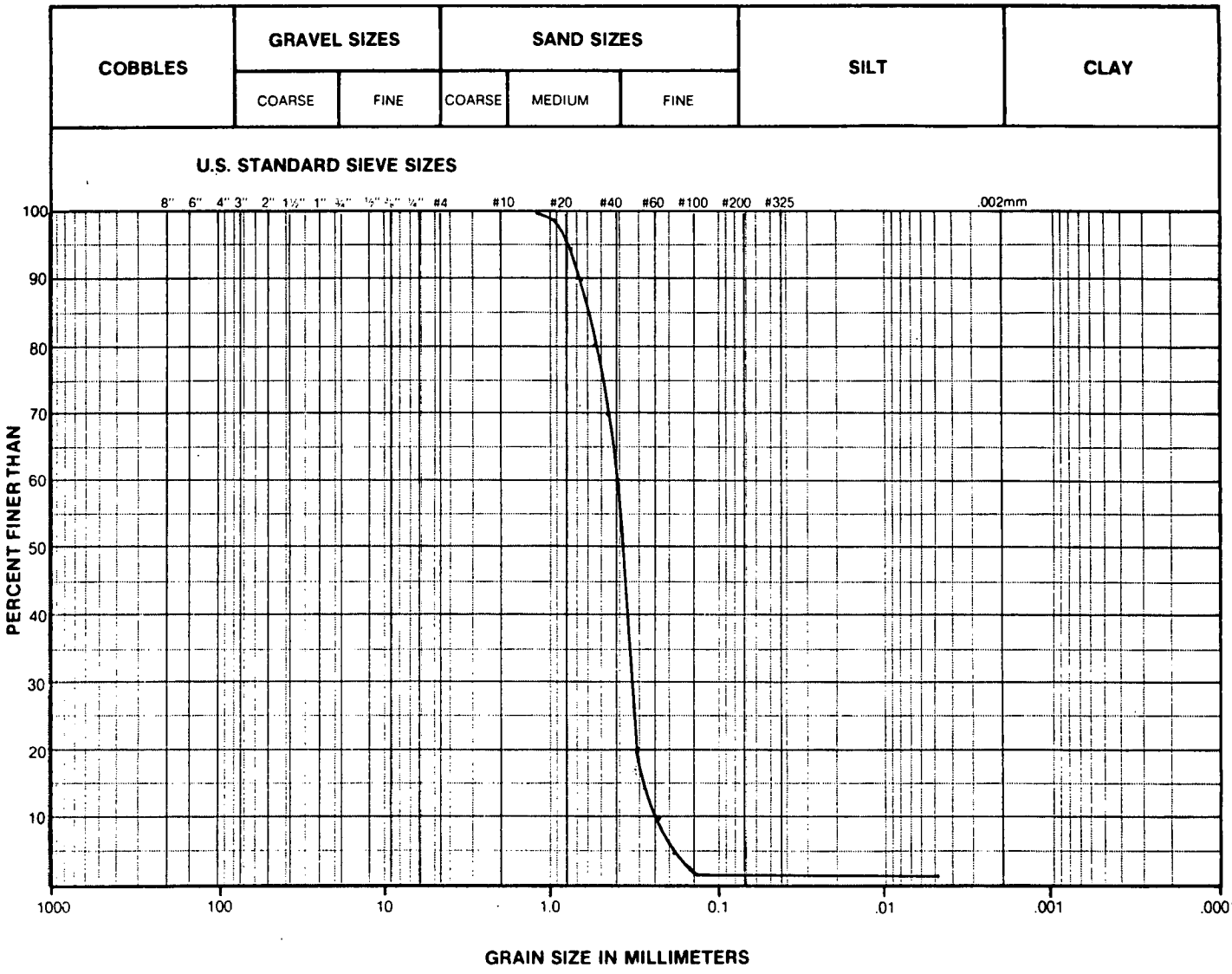

REMARKS: D_{50} = 0.40 mm , D_{90} = 0.69 mm

NOTE. UNIFIED SOIL CLASSIFICATION SYSTEM

SUMMARY

D_{10} =	mm	GRAVEL	0.30 %
D_{30} =	mm	SAND	98.80 %
D_{60} =	mm	SILT	0.45 %
C_U =	mm	CLAY	0.45 %
C_C =	mm		

Seaconsult Marine Research Ltd.

GRAIN SIZE CURVE

CLIENT:	
PROJECT NUMBER:	
LAB. NUMBER:	
LOCATION:	Grab #9 Olympia
HOLE:	SAMPLE:
DEPTH:	
TECHNICIAN:	DATE:

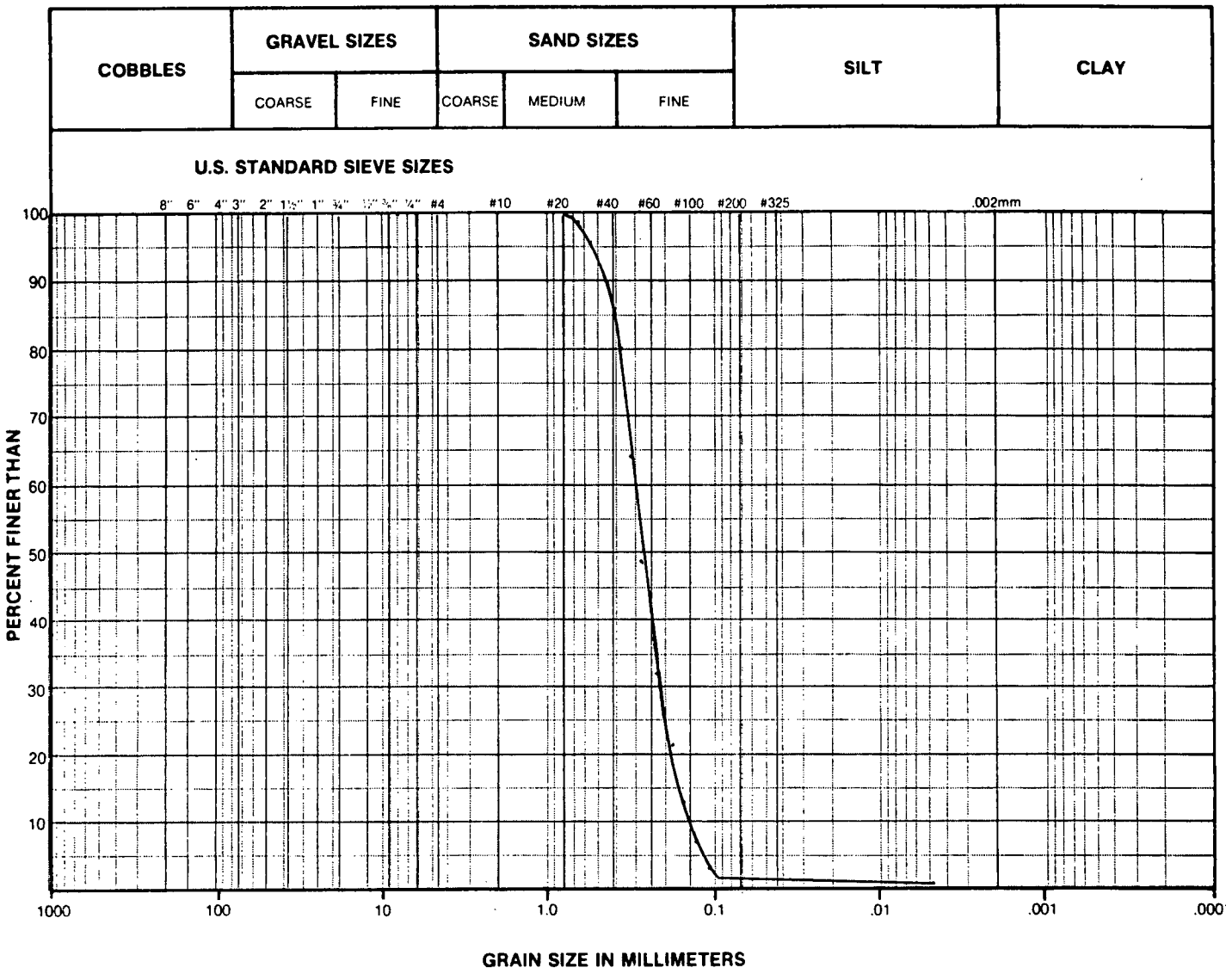

REMARKS: D_{50} = 0.27 mm , D_{90} = 0.45 mm

NOTE: UNIFIED SOIL CLASSIFICATION SYSTEM

SUMMARY

D_{10} =	mm	GRAVEL	0.30 %
D_{30} =	mm	SAND	98.50 %
D_{60} =	mm	SILT	0.60 %
C_U =	mm	CLAY	0.60 %
C_C =	mm		

Seaconsult Marine Research Ltd.

GRAIN SIZE CURVE

CLIENT:	
PROJECT NUMBER:	
LAB. NUMBER:	
LOCATION:	Grab #10 Olympia
HOLE:	SAMPLE:
DEPTH:	
TECHNICIAN:	DATE:

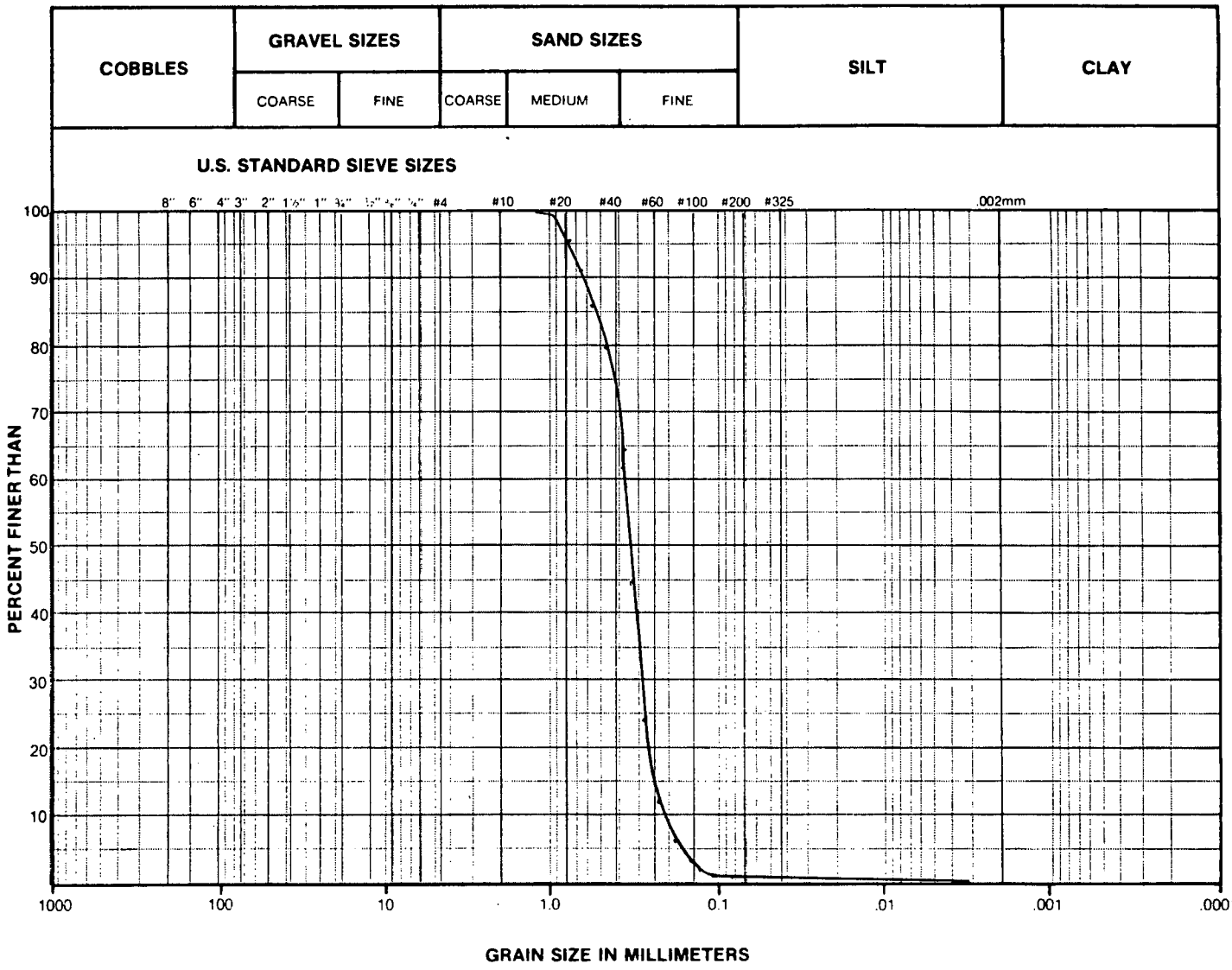

REMARKS: D_{50}= 0.34 mm , D_{90}= 0.63 mm

NOTE: UNIFIED SOIL CLASSIFICATION SYSTEM

SUMMARY

D_{10} =	mm	GRAVEL	0.10 %
D_{30} =	mm	SAND	98.91 %
D_{60} =	mm	SILT	0.59 %
C_U =	mm	CLAY	0.40 %
C_C =	mm		

Seaconsult Marine Research Ltd.

GRAIN SIZE CURVE

CLIENT:	
PROJECT NUMBER:	
LAB. NUMBER:	
LOCATION:	Grab #2 Venture
HOLE:	SAMPLE:
DEPTH:	
TECHNICIAN:	DATE:

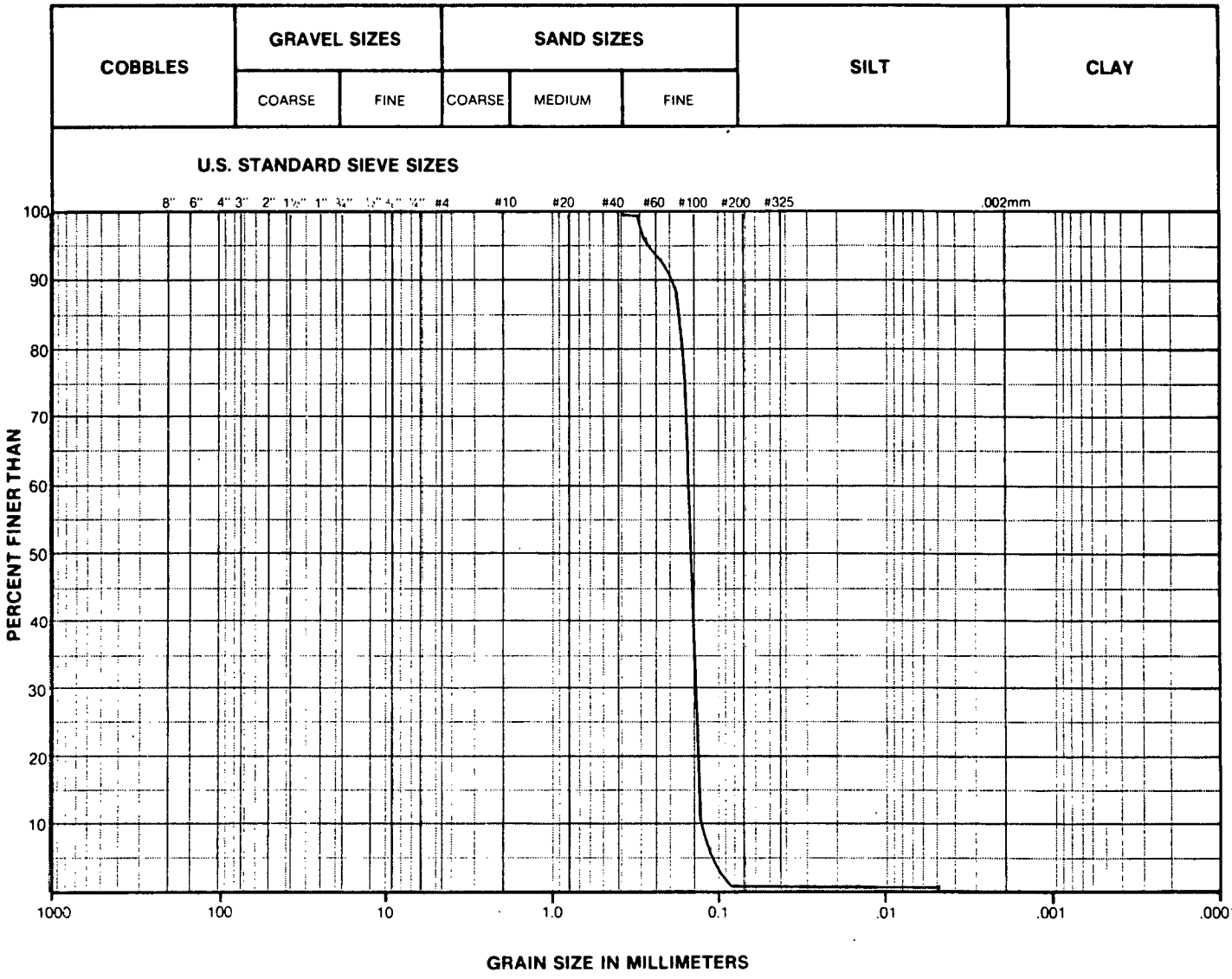

REMARKS: D_{50} = 0.15 mm , D_{90} = 0.20 mm

NOTE: UNIFIED SOIL CLASSIFICATION SYSTEM

SUMMARY

D_{10} =	mm	GRAVEL	0.10 %
D_{30} =	mm	SAND	98.57 %
D_{60} =	mm	SILT	0.78 %
C_U =	mm	CLAY	0.55 %
C_C =	mm		

Seaconsult Marine Research Ltd.

GRAIN SIZE CURVE

CLIENT:	
PROJECT NUMBER:	
LAB. NUMBER:	
LOCATION:	Grab #3 Venture
HOLE:	SAMPLE:
DEPTH:	
TECHNICIAN:	DATE:

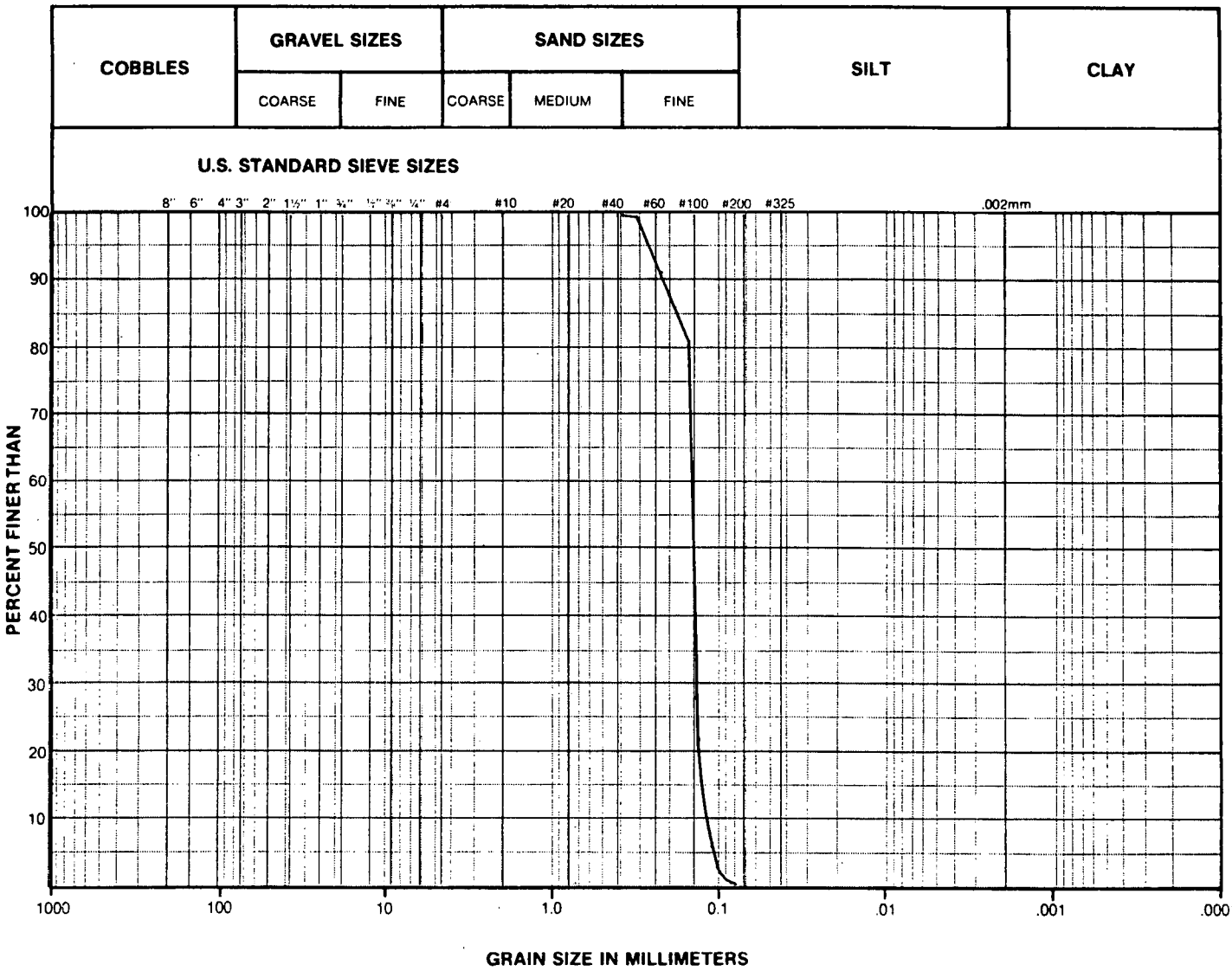

REMARKS: D_{50} = 0.15 mm , D_{90} = 0.16 mm

NOTE: UNIFIED SOIL CLASSIFICATION SYSTEM

SUMMARY

D_{10} =	mm	GRAVEL	0.00 %
D_{30} =	mm	SAND	99.00 %
D_{60} =	mm	SILT	0.50 %
C_U =	mm	CLAY	0.50 %
C_C =	mm		

Seaconsult Marine Research Ltd.

GRAIN SIZE CURVE

CLIENT:	
PROJECT NUMBER:	
LAB. NUMBER:	
LOCATION:	Grab #4 Venture
HOLE:	SAMPLE:
DEPTH:	
TECHNICIAN:	DATE:

COBBLES	GRAVEL SIZES		SAND SIZES			SILT	CLAY
	COARSE	FINE	COARSE	MEDIUM	FINE		

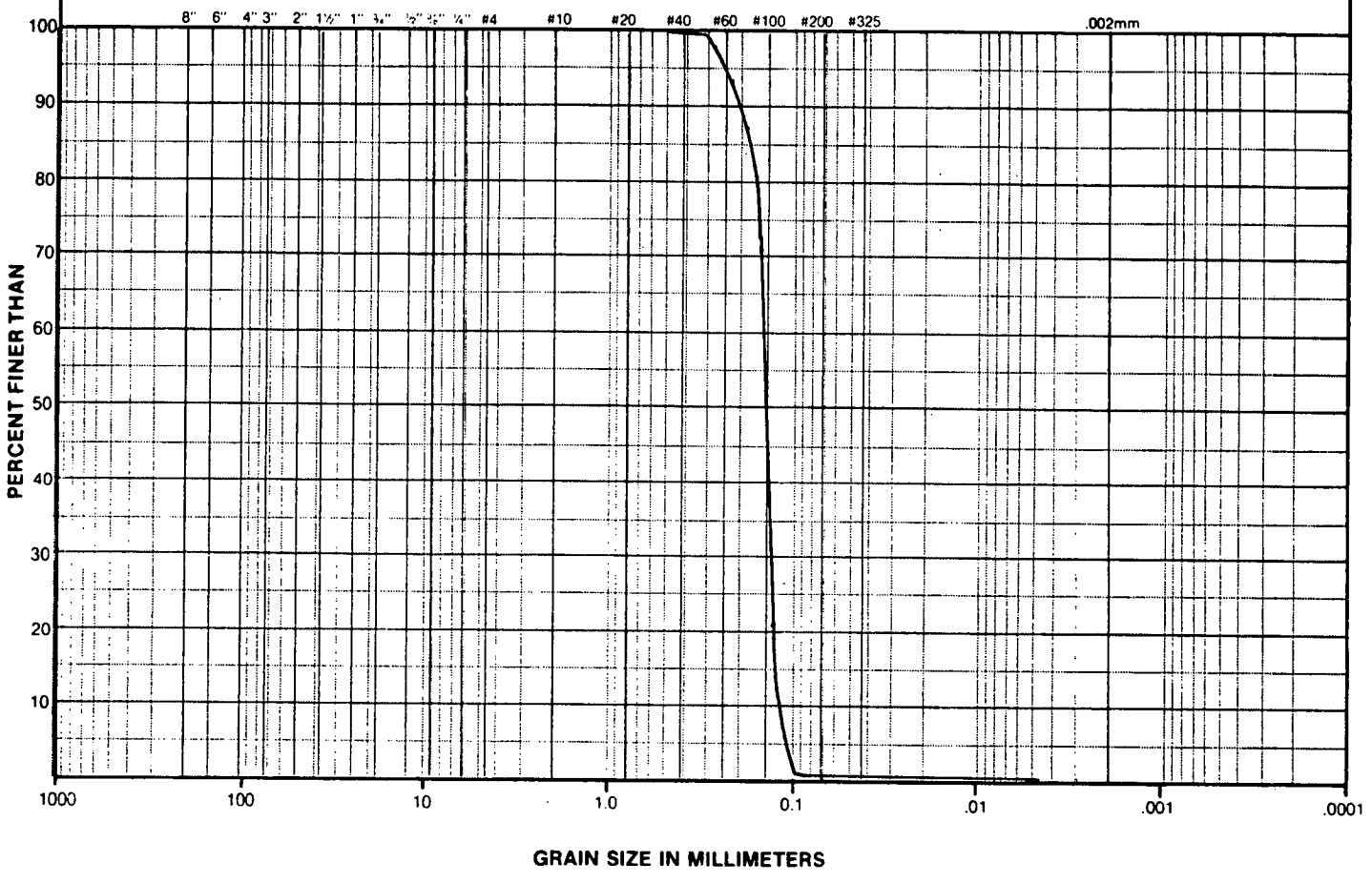

REMARKS: D_{50} = 0.15 mm , D_{90} = 0.20 mm

NOTE: UNIFIED SOIL CLASSIFICATION SYSTEM

SUMMARY

D_{10} =	mm	GRAVEL	0.00 %
D_{30} =	mm	SAND	99.10 %
D_{60} =	mm	SILT	0.45 %
C_U =	mm	CLAY	0.45 %
C_C =	mm		

Seaconsult Marine Research Ltd.

GRAIN SIZE CURVE

CLIENT:	
PROJECT NUMBER:	
LAB. NUMBER:	
LOCATION:	Grab #5 Venture
HOLE:	SAMPLE:
DEPTH:	
TECHNICIAN:	DATE:

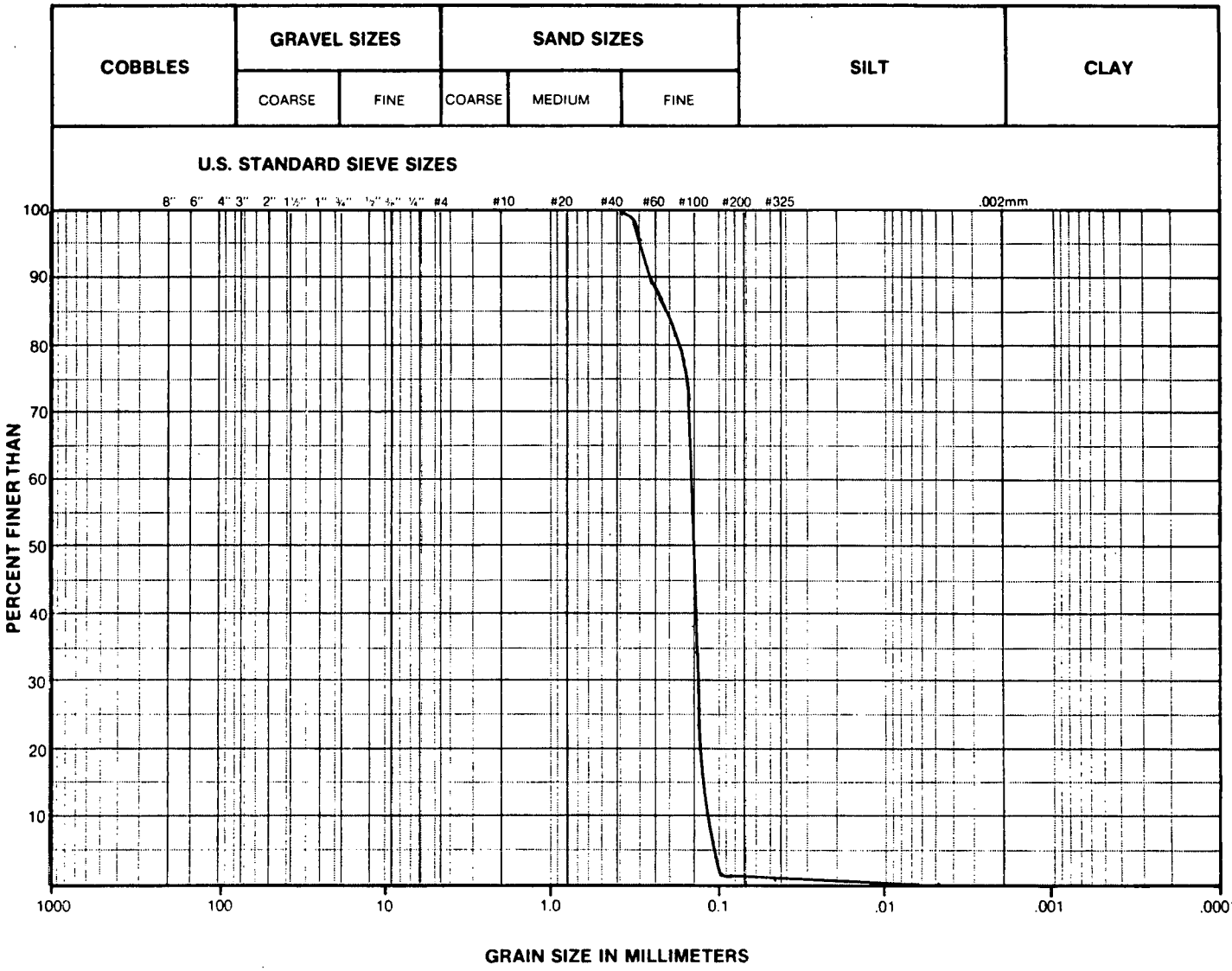

REMARKS: D_{50}= 0.15 mm , D_{90}= 0.26 mm

NOTE UNIFIED SOIL CLASSIFICATION SYSTEM

SUMMARY

D_{10} =	mm	GRAVEL	0.00 %
D_{30} =	mm	SAND	98.84 %
D_{60} =	mm	SILT	0.71 %
C_U =	mm	CLAY	0.45 %
C_C =	mm		

Seaconsult Marine Research Ltd.

GRAIN SIZE CURVE

CLIENT:	
PROJECT NUMBER:	
LAB. NUMBER:	
LOCATION:	Grab #6 Venture
HOLE:	SAMPLE:
DEPTH:	
TECHNICIAN:	DATE:

COBBLES	GRAVEL SIZES		SAND SIZES			SILT	CLAY
	COARSE	FINE	COARSE	MEDIUM	FINE		

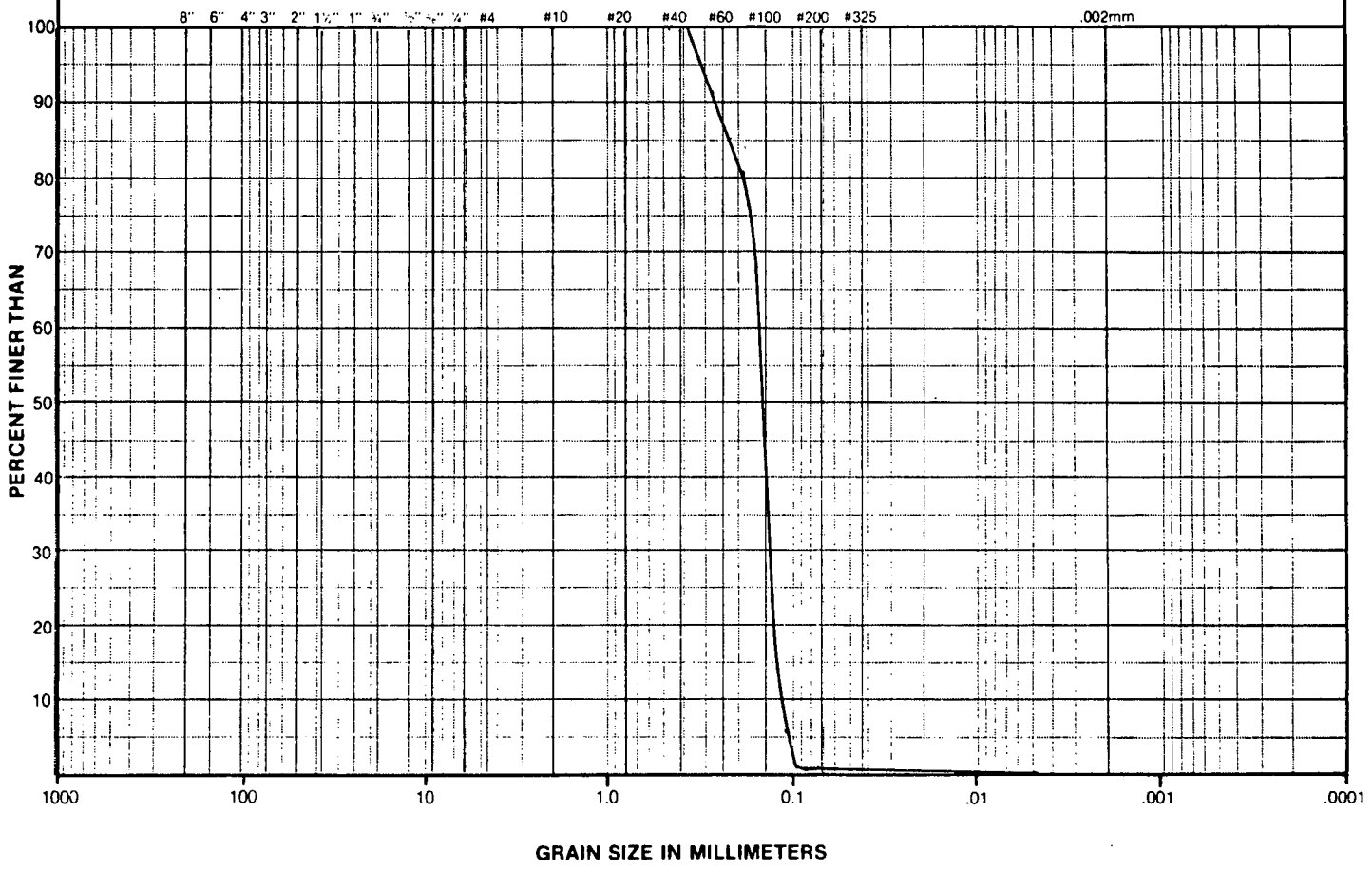

REMARKS: D_{50} = 0.15 mm , D_{90} = 0.27 mm

NOTE: UNIFIED SOIL CLASSIFICATION SYSTEM

SUMMARY

D_{10} =	mm	GRAVEL	0.10 %
D_{30} =	mm	SAND	99.00 %
D_{60} =	mm	SILT	0.45 %
C_U =	mm	CLAY	0.45 %
C_C =	mm		

Seaconsult Marine Research Ltd.

GRAIN SIZE CURVE

CLIENT:	
PROJECT NUMBER:	
LAB. NUMBER:	
LOCATION:	Grab #11 Venture
HOLE:	SAMPLE:
DEPTH:	
TECHNICIAN:	DATE:

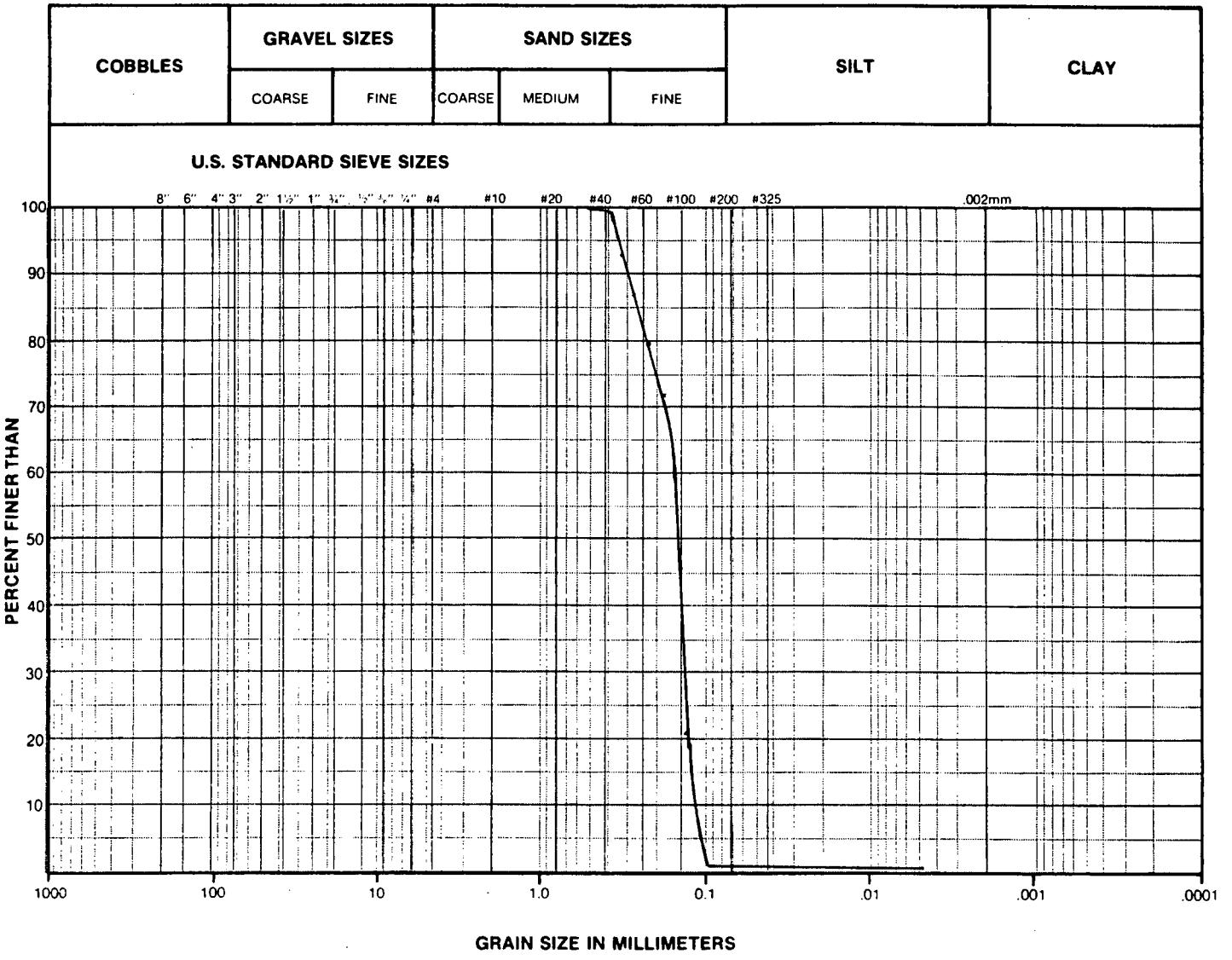

REMARKS: D_{50} = 0.16 mm , D_{90} = 0.30 mm

NOTE: UNIFIED SOIL CLASSIFICATION SYSTEM

SUMMARY

D_{10} =	mm	GRAVEL	0.10 %
D_{30} =	mm	SAND	98.66 %
D_{60} =	mm	SILT	0.74 %
C_U =	mm	CLAY	0.50 %
C_C =	mm		

Seaconsult Marine Research Ltd.

GRAIN SIZE CURVE

CLIENT:	
PROJECT NUMBER:	
LAB. NUMBER:	
LOCATION:	Grab #12 Venture
HOLE:	SAMPLE:
DEPTH:	
TECHNICIAN:	DATE:

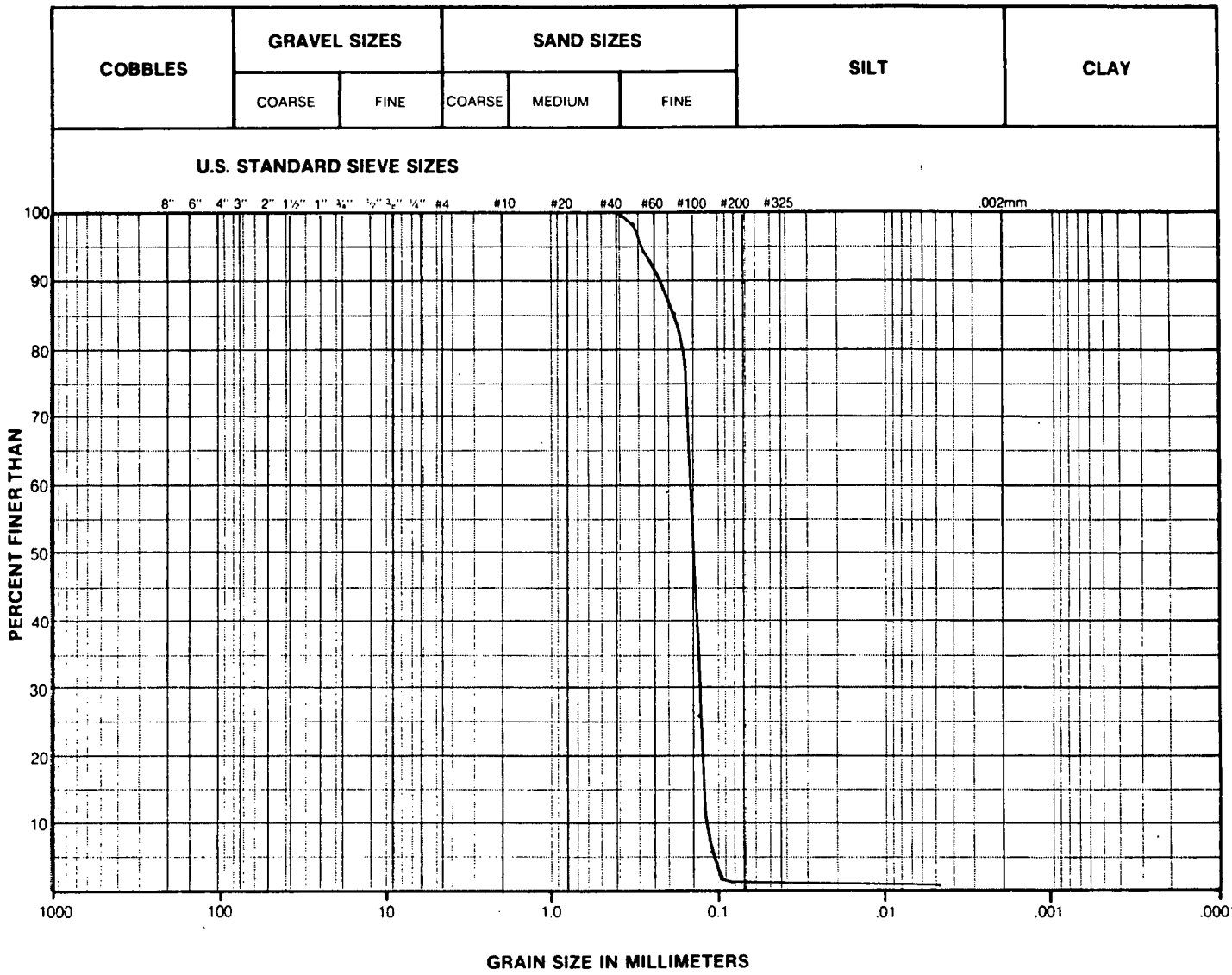

REMARKS: D_{50} = 0.15 mm , D_{90} = 0.23 mm

NOTE: UNIFIED SOIL CLASSIFICATION SYSTEM

SUMMARY

D_{10} =	mm	GRAVEL	0.20 %
D_{30} =	mm	SAND	98.70 %
D_{60} =	mm	SILT	0.55 %
C_U =	mm	CLAY	0.55 %
C_C =	mm		

Seaconsult Marine Research Ltd.

GRAIN SIZE CURVE

CLIENT:	
PROJECT NUMBER:	
LAB. NUMBER:	
LOCATION:	Grab #13 Venture
HOLE:	SAMPLE:
DEPTH:	
TECHNICIAN:	DATE:

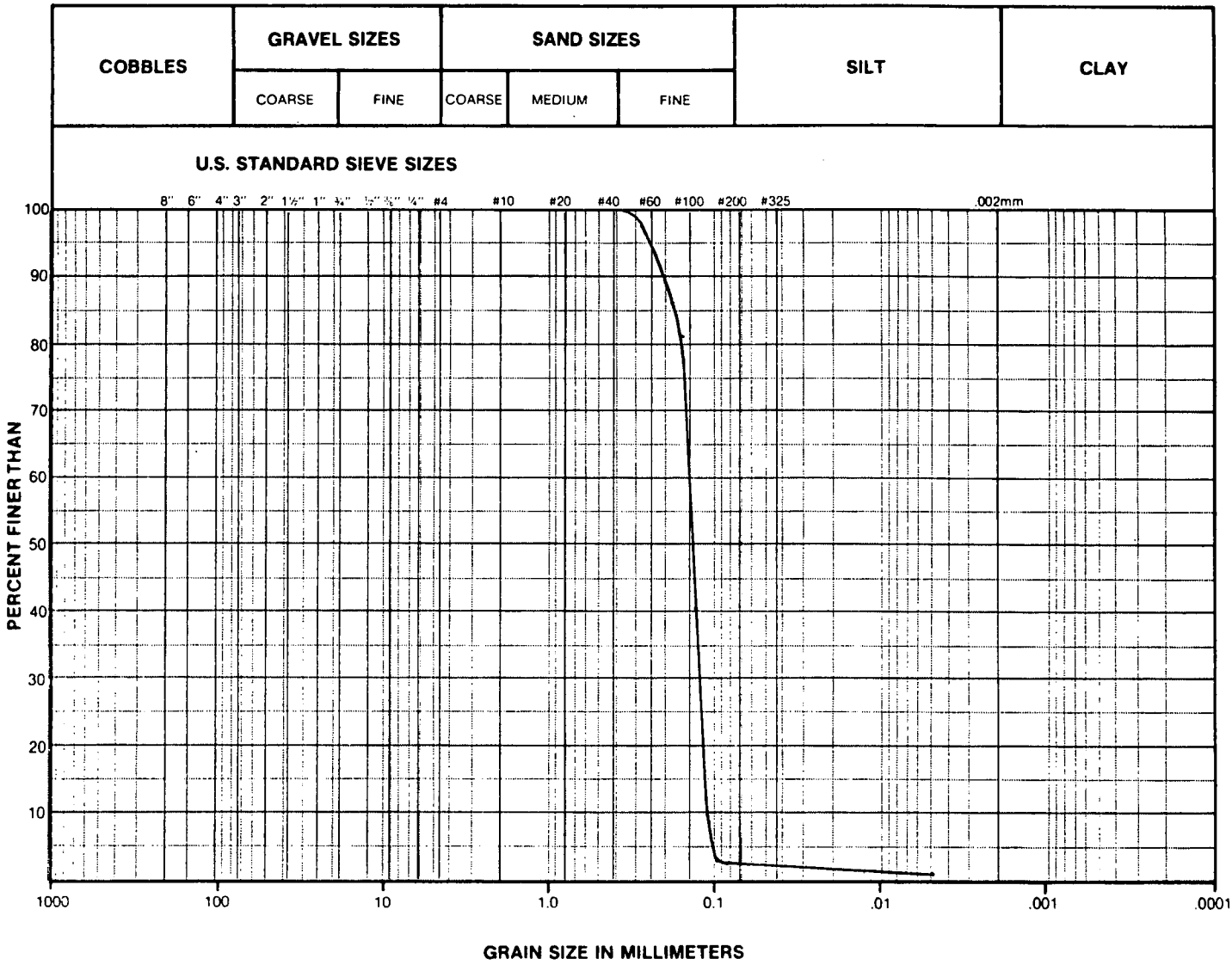

REMARKS: D_{50} = 0.14 mm , D_{90} = 0.20 mm

NOTE. UNIFIED SOIL CLASSIFICATION SYSTEM

SUMMARY

D_{10} =	mm	GRAVEL	0.10 %
D_{30} =	mm	SAND	98.80 %
D_{60} =	mm	SILT	0.55 %
C_U =	mm	CLAY	0.55 %
C_C =	mm		

Seaconsult Marine Research Ltd.

GRAIN SIZE CURVE

CLIENT:	
PROJECT NUMBER:	
LAB. NUMBER:	
LOCATION:	Grab #14 Venture
HOLE:	SAMPLE:
DEPTH:	
TECHNICIAN:	DATE:

COBBLES	GRAVEL SIZES		SAND SIZES			SILT	CLAY
	COARSE	FINE	COARSE	MEDIUM	FINE		

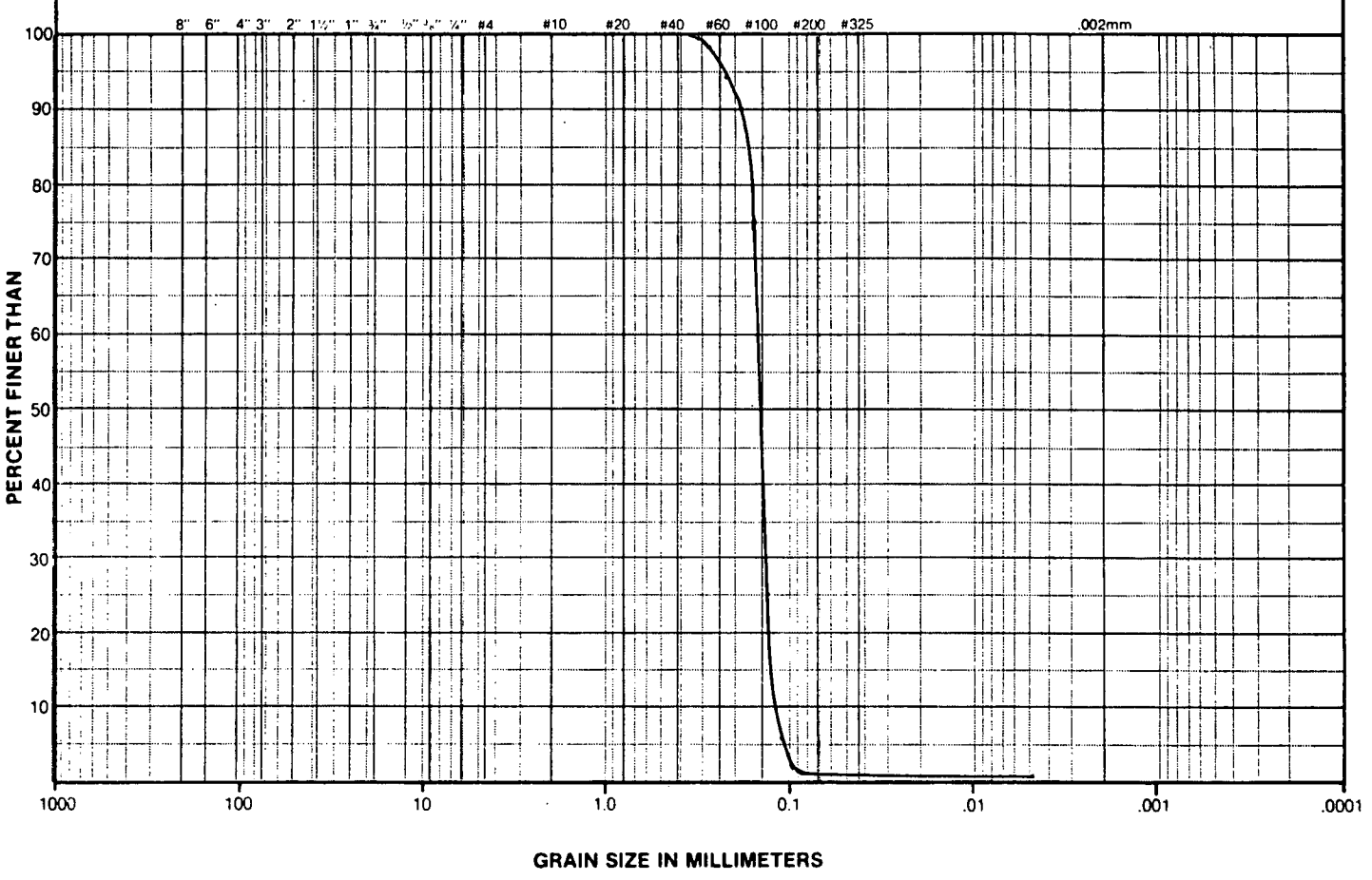

REMARKS: D_{50} = 0.15 mm , D_{90} = 0.18 mm

NOTE: UNIFIED SOIL CLASSIFICATION SYSTEM

SUMMARY

D_{10} =	mm	GRAVEL	0.10 %
D_{30} =	mm	SAND	98.70 %
D_{60} =	mm	SILT	0.60 %
C_U =	mm	CLAY	0.60 %
C_C =	mm		

Seaconsult Marine Research Ltd.

GRAIN SIZE CURVE

CLIENT:	
PROJECT NUMBER:	
LAB. NUMBER:	
LOCATION:	Grab #15 Venture
HOLE:	SAMPLE:
DEPTH:	
TECHNICIAN:	DATE:

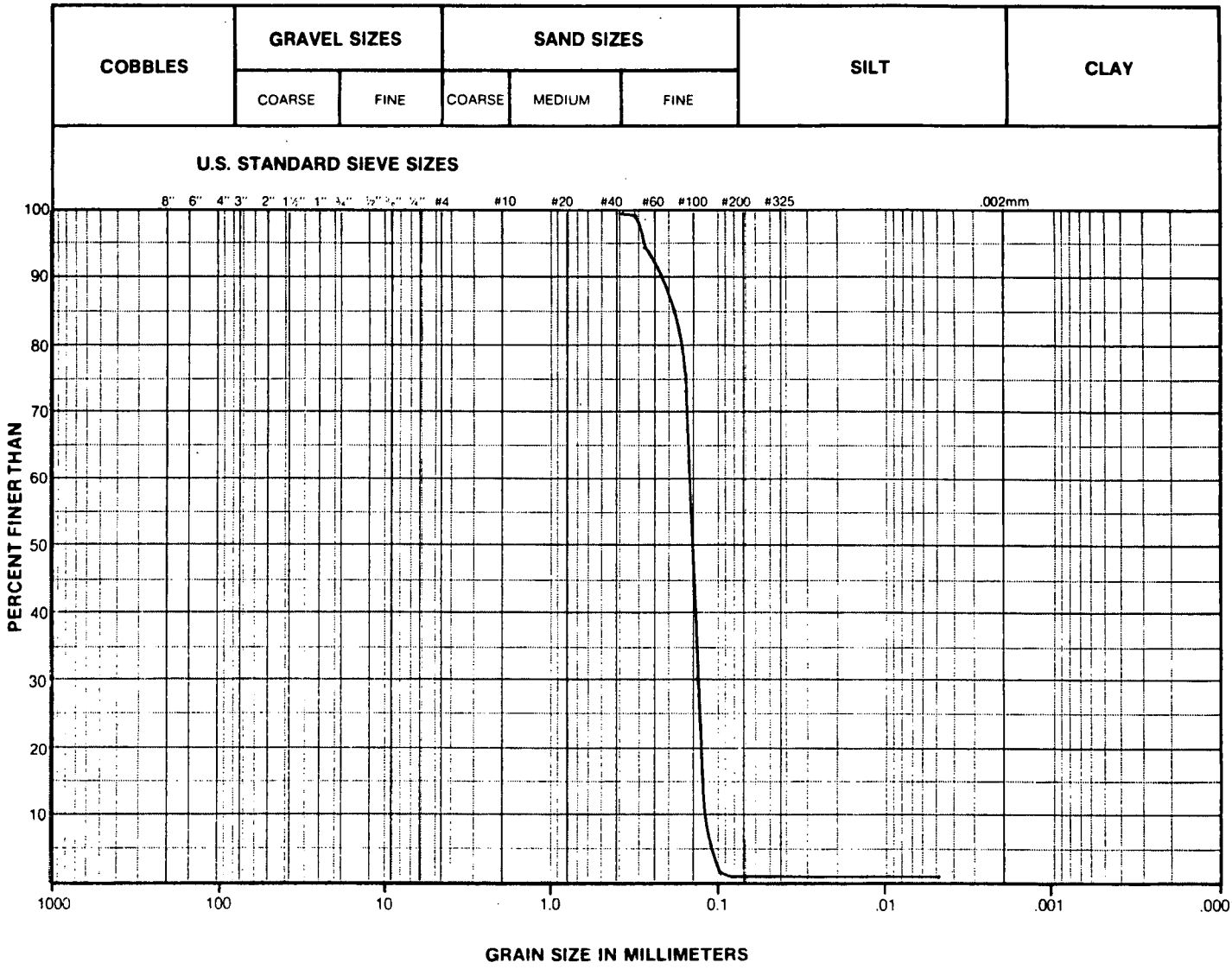

REMARKS: D_{50} = 0.15 mm , D_{90} = 0.23 mm

NOTE: UNIFIED SOIL CLASSIFICATION SYSTEM

SUMMARY

D_{10} =	mm	GRAVEL	0.10 %
D_{30} =	mm	SAND	98.80 %
D_{60} =	mm	SILT	0.55 %
C_U =	mm	CLAY	0.55 %
C_C =	mm		

Seaconsult Marine Research Ltd.

GRAIN SIZE CURVE

CLIENT:	
PROJECT NUMBER:	
LAB. NUMBER:	
LOCATION:	Grab #19 Venture
HOLE:	SAMPLE:
DEPTH:	
TECHNICIAN:	DATE:

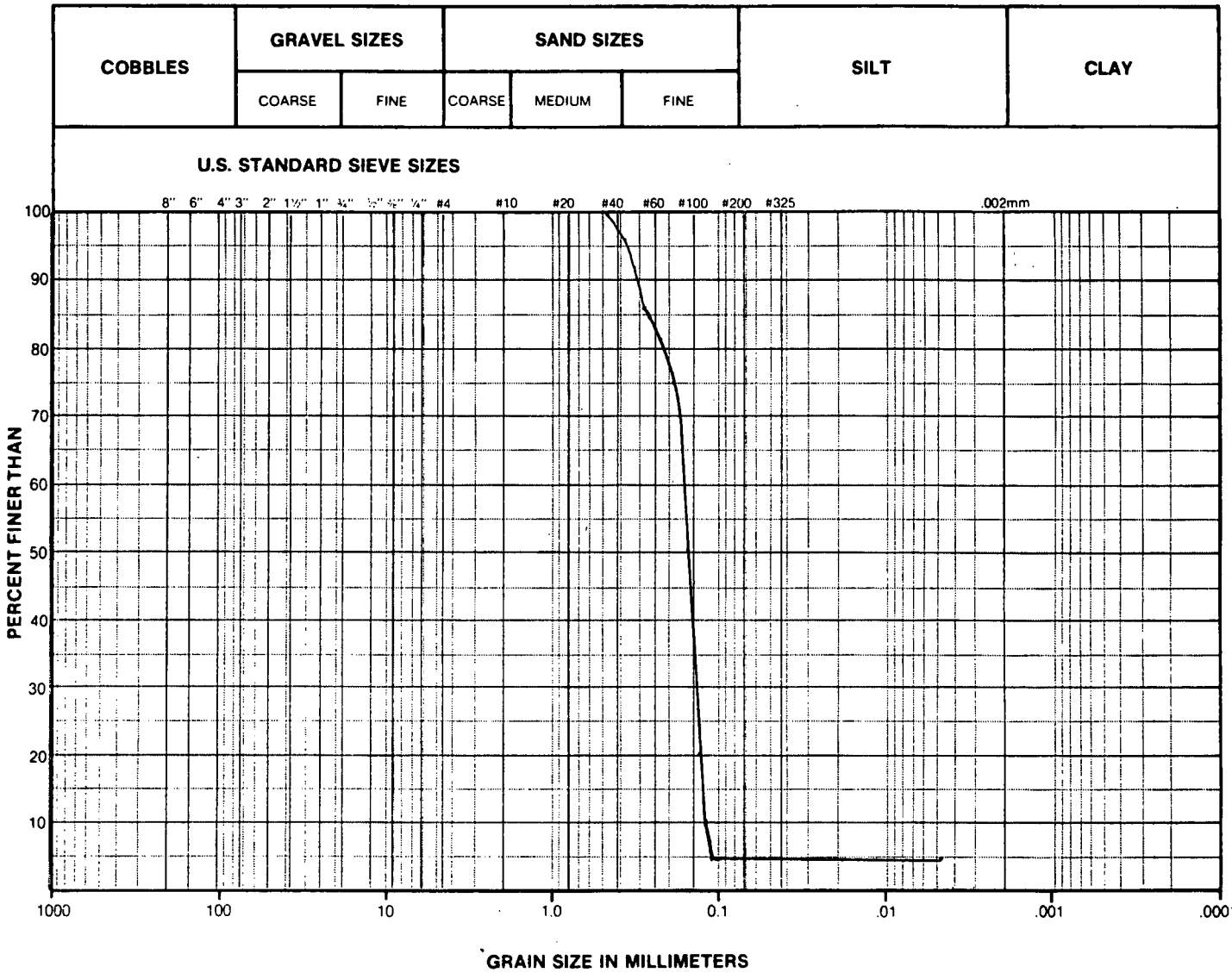

REMARKS: D_{50} = 0.16 mm , D_{90} = 0.31 mm

NOTE: UNIFIED SOIL CLASSIFICATION SYSTEM

SUMMARY

D_{10} =	mm	GRAVEL	0.10 %
D_{30} =	mm	SAND	98.70 %
D_{60} =	mm	SILT	0.60 %
C_U =	mm	CLAY	0.60 %
C_C =	mm		

Seaconsult Marine Research Ltd.

GRAIN SIZE CURVE

CLIENT:	
PROJECT NUMBER:	
LAB. NUMBER:	
LOCATION:	Grab #20 Venture
HOLE:	SAMPLE:
DEPTH:	
TECHNICIAN:	DATE:

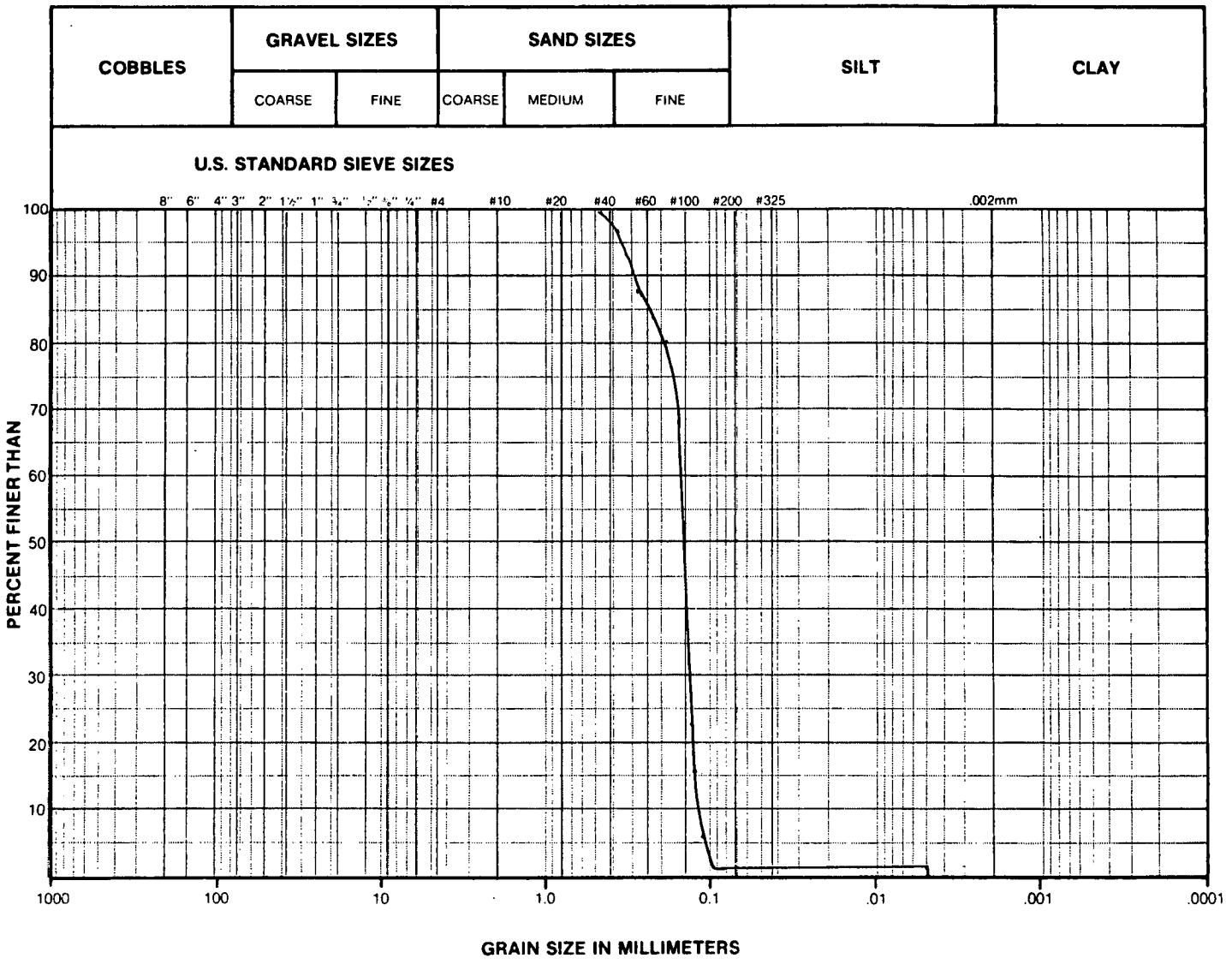

REMARKS: D_{50} = 0.15 mm , D_{90} = 0.30 mm

NOTE UNIFIED SOIL CLASSIFICATION SYSTEM

SUMMARY

D_{10} =	mm	GRAVEL	0.10 %
D_{30} =	mm	SAND	98.70 %
D_{60} =	mm	SILT	0.60 %
C_U =	mm	CLAY	0.60 %
C_C =	mm		

OLYMPIA SITE GRAIN SIZE ANALYSIS

GRAB NO. 1

INTERVAL	GRAIN SIZE (mm)	FREQUENCY FRACTION	CUMULATIVE FREQUENCY FRACTION
1	.0039	.0110	.0110
2	.0410	.0000	.0110
3	.0480	.0000	.0110
4	.0570	.0000	.0110
5	.0680	.0000	.0110
6	.0810	.0024	.0134
7	.0960	.0024	.0158
8	.1100	.0071	.0229
9	.1400	.0306	.0535
10	.1800	.0447	.0982
11	.1900	.0918	.1900
12	.2300	.1241	.3141
13	.2700	.1805	.4946
14	.3200	.2307	.7253
15	.3900	.1544	.8797
16	.4600	.0776	.9573
17	.5500	.0303	.9876
18	.6500	.0083	.9959
19	.7700	.0031	.9990
20	.9200	.0000	.9990
21	1.1000	.0000	.9990
22	1.3000	.0000	.9990
23	1.5000	.0000	.9990
24	1.8000	.0000	.9990
25	8.0000	.0010	1.0000

OLYMPIA SITE GRAIN SIZE ANALYSIS

GRAB NO. 7

INTERVAL	GRAIN SIZE (mm)	FREQUENCY FRACTION	CUMULATIVE FREQUENCY FRACTION
1	.0039	.0090	.0090
2	.0410	.0000	.0090
3	.0480	.0000	.0090
4	.0570	.0000	.0090
5	.0680	.0000	.0090
6	.0810	.0000	.0090
7	.0960	.0019	.0109
8	.1100	.0057	.0166
9	.1400	.0226	.0392
10	.1600	.0339	.0731
11	.1900	.0659	.1390
12	.2300	.1101	.2491
13	.2700	.0748	.3239
14	.3200	.1370	.4609
15	.3900	.1490	.6099
16	.4600	.1059	.7158
17	.5500	.0811	.7969
18	.6500	.0600	.8569
19	.7700	.0585	.9154
20	.9200	.0497	.9651
21	1.1000	.0224	.9875
22	1.3000	.0078	.9953
23	1.5000	.0027	.9980
24	1.8000	.0000	.9980
25	8.0000	.0020	1.0000

OLYMPIA SITE GRAIN SIZE ANALYSIS

GRAB NO. 8

INTERVAL	GRAIN SIZE (mm)	FREQUENCY FRACTION	CUMULATIVE FREQUENCY FRACTION
1	.0039	.0090	.0090
2	.0410	.0000	.0090
3	.0480	.0000	.0090
4	.0570	.0000	.0090
5	.0680	.0000	.0090
6	.0810	.0000	.0090
7	.0960	.0000	.0090
8	.1100	.0000	.0090
9	.1400	.0138	.0228
10	.1600	.0059	.0287
11	.1900	.0158	.0445
12	.2300	.0528	.0973
13	.2700	.0448	.1421
14	.3200	.1329	.2750
15	.3900	.2248	.4998
16	.4600	.1917	.6915
17	.5500	.1148	.8063
18	.6500	.0922	.8985
19	.7700	.0443	.9428
20	.9200	.0363	.9791
21	1.1000	.0112	.9903
22	1.3000	.0021	.9924
23	1.5000	.0046	.9970
24	1.8000	.0000	.9970
25	8.0000	.0030	1.0000

OLYMPIA SITE GRAIN SIZE ANALYSIS

GRAB NO. 9

INTERVAL	GRAIN SIZE (mm)	FREQUENCY FRACTION	CUMULATIVE FREQUENCY FRACTION
1	.0039	.0120	.0120
2	.0410	.0000	.0120
3	.0480	.0000	.0120
4	.0570	.0000	.0120
5	.0680	.0041	.0161
6	.0810	.0000	.0161
7	.0960	.0041	.0202
8	.1100	.0102	.0304
9	.1400	.0430	.0734
10	.1600	.0573	.1307
11	.1900	.0860	.2167
12	.2300	.1081	.3248
13	.2700	.1531	.4779
14	.3200	.1675	.6454
15	.3900	.1499	.7953
16	.4600	.1103	.9056
17	.5500	.0511	.9567
18	.6500	.0232	.9799
19	.7700	.0108	.9907
20	.9200	.0063	.9970
21	1.1000	.0000	.9970
22	1.3000	.0000	.9970
23	1.5000	.0000	.9970
24	1.8000	.0000	.9970
25	8.0000	.0030	1.0000

OLYMPIA SITE GRAIN SIZE ANALYSIS

GRAB NO. 10

INTERVAL	GRAIN SIZE (mm)	FREQUENCY FRACTION	CUMULATIVE FREQUENCY FRACTION
1	.0039	.0080	.0080
2	.0410	.0000	.0080
3	.0480	.0019	.0099
4	.0570	.0000	.0099
5	.0680	.0000	.0099
6	.0810	.0019	.0118
7	.0960	.0000	.0118
8	.1100	.0000	.0118
9	.1400	.0095	.0213
10	.1600	.0095	.0308
11	.1900	.0267	.0575
12	.2300	.0644	.1219
13	.2700	.1136	.2355
14	.3200	.2107	.4462
15	.3900	.1947	.6409
16	.4600	.1532	.7941
17	.5500	.0735	.8676
18	.6500	.0486	.9162
19	.7700	.0416	.9578
20	.9200	.0222	.9800
21	1.1000	.0151	.9951
22	1.3000	.0039	.9990
23	1.5000	.0000	.9990
24	1.8000	.0000	.9990
25	8.0000	.0010	1.0000

VENTURE SITE GRAIN SIZE ANALYSIS

GRAB NO. 2

INTERVAL	GRAIN SIZE (mm)	FREQUENCY FRACTION	CUMULATIVE FREQUENCY FRACTION
1	.0039	.0110	.0110
2	.0410	.0023	.0133
3	.0480	.0000	.0133
4	.0570	.0000	.0133
5	.0680	.0000	.0133
6	.0810	.0045	.0178
7	.0960	.0068	.0246
8	.1100	.0431	.0677
9	.1400	.1612	.2289
10	.1600	.4199	.6488
11	.1900	.2451	.8939
12	.2300	.0407	.9346
13	.2700	.0322	.9668
14	.3200	.0245	.9913
15	.3900	.0077	.9990
16	.4600	.0000	.9990
17	.5500	.0000	.9990
18	.6500	.0000	.9990
19	.7700	.0000	.9990
20	.9200	.0000	.9990
21	1.1000	.0000	.9990
22	1.3000	.0000	.9990
23	1.5000	.0000	.9990
24	1.8000	.0000	.9990
25	8.0000	.0010	1.0000

VENTURE SITE GRAIN SIZE ANALYSIS

GRAB NO. 3

INTERVAL	GRAIN SIZE (mm)	FREQUENCY FRACTION	CUMULATIVE FREQUENCY FRACTION
1	.0039	.0100	.0100
2	.0410	.0000	.0100
3	.0480	.0000	.0100
4	.0570	.0000	.0100
5	.0680	.0000	.0100
6	.0810	.0053	.0153
7	.0960	.0080	.0233
8	.1100	.0428	.0661
9	.1400	.2141	.2802
10	.1600	.5246	.8048
11	.1900	.0589	.8637
12	.2300	.0506	.9143
13	.2700	.0431	.9574
14	.3200	.0289	.9863
15	.3900	.0137	1.0000
16	.4600	.0000	1.0000
17	.5500	.0000	1.0000
18	.6500	.0000	1.0000
19	.7700	.0000	1.0000
20	.9200	.0000	1.0000
21	1.1000	.0000	1.0000
22	1.3000	.0000	1.0000
23	1.5000	.0000	1.0000
24	1.8000	.0000	1.0000
25	8.0000	.0000	1.0000

VENTURE SITE GRAIN SIZE ANALYSIS

GRAB NO. 4

INTERVAL	GRAIN SIZE (mm)	FREQUENCY FRACTION	CUMULATIVE FREQUENCY FRACTION
1	.0039	.0090	.0090
2	.0410	.0000	.0090
3	.0480	.0000	.0090
4	.0570	.0000	.0090
5	.0680	.0000	.0090
6	.0810	.0000	.0090
7	.0960	.0048	.0138
8	.1100	.0433	.0571
9	.1400	.1444	.2015
10	.1600	.5296	.7311
11	.1900	.1396	.8707
12	.2300	.0599	.9306
13	.2700	.0478	.9784
14	.3200	.0195	.9979
15	.3900	.0021	1.0000
16	.4600	.0000	1.0000
17	.5500	.0000	1.0000
18	.6500	.0000	1.0000
19	.7700	.0000	1.0000
20	.9200	.0000	1.0000
21	1.1000	.0000	1.0000
22	1.3000	.0000	1.0000
23	1.5000	.0000	1.0000
24	1.8000	.0000	1.0000
25	8.0000	.0000	1.0000

VENTURE SITE GRAIN SIZE ANALYSIS

GRAB NO. 5

INTERVAL	GRAIN SIZE (mm)	FREQUENCY FRACTION	CUMULATIVE FREQUENCY FRACTION
1	.0039	.0090	.0090
2	.0410	.0000	.0090
3	.0480	.0026	.0116
4	.0570	.0000	.0116
5	.0680	.0000	.0116
6	.0810	.0000	.0116
7	.0960	.0078	.0194
8	.1100	.0417	.0611
9	.1400	.1744	.2355
10	.1600	.5103	.7458
11	.1900	.0781	.8239
12	.2300	.0439	.8678
13	.2700	.0542	.9220
14	.3200	.0515	.9735
15	.3900	.0244	.9979
16	.4600	.0021	1.0000
17	.5500	.0000	1.0000
18	.6500	.0000	1.0000
19	.7700	.0000	1.0000
20	.9200	.0000	1.0000
21	1.1000	.0000	1.0000
22	1.3000	.0000	1.0000
23	1.5000	.0000	1.0000
24	1.8000	.0000	1.0000
25	8.0000	.0000	1.0000

VENTURE SITE GRAIN SIZE ANALYSIS

GRAB NO. 6

INTERVAL	GRAIN SIZE (mm)	FREQUENCY FRACTION	CUMULATIVE FREQUENCY FRACTION
1	.0039	.0090	.0090
2	.0410	.0000	.0090
3	.0480	.0000	.0090
4	.0570	.0000	.0090
5	.0680	.0000	.0090
6	.0810	.0000	.0090
7	.0960	.0029	.0119
8	.1100	.0467	.0586
9	.1400	.1720	.2306
10	.1600	.4520	.6826
11	.1900	.1312	.8138
12	.2300	.0407	.8545
13	.2700	.0579	.9124
14	.3200	.0498	.9622
15	.3900	.0298	.9920
16	.4600	.0070	.9990
17	.5500	.0000	.9990
18	.6500	.0000	.9990
19	.7700	.0000	.9990
20	.9200	.0000	.9990
21	1.1000	.0000	.9990
22	1.3000	.0000	.9990
23	1.5000	.0000	.9990
24	1.8000	.0000	.9990
25	8.0000	.0010	1.0000

VENTURE SITE GRAIN SIZE ANALYSIS

GRAB NO. 11

INTERVAL	GRAIN SIZE (mm)	FREQUENCY FRACTION	CUMULATIVE FREQUENCY FRACTION
1	.0039	.0100	.0100
2	.0410	.0000	.0100
3	.0480	.0000	.0100
4	.0570	.0024	.0124
5	.0680	.0000	.0124
6	.0810	.0000	.0124
7	.0960	.0048	.0172
8	.1100	.0404	.0576
9	.1400	.1522	.2098
10	.1600	.4187	.6285
11	.1900	.0999	.7284
12	.2300	.0615	.7899
13	.2700	.0833	.8732
14	.3200	.0620	.9352
15	.3900	.0466	.9818
16	.4600	.0172	.9990
17	.5500	.0000	.9990
18	.6500	.0000	.9990
19	.7700	.0000	.9990
20	.9200	.0000	.9990
21	1.1000	.0000	.9990
22	1.3000	.0000	.9990
23	1.5000	.0000	.9990
24	1.8000	.0000	.9990
25	8.0000	.0010	1.0000

VENTURE SITE GRAIN SIZE ANALYSIS

GRAB NO. 12

INTERVAL	GRAIN SIZE (mm)	FREQUENCY FRACTION	CUMULATIVE FREQUENCY FRACTION
1	.0039	.0110	.0110
2	.0410	.0000	.0110
3	.0480	.0000	.0110
4	.0570	.0000	.0110
5	.0680	.0024	.0134
6	.0810	.0047	.0181
7	.0960	.0024	.0205
8	.1100	.0447	.0652
9	.1400	.1928	.2580
10	.1600	.4586	.7166
11	.1900	.1341	.8507
12	.2300	.0490	.8997
13	.2700	.0445	.9442
14	.3200	.0338	.9780
15	.3900	.0200	.9980
16	.4600	.0000	.9980
17	.5500	.0000	.9980
18	.6500	.0000	.9980
19	.7700	.0000	.9980
20	.9200	.0000	.9980
21	1.1000	.0000	.9980
22	1.3000	.0000	.9980
23	1.5000	.0000	.9980
24	1.8000	.0000	.9980
25	8.0000	.0020	1.0000

VENTURE SITE GRAIN SIZE ANALYSIS

GRAB NO. 13

INTERVAL	GRAIN SIZE (mm)	FREQUENCY FRACTION	CUMULATIVE FREQUENCY FRACTION
1	.0039	.0110	.0110
2	.0410	.0000	.0110
3	.0480	.0000	.0110
4	.0570	.0000	.0110
5	.0680	.0026	.0136
6	.0810	.0026	.0162
7	.0960	.0105	.0267
8	.1100	.0654	.0921
9	.1400	.3111	.4032
10	.1600	.4079	.8111
11	.1900	.0523	.8634
12	.2300	.0679	.9313
13	.2700	.0520	.9833
14	.3200	.0094	.9927
15	.3900	.0000	.9927
16	.4600	.0000	.9927
17	.5500	.0000	.9927
18	.6500	.0000	.9927
19	.7700	.0000	.9927
20	.9200	.0000	.9927
21	1.1000	.0000	.9927
22	1.3000	.0063	.9990
23	1.5000	.0000	.9990
24	1.8000	.0000	.9990
25	8.0000	.0010	1.0000

VENTURE SITE GRAIN SIZE ANALYSIS

GRAB NO. 14

INTERVAL	GRAIN SIZE (mm)	FREQUENCY FRACTION	CUMULATIVE FREQUENCY FRACTION
1	.0039	.0120	.0120
2	.0410	.0000	.0120
3	.0480	.0000	.0120
4	.0570	.0000	.0120
5	.0680	.0000	.0120
6	.0810	.0023	.0143
7	.0960	.0070	.0213
8	.1100	.0419	.0632
9	.1400	.1885	.2517
10	.1600	.5026	.7543
11	.1900	.1489	.9032
12	.2300	.0440	.9472
13	.2700	.0330	.9802
14	.3200	.0188	.9990
15	.3900	.0000	.9990
16	.4600	.0000	.9990
17	.5500	.0000	.9990
18	.6500	.0000	.9990
19	.7700	.0000	.9990
20	.9200	.0000	.9990
21	1.1000	.0000	.9990
22	1.3000	.0000	.9990
23	1.5000	.0000	.9990
24	1.8000	.0000	.9990
25	8.0000	.0010	1.0000

VENTURE SITE GRAIN SIZE ANALYSIS

GRAB NO. 15

INTERVAL	GRAIN SIZE (mm)	FREQUENCY FRACTION	CUMULATIVE FREQUENCY FRACTION
1	.0039	.0110	.0110
2	.0410	.0000	.0110
3	.0480	.0000	.0110
4	.0570	.0000	.0110
5	.0680	.0000	.0110
6	.0810	.0025	.0135
7	.0960	.0051	.0186
8	.1100	.0405	.0591
9	.1400	.2380	.2971
10	.1600	.4381	.7352
11	.1900	.1190	.8542
12	.2300	.0504	.9046
13	.2700	.0431	.9477
14	.3200	.0319	.9796
15	.3900	.0194	.9990
16	.4600	.0000	.9990
17	.5500	.0000	.9990
18	.6500	.0000	.9990
19	.7700	.0000	.9990
20	.9200	.0000	.9990
21	1.1000	.0000	.9990
22	1.3000	.0000	.9990
23	1.5000	.0000	.9990
24	1.8000	.0000	.9990
25	8.0000	.0010	1.0000

VENTURE SITE GRAIN SIZE ANALYSIS

GRAB NO. 19

INTERVAL	GRAIN SIZE (mm)	FREQUENCY FRACTION	CUMULATIVE FREQUENCY FRACTION
1	.0039	.0120	.0120
2	.0410	.0000	.0120
3	.0480	.0000	.0120
4	.0570	.0000	.0120
5	.0680	.0000	.0120
6	.0810	.0000	.0120
7	.0960	.0000	.0120
8	.1100	.0368	.0488
9	.1400	.1542	.2030
10	.1600	.2991	.5021
11	.1900	.2508	.7529
12	.2300	.0640	.8169
13	.2700	.0479	.8648
14	.3200	.0600	.9248
15	.3900	.0431	.9679
16	.4600	.0259	.9938
17	.5500	.0052	.9990
18	.6500	.0000	.9990
19	.7700	.0000	.9990
20	.9200	.0000	.9990
21	1.1000	.0000	.9990
22	1.3000	.0000	.9990
23	1.5000	.0000	.9990
24	1.8000	.0000	.9990
25	8.0000	.0010	1.0000

VENTURE SITE GRAIN SIZE ANALYSIS

GRAB NO. 20

INTERVAL	GRAIN SIZE (mm)	FREQUENCY FRACTION	CUMULATIVE FREQUENCY FRACTION
1	.0039	.0090	.0090
2	.0410	.0000	.0090
3	.0480	.0000	.0090
4	.0570	.0000	.0090
5	.0680	.0000	.0090
6	.0810	.0000	.0090
7	.0960	.0045	.0135
8	.1100	.0473	.0608
9	.1400	.1735	.2343
10	.1600	.4033	.6376
11	.1900	.1667	.8043
12	.2300	.0403	.8446
13	.2700	.0448	.8894
14	.3200	.0445	.9339
15	.3900	.0345	.9684
16	.4600	.0272	.9956
17	.5500	.0034	.9990
18	.6500	.0000	.9990
19	.7700	.0000	.9990
20	.9200	.0000	.9990
21	1.1000	.0000	.9990
22	1.3000	.0000	.9990
23	1.5000	.0000	.9990
24	1.8000	.0000	.9990
25	8.0000	.0010	1.0000

The following graphs present the grain size distributions from grab samples taken at the Venture site on Cruise 4 (February 20/21, 1985). The analysis was performed by the Bedford Institute of Oceanography (Atlantic Geoscience Centre) and the results were available only in this format.

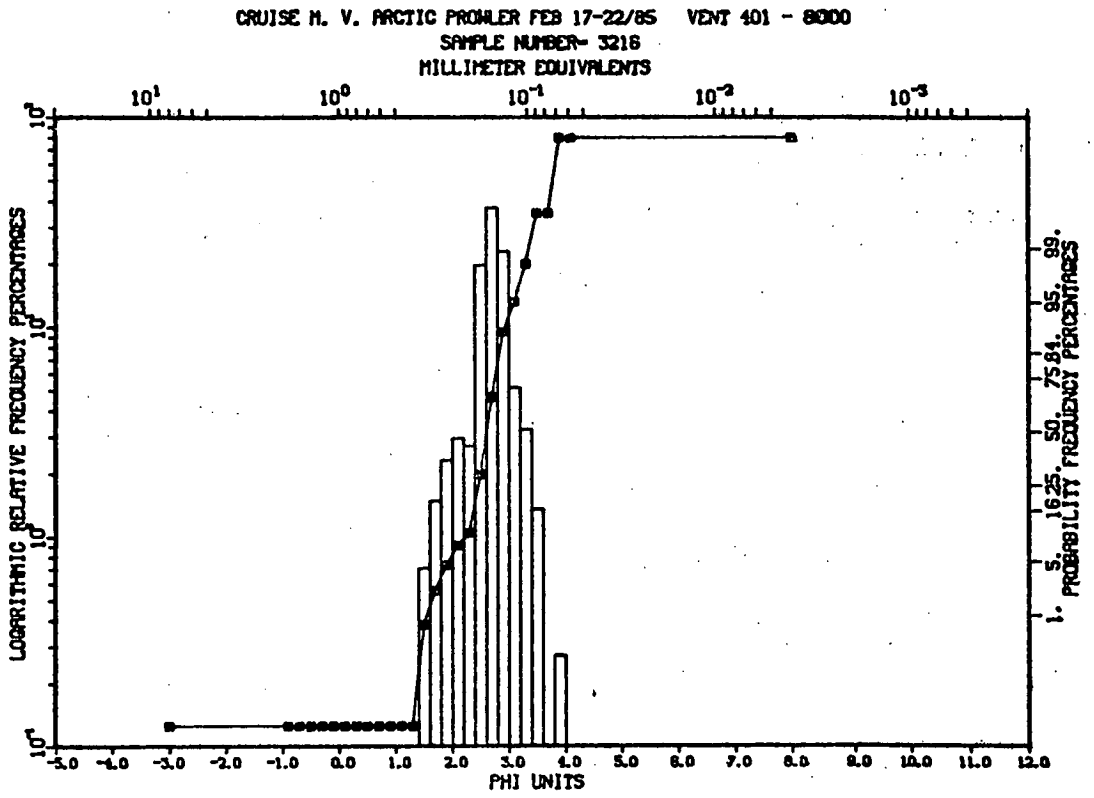
CRUISE M. V. ARCTIC PROWLER FEB 17-22/85 VENT 401 - 80D0
SAMPLE NUMBER- 3216
MILLIMETER EQUIVALENTS
LOGARITHMIC RELATIVE FREQUENCY PERCENTAGES
PROBABILITY FREQUENCY PERCENTAGES
PHI UNITS

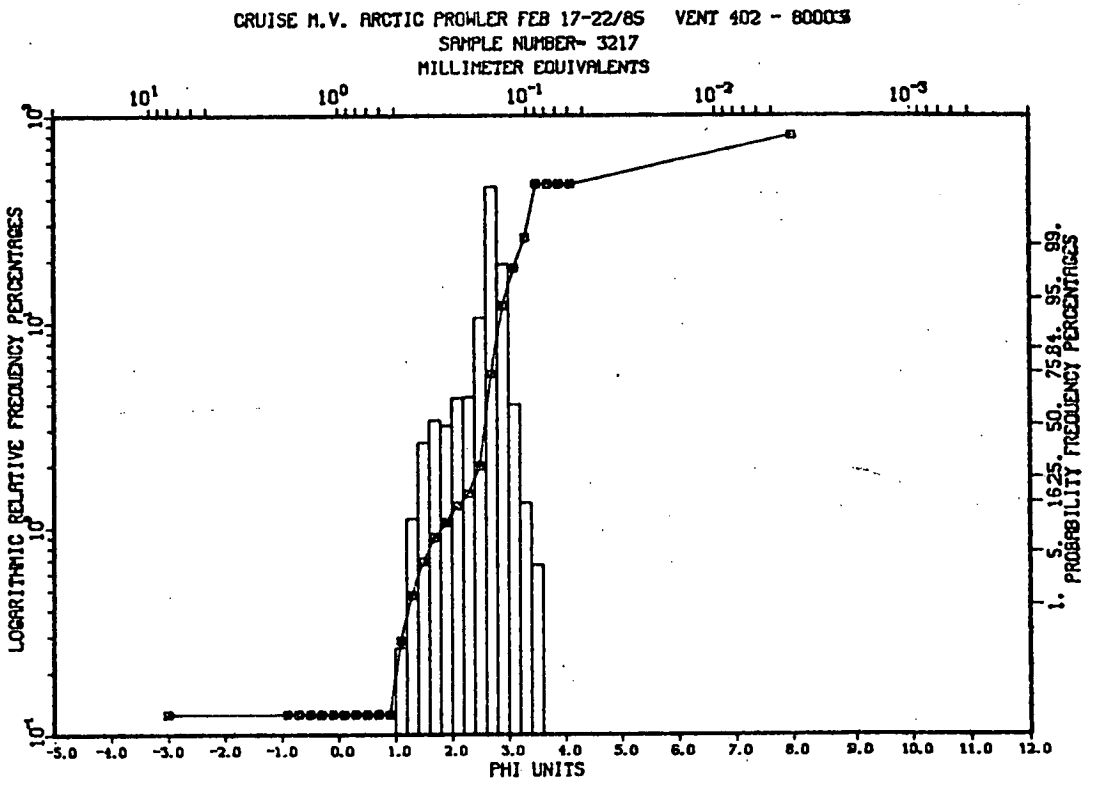
CRUISE M.V. ARCTIC PROWLER FEB 17-22/85 VENT 402 - 80003
SAMPLE NUMBER- 3217
MILLIMETER EQUIVALENTS
LOGARITHMIC RELATIVE FREQUENCY PERCENTAGES
PROBABILITY FREQUENCY PERCENTAGES
PHI UNITS

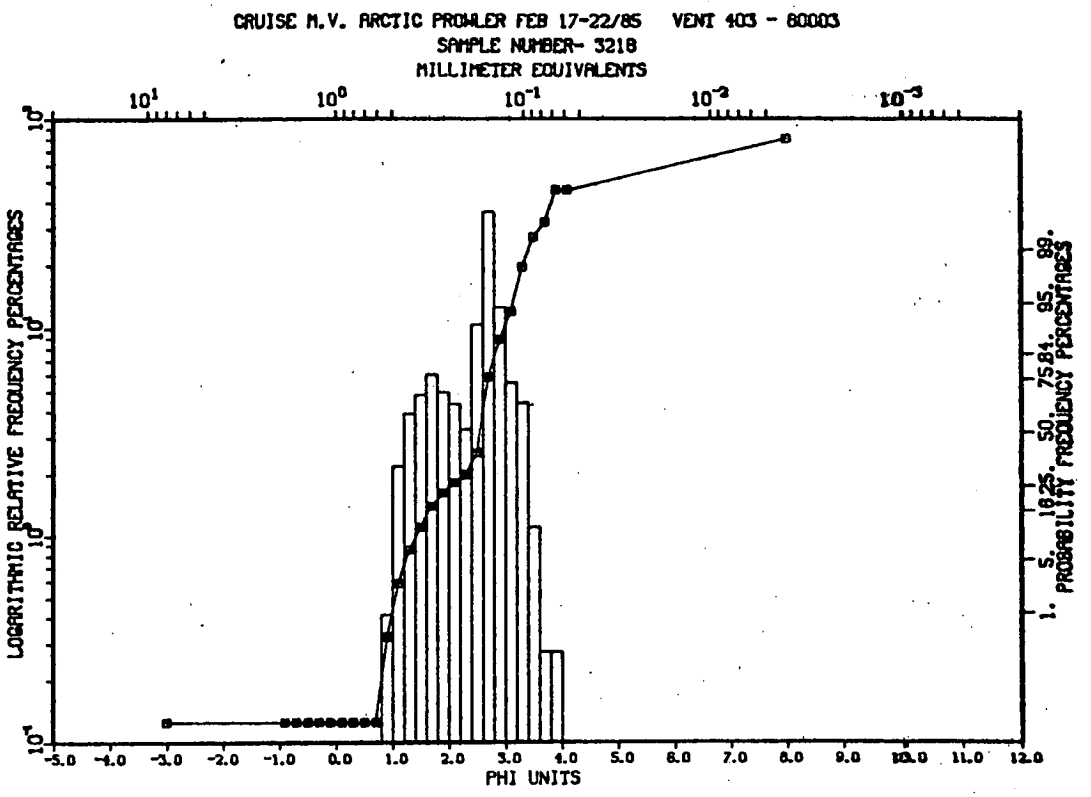
CRUISE M.V. ARCTIC PROWLER FEB 17-22/85 VENT 403 - 80003
SAMPLE NUMBER- 3218
MILLIMETER EQUIVALENTS
LOGARITHMIC RELATIVE FREQUENCY PERCENTAGES
PROBABILITY FREQUENCY PERCENTAGES
PHI UNITS

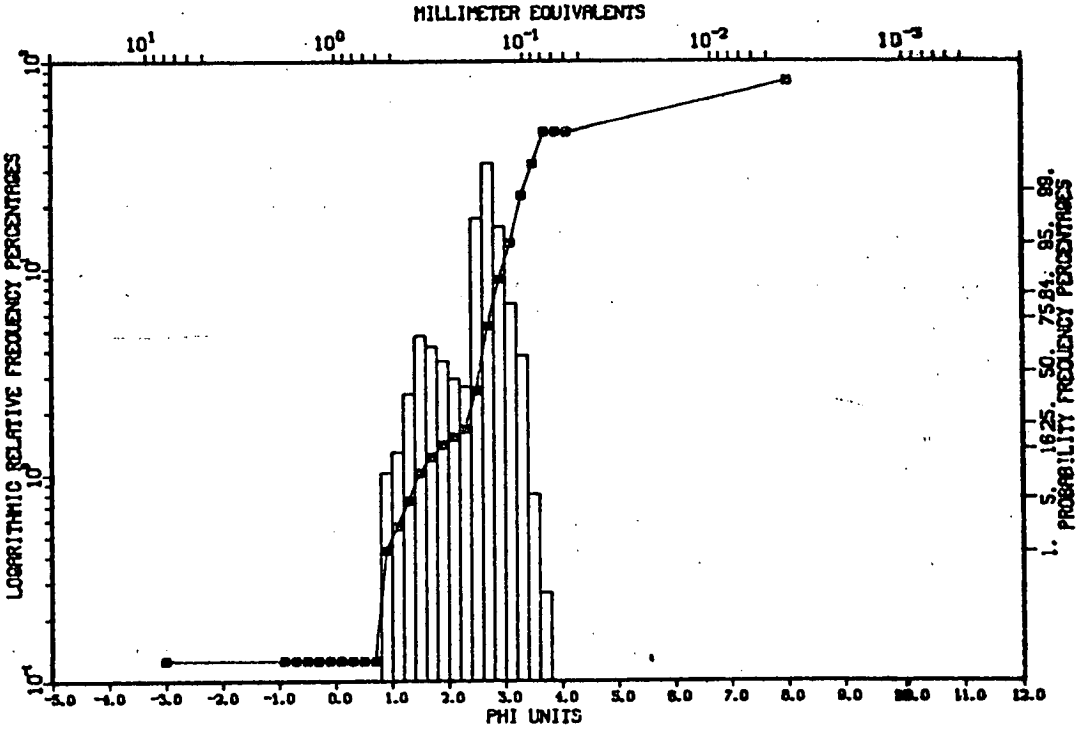
CRUISE M.V. ARCTIC PROWLER FEB 17-22/85 VENT 404 - 80003
SAMPLE NUMBER- 3219
MILLIMETER EQUIVALENTS
LOGARITHMIC RELATIVE FREQUENCY PERCENTAGES
PROBABILITY FREQUENCY PERCENTAGES
PHI UNITS

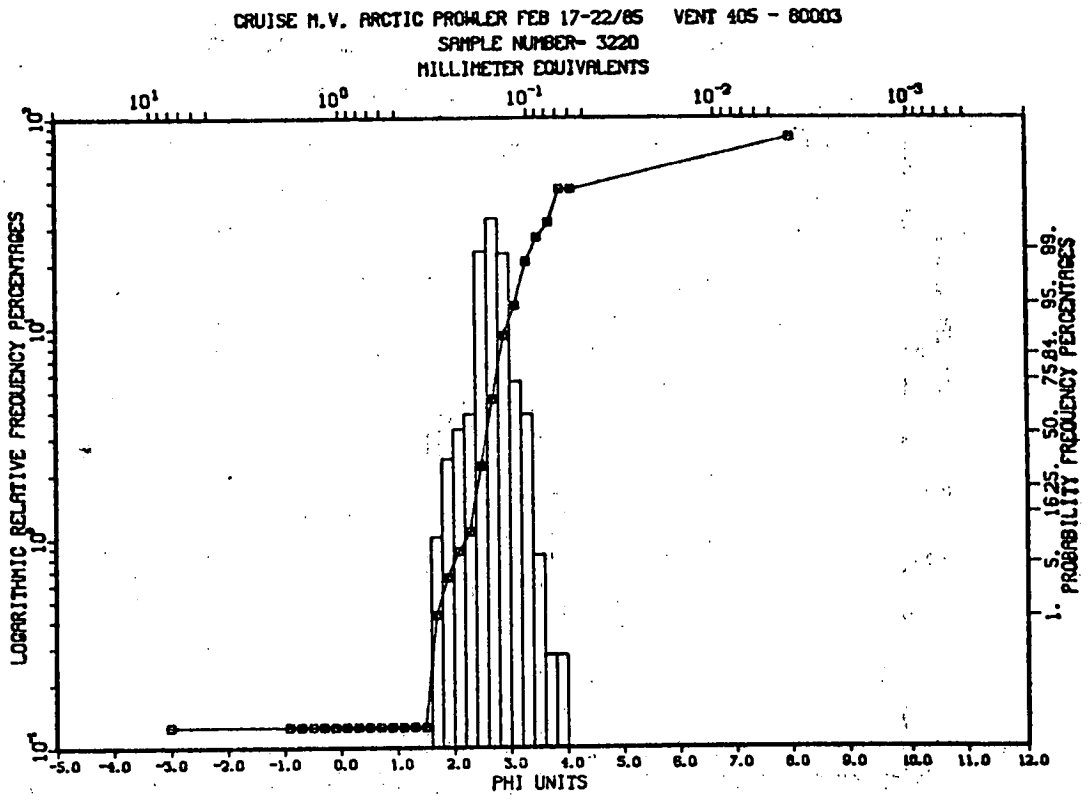
CRUISE M.V. ARCTIC PROWLER FEB 17-22/85 VENT 405 - 80003
SAMPLE NUMBER- 3220
MILLIMETER EQUIVALENTS
LOGARITHMIC RELATIVE FREQUENCY PERCENTAGES
PROBABILITY FREQUENCY PERCENTAGES
PHI UNITS

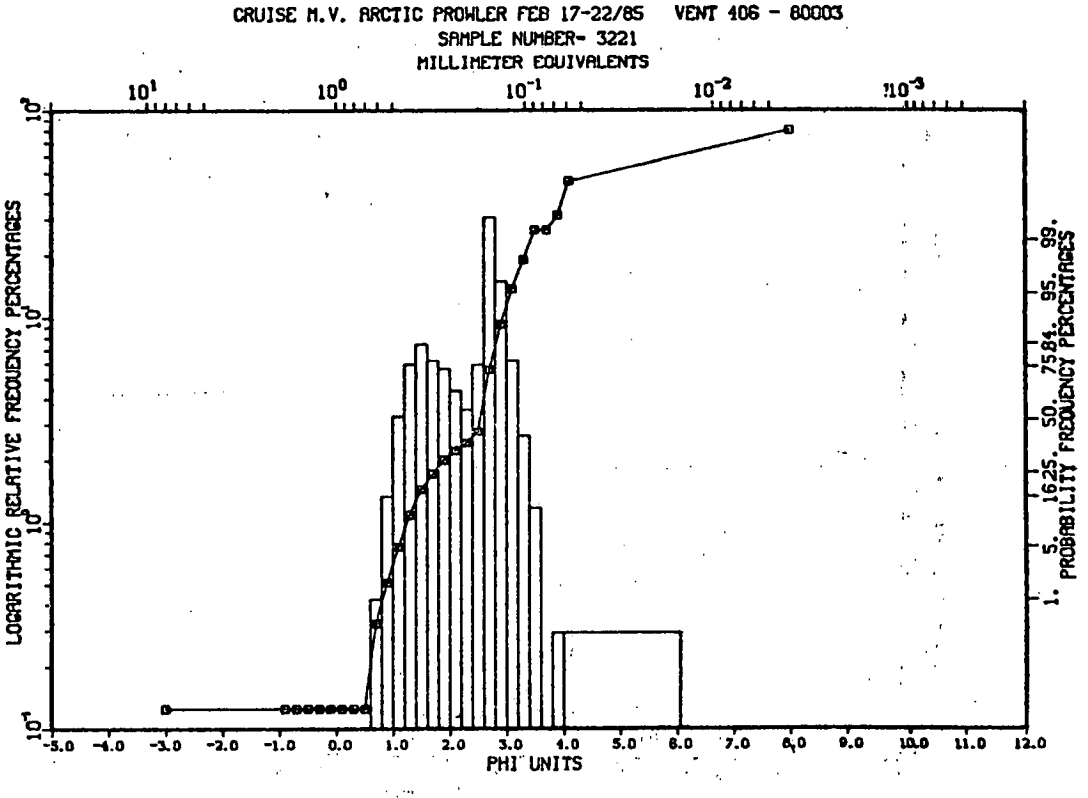
CRUISE M.V. ARCTIC PROWLER FEB 17-22/85 VENT 406 - 80003
SAMPLE NUMBER- 3221
MILLIMETER EQUIVALENTS
LOGARITHMIC RELATIVE FREQUENCY PERCENTAGES
PROBABILITY FREQUENCY PERCENTAGES
PHI UNITS

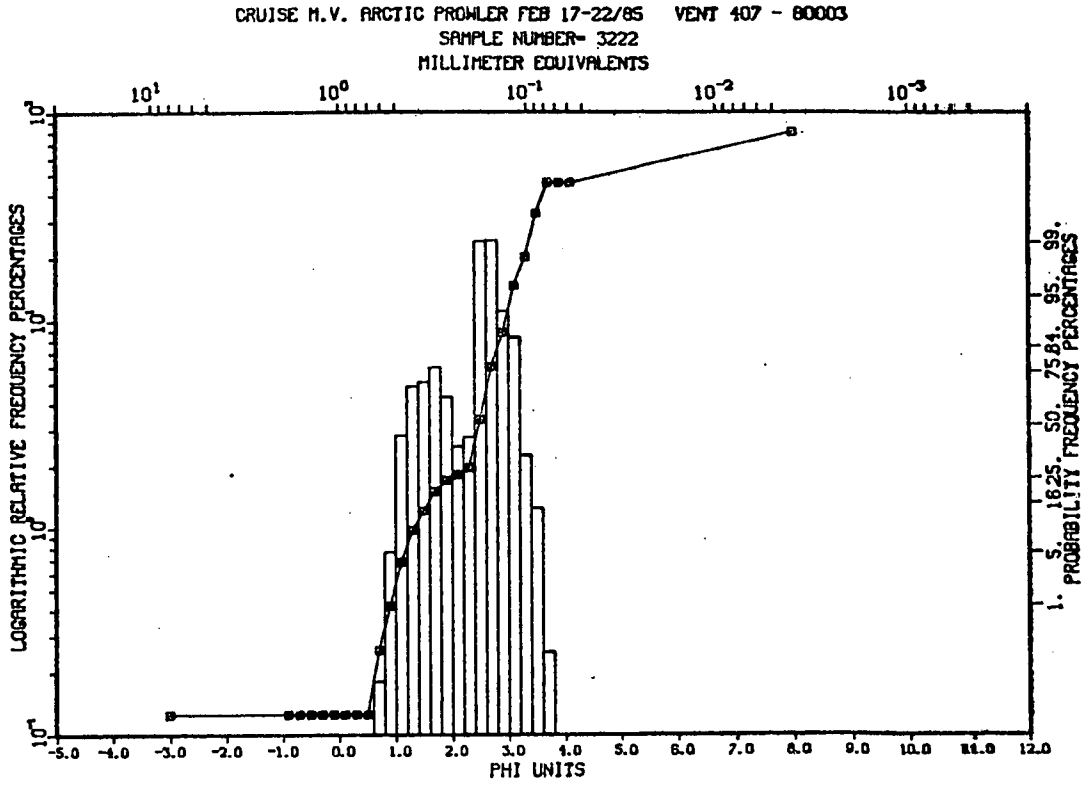
CRUISE M.V. ARCTIC PROWLER FEB 17-22/85 VENT 407 - 80003
SAMPLE NUMBER- 3222
MILLIMETER EQUIVALENTS
LOGARITHMIC RELATIVE FREQUENCY PERCENTAGES
PROBABILITY FREQUENCY PERCENTAGES
PHI UNITS

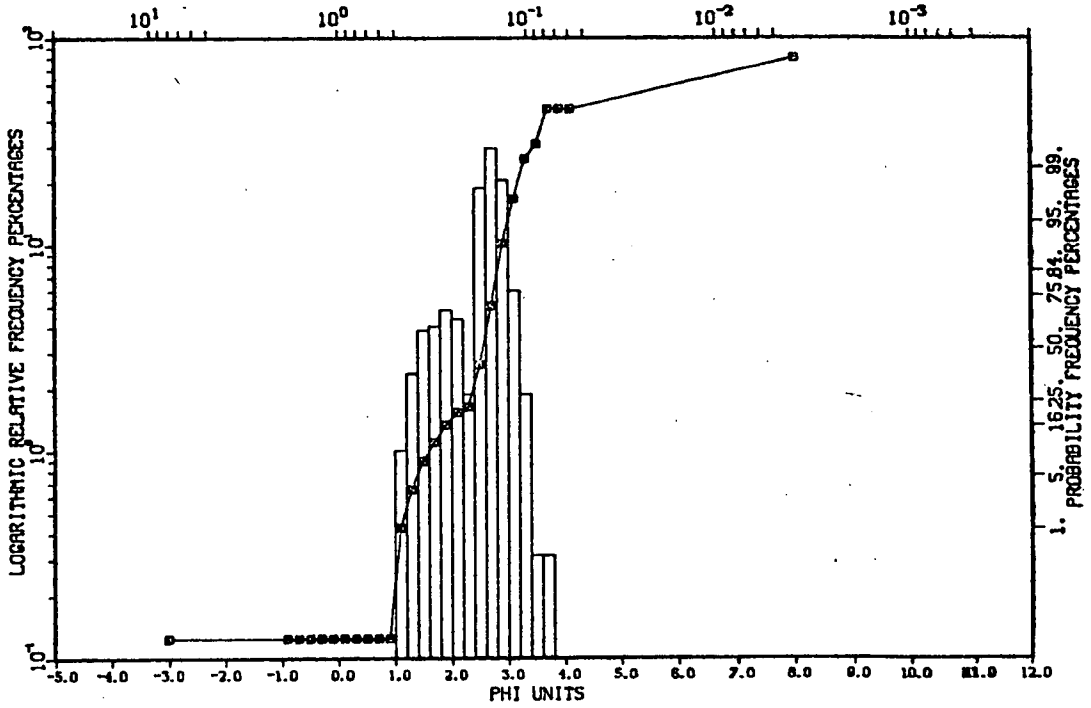
CRUISE M.V. ARCTIC PROWLER FEB 17-22/85 VENT 408 - 80003
SAMPLE NUMBER- 3223
MILLIMETER EQUIVALENTS
LOGARITHMIC RELATIVE FREQUENCY PERCENTAGES
PROBABILITY FREQUENCY PERCENTAGES
PHI UNITS

Appendix 8.2 Wind, temperature, and MSL pressure histories at Sable Island

Prepared by Seaconsult Limited
1:20 PM THU., 23 MAY , 1985

SABLE ISLAND METEOROLOGICAL OBSERVATIONS

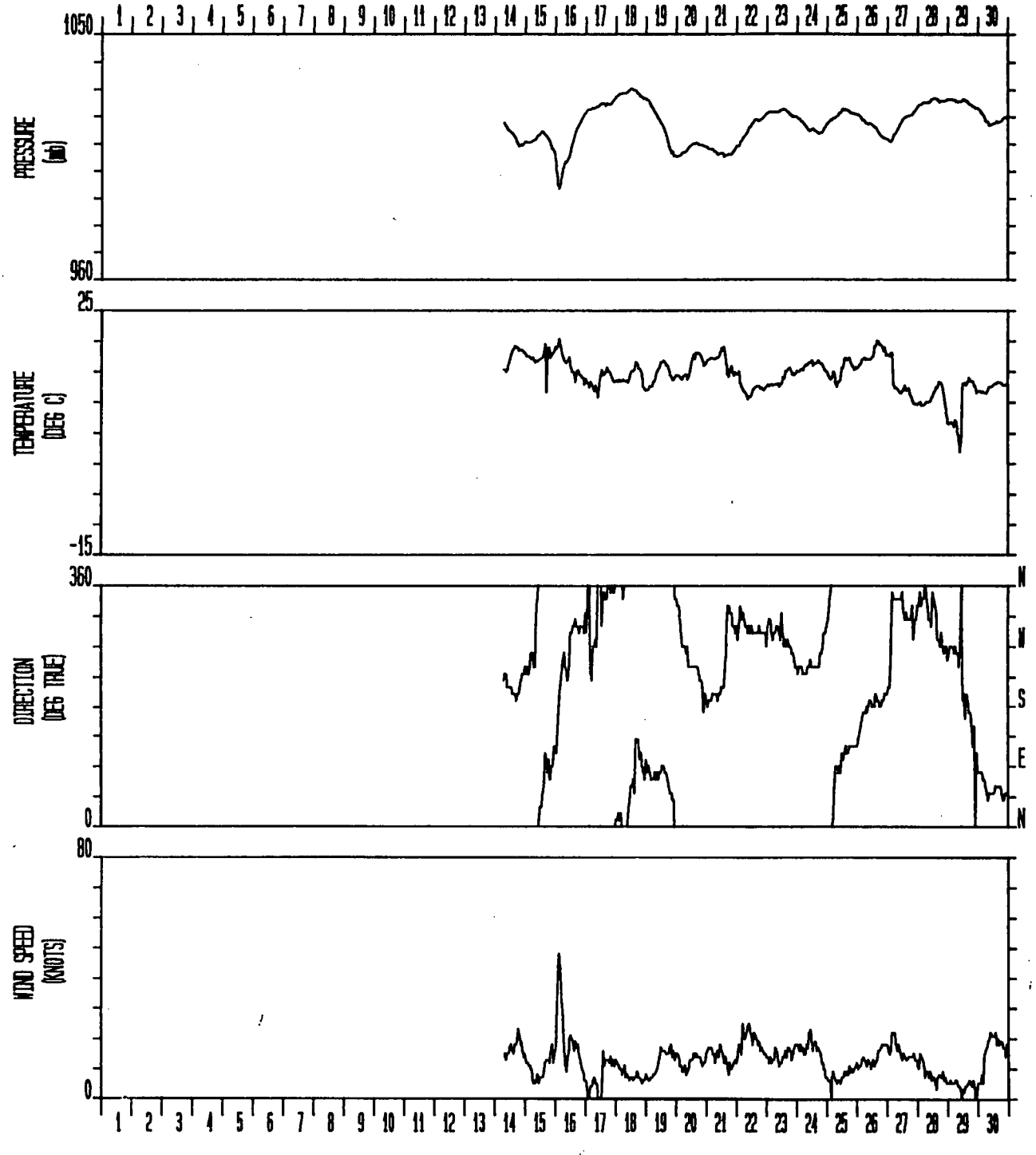

Prepared by Seaconsult Limited
10:26 AM TUE., 21 MAY , 1985

SABLE ISLAND METEOROLOGICAL OBSERVATIONS

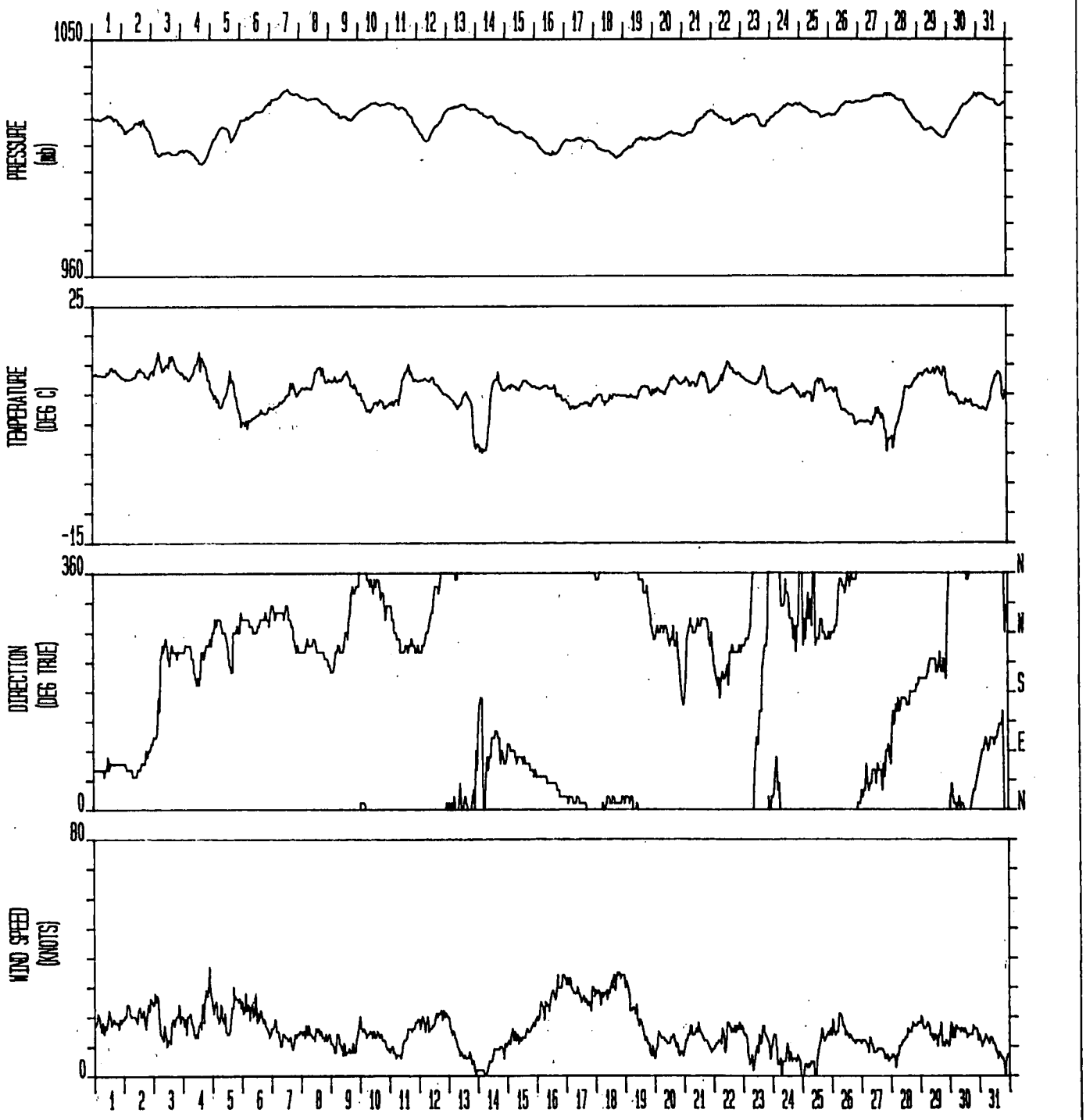

Prepared by Seaconsult Limited
10:31 AM TUE., 21 MAY , 1985

SABLE ISLAND METEOROLOGICAL OBSERVATIONS

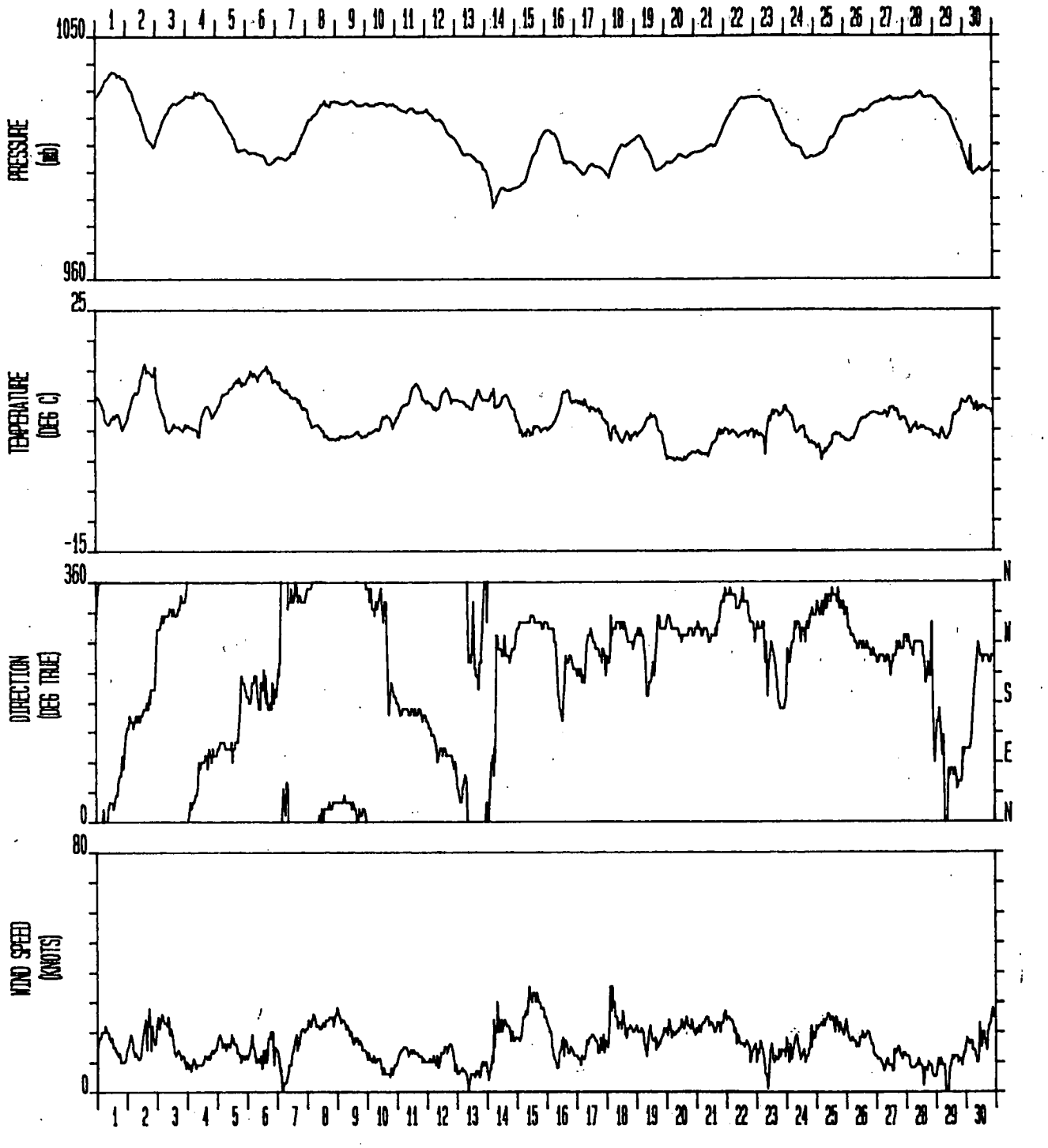

Prepared by Seaconsult Limited
10:37 AM TUE., 21 MAY , 1985

SABLE ISLAND METEOROLOGICAL OBSERVATIONS

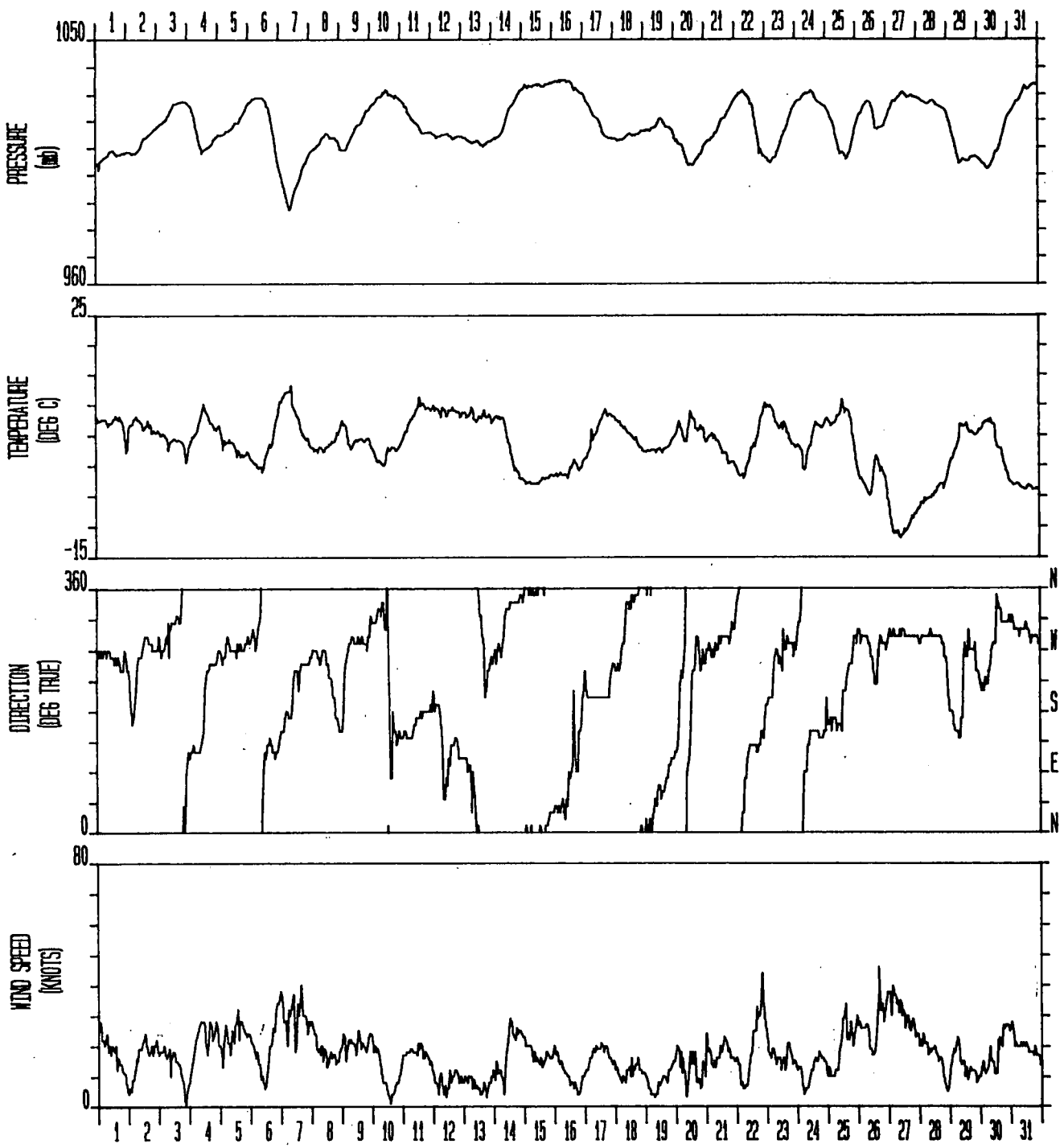

DECEMBER 1984

Prepared by Seaconsult Limited
2:00 PM WED., 22 MAY , 1985

SABLE ISLAND METEOROLOGICAL OBSERVATIONS

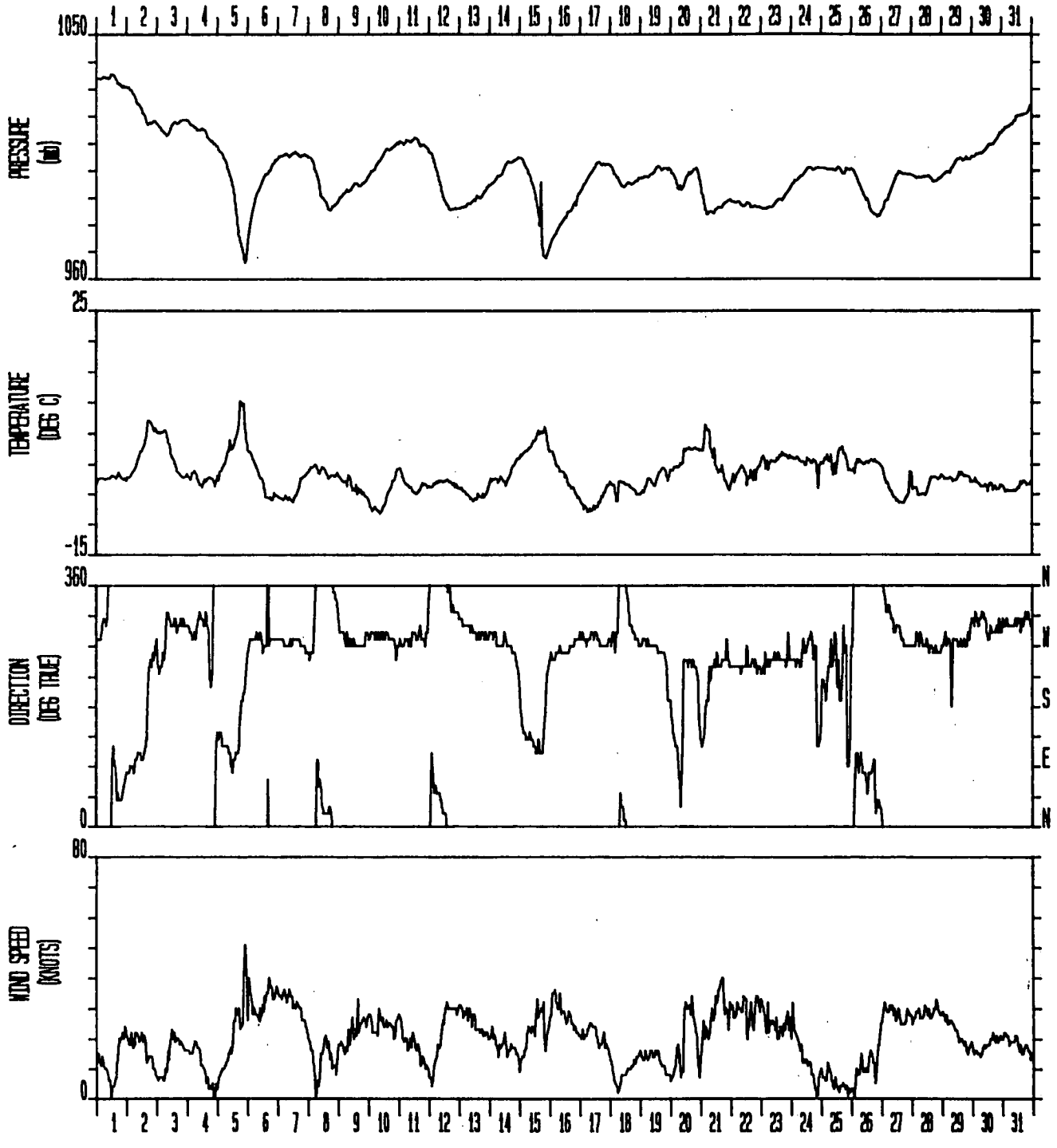

Prepared by Seaconsult Limited
4:12 PM WED., 22 MAY , 1985

SABLE ISLAND METEOROLOGICAL OBSERVATIONS

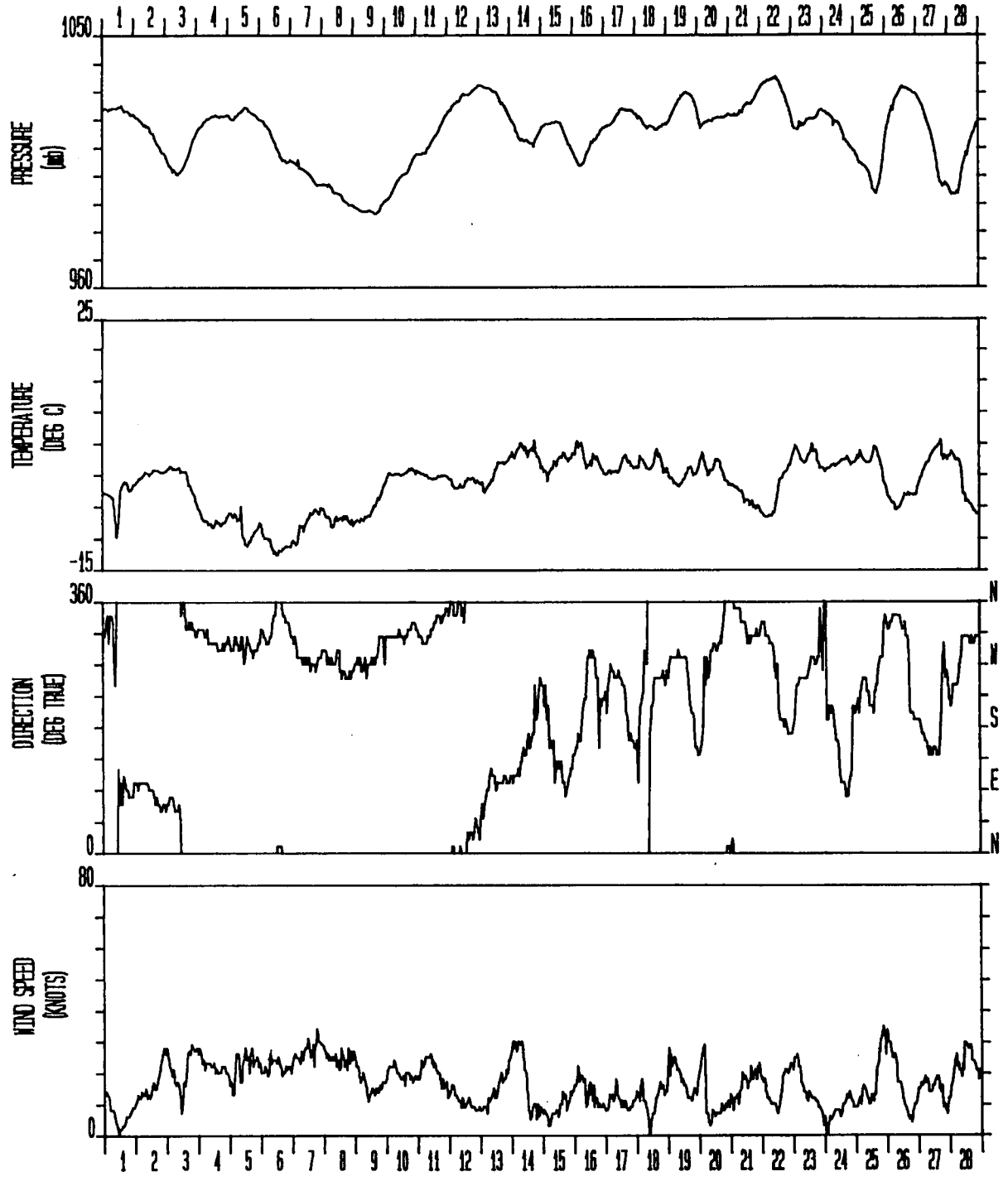

FEBRUARY 1985

Appendix 8.3 Significant wave height histories around Sable Island

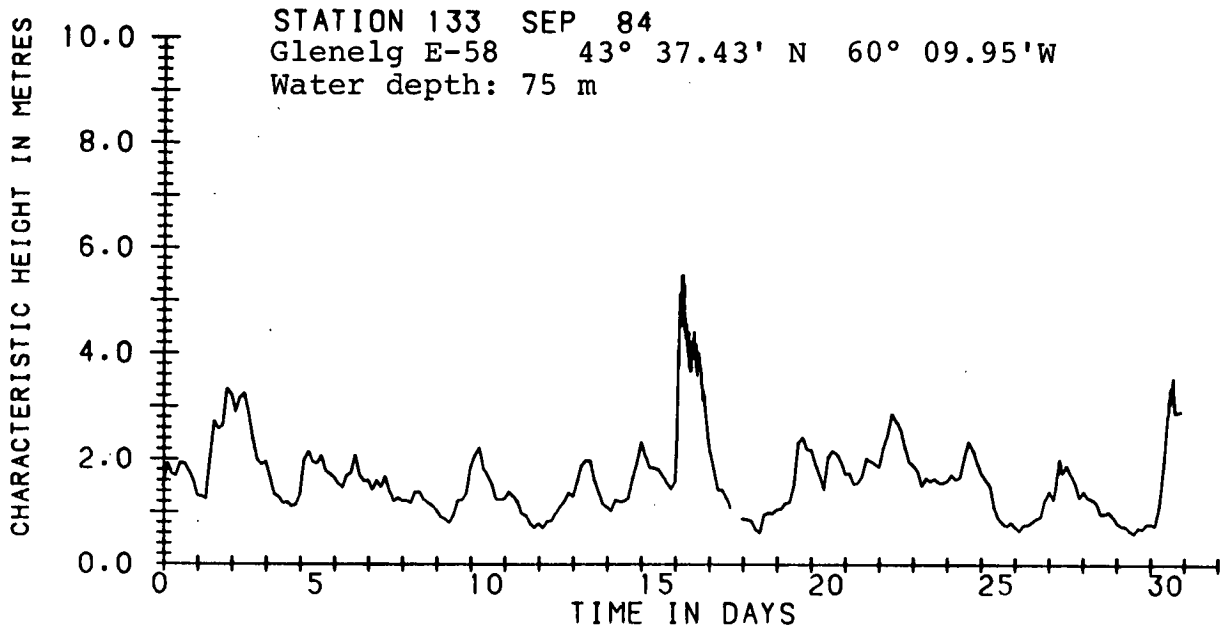
STATION 133 SEP 84
Glenelg E-58 43° 37.43' N 60° 09.95'W
Water depth: 75 m
CHARACTERISTIC HEIGHT IN METRES
10.0
8.0
6.0
4.0
2.0
0.0
0
5
10
15
20
25
30
TIME IN DAYS

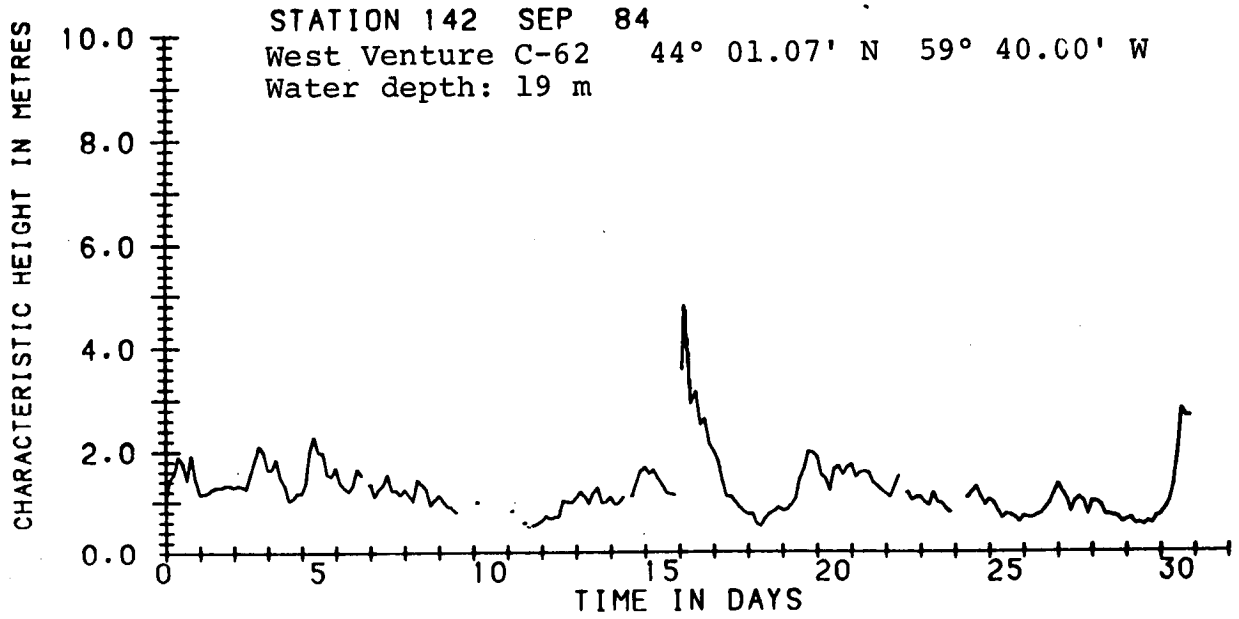
STATION 142 SEP 84
West Venture C-62 44° 01.07' N 59° 40.00' W
Water depth: 19 m
CHARACTERISTIC HEIGHT IN METRES
10.0
8.0
6.0
4.0
2.0
0.0
0
5
10
15
20
25
30
TIME IN DAYS

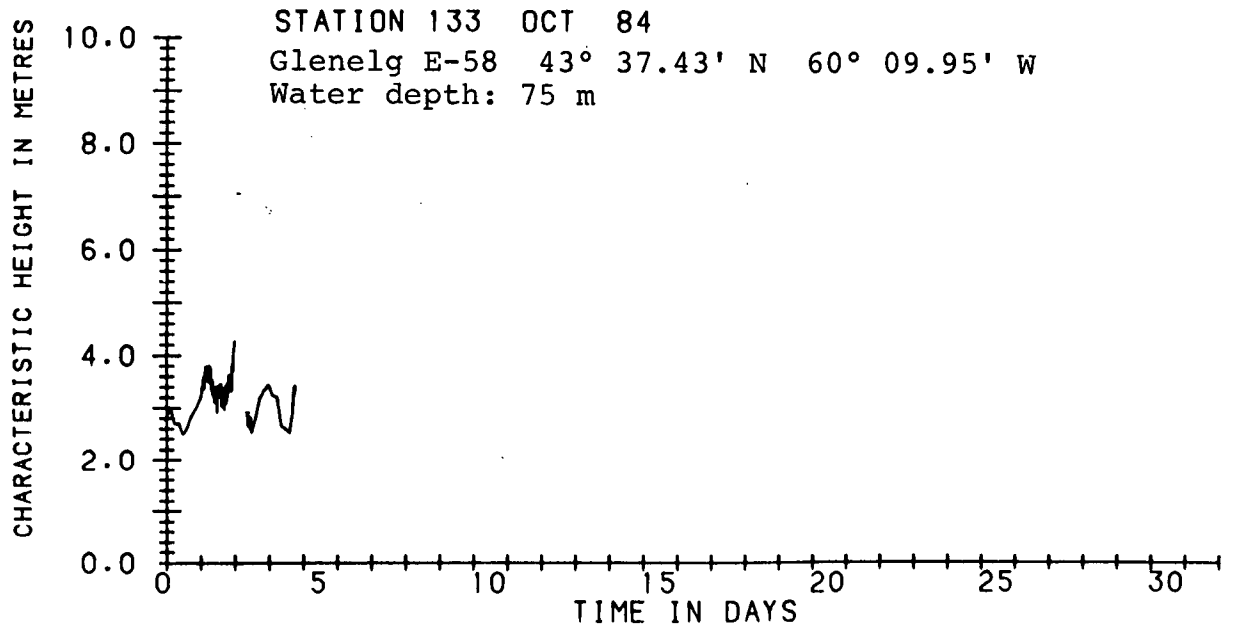
STATION 133 OCT 84
Glenelg E-58 43° 37.43' N 60° 09.95' W
Water depth: 75 m
CHARACTERISTIC HEIGHT IN METRES
10.0
8.0
6.0
4.0
2.0
0.0
0
5
10
15
20
25
30
TIME IN DAYS

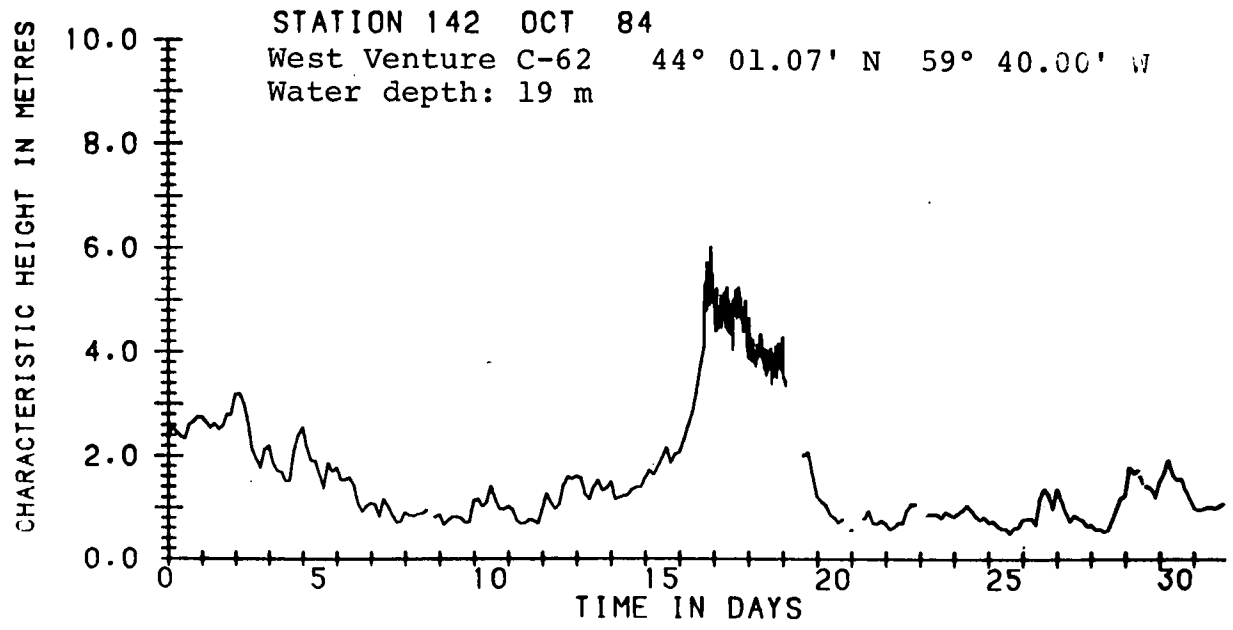
STATION 142 OCT 84
West Venture C-62 44° 01.07' N 59° 40.00' W
Water depth: 19 m
CHARACTERISTIC HEIGHT IN METRES
10.0
8.0
6.0
4.0
2.0
0.0
0
5
10
15
20
25
30
TIME IN DAYS

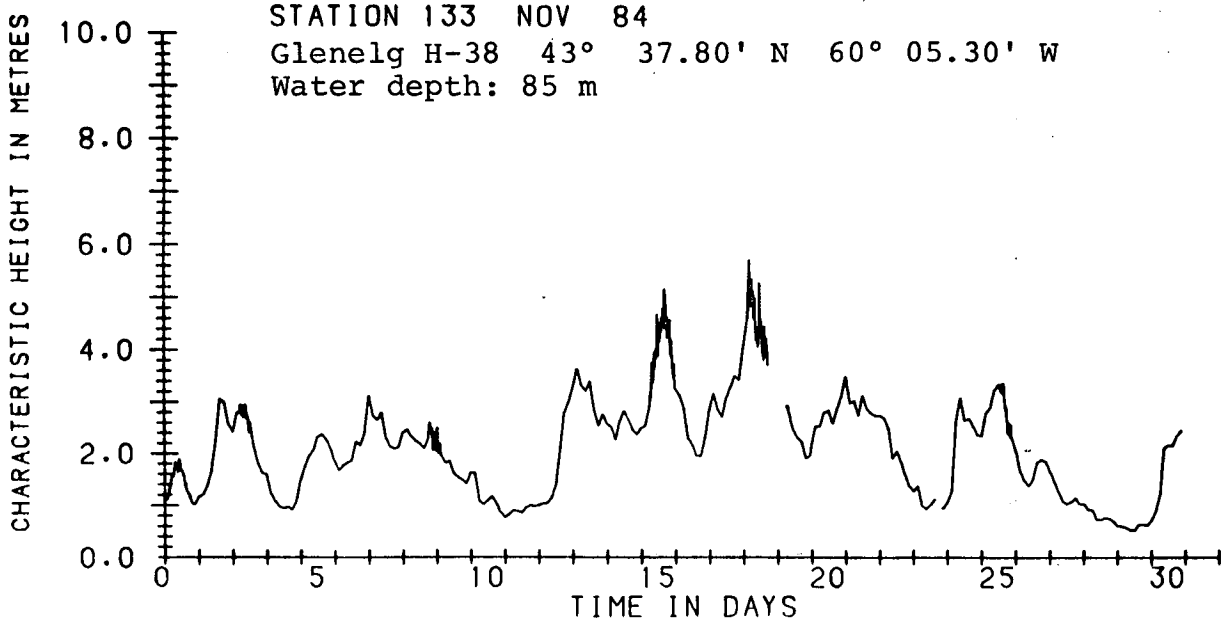
STATION 133 NOV 84
Glenelg H-38 43° 37.80' N 60° 05.30' W
Water depth: 85 m
CHARACTERISTIC HEIGHT IN METRES
10.0
8.0
6.0
4.0
2.0
0.0
0
5
10
15
20
25
30
TIME IN DAYS

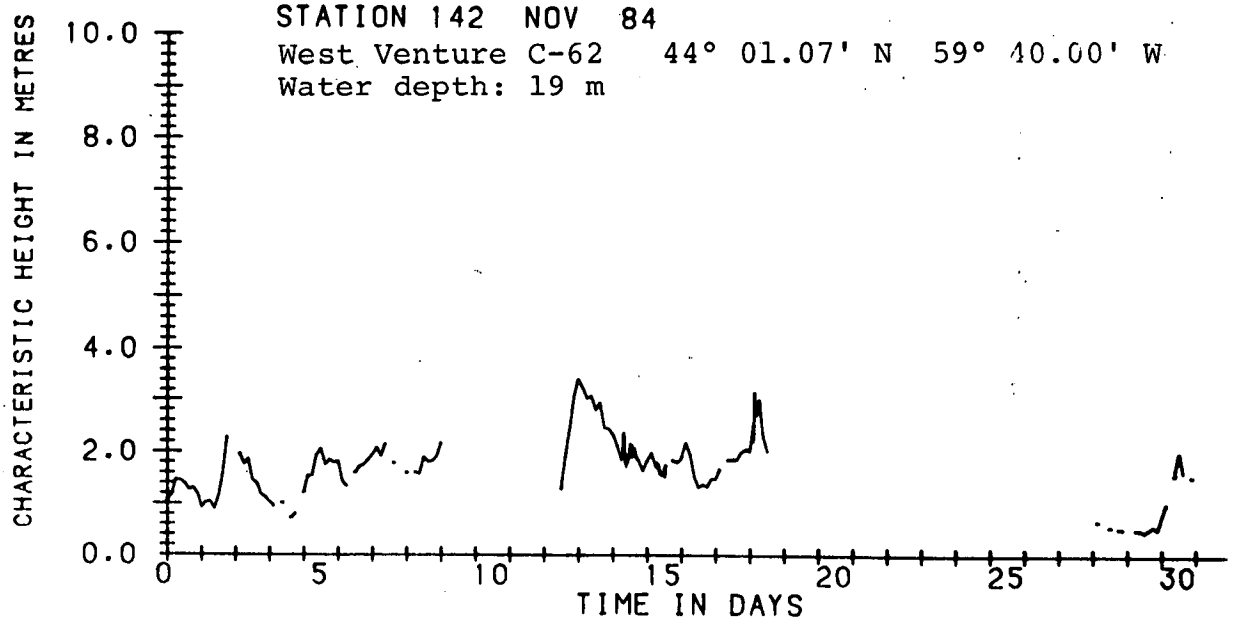
STATION 142 NOV 84
West Venture C-62 44° 01.07' N 59° 40.00' W
Water depth: 19 m
CHARACTERISTIC HEIGHT IN METRES
10.0
8.0
6.0
4.0
2.0
0.0
0
5
10
15
20
25
30
TIME IN DAYS

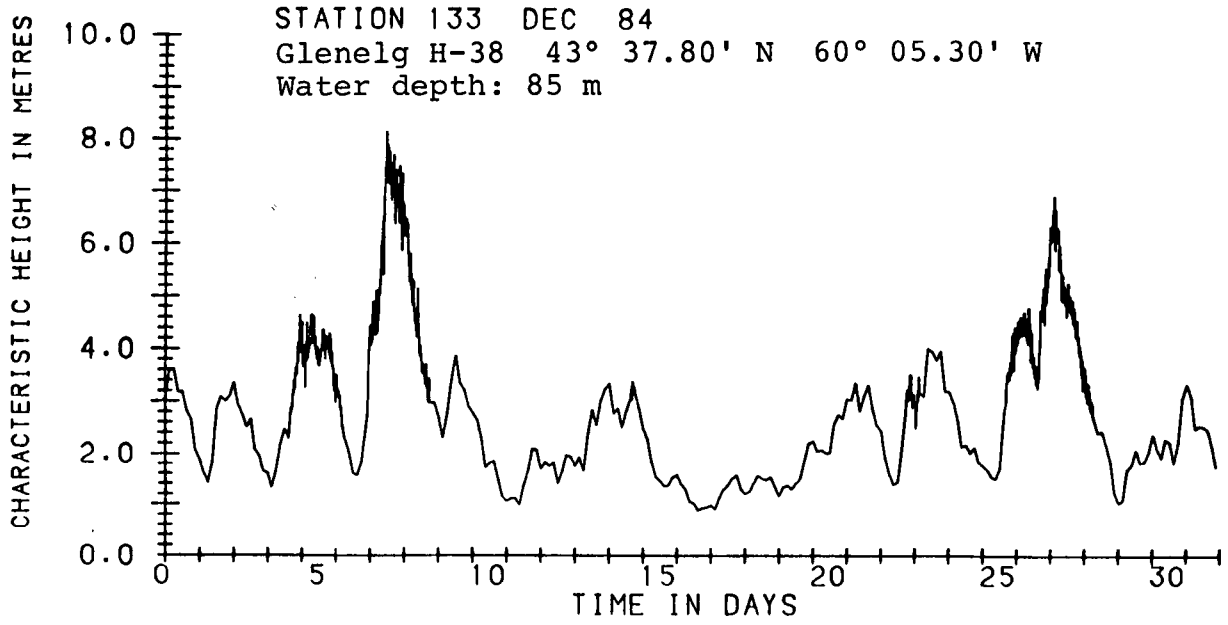
STATION 133 DEC 84
Glenelg H-38 43° 37.80' N 60° 05.30' W
Water depth: 85 m
CHARACTERISTIC HEIGHT IN METRES
10.0
8.0
6.0
4.0
2.0
0.0
0
5
10
15
20
25
30
TIME IN DAYS

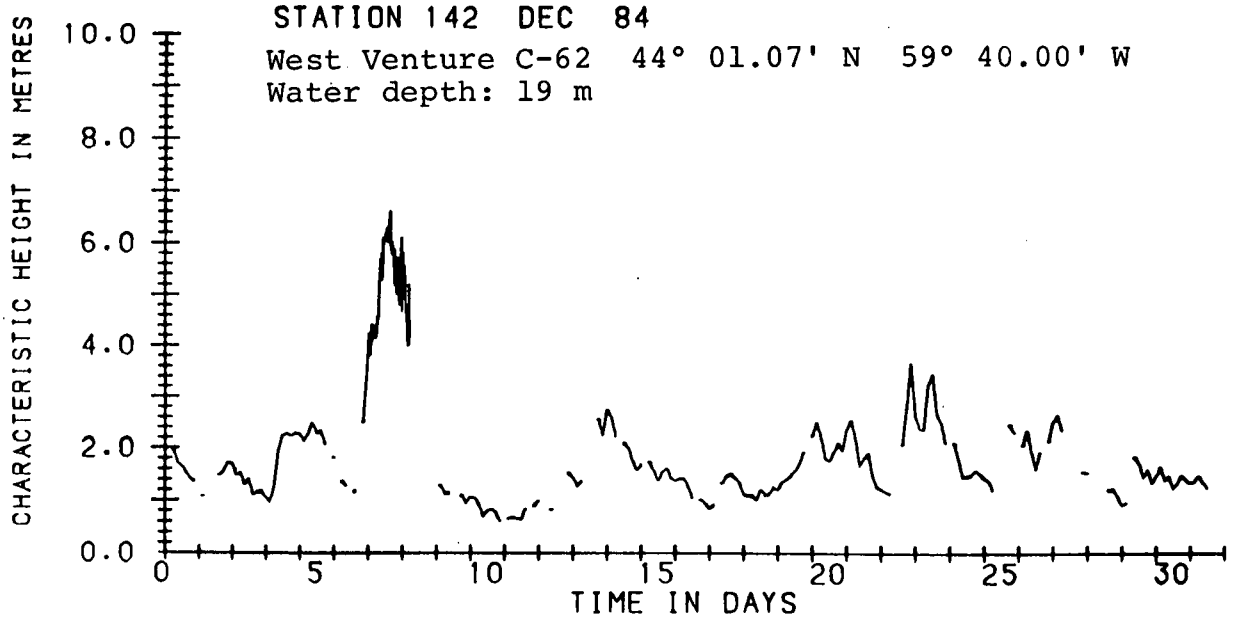
STATION 142 DEC 84
West Venture C-62 44° 01.07' N 59° 40.00' W
Water depth: 19 m
CHARACTERISTIC HEIGHT IN METRES
10.0
8.0
6.0
4.0
2.0
0.0
0
5
10
15
20
25
30
TIME IN DAYS

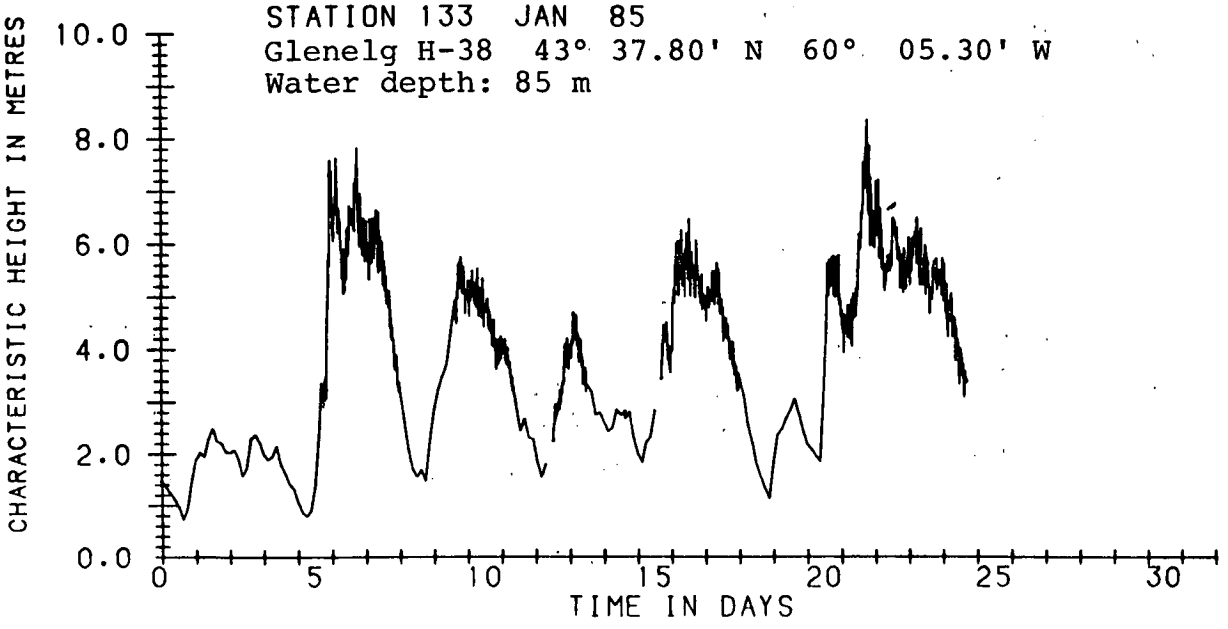
STATION 133 JAN 85
Glenelg H-38 43° 37.80' N 60° 05.30' W
Water depth: 85 m
CHARACTERISTIC HEIGHT IN METRES
10.0
8.0
6.0
4.0
2.0
0.0
0
5
10
15
20
25
30
TIME IN DAYS

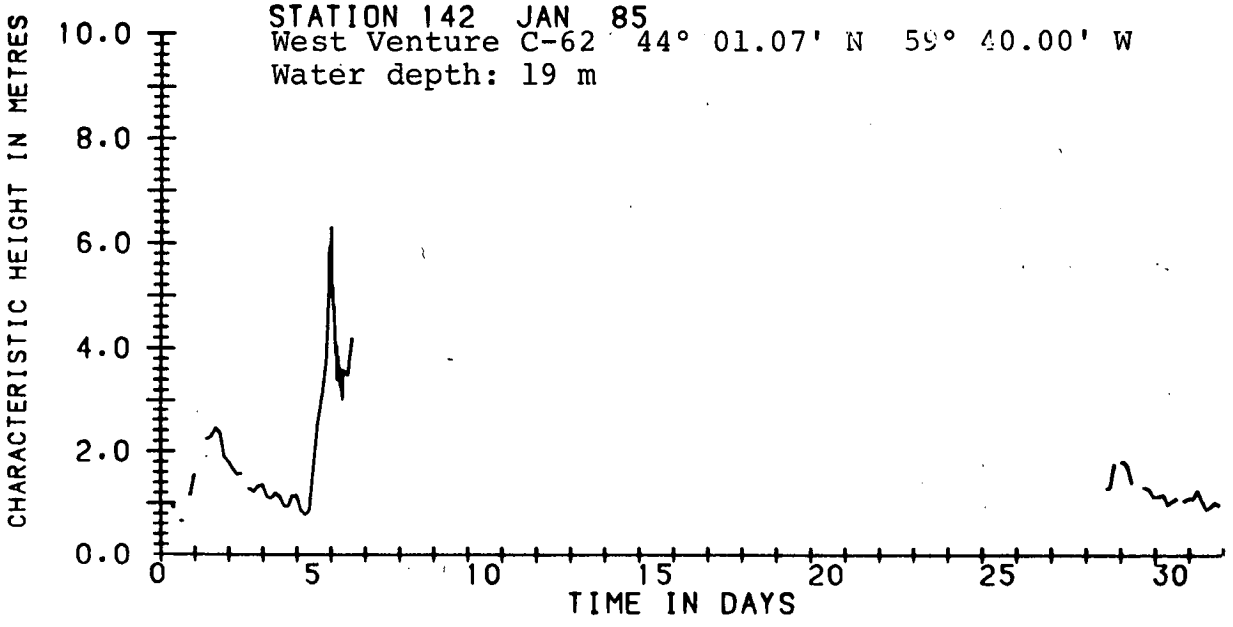
STATION 142 JAN 85
West Venture C-62 44° 01.07' N 59° 40.00' W
Water depth: 19 m
CHARACTERISTIC HEIGHT IN METRES
10.0
8.0
6.0
4.0
2.0
0.0
0
5
10
15
20
25
30
TIME IN DAYS

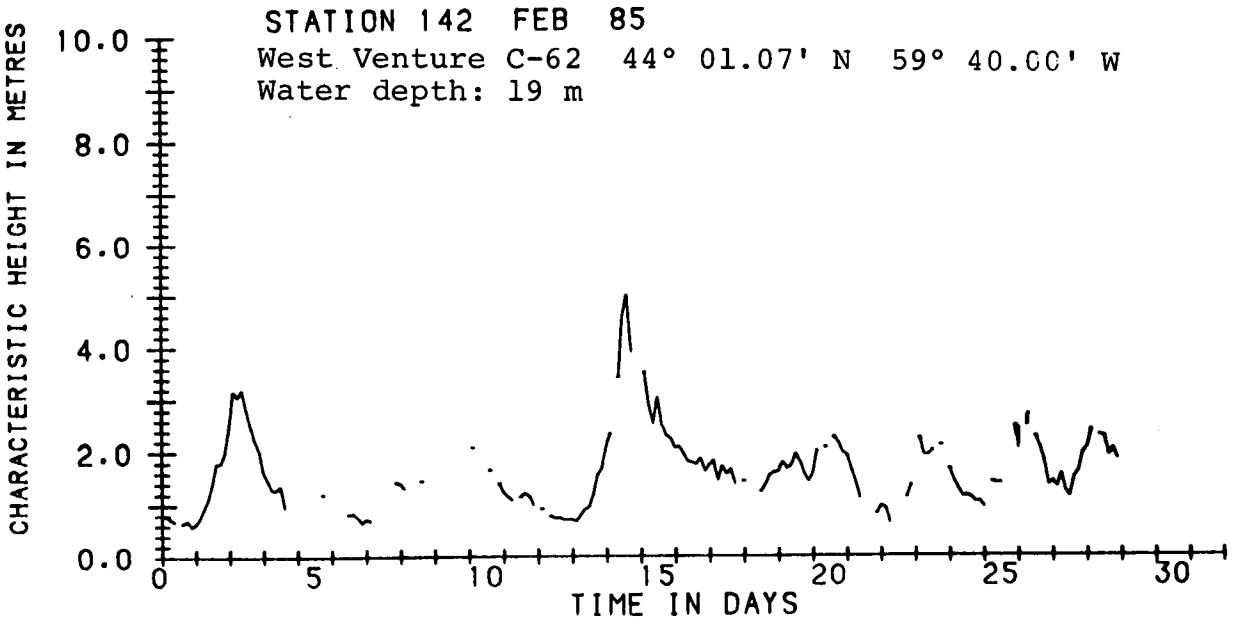
STATION 142 FEB 85
West Venture C-62 44° 01.07' N 59° 40.00' W
Water depth: 19 m
CHARACTERISTIC HEIGHT IN METRES
10.0
8.0
6.0
4.0
2.0
0.0
0
5
10
15
20
25
30
TIME IN DAYS

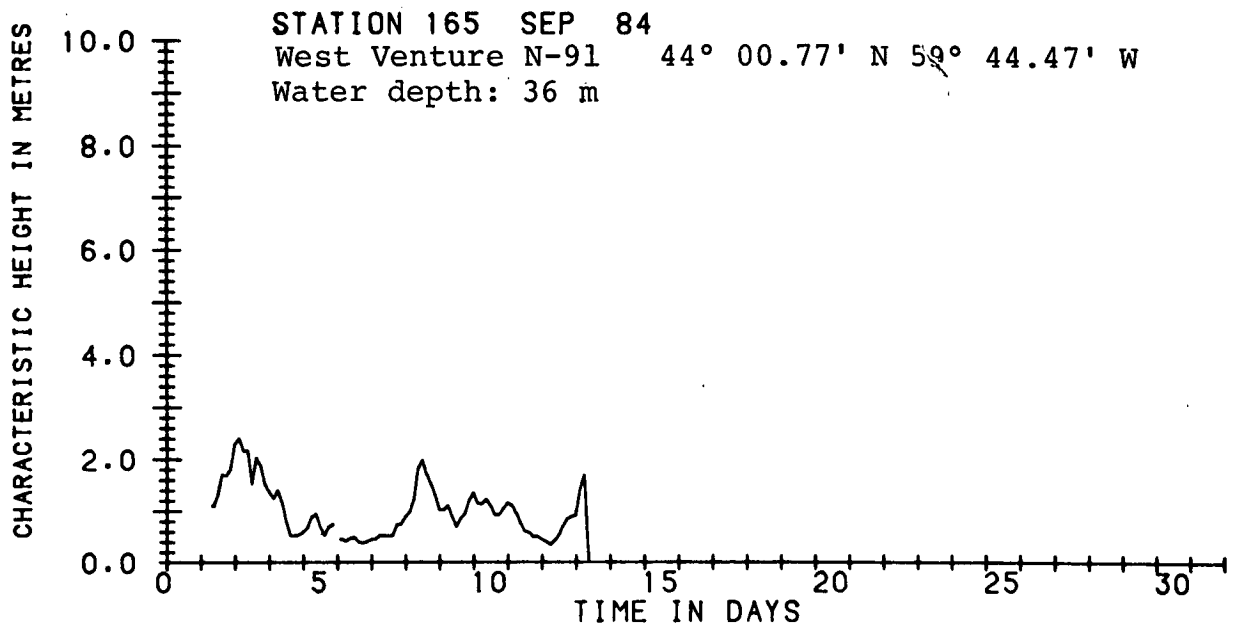

NO DATA FOR OCTOBER

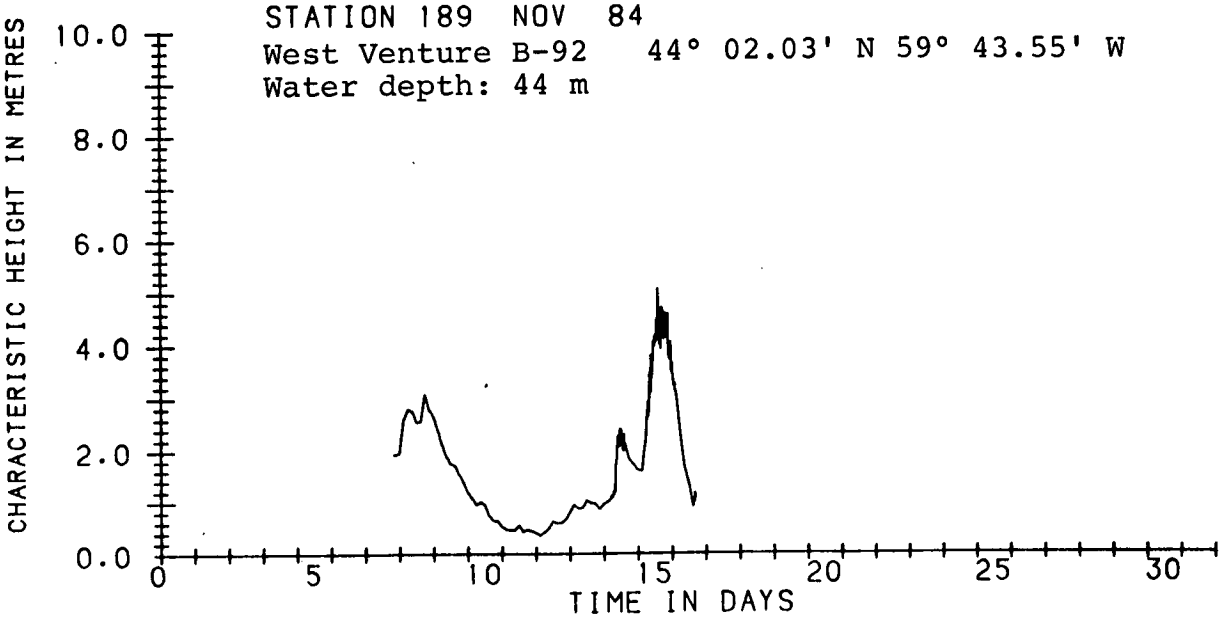
STATION 189 NOV 84
West Venture B-92 44° 02.03' N 59° 43.55' W
Water depth: 44 m
CHARACTERISTIC HEIGHT IN METRES
10.0
8.0
6.0
4.0
2.0
0.0
0
5
10
15
20
25
30
TIME IN DAYS

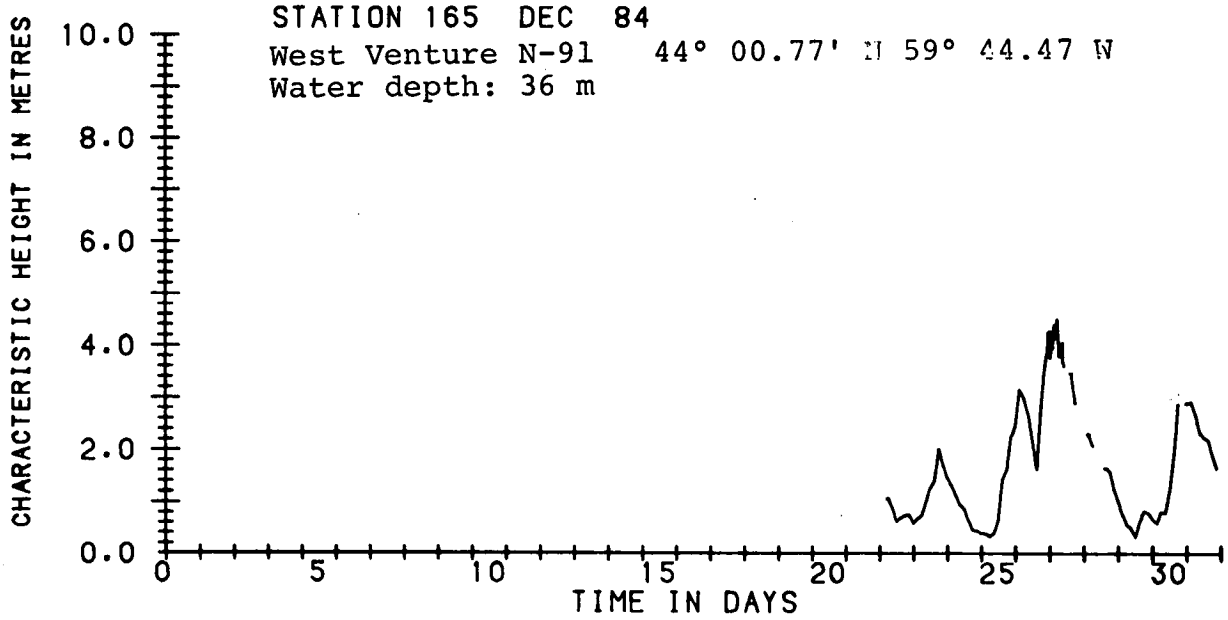
STATION 165 DEC 84
West Venture N-91 44° 00.77' N 59° 44.47 W
Water depth: 36 m
CHARACTERISTIC HEIGHT IN METRES
10.0
8.0
6.0
4.0
2.0
0.0
0
5
10
15
20
25
30
TIME IN DAYS

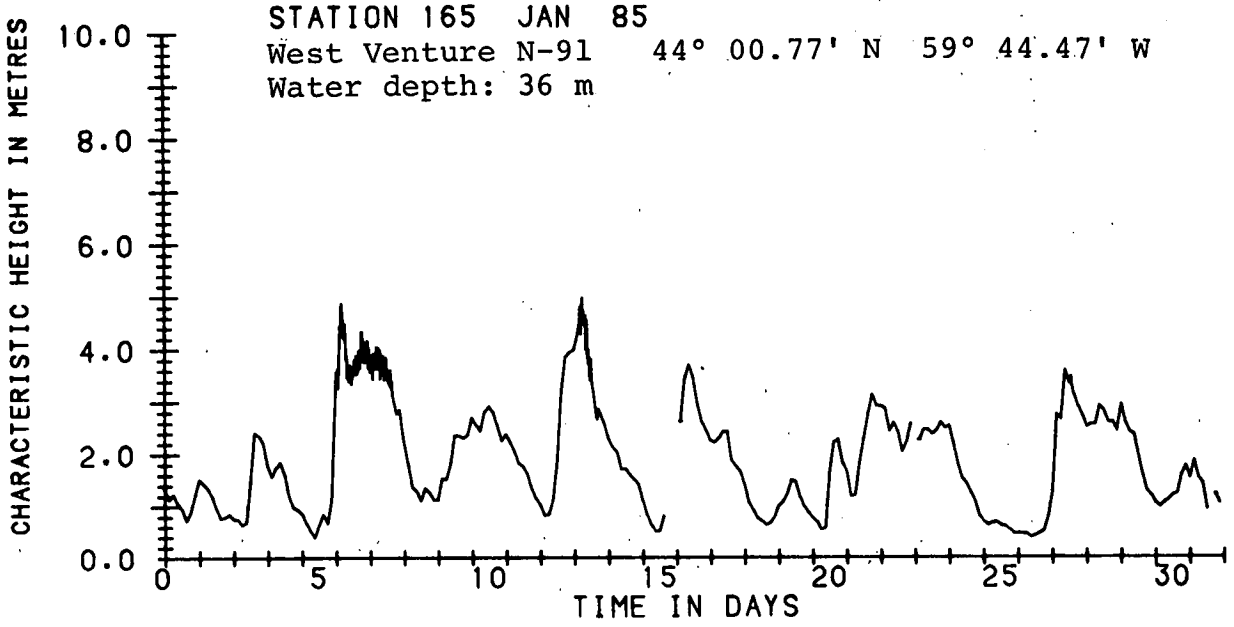
STATION 165 JAN 85
West Venture N-91 44° 00.77' N 59° 44.47' W
Water depth: 36 m
CHARACTERISTIC HEIGHT IN METRES
10.0
8.0
6.0
4.0
2.0
0.0
0
5
10
15
20
25
30
TIME IN DAYS

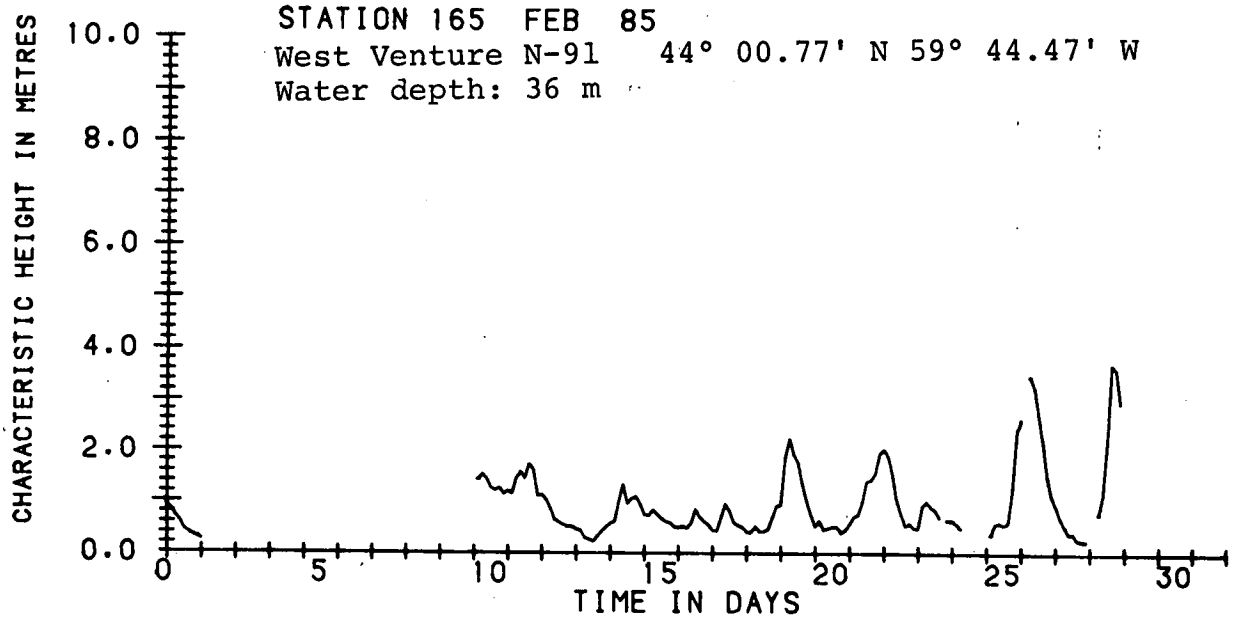
STATION 165 FEB 85
West Venture N-91 44° 00.77' N 59° 44.47' W
Water depth: 36 m
CHARACTERISTIC HEIGHT IN METRES
10.0
8.0
6.0
4.0
2.0
0.0
0
5
10
15
20
25
30
TIME IN DAYS

INSERT

OVERSIZE

IMAGE

HERE